Norwegian University of Life Sciences
Faculty of veterinary medicine
Department of Production Animal Clinical Sciences

Philosophiae Doctor (PhD)
Thesis 2021:63

Neurodevelopmental toxicity of a human relevant mixture of persistent organic pollutants (POPs) and perfluorooctane sulfonic acid (PFOS)

Skadelige effekter på nevroutvikling forårsaket av en humanrelevant blanding av persistente organiske miljøgifter (POPs) og perfluorooktansulfonsyre (PFOS)

Ajay Yadav

Neurodevelopmental toxicity of a human relevant mixture of persistent organic pollutants (POPs) and perfluorooctane sulfonic acid (PFOS)

Skadelige effekter på nevroutvikling forårsaket av en humanrelevant blanding av persistente organiske miljøgifter (POPs) og perfluorooktansulfonsyre (PFOS)

Philosophiae Doctor (PhD) Thesis

Ajay Yadav

Norwegian University of Life Sciences
Faculty of veterinary medicine
Department of Production Animal Clinical Sciences

Ås (2021)

Thesis number 2021:63
ISSN 1894-6402
ISBN 978-82-575-1837-0

Table of Contents

Acknowledgements

The work presented in this thesis was funded by the European Union's Horizon 2020 research and innovation program under the Marie Skłodowska-Curie grant agreement No. 722634: Protection against endocrine disruptors “ProtectED”.

I would like to thank the Norwegian University of Life Sciences (NMBU) for giving me this opportunity. Further, I would like to thank the previous and current head of the Department of Production Animal Clinical Sciences (PRODMED), Irma Oskam and Olav Reksen, for their support. I would like to thank the Section for Pharmacology and Pharmaceutical Biosciences, University of Oslo (UiO), where the experiments described in this thesis were mainly carried out.

This research would not have been completed without the guidance and motivation from all of my supervisors, Erik Ropstad, Steven Verhaegen, Karin Elisabeth Zimmer and Ragnhild Elisabeth Paulsen. I would like to specially thanks to my main supervisor Erik Ropstad for giving me an opportunity to pursue PhD in Norway. Thank you, Erik, for always being available whenever I needed any suggestions, being so friendly and very supportive. Thank you also for helping me with statistics. I would like to thank my co-supervisor Ragnhild for giving me an opportunity to work under her supervision at UiO. Ragnhild, thank you for your support, guidance and allowing me to work independently. Your office was always open for me to answer my questions. I want to thank my co-supervisor Karin, for reading my manuscripts/thesis and providing very useful comments/feedbacks. I would like to thank sincerely my co-supervisor Steven for his support and being so friendly. Thank you for always being available whenever I needed any suggestions/help and guiding me. Thank you for sharing your excellent ideas and correcting my writing style.

This project gave me the opportunities to learn some new scientific skills during my secondments abroad. I would like to thank Lisa Connolly (Institute for Global Food Security School of Biological Sciences Queen’s University Belfast, Northern Ireland) for giving me this opportunity and being very supportive. I want to thank Paul A Fowler (Institute of Medical Sciences School of Medicine, Medical Sciences & Nutrition, University of Aberdeen, Scotland) for this opportunity and for all scientific discussions. Special thanks to Panagiotis Filis, university of Aberdeen for his guidance and helping me with Omics data, manuscripts, and all.

I would like to thank Mona Aleksandersen for histological analysis, and Gunn C. Østby for preparation of samples and conducting histological experiments. Thanks to Diana Domanska for helping me with Omics data and being friendly. Thanks to Arvind Y.M. Sundaram for analysing the RNA-seq data. I would like to thank Shan Narui for being very supportive and giving access to the lab at STAMI. Thanks to Johanna Samulin Erdemd for her guidance and Fred Haugen for providing the resources at STAMI. Thanks to Mazia Amber, Queen's University Belfast for her great contribution to PC12 paper and for her help. I would like to thank Fernando Boix (Section for Drug Abuse Research, Dept. of Forensic Sciences, Division of Laboratory Medicine, Oslo University Hospital) for his help in conducting the Pharmacokinetics modelling and analysis. The contributions of all my co-authors are highly acknowledged.

Thanks to my friends/colleague, Nils, Marvin, Denis and others for making PhD life enjoyable at ZEB UiO. Nils, for organizing social events and always inviting me. Special thanks to Mussie Ghezu Hadera for his guidance and help at UiO. Mona Gaarder for her support in the lab during a PhD degree. Beata for her help at ZEB and concerns about my well-being. I would also like to thank my officemates at Adamstuen NMBU Maria and Silje for always being very helpful. Thank you, Rakesh, for your encouraging words.

Finally, I would like to thank my family, my brothers for their support, my parents for their blessing and unconditional love, my wife Lisha for always being so patient and encouraging me, and my little son Jason, who lights my life up.

Abbreviations and definitions

ADHD	Attention deficit hyperactivity disorder
AhR	Aryl hydrocarbon receptor
AMPA	α-amino-3-hydroxy-5-methylisoxazole-4-propionic acid
AOPs	Adverse outcome pathways
ASD	Autism spectrum disorders
AUC	Area under the curve
BBB	Blood-brain-barrier
BFRs	Brominated flame retardants
Ca^{2+}	Calcium ions
CAM	Chorioallantoic membrane
CGNs	Cerebellar granule neurons
CNS	Central nervous system
CPP	3-((R)-2-Carboxypiperazin-4-yl)-propyl-1-phosphonic acid
DDE	Dichlorodiphenyldichloroethylene
DDT	Dichlorodiphenyltrichloroethane
DENAMIC	Developmental neurotoxicity assessment of mixtures in children
DIV	Days *in vitro*
E	Embryonic day
EGL	External granule layer
EPA	U.S. Environmental Protection Agency
ER	Endoplasmic reticulum
GC	Granule cell
GDH	Glutamate dehydrogenase
GS	Glutamine synthase
HBB	Hexabromobiphenyl
HBCD	Hexabromocyclododecane
HCB	Hexachlorobenzene
HCBD	Hexachlorobutadiene
HCH	Hexachlorocyclohexane
HiPSCs	Human-induced pluripotent stem cells
IGL	Internal granule layer

LC-MS	Liquid Chromatography Mass Spectrometry
LDH	Lactate dehydrogenase
mBCl	Monochlorobimane
ML	Molecular layer
MRT	Mean residence time
MTT	3-(4,5-dimethylthiazol-2-yl)-2,5-diphenyl tetrazolium bromide
NGF	Nerve growth factor
NMDA-R	N-methyl-D-aspartate receptor
NO	Nitric oxide
OCPs	Organochlorine pesticides
PAH	Polycyclic aromatic hydrocarbon
PBDE	Polybrominated diphenyl ether
PC12	Rat pheochromocytoma cells
PCB	Polychlorinated biphenyl
PCDD	Polychlorinated dibenzo-*p*-dioxin
PCDF	Polychlorinated dibenzofuran
PCL	Purkinje cell layer
PD	Parkinson's disease
PFAA	Perfluoroalkyl acids
PFAS	Per- and polyfluoroalkyl substances
PFDA	Perfluorodecanoic acid
PFHxS	Perfluorohexane sulfonic acid
PFNA	Perfluorononanoic acid
PFOA	Perfluorooctanoic acid
PFOS	Perfluorooctanesulfonic acid
PFSA	Perfluoroalkyl sulfonic acid
PFUnDA	Perfluoroundecanoic acid
PK	Pharmacokinetic
PND	Postnatal day
POPs	Persistent organic pollutants
ROS	Reactive oxygen species
SCCP	Short-chain chlorinated paraffin
SCPOP	Stockholm Convention on Persistent Organic Pollutants

List of papers

Paper I:

Reprod Toxicol. 2021 Jan 23; 100:109-119.

doi: 10.1016/j.reprotox.2021.01.008.

A human relevant mixture of persistent organic pollutants (POPs) and perfluorooctane sulfonic acid (PFOS) differentially affect glutamate induced excitotoxic responses in chicken cerebellum granule neurons (CGNs) in vitro

Ajay Yadav, Steven Verhaegen, Evelien Verbruggen, Marie Kerhoas, Eva Henriëtte Willemijn Huiberts, Mussie Ghezu Hadera, Hanne Friis Berntsen, Karin Elisabeth Zimmer, Erik Ropstad, Ragnhild Elisabeth Paulsen

Paper II:

Toxicol Lett. 2021 Mar 1;338:85-96. doi: 10.1016/j.toxlet.2020.12.007.

A human relevant mixture of persistent organic pollutants (POPs) and perfluorooctane sulfonic acid (PFOS) enhance nerve growth factor (NGF)-induced neurite outgrowth in PC12 cells

Ajay Yadav, Mazia Amber, Denis Zosen, Nils Anders Labba, Eva Henriette Willemijn Huiberts, Johanna Samulin Erdem, Fred Haugen, Hanne Friis Berntsen, Shanbeh Zienolddiny, Ragnhild Elisabeth Paulsen, Erik Ropstad, Lisa Connolly, Steven Verhaegen

Paper III:

Under review (2021)

Peripherally Administered Persistent Organic Pollutants Distribute to the Brain of Developing Chicken Embryo in Concentrations Relevant for Human Exposure

Ajay Yadav, Steven Verhaegen, Mussie Ghezu Hadera, Hanne Friis Berntsen, Vidar Berg, Jan Ludvig Lyche, Azemira Sabaredzovic, Line Småstuen Haug, Oddvar Myhre, Karin Elisabeth Zimmer, Ragnhild Elisabeth Paulsen, Erik Ropstad, Fernando Boix

Paper IV:

Manuscript

Exposure to a Human Relevant Mixture of Persistent Organic Pollutants (POPs) or to Perfluorooctane Sulfonic Acid (PFOS) Alone Dysregulates the Developing Cerebellum of Chicken Embryo

Ajay Yadav, Steven Verhaegen, Panagiotis Filis, Diana Domanska, Robert Lyle, Arvind Y.M. Sundaram, Magnus Leithaug, Gunn Charlotte Østby, Mona Aleksandersen, Hanne Friis Berntsen, Karin Elisabeth Zimmer, Paul A. Fowler, Ragnhild Elisabeth Paulsen, Erik Ropstad

Summary

Persistent organic pollutants (POPs) are ubiquitous in the environment. Humans are continuously exposed to chemical mixtures through food and the environment. Exposure to POPs have been associated with several adverse effects on human health including impaired brain development, cognition, and behaviour. The developing central nervous system appears to be more susceptible to toxic insults and several POPs are suspected to be developmental neurotoxicants. In the present thesis we used a POP mixture, containing 29 different compounds, based on being prominent in food, breast milk or blood from the Scandinavian human population. Perfluorooctane sulfonic acid (PFOS) alone, a potential neurodevelopmental toxicant, was also evaluated. We hypothesized that exposure to POPs during sensitive periods of early development could adversely affect key neurodevelopmental processes. To address this, we used the chicken embryo focussing on cerebellum and PC12 rat pheochromocytoma cells, as experimental models. Our results showed that exposure to POPs not only induced toxicity on their own but also aggravated glutamate-induced excitotoxicity in cultured cerebellar granule neurons (CGNs). Observations indicated a Ca^{2+}-independent, but still N-methyl-D-aspartate receptor (NMDA-R) dependent mechanism in the absence of glutamate, and a Ca^{2+}- and NMDA-R dependent mechanism in the presence of glutamate. Further, we found that CGN-sensitivity increased with the maturation in culture. POP exposures enhanced neurite length and branched networks of neurites in nerve growth factor (NGF)-induced PC12 cells, indicating the POPs interference with neuronal connectivity. However, in the absence of NGF, the effects of POPs on neurite outgrowth were marginal, suggesting that exposure cannot mimic the NGF-receptor signal on its own. POP mixture injected into the allantois distributed to the brain of developing chicken embryo in a concentration relevant for human exposure. However, the speed of distribution differed, with the protein binding per- and polyfluoroalkyl substances (PFASs) reaching the brain slower than the lipophilic polychlorinated biphenyls (PCBs), organochlorine pesticides (OCPs) and brominated flame retardants (BFRs). This reflects that distribution speed of the compounds depends on the chemical properties of different classes of compounds present in the mixture. POP exposure induced alterations at the levels of cerebellar morphology and affected gene and protein expression profiles that can interfere with fundamental aspects of neurodevelopmental processes. Our results showed alterations in molecular events linked to neuronal cell proliferation and migration, cellular stress responses including unfolded protein response,

lipid metabolism, and myelination. Exposure to the POP mixture increased protein oxidation, whereas PFOS decreased oxidation. Our studies provide possible mechanistic explanations for associations between POP exposure and adverse neurodevelopmental and cognitive outcomes observed in epidemiological studies. Overall, we conclude that exposure to POPs could lead to morphological and molecular changes that interfere with fundamental aspects of neurodevelopment.

Norsk sammendrag

Persistente organiske miljøgifter (POP) finnes over alt i miljøet. Mennesker blir kontinuerlig eksponert for blandinger av disse kjemikaliene fra ulike kilder. Eksponering for POP har vært assosiert med flere uønskede effekter på menneskers helse, blant annet effekter på hjernens utvikling og funksjon. Utviklingen av sentralnervesystemet synes å være særlig utsatt for skadelige effekter knyttet til eksponering med POPs. I denne oppgaven brukte vi en POP-blanding, som inneholder 29 forskjellige forbindelser. Disse er basert på forekomst i mat, morsmelk eller blod fra den skandinaviske befolkningen. Perfluorooktansulfonsyre (PFOS), som er vist å ha skadelige effekter på nevroutvikling, ble i tillegg undersøkt som enkeltstoff. Vår hypotese var at eksponering for POPs i tidlige utviklingsstadier kunne ha negative effekter på viktige trinn i nevroutviklingen. For å belyse denne problemstillingen eksperimentelt, brukte vi kyllingembryo og isolerte granulærceller fra kyllingenes lillehjerne (CGN). I tillegg brukte vi en feokromocytomcellelinje fra rotte (PC12). Resultatene viste at eksponering for POPs ikke bare induserte toksisitet alene, men også forverret glutamatindusert eksitotoksisitet i isolerte CGN-celler. Våre funn indikerte en Ca^{2+} -uavhengig, men fortsatt N-metyl-D-aspartat reseptor (NMDA-R) -avhengig mekanisme i fravær av glutamat, og en Ca^{2+}- og NMDA-R-avhengig mekanisme i nærvær av glutamat. Videre fant vi at granulærcellenes følsomhet for eksponering i kultur økte med modningsgraden. Eksponering med POPs førte til økt neurittlengde og antall forgrenede nettverk av neuritter i PC12-celler som var tilsatt nervevekstfaktor (NGF). Dette indikerer at POPs kan forstyrre forbindelsen mellom nervecellene. I fravær av NGF, var imidlertid effekten av POPs på neurittutvekst marginal, noe som tyder på at POPs alene ikke kan etterligne NGF-reseptorsignalet. Blandingen av POPs ble injisert i kyllingegg for å undersøke om og hvordan de ulike stoffene i blandingen distribueres til hjernen hos kyllingembryo. Vi fant at POP-blanding injisert i allantois ble distribuert til hjernen i konsentrasjoner som er relevante for human eksponering. Distribusjonshastigheten varierte avhengig av stoffenes kjemiske egenskaper. Proteinbindende per- og polyfluoralkylstoffer (PFAS) nådde hjernen langsommere enn de lipofile polyklorerte bifenylene (PCB), organoklorpesticider (OCP) og bromerte flammehemmere (BFR). POP-eksponering av kyllingembryo induserte endringer i lillehjernens morfologi og påvirket gen- og proteinuttrykksprofiler knyttet til nevroutviklingsprosesser. Resultatene viste endringer knyttet til neuronal celleproliferasjon og migrasjon, cellulære stressresponser inkludert utfoldet proteinrespons, lipidmetabolisme og myelinisering. Eksponering for POP-

blandingen økte proteinoksidasjonen, mens PFOS reduserte oksidasjonen. Våre studier peker på mulige mekanistiske forklaringer knyttet til sammenhenger mellom POP-eksponering og uønskede nevroutviklings- og kognitive utfall påvist i epidemiologiske studier. Samlet sett fant vi at eksponering med POPs er forbundet med morfologiske og molekylære endringer som kan interferere med nevroutvikling.

1 Introduction

1.1 Persistent organic pollutants (POPs)

Humans are continuously exposed to a large number of chemicals in our everyday lives from sources such as the environment, food, and consumer products. Some of these chemicals belong to the group of POPs. Due to their adverse effects on human health and the environment these chemical are of global concern (EPA, 2021). POPs are organic carbon-based chemicals that are highly resistant to environmental degradation, and bioaccumulate and biomagnify in living organisms (Secretariat of the Stockholm Convention, 2019c). While POPs are mainly synthetic (man-made) organic chemicals, some are also natural products such as polybrominated diphenyl ethers (PBDEs) and their hydroxylated derivatives, which may be naturally biosynthesized by marine bacteria (Agarwal et al., 2014). POPs are semi-volatile, enabling them to travel long distances in the atmosphere. This results in widespread distribution across the earth, including regions where they have never been used (WHO, 2010). Thus, they are ubiquitous in the environment and human exposure is inevitable.

1.1.1 The Stockholm convention

The significance of researching and regulating POPs is exemplified in the Stockholm Convention, an international treaty to protect human health and the environment from POPs by eliminating and reducing the worldwide production, use and emission of POPs (Secretariat of the Stockholm Convention, 2019b). It was adopted in 2001 and entered into force in 2004 initially covering 12 POPs (the “dirty dozen”), causing adverse effects on humans and the ecosystem. The Convention is managed by the United Nations Environment Program. Currently the Stockholm Convention is ratified by 184 countries, and the parties have committed to implement national regulations to either eliminate (Annex A), restrict (Annex B) or reduce the unintentional release (Annex C) of chemicals listed in Table 1. As of now there are 30 POPs listed in the Stockholm Convention Table 1 (Secretariat of the Stockholm Convention, 2019a). They are placed in 3 categories: pesticides, industrial chemicals, and unintended by-products. These chemicals are halogenated and comprise three classes of compounds i.e. chlorinated, brominated, and fluorinated.

Table 1: Lists of POPs included or under consideration in the Annexes of the Stockholm Convention

Initial 12 POPs ("The Dirty dozen")	*POPs included till 2019*	*Under consideration*
Aldrin[1]	α-HCH[1,3]	Dechlorane Plus[2]
Chlordane[1]	β-HCH[1,3]	Methoxychlor[1]
DDT[1]	Chlordecone[1]	PFHxS, its salts and PFHxS-related compounds [2]
Dieldrin[1]	Dicofol[1]	
Endrin[1]	DecaBDEs[2]	
Heptachlor[1]	Endosulfan[1]	
HCB[1,2,3]	HBB[2]	
Mirex[1]	HBCD[2]	
Toxaphene[1]	Hexa- and heptaBDEs[2]	
PCBs[2,3]	HCBD[3]	
PCDDs[3]	Lindane[1]	
PCDFs[3]	PeCB[1,2,3]	
	PCP[1,2]	
	PCN[2]	
	Tetra- and pentaBDEs[2]	
	SCCPs[2]	
	PFOS, its salts and PFOS-F[1,2]	
	PFOA, its salts and PFOA-related compounds[2]	

[1]Pesticides; [2]Industrial chemicals; [3]By-products. See abbreviations for full chemical names

1.1.2 Categorisation and uses

PCBs are synthetic chlorinated aromatic hydrocarbons and are composed of a biphenyl molecule with 2–10 chlorine atoms attached, with a total of 209 possible congeners (Figure 1). Based on their stereochemical differences associated with chlorine binding positions onto the biphenyl molecule, PCBs are divided into coplanar and non-coplanar. Non-*ortho* or mono-*ortho* substituted PCBs are commonly referred to as planar or coplanar congeners, while other congeners are unable to conform to a planar configuration and are referred as non-planar or non-coplanar (Perkins et al., 2016). Non-ortho PCBs are "dioxin-like" that bind the aryl hydrocarbon receptor (AhR) and have a greater biological toxicity than the non-coplanar PCBs (Bruner-Tran and Osteen, 2010). PCBs have been used as dielectric and heat transfer fluids, coolants, lubricants, flame-retardants, and plasticizers due to their high thermal conductivity and chemical inertness. These compounds were produced beginning in 1930 until their production was banned in the USA in 1979 by the United States Congress and later under the Stockholm Convention in 2001 (Perkins et al., 2016). The Convention prohibits any new production and use of PCBs. The parties to the Convention are obliged to

eliminate the use of PCBs in existing equipment by 2025 and ensure environmentally sound waste management of them by 2028 (Secretariat of the Stockholm Convention, 2019).

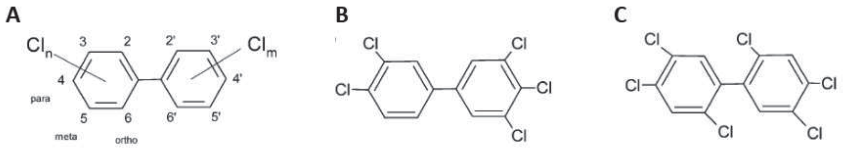

Figure 1. Chemical structures of selected PCBs. A) general structure of PCB; B) structure of PCB 126, a coplanar, non-ortho substituted PCB; and C) structure of PCB 153, a non-coplanar, di-ortho substituted PCB. Figure adapted from Perkins et al. (2016), with permission from publisher Springer Nature.

Organochlorine pesticides (OCPs) belong to another group of chlorinated compounds that have been applied to eradicate pests and vectors of diseases in agriculture, homes, and public health sector. Some examples of OCPs are dichlorodiphenyltrichloroethane (DDT) and its most dominant metabolite dichlorodiphenyldichloroethylene (DDE), dieldrin, chlordane, hexachlorocyclohexane (HCH) and hexachlorobenzene (HCB). Despite being banned in many developed countries, OCPs are still used in developing countries. This might be related to low cost and effectiveness of controlling different kinds of pests (Taiwo, 2019).

Brominated flame retardants (BFRs) have been used to a wide variety of commercial and industrial products for furnishings, textiles, paints, polymers, and electronic equipment to decrease the spread of fire. PBDEs and hexabromocyclododecanes (HBCDs) were the most widely used BFRs. PBDEs consist of 209 congeners and were produced in three major technical mixtures, characterized by different bromination degree (penta-BDE, octa-BDE, and deca-BDE). The EU has banned the use of penta and octa-BDE since 2004, HBCDs in 2013, and deca-BDE in 2017 (Tavoloni et al., 2021).

Per- and polyfluoroalkyl substances (PFAS) belong to a large class of synthetic chemicals that contain an alkyl chain with at least one fully fluorinated carbon atom (Figure 2). The carbon–fluorine bond shared by all members of this class is extremely strong and stable. This makes perfluoroalkyl acids (PFAAs), a subgroup of PFAS so extremely persistent in the environment that they are often referred to as “forever chemicals” (Bălan et al., 2021). Because of their hydrophobic and oleophobic properties they have been widely used in consumer products such as disposable food packaging, cookware, outdoor gear, furniture, and carpets. They are also one of the main components of aqueous film forming

foams and used frequently at airports and military bases for firefighting and training activities (Sunderland et al., 2019). Among PFAS, perfluorooctanoic acid (PFOA) and perfluorooctane sulfonic acid (PFOS) are the most studied chemicals (EPA, 2021).

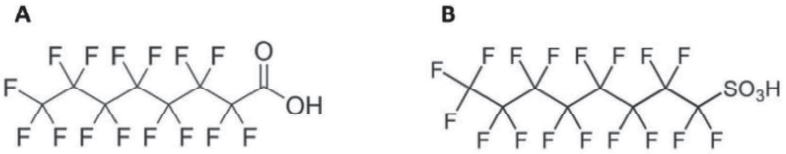

Figure 2. Chemical structures of selected PFAS, A) PFOA and B) PFOS

1.1.3 Human exposure to POPs

Humans are exposed to POPs mainly through ingestion, although exposure can also occur through inhalation and dermal absorption (WHO, 2010). POPs can be transferred through the placenta and breast milk to the developing offspring (EPA, 2020).

POPs can be detected in human blood (Göckener et al., 2020). The body burden of POPs is higher in occupational workers (Fu et al., 2016), in the Inuit population (Laird et al., 2013), and in children living in a sprayed area of insecticides (Verner et al., 2018). Once they enter the human body, chlorinated and brominated POPs are predominantly distributed in lipid rich tissues such as adipose tissue and blood lipids, while perfluorinated compounds are associated with proteins, and are found in the highest concentrations in liver, kidney, and blood (Karrman et al., 2006, Lau, 2015). All three classes of compounds have been detected in the human brain (Dewailly et al., 1999, Maestri et al., 2006, Mitchell et al., 2012, Pérez et al., 2013). POPs are present in human breast milk (Aerts et al., 2019, Ryan and Rawn, 2014, Zhang et al., 2017, Zheng et al., 2021), are found to cross the placenta (Fisher et al., 2016, Vizcaino et al., 2014), and are detected in the brain of human fetuses (Mamsen et al., 2019). This leads to exposure to these chemicals during the sensitive perinatal period of life.

1.1.4 Experimental mixture studies

Despite the fact that cocktail or mixture effects have been observed in various experimental models, chemical risk is traditionally assessed on a one-by-one basis of single chemicals (Svingen and Vinggaard, 2016). This approach overlooks the potential for chemicals to 'join forces' to cause an effect, even at very low doses. A recent review based on experimental mixture studies published between 2007 and 2017 found that that approximately two thirds of studies did not include more than 2 components (Martin et al., 2021).

Analysis of human blood, breast milk, and tissue samples have identified multiple chemicals present in an organism simultaneously (Aerts et al., 2019, Nøst et al., 2017, Pérez et al., 2013, Svarcova et al., 2019, Lenters et al., 2019). Studies *in vitro* and *in vivo* with mixtures showed that low-level exposure to chemicals that are not toxic on an individual basis can together lead to a biological or toxic effect if present in a mixture (DENAMIC, 2012). When chemicals co-occur, they may act additively, displaying non-interaction, which is currently believed to be the most common scenario, especially at low concentrations (Kortenkamp et al., 2009, Martin et al., 2021). Although less commonly observed, they may also display interactive synergistic (more than additive) or antagonistic (less than additive) effects. It is possible to predict the mixture effect by concentration addition for example by summing up the contribution of all individual compounds based on the toxicity and the concentration of individual components in the mixture. As it is not feasible to test every chemical mixture, this is of importance for risk assessment, because we could estimate the mixture effect based on knowledge of hazard and exposure data of single chemicals (Vinggaard et al., 2021). Yet another approach may be to study the effect of natural (extracted) mixtures of POPs at environmental relevant concentrations (Lyche et al., 2010, Montaño et al., 2011, Nourizadeh-Lillabadi et al., 2009, Zimmer et al., 2011). Alternatively, exposure scenarios could use a mixture with its composition based on biomonitoring data. In the present thesis we used a realistic mixture of contaminants, reflecting the relative levels of POPs to which the general human population are exposed (Berntsen et al., 2017a). However, a drawback with designed mixtures is that the predictions are limited to chemicals with known effects. Also, chemicals not included in the mixture but present in the tissue of question could contribute to an overall effect. A limitation with natural extracts is that the chemicals present in the extract but not measured could be major drivers of an adverse effect.

There are various other approaches for assessment of associations between chemical exposures and disease outcomes, as illustrated in Figure 3.

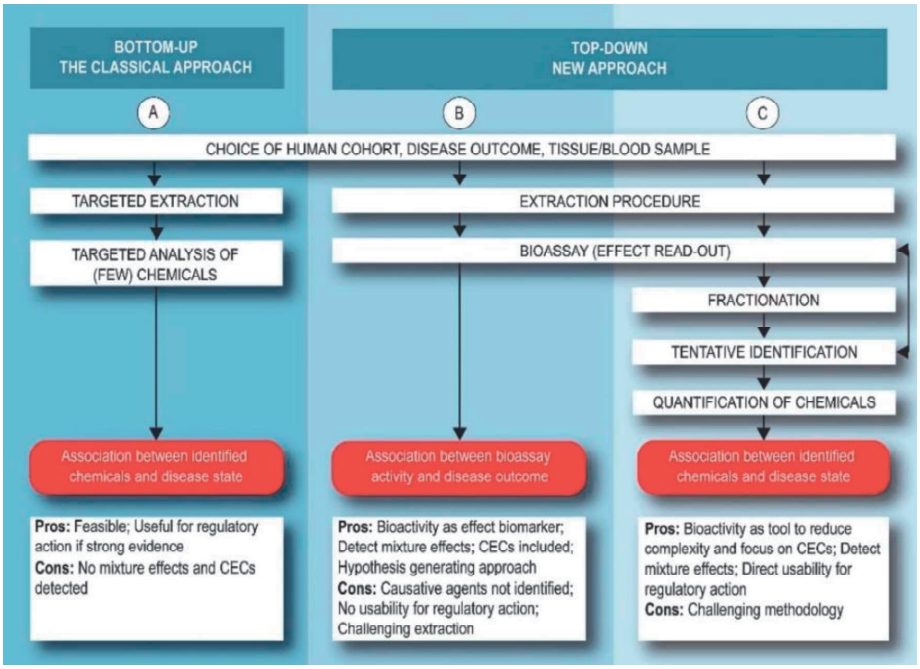

Figure 3. Illustration of various approaches for the assessment of chemical exposures to disease outcomes. (A) Bottom-up approach in which targeted chemical analysis performed on human tissues is associated with a disease outcome. (B) Top-Down approach where a specific *in vitro* activity caused by a group of chemicals defined by the extraction procedure is associated with a disease outcome without identifying the specific responsible chemicals. (C) Top-Down approach based on effect-directed analysis (EDA), which is used with a combination of *in vitro* tests, detailed fractionation procedures and chemical analytical methods to identify the responsible chemicals. CECs = Chemicals of Emerging Concern. Figure adapted from Vinggaard et al. (2021) with permission from publisher Elsevier.

1.1.5 Effects of POPs on neurodevelopment

Human exposure to POPs has been linked to reproductive, developmental, behavioural, neurologic, endocrine, and immunologic adverse health effects (EPA, 2021, Secretariat of the Stockholm Convention, 2019c). Early life is a critical period for human development, which determines lifelong patterns of health and disease. Brain development is an extraordinarily complex phenomenon which is initiated in early gestational stages and continues for several years postnatally. Within this period, several cellular processes such as

neurogenesis, migration, neuronal differentiation, synaptogenesis, myelination, apoptosis, and synaptic plasticity take place within a controlled time frame in which each neurodevelopmental stage follows a well-determined sequence. Environmental insult during these vulnerable windows could adversely impact these processes and cause irreversible damage which may become evident in new-borns or much later in life (Grova et al., 2019, Rice and Barone, 2000). Despite the presence of two important biological barriers the placenta and the blood-brain barrier (BBB), the developing brain is poorly protected from chemical exposure during foetal and early postnatal life (Grova et al., 2019). Mounting evidence from epidemiological studies suggests that early life exposure to certain environmental pollutants adversely affects neurodevelopment. POPs, including PBDEs, PCBs, PFAS, and organochlorine pesticides DDT and its metabolite DDE, are recognized for their potential role as (developmental) neurotoxicants (Goodman et al., 2011, Lam et al., 2017, Polańska et al., 2013, Vuong et al., 2020a, Vuong et al., 2018). There has been increasing awareness concerning the role of different toxicants in neurodevelopmental disorders. For example, in a multi-pollutant analysis of 27 POPs in a Norwegian birth cohort study, early-life exposure to β-hexachlorocyclohexane (HCH) and PFOS was associated with increased risk of ADHD (Lenters et al., 2019). In addition, prenatal exposure to POPs including PBDEs, β-HCH, PFOS, PFOA has been associated with poorer attention and executive function, decreased motor development, reduced IQ, and effects on neuro-behavioural development and hyperactive behaviour, in infants or in school age children (Sagiv et al., 2015, Wang et al., 2021, Lam et al., 2017, Vuong et al., 2016, Hoyer et al., 2015). Further, several POPs have been shown to interfere with the outgrowth of axonal and dendritic processes (collectively called neurites) in different neuronal systems (Addae et al., 2013, Angus and Contreras, 1995, Christen et al., 2017, Liao et al., 2008, Liao et al., 2009, Shinomiya and Shinomiya, 2003, Tofighi et al., 2011, Wan Ibrahim et al., 2013). Neurite outgrowth is essential for neuronal connectivity or for wiring the nervous system during development and regeneration (Miller and Suter, 2018).

In real life humans are exposed not to a single chemical but to several chemicals simultaneously. Thus, it is necessary to investigate the adverse effects of relevant POP mixtures, in addition to the study of the toxicity caused by single POPs. Although, some studies reported neurotoxicological effects of commercial mixtures of chlorinated or brominated compounds in cultured rat CGNs (Mariussen et al., 2002, Reistad et al., 2006), mixtures reflecting the human exposure scenario are especially relevant. For example, a mixture reflecting the blood contaminant profile of Canadian arctic populations was used by

Padhi et al. (2008) to study the neurodevelopmental effects in perinatally exposed rat. Adverse effects of human based mixture of POPs, containing all three groups of chemicals on brain development and function have been reported in several studies *in vivo* as well as in *vitro* models (Berntsen et al., 2017b, Berntsen et al., 2018, Berntsen et al., 2020, Davidsen et al., 2021, Khezri et al., 2017, Myhre et al., 2021).

1.2 Experimental models

In the present thesis (**in paper I, III and IV**) we used chicken embryo focussing on cerebellum, and PC12 rat pheochromocytoma cells (**paper II**), as experimental models to study the neurodevelopmental effects of POPs. The developing chicken embryo has been used as a model to study cerebellar development after exposure to POPs (Berntsen et al., 2020), various pharmaceuticals (Aden et al., 2008, Austdal et al., 2016) and environmental toxicants (Mathisen et al., 2013). Similarly, PC12 has widely been used to investigate the adverse neurodevelopmental effects of toxicants including POPs (Radio et al., 2008, Christen et al., 2017, Slotkin et al., 2008). Details on chicken CGNs are discussed in section 4.3.2, and on PC12 in section 4.3.3.

1.2.1 Overview of cerebellar development

The cerebellum is well known for its roles in motor functions, including coordination, posture, balance, and learning. However, recent studies found strong support for cerebellar contributions to non-motor functions such as cognition, emotion, and language (Lackey et al., 2018). Further, structural and functional cerebellar abnormalities have been associated with a number of neurological disorders such as ataxia, tremor, dystonia, autism spectrum disorder, schizophrenia, and attention-deficit/hyperactivity disorder (Lackey et al., 2018). Comparative anatomy studies have revealed that the cerebellum is well conserved between species (Sultan and Glickstein, 2007). In adult humans, the cerebellum represents 10% of the total brain weight (Azevedo et al., 2009).

The cerebellum is located inferior to the cerebrum and posterior to the brainstem, comprising the dorsal wall of the fourth ventricle. Anatomically, the cerebellum is tightly organized as a dense trilaminar structure that consist of an internal granule cell layer (IGL), Purkinje cell layer (PL) and molecular layer (ML). These layers contain the neurons that form the canonical microcircuit of the cerebellar cortex, as represented in Figure 4. ML, the most

superficial layer consists of stellate cells and basket cells, and Golgi and Purkinje cell dendrites. The PL is the middle layer of the cerebellar cortex and contains the cell bodies of the large Purkinje cells (PCs), which are the main cell type of the cerebellum and the sole output of the cerebellar cortex. The PL also contains the cell bodies of candelabrum cells and a specialized type of astrocyte called the Bergmann glia. PCs receive input in the ML, forming synapses with granule cells, climbing fibers (CFs), and interneurons. The GL, which in amniotes is the innermost layer of the cerebellar cortex, consists of granule cells and Golgi cells (Iulianella et al., 2019, Lackey et al., 2018). An external granular layer (EGL) is a transient layer during development. After birth the EGL progressively reduces in thickness and disappears, after a time interval that varies according to the species (Lavezzi et al., 2006). Granule cells are the most numerous neurons in the cerebellum. The whole brain of adult human contains about 90 billion neurons and from them cerebellar granule cells represent 80% of all neurons (Azevedo et al., 2009).

CGNs from rodent or chicken can be grown in culture as a relatively pure/ homogeneous population of neurons (Giordano and Costa, 2011, Krämer and Minichiello, 2010, Jacobs et al., 2006).

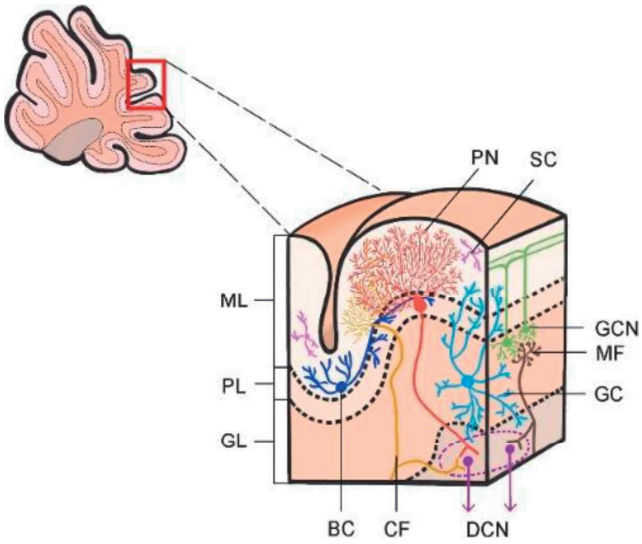

Figure 4. Schematic overview of the microarchitecture of the cerebellar cortex circuitry with three different layers, i.e. molecular layer (ML), Purkinje cell layer (PL), and granule cell layer (GL). The main excitatory neuronal connections include the mossy fibers (MFs), climbing fibers (CFs), granule cell neurons (GCN), and parallel fibers (PFs, in green). The principal inhibitory connections include Purkinje neurons (PN), and a diversity of interneuron types including stellate cells (SCs), basket cells (BCs), and Golgi cell (GC). The local circuit excitatory input pathways include CF and MF. MF synapse onto GCN, giving rise to excitatory PF. Both PF and CF synapse directly onto PN, that brings signal from the cerebellar cortex through synapses on the deep cerebellar nuclei (DCN). Figure adapted from Iulianella et al. (2019) with permission from publisher John Wiley and Sons.

1.2.2 The chicken embryo as an animal model

The chicken embryo has a long and distinguished history in developmental neurobiology with some major discoveries such as origin of neural crest and NGF in this model system (Aloe, 2004, Davey and Tickle, 2007). This model has several advantageous features: e.g., it is inexpensive, has a short incubation period of 21 days, and is nutritionally self-sufficient and does not require extra animal facilities (Bjornstad et al., 2015). The embryo is accessible, and it is easy to manipulate the individual offspring during development. In accordance with the 3R principles, the mother is excluded from the experiments and the number of fertilized eggs or live embryos are easy to control.

The basic histological cerebellar structure is similar in all mammals and birds (Sultan and Glickstein, 2007). Both have the foliated cerebellum, however the folial pattern of mammals is more complicated (Voogd and Glickstein, 1998). The most pronounced

difference between birds and mammals is that bird cerebellum lacks a distinct vermis, this medial expansion of cerebellar hemispheres is only present in humans and higher primates (Sultan and Glickstein, 2007).

The migration of the postmitotic granule neurons form EGL through ML to the IGL, where they differentiate into mature neurons, is a key feature of cerebellar development (Bjornstad et al., 2015). We performed the histological analysis of these layers in chicken embryo following POP exposure, detailed in **paper IV**. The importance of these layers in brain development associated with NMDA-Rs has been discussed in **paper I**. To a large extent, this migration process occurs before hatching in chicken and postnatally in some mammals, including humans (Bjornstad et al., 2015). As it can be seen in Table 2, chicken cerebellar development from E12 - E21 corresponds roughly to the last gestational trimester and first postnatal year in human. Details on the chicken embryo model are also discussed in section 4.3.1.

Table 2. Comparison of chicken and human cerebellar development focussing on different cerebellar layers.

	Chicken Embryonic day (E)	**Human** (Closest corresponding times)
External granule layer (EGL)		
Peak thickness ‘	~ E15	~ 34th gestational week
Layer thickness appears relatively even	~ E12 - 17	~ 25th gestational week - 1st postnatal month
Layer thickness reduced from	~ E17	~ 3rd postnatal month
Molecular layer (ML)		
Layer thickness appears relatively even	~ E12 - E16	-
Layer thick increases from (growth phase)	~ E16 - E20	~ 24th gestational week - 1st postnatal year
Internal granule layer (IGL)		
Layer thick increases from (growth phase)	~ E16 - E21	~ mid-gestation - 1st postnatal year

Notes to **Table 2**: The information gathered here are from (Abrahám et al., 2001, Austdal et al., 2016, Bjornstad et al., 2015, Volpe, 2009) and from a PhD thesis from our group (Austdal, 2018).

1.3 Mechanisms of neurodevelopmental toxicity

Neurodevelopmental toxicity may be caused by direct cytotoxicity (discussed below) or by cellular dysfunction. Effects on neurite outgrowth are discussed in 1.1.5 and in **paper II**.

1.3.1 Oxidative stress

Oxidative stress is an imbalance between production of reactive oxygen species (ROS) and antioxidant defence in a biological system. Excessive ROS can damage all major biological macromolecules, including nucleic acids, lipids and proteins, leading to an overall progressive decline in physiological function (Sanders and Timothy Greenamyre, 2013, Singh et al., 2019). The developing brain is particularly vulnerable to oxidative damage, reasons include its high concentrations of unsaturated fatty acids, high rate of oxygen consumption, low concentrations of antioxidants, high content of metals catalyzing free radical formation, and large proportion of sensitive immature cells (Ikonomidou and Kaindl, 2011). Oxidative stress has been proposed as one of the major factors linked with neuronal dysfunction and neurodegenerative diseases (Singh et al., 2019). The use of proteins as markers of oxidative stress has distinct advantages because proteins are the key molecules in maintaining cellular structure and functions. Thus, alterations in protein structure due to oxidative modification may be reflected at the functional level since such changes are relatively stable (Chakravarti and Chakravarti, 2007). Protein oxidation is one of a number of brain biomarkers of oxidative stress. Increased levels are found in several neurodegenerative disorders including Alzheimer's disease, Huntington's disease, Parkinson's disease and prion disorders (Butterfield and Kanski, 2001).

1.3.2 Glutathione as an antioxidant

The brain represents about 2% of the bodyweight but utilizes 20% of the O_2 used by the whole body. Due to the high O_2 consumption and poor antioxidant status, the brain is more susceptible to oxidative stress. To maintain redox homeostasis, the cells possess an antioxidant defence system as a counteractive mechanism. This includes various antioxidants such as superoxide dismutase (SOD), catalase, vitamin C, vitamin E, and glutathione (GSH) (Dwivedi et al., 2020). Glutathione (GSH, γ-glutamyl-cysteinyl-glycine) is an intracellular tripeptide comprising of glutamic acid (Glu), cysteine (Cys) and glycine (Gly) amino acids found in all mammalian cells. GSH is synthesized in two steps where Glu and Cys combine to form γ-Glu-Cys in the presence of the enzyme glutamate cysteine ligase (GCL), this further combines with Gly in the presence of GS (Glutathione synthetase) to synthesize GSH. GCL is a heterodimer which is composed of two subunits: catalytically active heavy subunit GCLC (73 kDa), and light modifier subunit GCLM (30 kDa). GCLC

functions as a substrate-binding unit whereas the GCLM modulates the binding affinity of GCLC by altering the K_m value. The presence of the sulfhydryl (SH) group of the Cys moiety, renders GSH a potent antioxidant property and can interact with reactive oxygen species /reactive nitrogen species (ROS/RNS) enzymatically and/or non-enzymatically. The antioxidant function of GSH involves catalytic oxidation of thiol group of its Cys moiety in the presence of glutathione peroxidase to produce GSSG (two molecules of disulfide-bonded GSH) which in turn is reduced to GSH in the presence of glutathione reductase. The reduced (GSH) form and oxidized disulfide form (GSSG) are interconvertible, with reduced GSH present as the predominant form. Other important functions of GSH include detoxification of xenobiotics, regulation of cellular events including gene expression, DNA and protein synthesis, apoptosis, signal transduction, protein glutathionylation, cytokine production and immune response. Dysregulation of GSH homeostasis due to increased oxidative stress has also been reported in various neurological disorders (Dwivedi et al., 2020).

1.3.3 Glutamate, excitotoxicity and the NMDA-R

Glutamate is a major excitatory neurotransmitter in the mammalian brain. It plays a major role in cognition, learning, memory, and many more ongoing and fundamental brain processes. It also contributes markedly to the development of the CNS by contributing to the formation and elimination of nerve contacts-the synapses, as well as to cell migration, differentiation, and regulation of cell death (Levite, 2017). However, excessive extracellular glutamate concentration can lead to excitotoxicity, leading to neuronal death (Choi, 1985, Choi, 1988) and loss of brain function. Glutamate-mediated neurotoxicity occurs through two different pathways: the glutamate receptor-dependent and -independent pathways, as illustrated in Figure 5. Excitotoxicity is involved in many neurodegenerative diseases such as Huntington's disease, Alzheimer's disease, lateral amyotrophic sclerosis, Parkinson's disease, and stroke or traumatic brain injury (Kritis et al., 2015).

Both the beneficial as well as the detrimental effects of glutamate are mediated by a large family of glutamate receptors (GluRs): the ionotropic glutamate receptors (iGluRs) and the metabotropic glutamate receptors (mGluRs). There are three types of iGluRs, NMDA (N-methyl-D-aspartate), AMPA (α-amino-3-hydroxy-5-methylisoxazole-4-propionic acid) and Kainate receptors. While all iGluR is in the first line of the excitotoxic response, NMDA-R has been suggested as the main culprit in glutamate-induced

neurotoxicity, due to their permeability to calcium ions (Armada-Moreira et al., 2020). NMDA-R is important for brain development such as neural stem cell proliferation and differentiation (Chakraborty et al., 2017); neuronal differentiation, establishment or elimination of synapses and migration of neurons (Komuro and Rakic, 1993). For activation this receptor exhibits a voltage-dependent magnesium-blockade, high permeability to calcium, and requires simultaneous binding of glutamate and a co-agonist, such as glycine and D-serine (Armada-Moreira et al., 2020). NMDARs function as heterotetrameric assemblies that typically associate GluN1 subunits with GluN2 subunits or a mixture of GluN2 and GluN3 subunits. The composition and localization of NMDA-R subunits are dynamic and vary across the CNS, especially during development (Paoletti et al., 2013). These changes are required for and determine accurate postnatal cerebellar development and function. In rat during early cerebellar development, NR2B (also known as GluN2B) is expressed at early developmental stages, during the period of neuronal cells migration from the external germinal layer to the inner granular layer before synapse formation. During the second postnatal week, NR2B subunit is gradually exchanged for NR2A (also known as GluN2A) and NR2C (also known as GluN2C) in mature post migratory cells (Llansola et al., 2005).

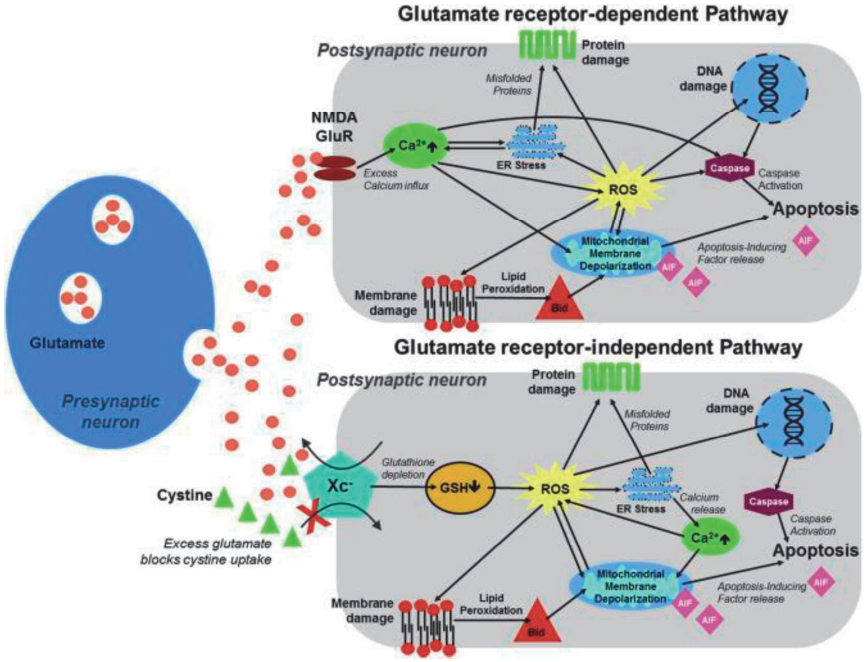

Figure 5. Overview of mechanisms involved in glutamate toxicity in neuronal cells. Glutamate-mediated neurotoxicity occurs through two different pathways: the glutamate receptor-dependent and -independent. The "classical" receptor-mediated pathway, which is known as excitotoxicity, occurs through excessive activation of the glutamate receptors, especially through the NMDA subtype. Overstimulation of these receptors leads to an excess of Ca^{2+} influx into the neurons, triggering a cascade of signalling events, subsequently resulting in cell death. These downstream effects include the activation of cellular-structure degrading agents (e.g. nucleases, proteases, and lipases), cell death signalling molecules (e.g. caspases), endoplasmic reticulum (ER) stress, mitochondrial depolarization and the production of ROS. The other glutamate toxicity pathway is independent of the glutamate receptor and involves oxidative glutamate toxicity. In this pathway, the excess extracellular glutamate blocks the cystine-glutamate antiporter (system Xc^{-}), which prevents the cellular uptake of cystine. Cystine is the rate-limiting molecule in the production of GSH, this results in a shortage of GSH and thereby an increase in ROS and cellular oxidative stress. Excessive ROS could impair mitochondria's structure and function that facilitates programmed cell death, where mitochondrial apoptosis-inducing factor (AIF) signalling, rather than caspase activation, is supposed to be the underlying mechanism. Figure adapted from Prasansuklab et al. (2020).

2 Aim of the thesis

POPs are ubiquitous in the environment. Exposures in humans to pollutants are suspected to cause adverse health outcomes including neurodevelopmental effects. Most studies examining effects of POPs use single compounds, and often at high concentrations. However, in real life we are exposed simultaneously to complex and variable combinations of chemical compounds, thus mixture studies at environmentally relevant concentrations are of great importance. In the present study we used a POP mixture with concentrations based on those measured in human blood in Scandinavia (Berntsen et al., 2017a). We also evaluated exposure to a prominent compound in the mixture, PFOS alone. In this thesis we hypothesise that POP exposure during embryonic growth adversely affect neurodevelopmental processes. To address this hypothesis, we investigated specific processes related to neurodevelopment and neurotoxicity as well as toxicokinetic properties of compounds used for exposure in different experimental models.

- We investigated if POP mixture or PFOS could induce or aggravate glutamate excitotoxicity in cultured chicken CGNs via NMDA-R and whether GGNs display a developmental increase in their sensitivity at different stages of maturation. (**Paper I**)
- We examined if a POP mixture or PFOS could affect the outgrowth of axons and dendrites (collectively known as neurites) in nerve growth factor (NGF)-induced PC12 cells. (**Paper II**)
- We predicted that peripherally administrated POP mixture would distribute to the developing chicken brain in a concentration relevant for human exposure and that the compounds reaching the brain depend on the chemical property of the individual compound. (**Paper III**)
- Based on paper III we explored if a POP mixture or PFOS alone would induce alterations at the levels of brain morphology, RNA-seq transcriptomics and proteomics, and possibly affect molecular pathways fundamental for brain development and function. (**Paper IV**)

3 Results: Summary of papers

3.1 Paper I

A human relevant mixture of persistent organic pollutants (POPs) and perfluorooctane sulfonic acid (PFOS) differentially affect glutamate induced excitotoxic responses in chicken cerebellum granule neurons (CGNs) in vitro

In this publication, we exposed primary cultures of cerebellar granule neurons (CGNs) derived from chicken embryos to explore the effects on developmental neurotoxicity by using a complex defined mixture of persistent organic pollutants (POPs). The chemical composition and concentrations of a POP mixture were based on blood levels in the Scandinavian population. We also evaluated exposure to a prominent compound in the mixture, perfluorooctane sulfonic acid (PFOS) alone. CGNs at different stages of maturation, between day in vitro (DIV) 1, 3, and 5 were exposed to the POP mixture, or PFOS alone. Their combination with glutamate, an excitatory endogenous neurotransmitter important in neurodevelopment, also known to cause excitotoxicity was evaluated. Outcomes with the mixture at 500x blood levels were compared to PFOS at its corresponding concentration of 20 μM. The POP mixture reduced cell viability at earlier stages of maturation, compared to PFOS alone, as measured by tetrazolium salt (MTT) conversion. Glutamate-induced excitotoxicity was enhanced above the level of that induced by glutamate alone, especially in mature CGNs at DIV5. Glutathione (GSH) concentrations seemed to set the level of sensitivity for the toxic insults from exposures to the pollutants. The role of N-methyl-D-aspartate receptor (NMDA-R) mediated calcium influx in pollutant exposures was investigated using the non-competitive and competitive receptor antagonists MK-801 and CGP 39551. Our observations indicate a calcium-independent, but still NMDA-R dependent mechanism in the absence of glutamate, and a calcium- and NMDA-R dependent one in the presence of glutamate. The outcomes for the POP mixture cannot be explained by PFOS alone, indicating that other chemicals in the mixture contribute its overall effect.

3.2 Paper II

A human relevant mixture of persistent organic pollutants (POPs) and perfluorooctane sulfonic acid (PFOS) enhance nerve growth factor (NGF)-induced neurite outgrowth in PC12 cells

Establishing neuronal connectivity, the physical network of axonal and dendritic extensions of neurons, is a key process during brain development. These extensions are collectively referred to as neurite outgrowth. Disruption of neurite outgrowth is a marker for neurotoxicity. Persistent organic pollutants (POPs) are potential developmental neurotoxicants. We investigated their effect on neurite outgrowth in PC12 rat pheochromocytoma cells, in absence or presence of nerve growth factor (NGF), an inducer of neuronal differentiation. Cells were exposed for 72 h to a defined mixture of POPs with chemical composition and concentrations based on blood levels in the Scandinavian population. Perfluorooctanesulfonic acid (PFOS) alone, the most abundant compound in the POP mixture, was also evaluated. We found that only higher concentrations of POP mixture reduced cell viability, as measured by tetrazolium salt (MTT) conversion. High-content analysis showed a decrease in cell number, but no changes for nuclear and mitochondrial cellular health parameters. Robust glutathione levels were observed in NGF-differentiated cells. Live imaging, using the IncuCyte ZOOM platform indicated ongoing cell proliferation over time, but slower in presence of NGF. The pollutants did not inhibit neuritogenesis, but rather increased NGF-induced neurite length. PFOS induced neurite outgrowth to about 50 % of the level seen with the POP mixture. Neither the POP mixture nor PFOS affected neurite length in the absence of NGF. Our observations indicate that realistic complex mixtures of environmental pollutants can affect neuronal connectivity via NGF-induced neurite outgrowth.

3.3 Paper III

Peripherally Administered Persistent Organic Pollutants Distribute to the Brain of Developing Chicken Embryo in Concentrations Relevant for Human Exposure

In this paper, to explore the distribution of POPs to the fetal brain, we exposed chicken embryos to a POP mixture, containing 29 different compounds with concentrations based on blood levels measured in the Scandinavian human population. The mixture was injected into the allantois at embryonic day 13 (E13), aiming at a theoretical concentration of 10 times human blood levels. POPs concentrations in the brain were measured at 0.5, 1, 2, 4, 6, 24, 48, and 72 h after administration. We detected twenty-seven of the individual compounds during at least one of the time-points analysed. Generally, the concentrations of most of the measured compounds were within the order of magnitude of those reported in human brain samples. Differences in the speed of distribution to the brain were observed for the per- and polyfluoroalkyl substances (PFASs) which have protein binding potential, versus the lipophilic polychlorinated biphenyls (PCBs), organochlorine pesticides (OCPs) and brominated flame retardants (BFRs). Based on human pharmacokinetic modelling, protein binding PFASs were best described by a one compartment model. PFASs displayed relatively slow elimination (Kel) and persisted at high levels in the brain. Lipophilic OCPs and PCBs could be fitted to a 2-compartment model. These showed high levels in the brain relative to the dose administrated as calculated by area under the curve (AUC)/Dose. Altogether our study showed that chicken is a relevant model to explore the distribution of POPs in the developing brain at human relevant exposure.

3.4 Paper IV

Exposure to a Human Relevant Mixture of Persistent Organic Pollutants (POPs) or to Perfluorooctane Sulfonic Acid (PFOS) Alone Dysregulates the Developing Cerebellum of Chicken Embryo

In this paper, we explored whether a human-relevant POP mixture affects the development of the chicken embryo cerebellum. We used a defined mixture of 29 POPs, at human-relevant concentrations. We also evaluated exposure to a prominent compound in the mixture, perfluorooctane sulfonic acid (PFOS), alone. Embryos were exposed by injection directly into the allantois at embryonic day 13 (E13). Cerebella were isolated at E17 and subjected to morphological, RNA-seq and shot-gun proteomics analyses. There was up to 19% thinning of the molecular layer in both exposure scenarios. Exposure to the POP mixture significantly affected expression of 65 of 13,800 transcripts, and 43 of 2,568 proteins, when compared to solvent control. PFOS alone affected expression of 80 of 13,859 transcripts, and 69 of 2,555 proteins. Twenty-five genes and 15 proteins were common for both exposure groups. These point to alterations in molecular events linked to retinoid X receptor (RXR) signalling, neuronal cell proliferation and migration, cellular stress responses including unfolded protein response, lipid metabolism, and myelination. Exposure to the POP mixture increased methionine oxidation, whereas PFOS decreased oxidation. Several of the altered genes and proteins are involved in a wide variety of neurological disorders. We conclude that POP exposure can interfere with fundamental aspects of neurodevelopment, altering molecular pathways that are associated with adverse neurocognitive and behavioural outcomes.

4 Discussion of materials, methods and model systems

In this section we elaborate on the chosen materials/methods. We also compare our model systems with other mammalian models. Some methods are not discussed here but detailed in the corresponding papers.

4.1 Comparison of the exposure scenarios

In chicken, the cerebellum enters a growth spurt around E13 that last until around E17 (Austdal et al., 2016). Thus, exposures in **paper III** were scheduled so that exposure to chemicals coincide with peak cerebellar development. In **paper IV** we followed the same exposure scenario and extracted the whole brain or cerebellum at the endpoint E17. For the *in vitro* study in **paper I**, CGNs were isolated from unexposed cerebella at E17 and were exposed during maturation in culture for up to 5 days. In contrast to neurons from the central nervous system such as CGNs, PC12 cells lack functional expression of NMDA receptors (Edwards et al., 2007). This receptor has been shown to be involved in the excitotoxicity in cultured rat CGNs following exposure to POPs (Berntsen et al., 2018, Mariussen et al., 2002). Thus, in **paper II**, we used rat PC12 cell line to study the exposure effects independent of NMDA-receptor as a neural model. An overview of exposure scenarios is shown in Figure 6.

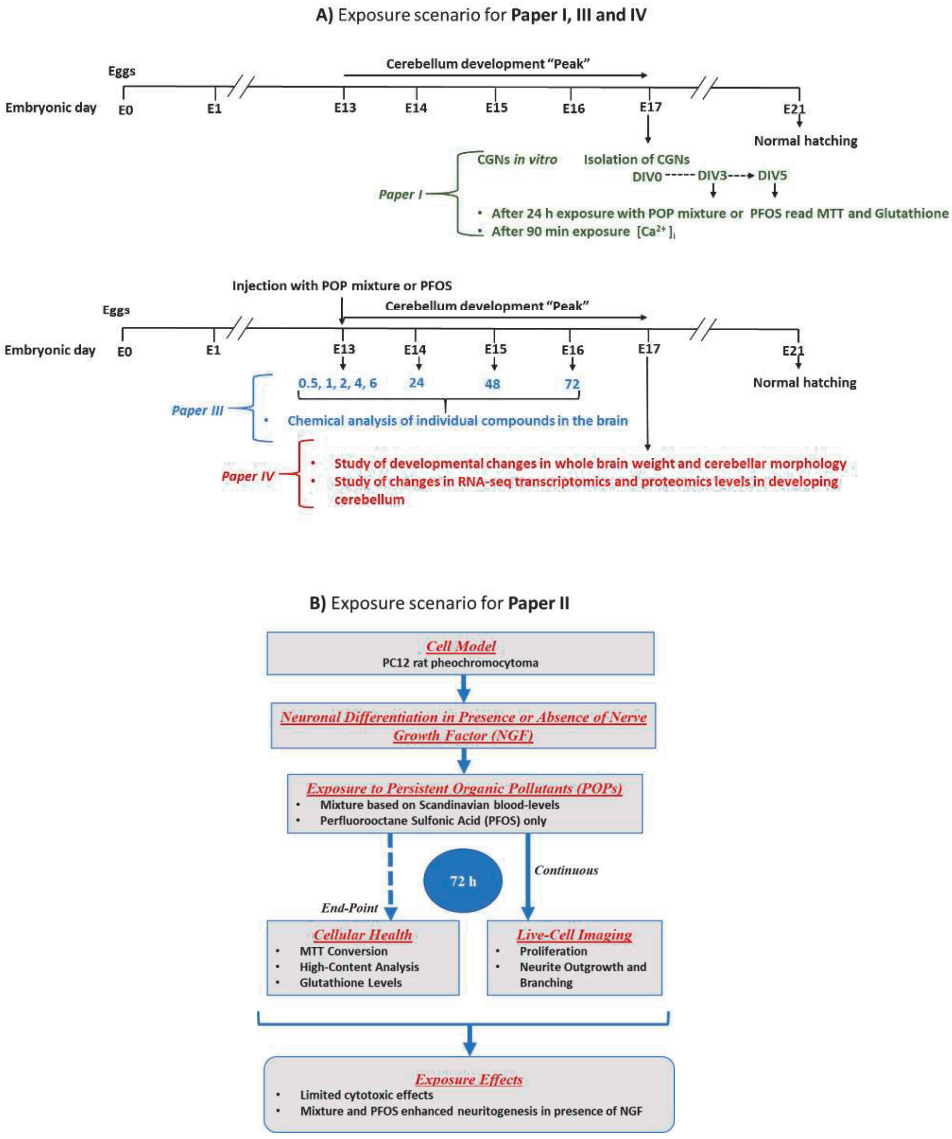

Figure 6. An overview of exposure scenarios used in paper I, III and IV (A) and II (B).

In paper I, chicken CGNs were cultured at E17 and then at different days *in vitro* (DIV) following exposure to POPs different toxicity assays were performed. In paper III and IV, chicken embryos were exposed by injection into the allantois at E13. After that whole brain or cerebellum was isolated at different embryonic days (E). We investigated different processes related to neurodevelopment and neurotoxicity as well as toxicokinetic properties of compounds used for exposure. In Paper II, we assessed the effects of POP exposures on cellular health and neurite dynamics in PC12 cells either in the absence or presence of NGF. Figure B is adapted from Yadav et al. (2021).

4.2 POP mixture and PFOS

The POP mixture used in the present thesis was designed and prepared at the Norwegian University of Life Sciences (NMBU), Oslo, Norway (Berntsen et al., 2017a). The mixture contained 29 different compounds (Table 3) including six perfluorinated, seven brominated compounds and sixteen chlorinated compounds. The compounds were selected from their respective compound groups based on prevalence in blood, breastmilk and/or food, and their relative concentrations were based on Scandinavian human blood levels. Some of the chlorinated compounds such as polychlorinated dibenzodioxins/polychlorinated dibenzofurans (PCDD/PCDF) as well as most dioxin-like PCB (with the exception of PCB 118) were excluded from the mixture because their relatively high toxicity at a lower concentration could have masked the effects of less potent POPs without clear mechanisms of action. Some other compounds such as toxaphenes and endosulfan were also excluded from the mixture due to few studies and limited information on relevant Scandinavian exposure levels. If the study population had been performed based on a non-Scandinavian setting, a different composition of POPs would have been needed. For example, one should consider regional differences in POP exposures such as the comparably high seafood intake in Scandinavia that could give increased body burden of certain POPs. One study reported that dietary exposure to brominated flame retardants correlated with blood levels in a selected group of Norwegians with a wide range of seafood consumption (Knutsen et al., 2008). It should be noted that we have not considered other routes of exposure, for example that BFR exposure through dust is/has been higher e.g. in the U.S. population (Varshavsky et al., 2020).

In the present thesis we used PFOS as a single compound. PFAAs were present in the Scandinavian food basket, and in comparison to the levels of the brominated and chlorinated compounds the concentration of PFAAs in blood in the Scandinavian population was high, likely due to their binding to serum proteins Therefore, the mixture contains relatively high levels of PFAAs. Amongst these, PFOS was the dominating congener present in the POP mixture (Berntsen et al., 2017a).

Table 3. The total *in vitro* mixture containing 29 different POPs based on human blood levels, detailed in ***(Berntsen et al., 2017a).***

Compound	*Average human blood levels [a] ng/g lipid*	*Average human blood levels [b] ng/ml*	*Total mixture stock nominal concentration [c] mg/ml*	*Total mixture stock Measured concentration [d] µM*
PCBs				
PCB 28	2.13	0.013	0.013	31.1
PCB 52	1.6	0.01	0.01	20.5
PCB 101	1.3	0.008	0.008	24.5
PCB 118	10.67	0.064	0.064	137.9
PCB 138	37	0.222	0.222	429.5
PCB 153	60.33	0.362	0.362	698.3
PCB 180	32.33	0.194	0.194	339
∑ PCBs	145.36	0.873	0.873	1680.8
OCP				
p,p'-DDE	83.67	0.502	0.502	1065.9
HCB	19.5	0.117	0.117	228.2
α-Chlordane	1.8	0.011	0.011	23.7
Oxychlordane	3.7	0.022	0.022	33
trans-Nonachlor	6.8	0.041	0.041	99.1
α-HCH	1	0.006	0.006	16.8
β-HCH	8.77	0.053	0.053	75.6
γ-HCH	1	0.006	0.006	16.8
Dieldrin	4	0.024	0.024	56.2
∑ OCPs	130.24	0.782	0.782	1615.3
∑ PCBs + OCPs	275.6	1.655	1.655	3296.1
BFRs				
PBDE 47	1.43	0.009	0.009	17.8
PBDE 99	0.59	0.004	0.004	7.5
PBDE 100	0.36	0.002	0.002	3.8
PBDE 153	1.64	0.01	0.001*	2.1
PBDE 154	0.29	0.002	0.002	3
PBDE 209	1.81	0.011	0.011	9.4
HBCD	4.1	0.025	0.025	54.5
∑ BFRs	10.22	0.063	0.053	98.1
PFAAs				
PFHxS	N/A	3.45	3.45	7809.2
PFOS	N/A	29.425	29.425	41522.1
PFOA	N/A	4.523	4.523	4209.4
PFNA	N/A	0.8	0.8	1092.5
PFDA	N/A	0.495	0.495	375.4
PFUnDA	N/A	0.56	0.56	336.8
∑ PFAAs	N/A	39.253	39.253	55345.4

[a] Average human blood levels of POPs based on a literature review of Scandinavian values, providing the basis for the in vitro mixture.

[b] Average human blood levels of POPs converted to ng/ml. A fat percentage of 0.6 % was used. 1 ml blood was considered to have a weight of 1 g.

[c] Nominal concentration of the various compounds in the total mixture stock – 1000000x the average concentration in blood.

[d] Measured concentrations of the various compounds in the total mixture stock converted to µM.

***** The nominal concentration of PBDE 153 included in the total mixture stock was ten times lower than originally intended.

4.3 *In ovo* and *in vitro* model systems

In this thesis we used *in ovo* chicken embryo (**paper III and IV**) and *in vitro* primary chicken CGNs (**paper I**) and rat pheochromocytoma PC12 (**paper II**) cell line to study the neurodevelopmental effects of POP exposures.

4.3.1 Comparison of chicken and mammalian cerebellum

Comparative genomics revealed that the chicken genome (approximately one billion base pairs) is three times smaller than the one of human or mouse (both about 3 billion base pairs), but contains approximately the same number of genes (chicken about 20,000–25,000, and human about 30,000 protein-coding genes). About 60% of chicken protein-coding genes have a single human orthologue. The proportion of mouse genes with a single identifiable orthologue in the human genome seems to be approximately 80% (Chinwalla et al., 2002, Hillier et al., 2004). Further, sequences expressed in the chicken brain, as indicated by expressed sequence tag (EST) data, are more conserved than those expressed by other tissues (Hillier et al., 2004).

Epidemiological studies have reported that there may be sex-specific effects between early life exposure to POPs and childhood neurodevelopment (Granillo et al., 2019, Spratlen et al., 2020, Lenters et al., 2019). Thus, we could expect that there are sex differences in response to POP exposures *in ovo* (**paper IV**). To identify the sex of individual embryos, DNA was also extracted during preparation of the cerebellar samples. This was subjected to PCR analysis allowing sexing of the samples (Figure 7). We found 11 samples (out of total 24) were female, without taking exposure group in account. However, we found skewed male/female ratios within some exposure groups (Table 4.) Given the small number of embryos per group, this is not unexpected. Thus, we performed the omics analysis without taking the sex of the samples into consideration.

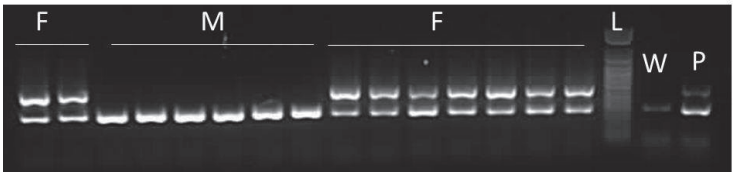

Figure 7. DNA sex identification from cerebellar tissue of chicken embryo at E17. PCR was performed using a 415 bp product of the Xhol repeat sequence present on W chromosome representing female DNA. Double band = F (female), single band = M (Male), L = ladder, W = water and P = positive control. Special thanks to Carol A Wallace for performing PCR at the University of Aberdeen, Scotland.

Table 4. Number of female and male embryos and sex ratios in the samples of cerebellar tissue of chicken embryo at E17 for POP mixture or PFOS exposure and relevant controls after performing PCR. These embryos were used for proteomics analysis.

Samples	Control	POP mixture	PFOS	Total
Female	2	4	5	11
Male	6	4	3	13
Total	8	8	8	24
Ratio Male/Female	3	1	0.6	1.18

In chicken during embryonic development, there are different regions through which an *in ovo* injection may be given. These regions include the allantois, the air cell, the amniotic fluid, the yolk or directly the embryo body (Roto et al., 2016). The different compartments in the chicken egg during embryonic development are shown in Figure 8. We exposed chicken embryo with POP by injection into the allantois at E13 (**paper III and IV**). We predicted that injected pollutants would distribute in the allantoic fluid, be absorbed through CAM, and distribute to the brain via the blood stream. This prediction was based on LC-MS analysis of the drug methadone which rapidly reached the developing chicken embryo brain in concentrations comparable to those obtained in rat (Hadera et al., 2017). The same injection procedure has been used in previous studies on exposure of drugs, pharmaceuticals and environmental toxicants, with apparent effects on the embryo (Austdal et al., 2016, Fjelldal et al., 2019, Mathisen et al., 2013). The CAM is highly vascularized and the development of CAM is completed by E10, however, it is only fully differentiated by E13 (Nowak-Sliwinska et al., 2014). The CAM has been compared to the mammalian placenta, but differs from it anatomically (Metcalfe and Stock, 1993). Chemicals applied to

the CAM can reach the systemic circulation, after absorption through the membrane and affect the development of the chick embryo (Ribatti, 2016).

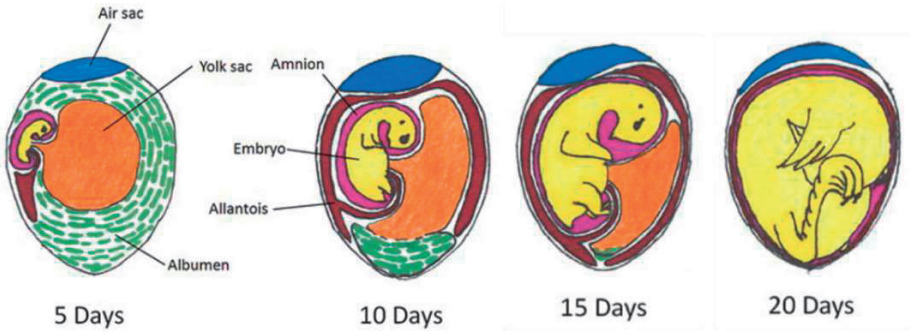

Figure 8. Representation of different compartments in the chicken embryo at 5, 10, 15 and 20 days of incubation. Colors indicate differing compartments: embryo = yellow; air sac = blue; amnion = pink; allantois = red; albumen = green. In **paper III and IV** chicken embryo was exposed at E13 by injection into the allantois. Figure adapted from Roto et al. (2016).

The development of BBB needs to be taken into consideration while exposing the developing chicken embryo with pollutants or chemicals. Compared to humans who might have well developed BBB at the time of birth, in chicken it is still less developed at the time (E13) of POP exposure (Goasdoué et al., 2017, Ribatti et al., 1993). In chicken, the BBB matures between E10 - E16 and the period of maturation of the BBB may be prolonged into or beyond the period of hatching (Stewart and Wiley, 1981). The BBB is characterized by the physical barrier of tight junctions, accompanied by a transport barrier comprising membrane enzymes, transporters and vesicular mechanisms (Schmitt et al., 2017). In chicken embryo tight junctions are observed at E14 (Grange-Messent et al., 1996). According to BBB characteristics, whether chemicals enter the brain is determined by factors like lipid solubility, molecular size, plasma protein binding effects, and the activity of carrier-mediated (e.g. glucose, amino acids), receptor-mediated (e.g. insulin, transferrin) or absorption-mediated transcytosis (e.g. albumin and other plasma proteins) mechanisms (Joly et al., 1995, Bagchi et al., 2019). Another mechanism that can prevent passage of various lipophilic substances is based on the presence of P-glycoprotein (P-gp), a 170 kD plasma transmembrane phosphoglycoprotein. P-gp is a membrane of ATP binding cassette transporter present in many tissues including BBB and plays an important role in limiting the entry of xenobiotic compounds into the brain (Lam et al., 2015).

As in all non-mammalian animal models there are challenges and features which cannot be mimicked correctly in avian models when translating results to a similar setting in mammals. For example, maternal metabolism, placental barrier, and an excretion from eggs are absent in the chicken embryo model, which may cause a prolonged effect of a single exposure (Bjornstad et al., 2015). Even so, the chicken embryo holds potential as a model system in screening procedures of formulation candidates, establishing an intermediate step between *in vitro* cellular tests and preclinical mammalian models (Vargas et al., 2007), and providing supplementary data.

4.3.2 Comparison of cultured chicken and rat cerebellar granule neurons

Primary cultures of cerebellar granule cells (CGNs) derived from rodents is a well-established *in vitro* model to study several aspects of developmental, functional and pathological neurobiology (Contestabile, 2002, Tehran and Pirazzini, 2018). Culturing chicken cerebellar granule neurons (CGNs) was first established by our group as an alternative to murine CGNs cultures. In comparison to rat CGNs culture which is dependent on depolarizing culture condition of 25 mM potassium (Gallo et al., 1982), chicken CGNs culture is dependent on physiological potassium concentration of 5 mM (Jacobs et al., 2006). CGNs isolated at ED17–18 from chicken (Figure 9) is comparable to postnatal day 7–8 in the rat (Jacobs et al., 2006, Mathisen et al., 2013). At these time points cultured chicken CGNs contain approximately 80% of neurons and rat about 95% of neurons. This reflects that CGNs constitute a large homogenous neuronal population in both species. Chicken CGNs develop NMDA-R mediated excitotoxicity rapidly in culture at 3 days compared to 7 days with cultures of rat CGNs. Chicken CGNs respond to glutamate excitotoxicity similar to rat cultures with ROS production and activation of caspase 3. Disadvantages with the chicken culture system may be that it shows higher basal cell death, less is known about the cell culture system, and some antibodies may not recognize avian proteins (Jacobs et al., 2006). Chicken CGNs were used to study the glutamate induced excitotoxicity at different stages of maturation following POP exposure (**paper I**).

Primary neuronal cultures retain many of the morphological, neurochemical, and electrophysiological properties of neurons *in situ*, a significant benefit of this model compared to cell lines. A disadvantage of primary cultures is their limited lifespan, typically

days to weeks. Isolated primary cultures are predominantly post-mitotic, and new animals are needed to prepare new cultures which increases the potential for culture to culture variability. Primary neuronal cultures are a mixture of neuronal and glial populations (Radio et al., 2010, Radio and Mundy, 2008). However, this seems to be less of a problem for the preparation of culture of CGNs, as the cytosine arabinoside (ARA-C) can be added after 18-20 hr to the culture medium to prevent the replication of nonneuronal cells (Gallo et al., 1982).

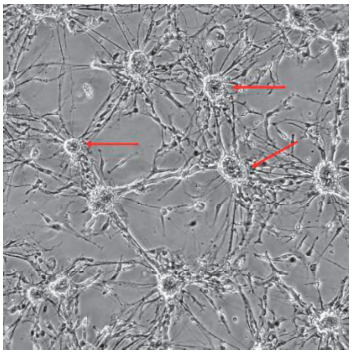

Figure 9. Chicken cerebellar granule neurons (CGNs) cultured at E17, DIV3. Red arrows indicate granule neurons aggregate. (Special thanks to Denis Zosen, UiO for this image).

4.3.3 PC12 cells

PC12 is a cell line established from a transplantable rat adrenal pheochromocytoma (Greene and Tischler, 1976). Serum-withdrawal together with stimulation with NGF results in the cells undergoing one population doubling and induction of neurite outgrowth (Greene, 1978). The elaboration of neurites occurs within 24 to 48 h of NGF exposure (Das et al., 2004). Figure 10 represents the PC12 in the absence or presence of NGF. PC12 has widely been used to assess the involvement of NGF-activated signalling pathways and possible mechanisms by which toxicants affect differentiation and neurite outgrowth (Radio et al., 2008). Even subtle perturbations of the neurite outgrowth by chemicals or pollutants could potentially lead to neurological adverse effects in rodents and humans (Radio and Mundy, 2008, Panesar et al., 2020). Chemicals that can affect neurite outgrowth have the potential to cause developmental neurotoxicity. Therefore, there is a need of screening methods where we can examine such effects. The advantages of immortalized cell lines including PC12 are: (1) they can be expanded in culture for an extended period of time and provide a

relatively homogenous population of cells in large quantities, (2) they are easy to obtain and can be stored indefinitely in liquid nitrogen and (3) the ability to precisely control the timing and onset of differentiation for screening chemical effects on neurite outgrowth (Radio et al., 2010, Radio and Mundy, 2008). However, there are limitations to use this cell line as a model to assess neurite outgrowth. Because these cells are tumour derived, they do not necessarily exhibit the same phenotype as the original primary neurons. For example, neurites derived from the commonly used PC12 cannot be distinguished as axons or dendrites and do not have functional synapses (Radio and Mundy, 2008). In addition, there can be phenotypic variability over time due to genetic instability with increasing passage number. To minimize this variability, we performed the experiments using passage numbers between 10 and 30. One should also consider that the effects of chemicals on neurite outgrowth inhibition or neural cell cytotoxicity could be cell type specific or species specific (Costa et al., 2007, Harrill et al., 2011). For example, human embryonic stem cell-derived neural cultures were more sensitive to neurite outgrowth inhibitors compared to rat primary cortical cultures (Harrill et al., 2011). Neural stem cells of human origin including human-induced pluripotent stem cell (hiPSC)-derived neurons could provide the opportunity to assess neurite outgrowth in cells that are almost identical to that found in the human nervous system (Radio et al., 2008, Cohen and Tanaka, 2018, Zhang et al., 2020). However, there are concerns with human stem cells for example, culture is expensive, it is unclear which developmental state of brain region they represent, and differentiation protocols may be lengthy (Schmidt et al., 2017). Overall, cell lines are proven to be useful in understanding the basic biological processes involved in neuronal differentiation.

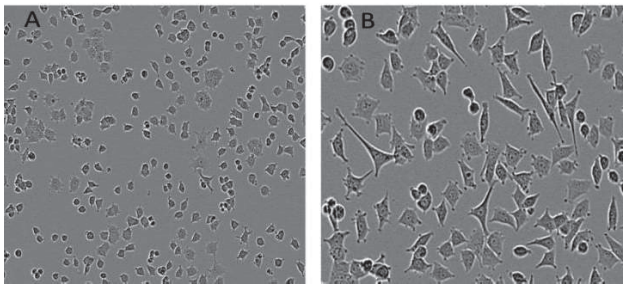

Figure 10. PC12 cells (A) in the absence, and (B) in the presence of NGF (treated for 28-32 h).

4.4 Quantifying the reduction of tetrazolium salt (MTT)

We used MTT assay (**paper I and II**) to measure the cell viability, which reflects the cellular metabolic activity of living cells (Mosmann, 1983). To determine the cell viability in *in vitro* studies more than one assay should be used, as this would increase the reliability of the results obtained (Fotakis and Timbrell, 2006). For example, the lactate dehydrogenase leakage assay (LDH) is based on the measurement of lactate dehydrogenase activity in the extracellular medium. The loss of intracellular LDH and its release into the culture medium is an indicator of irreversible cell death due to cell membrane damage. Further, the neutral red assay is also used to measure cell viability. This assay determines the accumulation of the neutral red dye in the lysosomes of viable, uninjured cells (Fotakis and Timbrell, 2006).

Another possible way to determine the cell viability is trypan blue dye exclusion staining. The dye is excluded from membrane-intact live cells but can enter and concentrate in membrane-compromised dead cells, rendering the cells dark blue (Chan et al., 2020). However, assessing cell membrane damage by this assay, is a more time-consuming assay, where the detection of dead and live cells is dependent on the individual evaluation of the investigator.

4.5 Glutathione measurements

Glutathione (GSH) acts as an important antioxidant. GSH levels were measured in the CGNs (**paper I**) and in the PC12 cells (**paper II**) with monochlorobimane (mBCl). This probe is cell-permeant and non-fluorescent and forms a stable fluorescent conjugate with GSH in a reaction catalysed by the GSH S-transferases (GST) (Fernandez-Checa and Kaplowitz, 1990). The probe detects the thiol group. One of the limitations to the use of mBCl is that the rate of mBCl and GSH conjugation by GST is isoenzyme specific. The GSTs are a complex multigene family of isoenzymes with differing substrate specificities, for example mBCl conjugation is preferentially catalysed by GST μ and to a lesser extent by GST α subunits. It is a poor substrate for GST π. PC12 cells are shown to express GST μ and π (Stevenson et al., 2002, Ublacker et al., 1991). Neurons throughout the brain contain GST (Nur et al., 2000). However, there are also regional differences in pattern of GST subunits expression for example in the rat cerebellum, the flocculus has a higher concentration of GST μ subunit than the vermis (Johnson et al., 1993).

4.6 Calcium influx measurements

The relative cytosolic free Ca^{2+} level in CGNs (**paper I**) was estimated with the ratiometric Ca^{2+} indicator Fura-2 acetoxymethyl (AM) ester. Fura-2 AM has been reported to be completely cleaved by cellular esterases to Fura-2 which is trapped within cells and is used to measure intracellular free Ca^{2+} concentration by a fluorescence ratio method (Oakes et al., 1988). Binding of Ca^{2+} to fura-2 causes an increase in fluorescence intensity and its peak absorbance shifts from 340 nm in the Ca^{2+} bound state to 380 nm in the Ca^{2+} free state. Fluorescence occurs at a peak wavelength of 510 nm for emission. The intracellular Ca^{2+} concentration is proportional to the ratio of fluorescence intensity at two wavelengths i.e. F340/F380. This ratio of fluorescence intensities of Fura-2 at two excitation wavelengths can be used to calculate Ca^{2+} concentrations independent of dye concentration, cell thickness, illumination intensity, emission collection efficiency and possible variability due to instrument efficiency (Grynkiewicz et al., 1985). The dye has wide sensitivity ranging from 100 nM to100 μM. The disadvantage of this probe is that it is a dual excitation dye and not suitable for confocal microscopy (Paredes et al., 2008). Since the fluorescence intensity can get affected by temperature and pH (Oliver et al., 2000), the experiment in CGNs (**paper I**) was conducted at a constant temperature and the solution were buffered to keep the pH at 7.4.

4.7 Omics analysis

4.7.1 RNA-seq transcriptomics and proteomics analysis

We used RNA-seq transcriptomic and label-free LC-MS-detection based proteomics approaches to study the changes in gene and protein expression profiles in cerebella of developing chicken embryos following exposure to the POP mixture or single PFOS (**paper IV**).

Traditional approaches to study function by focusing on a single gene is time-consuming and often limiting in scope. Often a critical change in gene function that causes a change in physiology and behaviour of a neuron can be the result of changes in the expression levels of the RNA and/or protein product of the gene or changes in the activity through specific post-translational modifications. Thus, to get more insight in gene function that underlie basic neurological functions or the brain's responses to external stimuli or

neurological disorders, it is highly recommended to study changes in all of the RNAs (transcriptome) or proteins (proteome) (Kadakkuzha and Puthanveettil, 2013).

Transcriptome consists of all the mRNA that is transcribed at a given time point in a specific tissue. As opposed to the genome or exome, which are fixed for all the cells of an organism, the transcriptome is highly variable and depends upon the environment (Singh et al., 2012). RNA-Seq technology can identify more differentially modulated transcripts of toxicological relevance, splice variants, and non-coding transcripts [e.g., microRNA (miRNA), long non-coding RNA (lncRNA), and pseudogenes]. These additional data could be informative for toxicity prediction, mechanistic investigations or biomarker discovery (Rao et al., 2019).

The proteome is defined as the expressed protein and peptide complement of a cell, organ or organism, which includes all isoforms and posttranslational variants. An organism has a single genome, while it possesses multiple proteomes depending on the cell compartment, type of cell, type of tissue and organ. Proteomes undergo constant changes. Proteomics summarizes the procedures required for analysis of a proteome, where populations of proteins rather than an individual protein are investigated (Christians et al., 2017). The MS techniques used alone or in tandem provide a high level of confidence in identification of protein, especially while analysing complex mixtures of proteins (Kadakkuzha and Puthanveettil, 2013).

Some of the limitations of RNA-seq approach include their dependence on cDNA synthesis and downstream processes, the efficiency of which depends on RNA sequence and structure. When it comes to proteomic approaches, a major issue includes accurate and reproducible protein quantitation in complex samples. Additional difficulties arise from inherent insolubility of some proteins and the post translational modifications, which require sophisticated detection and validation approaches. In addition to biological complexity, other technical challenges for these high-throughput platforms are as follows: data files are too large to handle, and the storage, retrieval and data processing require specific computer assemblies and highly trained bioinformatics specialists (Kadakkuzha and Puthanveettil, 2013).

4.8 Pharmacokinetic (PK) modelling

Pharmacokinetics is the mathematical description of the rates of absorption, distribution, metabolism, and excretion (ADME)-processes and of concentration-time

relationships (Alavijeh et al., 2005). In **paper III** we modelled the distribution of the POP mixture in the embryonic chicken egg by applying a human PK software with the brain considered as an extravascular compartment. This package has been applied in previous studies to calculate the different pharmacokinetic parameters determining the levels of drugs in blood and brain after administration in mice (Andersen et al., 2009, Boix et al., 2013). It should be noted that whether a molecule crosses the BBB is dependent on its physicochemical properties, along with its PK profile (i.e. ADME) of the compound in plasma (Bagchi et al., 2019). One limitation with our experiments was that in our model excretion from eggs is absent (a closed system). We could have measured the compounds in other compartments such as in blood and have included more time points.

5 Discussion of findings

In this thesis chicken embryos were exposed to a POP mixture by injection into the allantois. We detected most of the chemicals present in the mixture in the developing chicken brain, confirming that POP gets transferred to and could target the cells in the brain. The concentrations of most of the measured compounds in chicken embryo brains were within the same order as those reported in human brain samples, **paper III** and (Dewailly et al., 1999, Maestri et al., 2006, Mitchell et al., 2012, Pérez et al., 2013).This is in accordance with a recent study from our group, where POPs get transferred to mice offspring brains after maternal exposure to the POP mixture with a similar composition (Myhre et al., 2021).

There is increasing epidemiological evidence that exposure with POPs is associated with neurodevelopmental toxicity (Latchney and Majewska, 2021, Vuong et al., 2020b). Measuring the concentrations of POPs reaching the brain gives us a benchmark for concentrations relevant for *in vitro* exposures. However, even *in vitro* it could be advantageous to measure intracellular concentrations as these can be lower than the concentrations in the exposure media. For example, a study from our group using zebrafish exposed to POP mixture and PFOS, showed total concentrations recovered from the larval tissue were lower than the concentrations in the exposure media, thus resulting in a lower actual exposure level. The highest recovery rate was 50.2% for β-HCH incorporated in the POP mixture and 35.5% for the single PFOS exposure (Christou, 2020). A limitation in the current work using primary CGNs and PC12 cells is the absence of intracellular concentration measurements and thus we do not know the actual uptake and fate of chemicals in the cells.

We found that often the POP exposures aggravate the adverse neurodevelopmental effects rather than being the main driver. For example, in **paper I**, POP exposure not only induced toxicity on their own but also aggravated glutamate-induced excitotoxicity in cultured CGNs. Similarly, **in paper II**, the exposure enhanced neurite length and branched networks of neurites in NGF-induced PC12 cells. However, in the absence of NGF, the effects of POPs on neurite outgrowth were marginal, suggesting exposure cannot mimic the NGF-receptor signal on its own.

In **paper I** we found that CGNs sensitivity increases with the maturation in culture. This was in accordance with several other studies using CGNs (Berntsen et al., 2018,

Berntsen et al., 2020, Ceccon et al., 2000). The higher sensitivity at DIV5 could be due to a time-dependent changes in NMDA-R subunits expression. Also, similar to the cerebellum *in vivo*, the expression of subunits in cultures of CGNs *in vitro* changes with time, leading to maturation of neuronal cultures (Cebers et al., 2001, Vallano et al., 1996).

Our observations in cultured chicken CGNs indicated that POP exposure leads to NMDA-R mediated excitotoxity (**paper I).** In **paper IV** exposure to POPs did not indicate any significant changes in glutamate ionotropic NMDA-Rs or subunit types in cerebella from *in ovo* exposed chicken embryos. However, we found changes in gene or protein expression levels that affect regulators of the NMDA-R systems and calcium signaling. Our histological analysis revealed thinning of the ML in cerebellum after POP exposure. This ML thinning could be due to the observed dysregulation of genes and proteins involved in proliferative and/or migratory pathways. The migration of postmitotic CGNs through different cerebellar layers i.e. from the EGL through the ML to the IGL (where they mature) is a key feature for development of the cerebellum. The migration of neurons in a developing brain is guided through NMDA-R mediated Ca^{2+} influx, among other signals (Komuro and Rakic, 1993). Alterations in migration could be indicative of impaired neurodevelopment (Bjornstad et al., 2015).

In contrast to neurons from the CNS such as CGNs, PC12 is lacking functional expression of NMDA receptors (Edwards et al., 2007). PFOS-induced toxicity in PC12 cells was not found to be affected by the NMDA-R antagonists CPP, indicating no involvement of this receptor in PFOS-induced cytotoxicity (Berntsen et al., 2018). Thus, it is interesting to study the effect independent of NMDA-receptor as a neural model for example in PC12. In **paper II,** POP exposure was found to enhance neurite outgrowth indicating lack of cytotoxicity. Some effects on the rate of cell proliferation were observed, but nuclear and mitochondrial health parameters remained unaffected. However, other *in vitro* studies revealed changes in mitochondrial mass and mitochondrial membrane potential in several non-neuronal cell systems following exposure to POPs (Shannon et al., 2019; Wilson et al., 2016), so a similar effect in neuronal cells cannot be excluded. Indeed, in **paper IV**, we found that POP exposure led to alterations in genes or proteins in cerebellum of developing chicken related to mitochondrial health. In **paper I** and **IV**, POP exposure led to adverse effects on cerebellar development, in contrast the similar exposure in **paper II** indicated lack of toxicity. This discrepancy in neurotoxic outcomes in **paper I** and **IV** vs **paper II** might be explained by many factors, such as differences in types of neurons, or the experimental conditions used. The effects of POPs on neurite outgrowth in

PC12 could also be species specific or cell type specific. For example, human embryonic stem cell-derived neural cultures were supposed to be more sensitive to neurite outgrowth inhibitors compared to rat primary cortical cultures (Harrill et al., 2011). Another possible reason could be an ontogenetic effect linked to the developmental stage of the cells. For example, in **paper II**, we investigated the adverse developmental effects of POP exposure in PC12 cells that were not exposed previously to NGF (i.e. not differentiated, unprimed). The other possible way would be to use PC12 cells that have been exposed previously to NGF (primed).

In **paper III**, we observed differences in the speed of distribution of POPs to the brain, with the protein binding compounds PFASs being slower than the lipophilic PCBs, OCPs, BFRs. This reflects that compounds reaching the brain depend on the chemical property of the individual compounds. It is expected that small lipid soluble compounds such as chlorinated and brominated POPs will readily diffuse across the BBB whereas other compounds, such as protein binding PFASs would need carrier or receptor-mediated transport (Goasdoué et al., 2017). Our analysis revealed that PFUnDA would stay at relatively significant levels in the brain. This was further supported by recent study from our group where Myhre et al. (2021) reported that PFOS, PFUnDA and PFDA were the most abundant PFAS congeners in the brains of both dams and pups following maternal exposure to a POP mixture and among these PFAS, PFUnDA deposited to the greatest extent in the brain in comparison to blood. The longer residence time of this compound in our case and its possibly higher neurotoxicity could potentially make this a compound of high concern with respect to developmental neurotoxicity. The differences in the speed of distribution of POPs to the brain, moreover, also suggests the presence of a functional barrier at this time-point, most likely the BBB. In **paper IV** we identified a set of genes or proteins related to brain vascularization, integrity and function of the BBB, suggesting that POPs interfere with the BBB.

Further, in **paper I** and **II**, we did not observe an increase in ROS production in cultured chicken CGNs or in PC12 following exposure to POPs (result not shown) by using dihydrorhodamine 123 probe. However, our proteomics analysis (**paper IV**) indicated that exposure to mixture involves oxidative stress, with increased oxidation of peptides at methionine residues. This was in accordance with previous work in relation to oxidative stress where exposure to a POP mixture led to up-regulation of genes related to the antioxidant defence in cultured rat CGNs, also indicating mixture toxicity involves oxidative stress (Berntsen et al., 2020). In **paper I, II** and **IV**, we found that a single

compound (in our case PFOS) can explain only part of the effect seen with the POP mixture, and that additional compounds contribute to its overall effect.

In relation to adverse DNT outcomes in **paper I** we found that exposure to POPs can interfere with NMDA-R. Changes in the expression of ionotropic glutamate receptors have been observed in autism, for example an upregulation of NMDA-R subunit protein levels has also been reported in the cerebellum of human postmortem samples with autism (Rojas, 2014). In **paper II** exposure to POPs did not inhibit neuritogenesis, but rather increased NGF-induced neurite outgrowth in PC12 cells. However, we cannot exclude possible adverse effects on developmental outcomes with regards to overactive neuritogenesis, which might lead to improper neuronal connectivity. The development of nervous system comprised a series of unique and complex processes such as proliferation, migration, differentiation, synaptogenesis, gliogenesis/myelination, and apoptosis. It is assumed that DNT toxicants exert their toxicity by disturbing at least one of these processes. The disturbances of these processes are key events (KEs) of adverse outcome pathways (AOPs) relevant for DNT (Bal-Price et al., 2018). An example of the AOP relevant to DNT is the binding of an antagonist to the NMDA-R know as molecular initiating event (MIE). This MIE triggers a cascade of KEs at the cellular, organ and organism level and resulting in the adverse outcome (AO), defined as impairment of learning and memory (Sachana et al., 2018). In **paper IV**, our data identified changes in gene expression and proteins, many of which are multifunctional, and are involved in several key neurodevelopmental processes. These point to alterations in molecular events linked to neuronal cell proliferation and migration, cellular stress responses including unfolded protein response, lipid metabolism, and myelination, thus interfering with the fundamental aspects of brain development and function. Some have strong links to neurocognitive and neurobehavioral outcomes, as well as neurodegenerative disorders. The information gained from our studies is useful in the AOPs framework, where it can add knowledge into existing AOPs for DNT (Sachana et al., 2018) and/or form the basis of new AOPs.

6 General conclusions

Based on the observations in relevant model systems for studying the neurodevelopmental effects of POPs, we can state that:

- Often the POP exposures aggravate the adverse neurodevelopmental effects rather than being the main driver.
- It is important to study mixture effects since single compounds can only explain part of the effect.
- POP exposures showed an effect on neuronal connectivity.
- POP distributes to the chicken embryonic brain at human relevant exposure level.
- Our study provides information that add to mechanistic understanding of associations between POP exposures and adverse neurodevelopmental outcomes observed in epidemiological studies.

In support of our initial hypothesis, we conclude that exposure to POPs could lead to morphological and molecular changes that interfere with fundamental aspects of neurodevelopment.

7 Future perspectives

To gain more knowledge on the adverse neurodevelopmental effects of POPs, it would be interesting to consider the following studies in the future.

1. **Mechanistic studies**

Our observation indicated that exposure to POPs could interfere with NMDA glutamate receptors. This receptor modulates the migration of granule neurons through different cerebellar layers, a key feature for cerebellar development (Komuro and Rakic, 1993). We also found alteration in the molecular layer of the cerebellar cortex following exposure to POPs. It would be interesting to validate this observation further by immunohistological analysis for NR2B, a subunit of NMDA-R, as an important neurodevelopmental marker. Similarly, glial fibrillary acidic protein (GFAP) could be used as marker for astrocytic cells. We can also use the NR2B NMDA receptor ligand ^{11}C Ro 04-5595 as a potential radiotracer for positron emission tomography to assess developmental effects on NR2B expression in chicken embryo brain (Jakobsson et al., 2019).

In the present thesis we highlighted the relevance of chicken embryo to study the DNT. We found several altered genes and proteins that are involved in adverse neurocognitive and behavioural outcomes. It would be of interest to continue studies on development of exposed chicken embryos after hatching, including the study of cognitive and behavioural outcomes in adult chickens.

Our results showed that exposure to POPs enhanced NGF-induced neurite outgrowth. Further aspects of this, such as NGF signalling pathways should be explored in future studies.

2. **Internal concentration assessments**

Since we do not know the actual uptake and fate of chemicals in the cells *in vitro*, it would be interesting to assess the concentrations of chemicals in cells and in cell culture medium.

3. **Inclusion of emerging compounds**

PFOS and its salts; PFOA and its salts; and PFHxS compounds are under the Stockholm Convention. The production of these compounds has therefore been limited in many countries and are on the way to phase out (Bălan et al., 2021). But new replacement of those

PFAS, emerging compounds such as, hexafluoropropylene oxide dimer acid (HFPO-DA; tradename GenX) or 4,8-dioxa-3H-perfluorononanoic acid (DONA) are also of concern for their probable adverse effects on human health (Brase et al., 2021). It would be interesting to explore further the adverse neurodevelopmental effects, using the POP mixture as a background, then add other compounds not only POPs, but also bisphenol A, mycotoxins, phytoestrogens.

4. **Using other model systems**

Human induced pluripotent stem (iPS) cells can be grown in three-dimensions as neurospheres and brain organoids. These models have been used to explore the consequences of zika virus infection during neurogenesis and growth (Garcez et al., 2016). So, similar approaches can be used to study the neurotoxicity of the POPs. Also, the EU Reference Laboratory for alternatives to animal testing (EURL ECVAM) review comprises more than five hundred different models, compiled from publications between 2013 and 2018 in the field of neurodegenerative diseases and identified that the majority of the models are based on iPSCs (Gribaldo, 2021). They are more convenient for *in vitro* biomedical research than embryonic stem cells because of practical and ethical reasons. These models are also important to overcome species differences.

8 References

ABRAHÁM, H., TORNÓCZKY, T., KOSZTOLÁNYI, G. & SERESS, L. 2001. Cell formation in the cortical layers of the developing human cerebellum. *Int J Dev Neurosci,* 19**,** 53-62.

ADDAE, C., CHENG, H. & MARTINEZ-CEBALLOS, E. 2013. Effect of the environmental pollutant hexachlorobenzene (HCB) on the neuronal differentiation of mouse embryonic stem cells. *Int J Environ Res Public Health,* 10**,** 5244-56.

ADEN, P., GOVERUD, I., LIESTOL, K., LOBERG, E. M., PAULSEN, R. E., MAEHLEN, J. & LOMO, J. 2008. Low-potency glucocorticoid hydrocortisone has similar neurotoxic effects as high-potency glucocorticoid dexamethasone on neurons in the immature chicken cerebellum. *Brain Res,* 1236**,** 39-48.

AERTS, R., VAN OVERMEIRE, I., COLLES, A., ANDJELKOVIĆ, M., MALARVANNAN, G., POMA, G., DEN HOND, E., VAN DE MIEROOP, E., DEWOLF, M.-C., CHARLET, F., VAN NIEUWENHUYSE, A., VAN LOCO, J. & COVACI, A. 2019. Determinants of persistent organic pollutant (POP) concentrations in human breast milk of a cross-sectional sample of primiparous mothers in Belgium. *Environment International,* 131**,** 104979.

AGARWAL, V., EL GAMAL, A. A., YAMANAKA, K., POTH, D., KERSTEN, R. D., SCHORN, M., ALLEN, E. E. & MOORE, B. S. 2014. Biosynthesis of polybrominated aromatic organic compounds by marine bacteria. *Nat Chem Biol,* 10**,** 640-7.

ALAVIJEH, M. S., CHISHTY, M., QAISER, M. Z. & PALMER, A. M. 2005. Drug metabolism and pharmacokinetics, the blood-brain barrier, and central nervous system drug discovery. *NeuroRx,* 2**,** 554-71.

ALOE, L. 2004. Rita Levi-Montalcini: the discovery of nerve growth factor and modern neurobiology. *Trends Cell Biol,* 14**,** 395-9.

ANDERSEN, J. M., RIPEL, A., BOIX, F., NORMANN, P. T. & MØRLAND, J. 2009. Increased locomotor activity induced by heroin in mice: pharmacokinetic demonstration of heroin acting as a prodrug for the mediator 6-monoacetylmorphine in vivo. *J Pharmacol Exp Ther,* 331**,** 153-61.

ANGUS, W. G. & CONTRERAS, M. L. 1995. Aroclor 1254 alters the binding of 125I-labeled nerve growth factor in PC12 cells. *Neurosci Lett,* 191**,** 23-6.

ARMADA-MOREIRA, A., GOMES, J. I., PINA, C. C., SAVCHAK, O. K., GONÇALVES-RIBEIRO, J., REI, N., PINTO, S., MORAIS, T. P., MARTINS, R. S., RIBEIRO, F. F., SEBASTIÃO, A. M., CRUNELLI, V. & VAZ, S. H. 2020. Going the Extra (Synaptic) Mile: Excitotoxicity as the Road Toward Neurodegenerative Diseases. *Frontiers in cellular neuroscience,* 14**,** 90-90.

AUSTDAL, L. P., BJORNSTAD, S., MATHISEN, G. H., ADEN, P. K., MIKKOLA, I., PAULSEN, R. E. & RAKKESTAD, K. E. 2016. Glucocorticoid Effects on Cerebellar Development in a Chicken Embryo Model: Exploring Changes in PAX6 and Metalloproteinase-9 After Exposure to Dexamethasone. *J Neuroendocrinol,* 28.

AUSTDAL, L. P. E. 2018. New models for nonclinical safety assessment: targeting hallmark neurodevelopmental processes to examine if pharmaceuticals affect the immature brain.

AZEVEDO, F. A., CARVALHO, L. R., GRINBERG, L. T., FARFEL, J. M., FERRETTI, R. E., LEITE, R. E., JACOB FILHO, W., LENT, R. & HERCULANO-HOUZEL, S. 2009. Equal numbers of neuronal and nonneuronal cells make the human brain an isometrically scaled-up primate brain. *J Comp Neurol,* 513**,** 532-41.

BAGCHI, S., CHHIBBER, T., LAHOOTI, B., VERMA, A., BORSE, V. & JAYANT, R. D. 2019. In-vitro blood-brain barrier models for drug screening and permeation studies: an overview. *Drug Des Devel Ther,* 13**,** 3591-3605.

BAL-PRICE, A., HOGBERG, H. T., CROFTON, K. M., DANESHIAN, M., FITZGERALD, R. E., FRITSCHE, E., HEINONEN, T., HOUGAARD BENNEKOU, S., KLIMA, S., PIERSMA, A. H., SACHANA, M., SHAFER, T. J., TERRON, A., MONNET-TSCHUDI, F., VIVIANI, B., WALDMANN, T., WESTERINK, R. H. S., WILKS, M. F., WITTERS, H., ZURICH, M. G. & LEIST, M. 2018. Recommendation on test readiness criteria for new approach methods in toxicology: Exemplified for developmental neurotoxicity. *Altex,* 35**,** 306-352.

BĂLAN, S. A., MATHRANI, V. C., GUO, D. F. & ALGAZI, A. M. 2021. Regulating PFAS as a Chemical Class under the California Safer Consumer Products Program. *Environmental Health Perspectives,* 129**,** 025001.

BERNTSEN, H. F., BERG, V., THOMSEN, C., ROPSTAD, E. & ZIMMER, K. E. 2017a. The design of an environmentally relevant mixture of persistent organic pollutants for use in in vivo and in vitro studies. *J Toxicol Environ Health A***,** 1-15.

BERNTSEN, H. F., BJORKLUND, C. G., AUDINOT, J. N., HOFER, T., VERHAEGEN, S., LENTZEN, E., GUTLEB, A. C. & ROPSTAD, E. 2017b. Time-dependent effects of perfluorinated compounds on viability in cerebellar granule neurons: Dependence on carbon chain length and functional group attached. *Neurotoxicology,* 63**,** 70-83.

BERNTSEN, H. F., BJORKLUND, C. G., STRANDABO, R., HAUG, T. M., MOLDES-ANAYA, A., FUENTES-LAZARO, J., VERHAEGEN, S., PAULSEN, R. E., TASKER, R. A. & ROPSTAD, E. 2018. PFOS-induced excitotoxicity is dependent on Ca(2+) influx via NMDA receptors in rat cerebellar granule neurons. *Toxicol Appl Pharmacol,* 357**,** 19-32.

BERNTSEN, H. F., DUALE, N., BJØRKLUND, C. G., RANGEL-HUERTA, O. D., DYRBERG, K., HOFER, T., RAKKESTAD, K. E., ØSTBY, G., HALSNE, R., BOGE, G., PAULSEN, R. E., MYHRE, O. & ROPSTAD, E. 2020. Effects of a human-based mixture of persistent organic pollutants on the in vivo exposed cerebellum and cerebellar neuronal cultures exposed in vitro. *Environ Int,* 146**,** 106240.

BJORNSTAD, S., AUSTDAL, L. P., ROALD, B., GLOVER, J. C. & PAULSEN, R. E. 2015. Cracking the Egg: Potential of the Developing Chicken as a Model System for Nonclinical Safety Studies of Pharmaceuticals. *J Pharmacol Exp Ther,* 355**,** 386-96.

BOIX, F., ANDERSEN, J. M. & MØRLAND, J. 2013. Pharmacokinetic modeling of subcutaneous heroin and its metabolites in blood and brain of mice. *Addict Biol,* 18**,** 1-7.

BRASE, R. A., MULLIN, E. J. & SPINK, D. C. 2021. Legacy and Emerging Per- and Polyfluoroalkyl Substances: Analytical Techniques, Environmental Fate, and Health Effects. *Int J Mol Sci,* 22.

BRUNER-TRAN, K. L. & OSTEEN, K. G. 2010. Dioxin-like PCBs and endometriosis. *Systems biology in reproductive medicine,* 56**,** 132-146.

BUTTERFIELD, D. A. & KANSKI, J. 2001. Brain protein oxidation in age-related neurodegenerative disorders that are associated with aggregated proteins. *Mechanisms of Ageing and Development,* 122**,** 945-962.

CEBERS, G., CEBERE, A., KOVÁCS, A. D., HÖGBERG, H., MOREIRA, T. & LILJEQUIST, S. 2001. Increased ambient glutamate concentration alters the expression of NMDA receptor subunits in cerebellar granule neurons. *Neurochem Int,* 39**,** 151-60.

CECCON, M., GIUSTI, P., FACCI, L., BORIN, G., IMBESI, M., FLOREANI, M. & SKAPER, S. D. 2000. Intracellular glutathione levels determine cerebellar granule neuron sensitivity to excitotoxic injury by kainic acid. *Brain Res,* 862**,** 83-9.

CHAKRABORTY, A., MURPHY, S. & COLEMAN, N. 2017. The Role of NMDA Receptors in Neural Stem Cell Proliferation and Differentiation. *Stem Cells and Development,* 26**,** 798-807.

CHAKRAVARTI, B. & CHAKRAVARTI, D. N. 2007. Oxidative modification of proteins: age-related changes. *Gerontology,* 53**,** 128-39.

CHAN, L. L.-Y., RICE, W. L. & QIU, J. 2020. Observation and quantification of the morphological effect of trypan blue rupturing dead or dying cells. *PLOS ONE,* 15**,** e0227950.

CHINWALLA, A. T., COOK, L. L., DELEHAUNTY, K. D. & FEWELL, G. A., ET AL. 2002. Initial sequencing and comparative analysis of the mouse genome. *Nature,* 420**,** 520-562.

CHOI, D. W. 1985. Glutamate neurotoxicity in cortical cell culture is calcium dependent. *Neurosci Lett,* 58**,** 293-7.

CHOI, D. W. 1988. Glutamate neurotoxicity and diseases of the nervous system. *Neuron,* 1**,** 623-34.
CHRISTEN, V., RUSCONI, M., CRETTAZ, P. & FENT, K. 2017. Developmental neurotoxicity of different pesticides in PC-12 cells in vitro. *Toxicol Appl Pharmacol,* 325**,** 25-36.
CHRISTIANS, U., KLAWITTER, J., KLEPACKI, J. & KLAWITTER, J. 2017. Chapter Four - The Role of Proteomics in the Study of Kidney Diseases and in the Development of Diagnostic Tools. *In:* EDELSTEIN, C. L. (ed.) *Biomarkers of Kidney Disease (Second Edition).* Academic Press.
CHRISTOU, M. 2020. PhD Thesis Exploring the short and longterm effects of developmental exposure in zebrafish exposed to anthropogenic chemicals.
COHEN, J. D. & TANAKA, Y. 2018. Comparative Sensitivity of Human-Induced Pluripotent Stem Cell-Derived Neuronal Subtypes to Chemically Induced Neurodegeneration. *Applied In Vitro Toxicology,* 4**,** 347-364.
CONTESTABILE, A. 2002. Cerebellar granule cells as a model to study mechanisms of neuronal apoptosis or survival in vivo and in vitro. *Cerebellum,* 1**,** 41-55.
COSTA, L. G., FATTORI, V., GIORDANO, G. & VITALONE, A. 2007. An in vitro approach to assess the toxicity of certain food contaminants: methylmercury and polychlorinated biphenyls. *Toxicology,* 237**,** 65-76.
DAS, K. P., FREUDENRICH, T. M. & MUNDY, W. R. 2004. Assessment of PC12 cell differentiation and neurite growth: a comparison of morphological and neurochemical measures. *Neurotoxicol Teratol,* 26**,** 397-406.
DAVEY, M. G. & TICKLE, C. 2007. The chicken as a model for embryonic development. *Cytogenet Genome Res,* 117**,** 231-9.
DAVIDSEN, N., LAUVÅS, A. J., MYHRE, O., ROPSTAD, E., CARPI, D., GYVES, E. M.-D., BERNTSEN, H. F., DIRVEN, H., PAULSEN, R. E., BAL-PRICE, A. & PISTOLLATO, F. 2021. Exposure to human relevant mixtures of halogenated persistent organic pollutants (POPs) alters neurodevelopmental processes in human neural stem cells undergoing differentiation. *Reproductive Toxicology,* 100**,** 17-34.
DENAMIC 2012. DENAMIC Report Summary, Project ID: 282957. https://cordis.europa.eu/project/id/282957/reporting.
DEWAILLY, E., MULVAD, G., PEDERSEN, H. S., AYOTTE, P., DEMERS, A., WEBER, J. P. & HANSEN, J. C. 1999. Concentration of organochlorines in human brain, liver, and adipose tissue autopsy samples from Greenland. *Environ Health Perspect,* 107**,** 823-8.
DWIVEDI, D., MEGHA, K., MISHRA, R. & MANDAL, P. K. 2020. Glutathione in Brain: Overview of Its Conformations, Functions, Biochemical Characteristics, Quantitation and Potential Therapeutic Role in Brain Disorders. *Neurochemical Research,* 45**,** 1461-1480.
EDWARDS, M. A., LOXLEY, R. A., WILLIAMS, A. J., CONNOR, M. & PHILLIPS, J. K. 2007. Lack of functional expression of NMDA receptors in PC12 cells. *Neurotoxicology,* 28**,** 876-85.
EPA 2020. U.S. Environmental Protection Agency Report an environmental violation.https://www.epa.gov/international-cooperation/persistent-organic-pollutants-global-issue-global-response.
EPA 2021. U.S. Environmental Protection Agency Report an environmental violation (EPA), https://www.epa.gov/pfas/basic-information-pfas.
FERNANDEZ-CHECA, J. C. & KAPLOWITZ, N. 1990. The use of monochlorobimane to determine hepatic GSH levels and synthesis. *Anal Biochem,* 190**,** 212-9.
FISHER, M., ARBUCKLE, T. E., LIANG, C. L., LEBLANC, A., GAUDREAU, E., FOSTER, W. G., HAINES, D., DAVIS, K. & FRASER, W. D. 2016. Concentrations of persistent organic pollutants in maternal and cord blood from the maternal-infant research on environmental chemicals (MIREC) cohort study. *Environmental Health,* 15**,** 59.
FJELLDAL, M. F., HADERA, M. G., KONGSTORP, M., AUSTDAL, L. P. E., SULOVIC, A., ANDERSEN, J. M. & PAULSEN, R. E. 2019. Opioid receptor-mediated changes in the NMDA receptor in developing rat and chicken. *Int J Dev Neurosci,* 78**,** 19-27.

FOTAKIS, G. & TIMBRELL, J. A. 2006. In vitro cytotoxicity assays: Comparison of LDH, neutral red, MTT and protein assay in hepatoma cell lines following exposure to cadmium chloride. *Toxicology Letters,* 160**,** 171-177.

FU, J., GAO, Y., CUI, L., WANG, T., LIANG, Y., QU, G., YUAN, B., WANG, Y., ZHANG, A. & JIANG, G. 2016. Occurrence, temporal trends, and half-lives of perfluoroalkyl acids (PFAAs) in occupational workers in China. *Sci Rep,* 6**,** 38039.

GALLO, V., CIOTTI, M. T., COLETTI, A., ALOISI, F. & LEVI, G. 1982. Selective release of glutamate from cerebellar granule cells differentiating in culture. *Proc Natl Acad Sci U S A,* 79**,** 7919-23.

GARCEZ, P. P., LOIOLA, E. C., MADEIRO DA COSTA, R., HIGA, L. M., TRINDADE, P., DELVECCHIO, R., NASCIMENTO, J. M., BRINDEIRO, R., TANURI, A. & REHEN, S. K. 2016. Zika virus impairs growth in human neurospheres and brain organoids. *Science,* 352**,** 816-8.

GIORDANO, G. & COSTA, L. G. 2011. Primary Neurons in Culture and Neuronal Cell Lines for In Vitro Neurotoxicological Studies. *In:* COSTA, L. G., GIORDANO, G. & GUIZZETTI, M. (eds.) *In Vitro Neurotoxicology: Methods and Protocols.* Totowa, NJ: Humana Press.

GOASDOUÉ, K., MILLER, S. M., COLDITZ, P. B. & BJÖRKMAN, S. T. 2017. Review: The blood-brain barrier; protecting the developing fetal brain. *Placenta,* 54**,** 111-116.

GÖCKENER, B., WEBER, T., RÜDEL, H., BÜCKING, M. & KOLOSSA-GEHRING, M. 2020. Human biomonitoring of per- and polyfluoroalkyl substances in German blood plasma samples from 1982 to 2019. *Environment International,* 145**,** 106123.

GOODMAN, M., SQUIBB, K., YOUNGSTROM, E., ANTHONY, L. G., KENWORTHY, L., LIPKIN, P. H., MATTISON, D. R. & LAKIND, J. S. 2011. Using systematic reviews and meta-analyses to support regulatory decision making for neurotoxicants: lessons learned from a case study of PCBs. *Cien Saude Colet,* 16**,** 3207-20.

GRANGE-MESSENT, V., RAISON, D. & BOUCHAUD, C. 1996. Astrocyte-endothelial cell relationships during the establishment of the blood-brain barrier in the chick embryo. *Biology of the Cell,* 86**,** 45-51.

GRANILLO, L., SETHI, S., KEIL, K. P., LIN, Y., OZONOFF, S., IOSIF, A.-M., PUSCHNER, B. & SCHMIDT, R. J. 2019. Polychlorinated biphenyls influence on autism spectrum disorder risk in the MARBLES cohort. *Environmental Research,* 171**,** 177-184.

GREENE, L. A. 1978. Nerve growth factor prevents the death and stimulates the neuronal differentiation of clonal PC12 pheochromocytoma cells in serum-free medium. *J Cell Biol,* 78**,** 747-55.

GREENE, L. A. & TISCHLER, A. S. 1976. Establishment of a noradrenergic clonal line of rat adrenal pheochromocytoma cells which respond to nerve growth factor. *Proc Natl Acad Sci U S A,* 73**,** 2424-8.

GRIBALDO, L., DURA, A., AND WHELAN, M., 2021. Advanced Non-animal Models in Biomedical Research – Neurodegenrative Diseases – Executive Summary, EUR 30334 EN, Publications Office of the European Union, Luxembourg.

GROVA, N., SCHROEDER, H., OLIVIER, J. L. & TURNER, J. D. 2019. Epigenetic and Neurological Impairments Associated with Early Life Exposure to Persistent Organic Pollutants. *Int J Genomics,* 2019**,** 2085496.

GRYNKIEWICZ, G., POENIE, M. & TSIEN, R. Y. 1985. A new generation of Ca2+ indicators with greatly improved fluorescence properties. *J Biol Chem,* 260**,** 3440-50.

HADERA, M. G., ANDERSEN, J. M. & PAULSEN, R. E. 2017. Effects of methadone in the developing chicken embryo as a model of neurodevelopmental toxicity. *Reproductive Toxicology,* 72**,** 216-217.

HARRILL, J. A., FREUDENRICH, T. M., ROBINETTE, B. L. & MUNDY, W. R. 2011. Comparative sensitivity of human and rat neural cultures to chemical-induced inhibition of neurite outgrowth. *Toxicology and Applied Pharmacology,* 256**,** 268-280.

HILLIER, L. W., MILLER, W., BIRNEY, E. & WARREN, W., ET AL. 2004. Sequence and comparative analysis of the chicken genome provide unique perspectives on vertebrate evolution. *Nature,* 432**,** 695-716.

HOYER, B. B., RAMLAU-HANSEN, C. H., OBEL, C., PEDERSEN, H. S., HERNIK, A., OGNIEV, V., JONSSON, B. A., LINDH, C. H., RYLANDER, L., RIGNELL-HYDBOM, A., BONDE, J. P. & TOFT, G. 2015. Pregnancy serum concentrations of perfluorinated alkyl substances and offspring behaviour and motor development at age 5-9 years--a prospective study. *Environ Health,* 14**,** 2.

IKONOMIDOU, C. & KAINDL, A. M. 2011. Neuronal death and oxidative stress in the developing brain. *Antioxid Redox Signal,* 14**,** 1535-50.

IULIANELLA, A., WINGATE, R. J., MOENS, C. B. & CAPALDO, E. 2019. The generation of granule cells during the development and evolution of the cerebellum. *Developmental Dynamics,* 248**,** 506-513.

JACOBS, C. M., ADEN, P., MATHISEN, G. H., KHUONG, E., GAARDER, M., LØBERG, E. M., LØMO, J., MÆHLEN, J. & PAULSEN, R. E. 2006. Chicken cerebellar granule neurons rapidly develop excitotoxicity in culture. *Journal of Neuroscience Methods,* 156**,** 129-135.

JAKOBSSON, J. E., GOURNI, E., KHANAPUR, S., BRITO, B. & RISS, P. J. 2019. Synthesis and Characterization in Rodent Brain of the Subtype-Selective NR2B NMDA Receptor Ligand [11C]Ro04-5595 as a Potential Radiotracer for Positron Emission Tomography. *ACS Omega,* 4**,** 9925-9931.

JOHNSON, J. A., EL BARBARY, A., KORNGUTH, S. E., BRUGGE, J. F. & SIEGEL, F. L. 1993. Glutathione S-transferase isoenzymes in rat brain neurons and glia. *J Neurosci,* 13**,** 2013-23.

JOLY, B., FARDEL, O., CECCHELLI, R., CHESNÉ, C., PUOZZO, C. & GUILLOUZO, A. 1995. Selective drug transport and P-glycoprotein activity in an in vitro blood-brain barrier model. *Toxicol In Vitro,* 9**,** 357-64.

KADAKKUZHA, B. M. & PUTHANVEETTIL, S. V. 2013. Genomics and proteomics in solving brain complexity. *Molecular BioSystems,* 9**,** 1807-1821.

KARRMAN, A., VAN BAVEL, B., JARNBERG, U., HARDELL, L. & LINDSTROM, G. 2006. Perfluorinated chemicals in relation to other persistent organic pollutants in human blood. *Chemosphere,* 64**,** 1582-91.

KHEZRI, A., FRASER, T. W., NOURIZADEH-LILLABADI, R., KAMSTRA, J. H., BERG, V., ZIMMER, K. E. & ROPSTAD, E. 2017. A Mixture of Persistent Organic Pollutants and Perfluorooctanesulfonic Acid Induces Similar Behavioural Responses, but Different Gene Expression Profiles in Zebrafish Larvae. *Int J Mol Sci,* 18.

KNUTSEN, H. K., KVALEM, H. E., THOMSEN, C., FRØSHAUG, M., HAUGEN, M., BECHER, G., ALEXANDER, J. & MELTZER, H. M. 2008. Dietary exposure to brominated flame retardants correlates with male blood levels in a selected group of Norwegians with a wide range of seafood consumption. *Molecular Nutrition & Food Research,* 52**,** 217-227.

KOMURO, H. & RAKIC, P. 1993. Modulation of neuronal migration by NMDA receptors. *Science,* 260**,** 95-7.

KORTENKAMP, A., BACKHAUS, T. & FAUST, M. 2009. State of the Art Report on Mixture Toxicity. Final Report. Executive Summary.: The School of Pharmacy University of London (ULSOP).

KRÄMER, D. & MINICHIELLO, L. 2010. Cell Culture of Primary Cerebellar Granule Cells. *In:* WARD, A. & TOSH, D. (eds.) *Mouse Cell Culture: Methods and Protocols.* Totowa, NJ: Humana Press.

KRITIS, A. A., STAMOULA, E. G., PANISKAKI, K. A. & VAVILIS, T. D. 2015. Researching glutamate - induced cytotoxicity in different cell lines: a comparative/collective analysis/study. *Front Cell Neurosci,* 9**,** 91.

LACKEY, E. P., HECK, D. H. & SILLITOE, R. V. 2018. Recent advances in understanding the mechanisms of cerebellar granule cell development and function and their contribution to behavior. *F1000Research,* 7**,** F1000 Faculty Rev-1142.

LAIRD, B. D., GONCHAROV, A. B. & CHAN, H. M. 2013. Body burden of metals and persistent organic pollutants among Inuit in the Canadian Arctic. *Environ Int,* 59**,** 33-40.

LAM, J., BAELLO, S., IQBAL, M., KELLY, L. E., SHANNON, P. T., CHITAYAT, D., MATTHEWS, S. G. & KOREN, G. 2015. The ontogeny of P-glycoprotein in the developing human blood-brain barrier: implication for opioid toxicity in neonates. *Pediatr Res,* 78**,** 417-21.

LAM, J., LANPHEAR, B. P., BELLINGER, D., AXELRAD, D. A., MCPARTLAND, J., SUTTON, P., DAVIDSON, L., DANIELS, N., SEN, S. & WOODRUFF, T. J. 2017. Developmental PBDE Exposure and IQ/ADHD in Childhood: A Systematic Review and Meta-analysis. *Environ Health Perspect,* 125**,** 086001.

LATCHNEY, S. E. & MAJEWSKA, A. K. 2021. Persistent organic pollutants at the synapse: Shared phenotypes and converging mechanisms of developmental neurotoxicity. *Developmental Neurobiology,* n/a.

LAU, C. 2015. Perfluorinated Compounds: An Overview. *In:* DEWITT, J. C. (ed.) *Toxicological Effects of Perfluoroalkyl and Polyfluoroalkyl Substances.* Cham: Springer International Publishing.

LAVEZZI, A. M., OTTAVIANI, G., TERNI, L. & MATTURRI, L. 2006. Histological and biological developmental characterization of the human cerebellar cortex. *International Journal of Developmental Neuroscience,* 24**,** 365-371.

LENTERS, V., ISZATT, N., FORNS, J., CECHOVA, E., KOCAN, A., LEGLER, J., LEONARDS, P., STIGUM, H. & EGGESBO, M. 2019. Early-life exposure to persistent organic pollutants (OCPs, PBDEs, PCBs, PFASs) and attention-deficit/hyperactivity disorder: A multi-pollutant analysis of a Norwegian birth cohort. *Environ Int,* 125**,** 33-42.

LEVITE, M. 2017. Glutamate, T cells and multiple sclerosis. *Journal of Neural Transmission,* 124**,** 775-798.

LIAO, C., DUAN, S. & JIANG, G. 2008. Effect of polybrominated diphenyl ether on development of cultured hippocampal neuron. *Science in China Series B: Chemistry,* 51**,** 62-68.

LIAO, C., WANG, T., CUI, L., ZHOU, Q., DUAN, S. & JIANG, G. 2009. Changes in synaptic transmission, calcium current, and neurite growth by perfluorinated compounds are dependent on the chain length and functional group. *Environ Sci Technol,* 43**,** 2099-104.

LLANSOLA, M., SANCHEZ-PEREZ, A., CAULI, O. & FELIPO, V. 2005. Modulation of NMDA receptors in the cerebellum. 1. Properties of the NMDA receptor that modulate its function. *Cerebellum,* 4**,** 154-61.

LYCHE, J. L., NOURIZADEH-LILLABADI, R., ALMAAS, C., STAVIK, B., BERG, V., SKÅRE, J. U., ALESTRØM, P. & ROPSTAD, E. 2010. Natural mixtures of persistent organic pollutants (POP) increase weight gain, advance puberty, and induce changes in gene expression associated with steroid hormones and obesity in female zebrafish. *J Toxicol Environ Health A,* 73**,** 1032-57.

MAESTRI, L., NEGRI, S., FERRARI, M., GHITTORI, S., FABRIS, F., DANESINO, P. & IMBRIANI, M. 2006. Determination of perfluorooctanoic acid and perfluorooctanesulfonate in human tissues by liquid chromatography/single quadrupole mass spectrometry. *Rapid Commun Mass Spectrom,* 20**,** 2728-34.

MARIUSSEN, E., MYHRE, O., REISTAD, T. & FONNUM, F. 2002. The polychlorinated biphenyl mixture aroclor 1254 induces death of rat cerebellar granule cells: the involvement of the N-methyl-D-aspartate receptor and reactive oxygen species. *Toxicol Appl Pharmacol,* 179**,** 137-44.

MARTIN, O., SCHOLZE, M., ERMLER, S., MCPHIE, J., BOPP, S. K., KIENZLER, A., PARISSIS, N. & KORTENKAMP, A. 2021. Ten years of research on synergisms and antagonisms in chemical mixtures: A systematic review and quantitative reappraisal of mixture studies. *Environment International,* 146**,** 106206.

MATHISEN, G. H., YAZDANI, M., RAKKESTAD, K. E., ADEN, P. K., BODIN, J., SAMUELSEN, M., NYGAARD, U. C., GOVERUD, I. L., GAARDER, M., LOBERG, E. M., BOLLING, A. K., BECHER, R. & PAULSEN, R. E. 2013. Prenatal exposure to bisphenol A interferes with the development of cerebellar granule neurons in mice and chicken. *Int J Dev Neurosci,* 31**,** 762-9.

METCALFE, J. & STOCK, M. K. 1993. Current topic: oxygen exchange in the chorioallantoic membrane, avian homologue of the mammalian placenta. *Placenta,* 14**,** 605-13.
MILLER, K. E. & SUTER, D. M. 2018. An Integrated Cytoskeletal Model of Neurite Outgrowth. *Frontiers in Cellular Neuroscience,* 12.
MITCHELL, M. M., WOODS, R., CHI, L. H., SCHMIDT, R. J., PESSAH, I. N., KOSTYNIAK, P. J. & LASALLE, J. M. 2012. Levels of select PCB and PBDE congeners in human postmortem brain reveal possible environmental involvement in 15q11-q13 duplication autism spectrum disorder. *Environ Mol Mutagen,* 53**,** 589-98.
MONTAÑO, M., ZIMMER, K. E., DAHL, E., BERG, V., OLSAKER, I., SKAARE, J. U., MURK, A. J., ROPSTAD, E. & VERHAEGEN, S. 2011. Effects of mixtures of persistent organic pollutants (POPs) derived from cod liver oil on H295R steroidogenesis. *Food Chem Toxicol,* 49**,** 2328-35.
MOSMANN, T. 1983. Rapid colorimetric assay for cellular growth and survival: application to proliferation and cytotoxicity assays. *J Immunol Methods,* 65**,** 55-63.
MYHRE, O., ZIMMER, K. E., HUDECOVA, A. M., HANSEN, K. E. A., KHEZRI, A., BERNTSEN, H. F., BERG, V., LYCHE, J. L., MANDAL, S., DUALE, N. & ROPSTAD, E. 2021. Maternal exposure to a human based mixture of persistent organic pollutants (POPs) affect gene expression related to brain function in mice offspring hippocampus. *Chemosphere,* 276**,** 130123.
NØST, T. H., SANDANGER, T. M., NIEBOER, E., ODLAND, J. Ø. & BREIVIK, K. 2017. The impacts of emission trends of POPs on human concentration dynamics: Lessons learned from a longitudinal study in Norway (1979–2007). *International Journal of Hygiene and Environmental Health,* 220**,** 776-781.
NOURIZADEH-LILLABADI, R., LYCHE, J. L., ALMAAS, C., STAVIK, B., MOE, S. J., ALEKSANDERSEN, M., BERG, V., JAKOBSEN, K. S., STENSETH, N. C., SKÅRE, J. U., ALESTRØM, P. & ROPSTAD, E. 2009. Transcriptional regulation in liver and testis associated with developmental and reproductive effects in male zebrafish exposed to natural mixtures of persistent organic pollutants (POP). *J Toxicol Environ Health A,* 72**,** 112-30.
NOWAK-SLIWINSKA, P., SEGURA, T. & IRUELA-ARISPE, M. L. 2014. The chicken chorioallantoic membrane model in biology, medicine and bioengineering. *Angiogenesis,* 17**,** 779-804.
NUR, E. K. M. S., QURESHI, M. M., IJAZ, M. K., GALADARI, S. H. & RAZA, H. 2000. Proto-oncogene ras GTPase-linked induction of glutathione-S-transferase by growth factors in PC12 cells. *Int J Oncol,* 16**,** 1043-8.
OAKES, S. G., MARTIN, W. J., LISEK, C. A. & POWIS, G. 1988. Incomplete hydrolysis of the calcium indicator precursor fura-2 pentaacetoxymethyl ester (fura-2 AM) by cells. *Analytical Biochemistry,* 169**,** 159-166.
OLIVER, A. E., BAKER, G. A., FUGATE, R. D., TABLIN, F. & CROWE, J. H. 2000. Effects of temperature on calcium-sensitive fluorescent probes. *Biophys J,* 78**,** 2116-26.
PADHI, B. K., PELLETIER, G., WILLIAMS, A., BERNDT-WEIS, L., YAUK, C., BOWERS, W. J. & CHU, I. 2008. Gene expression profiling in rat cerebellum following in utero and lactational exposure to mixtures of methylmercury, polychlorinated biphenyls and organochlorine pesticides. *Toxicol Lett,* 176**,** 93-103.
PANESAR, H. K., KENNEDY, C. L., KEIL STIETZ, K. P. & LEIN, P. J. 2020. Polychlorinated Biphenyls (PCBs): Risk Factors for Autism Spectrum Disorder? *Toxics,* 8.
PAOLETTI, P., BELLONE, C. & ZHOU, Q. 2013. NMDA receptor subunit diversity: impact on receptor properties, synaptic plasticity and disease. *Nat Rev Neurosci,* 14**,** 383-400.
PAREDES, R. M., ETZLER, J. C., WATTS, L. T., ZHENG, W. & LECHLEITER, J. D. 2008. Chemical calcium indicators. *Methods,* 46**,** 143-51.
PÉREZ, F., NADAL, M., NAVARRO-ORTEGA, A., FÀBREGA, F., DOMINGO, J. L., BARCELÓ, D. & FARRÉ, M. 2013. Accumulation of perfluoroalkyl substances in human tissues. *Environment International,* 59**,** 354-362.

PERKINS, J. T., PETRIELLO, M. C., NEWSOME, B. J. & HENNIG, B. 2016. Polychlorinated biphenyls and links to cardiovascular disease. *Environmental Science and Pollution Research,* 23**,** 2160-2172.
POLAŃSKA, K., JUREWICZ, J. & HANKE, W. 2013. Review of current evidence on the impact of pesticides, polychlorinated biphenyls and selected metals on attention deficit / hyperactivity disorder in children. *International Journal of Occupational Medicine and Environmental Health,* 26**,** 16-38.
PRASANSUKLAB, A., BRIMSON, J. M. & TENCOMNAO, T. 2020. Potential Thai medicinal plants for neurodegenerative diseases: A review focusing on the anti-glutamate toxicity effect. *Journal of Traditional and Complementary Medicine,* 10**,** 301-308.
RADIO, N. M., BREIER, J. M., SHAFER, T. J. & MUNDY, W. R. 2008. Assessment of chemical effects on neurite outgrowth in PC12 cells using high content screening. *Toxicol Sci,* 105**,** 106-18.
RADIO, N. M., FREUDENRICH, T. M., ROBINETTE, B. L., CROFTON, K. M. & MUNDY, W. R. 2010. Comparison of PC12 and cerebellar granule cell cultures for evaluating neurite outgrowth using high content analysis. *Neurotoxicol Teratol,* 32**,** 25-35.
RADIO, N. M. & MUNDY, W. R. 2008. Developmental neurotoxicity testing in vitro: Models for assessing chemical effects on neurite outgrowth. *NeuroToxicology,* 29**,** 361-376.
RAO, M. S., VAN VLEET, T. R., CIURLIONIS, R., BUCK, W. R., MITTELSTADT, S. W., BLOMME, E. A. G. & LIGUORI, M. J. 2019. Comparison of RNA-Seq and Microarray Gene Expression Platforms for the Toxicogenomic Evaluation of Liver From Short-Term Rat Toxicity Studies. *Frontiers in Genetics,* 9.
REISTAD, T., FONNUM, F. & MARIUSSEN, E. 2006. Neurotoxicity of the pentabrominated diphenyl ether mixture, DE-71, and hexabromocyclododecane (HBCD) in rat cerebellar granule cells in vitro. *Archives of Toxicology,* 80**,** 785-796.
RIBATTI, D. 2016. The chick embryo chorioallantoic membrane (CAM). A multifaceted experimental model. *Mech Dev,* 141**,** 70-77.
RIBATTI, D., NICO, B. & BERTOSSI, M. 1993. The development of the blood-brain barrier in the chick. Studies with evans blue and horseradish peroxidase. *Ann Anat,* 175**,** 85-8.
RICE, D. & BARONE, S., JR. 2000. Critical periods of vulnerability for the developing nervous system: evidence from humans and animal models. *Environ Health Perspect,* 108 Suppl 3**,** 511-33.
ROJAS, D. C. 2014. The role of glutamate and its receptors in autism and the use of glutamate receptor antagonists in treatment. *J Neural Transm (Vienna),* 121**,** 891-905.
ROTO, S. M., KWON, Y. M. & RICKE, S. C. 2016. Applications of In Ovo Technique for the Optimal Development of the Gastrointestinal Tract and the Potential Influence on the Establishment of Its Microbiome in Poultry. *Front Vet Sci,* 3**,** 63.
RYAN, J. J. & RAWN, D. F. K. 2014. The brominated flame retardants, PBDEs and HBCD, in Canadian human milk samples collected from 1992 to 2005; concentrations and trends. *Environment International,* 70**,** 1-8.
SACHANA, M., ROLAKI, A. & BAL-PRICE, A. 2018. Development of the Adverse Outcome Pathway (AOP): Chronic binding of antagonist to N-methyl-d-aspartate receptors (NMDARs) during brain development induces impairment of learning and memory abilities of children. *Toxicology and applied pharmacology,* 354**,** 153-175.
SAGIV, S. K., KOGUT, K., GASPAR, F. W., GUNIER, R. B., HARLEY, K. G., PARRA, K., VILLASEÑOR, D., BRADMAN, A., HOLLAND, N. & ESKENAZI, B. 2015. Prenatal and childhood polybrominated diphenyl ether (PBDE) exposure and attention and executive function at 9-12 years of age. *Neurotoxicol Teratol,* 52**,** 151-61.
SANDERS, L. H. & TIMOTHY GREENAMYRE, J. 2013. Oxidative damage to macromolecules in human Parkinson disease and the rotenone model. *Free radical biology & medicine,* 62**,** 111-120.

SCHMIDT, B. Z., LEHMANN, M., GUTBIER, S., NEMBO, E., NOEL, S., SMIRNOVA, L., FORSBY, A., HESCHELER, J., AVCI, H. X., HARTUNG, T., LEIST, M., KOBOLÁK, J. & DINNYÉS, A. 2017. In vitro acute and developmental neurotoxicity screening: an overview of cellular platforms and high-throughput technical possibilities. *Arch Toxicol,* 91**,** 1-33.

SCHMITT, G., PARROTT, N., PRINSSEN, E. & BARROW, P. 2017. The great barrier belief: The blood-brain barrier and considerations for juvenile toxicity studies. *Reprod Toxicol,* 72**,** 129-135.

SECRETARIAT OF THE STOCKHOLM CONVENTION. 2019a. *All POPs listed in the Stockholm Convention.* *http://chm.pops.int/TheConvention/ThePOPs/AllPOPs/tabid/2509/Default.aspx* [Online]. [Accessed 8 January 2021].

SECRETARIAT OF THE STOCKHOLM CONVENTION 2019b. Stockholm Convention on persistent organic pollutions (POPs). http://chm.pops.int/TheConvention/Overview/TextoftheConvention/tabid/2232/Default.aspx.

SECRETARIAT OF THE STOCKHOLM CONVENTION. 2019c. *What are POPs?* *http://chm.pops.int/TheConvention/ThePOPs/tabid/673/Default.aspx* [Online]. [Accessed 8 January 2021].

SECRETARIAT OF THE STOCKHOLM CONVENTION 2019 The PCBs elimination network: the information exchange platform created for the risk reduction of polychlorinated biphenyls (PCBs), http://chm.pops.int/Default.aspx?tabid=3016.

SHINOMIYA, N. & SHINOMIYA, M. 2003. Dichlorodiphenyltrichloroethane suppresses neurite outgrowth and induces apoptosis in PC12 pheochromocytoma cells. *Toxicol Lett,* 137**,** 175-83.

SINGH, A., KUKRETI, R., SASO, L. & KUKRETI, S. 2019. Oxidative Stress: A Key Modulator in Neurodegenerative Diseases. *Molecules,* 24.

SINGH, D., SINGH, P. K., CHAUDHARY, S., MEHLA, K. & KUMAR, S. 2012. Chapter Three - Exome Sequencing and Advances in Crop Improvement. *In:* FRIEDMANN, T., DUNLAP, J. C. & GOODWIN, S. F. (eds.) *Advances in Genetics.* Academic Press.

SLOTKIN, T. A., MACKILLOP, E. A., MELNICK, R. L., THAYER, K. A. & SEIDLER, F. J. 2008. Developmental neurotoxicity of perfluorinated chemicals modeled in vitro. *Environ Health Perspect,* 116**,** 716-22.

SPRATLEN, M. J., PERERA, F. P., LEDERMAN, S. A., RAUH, V. A., ROBINSON, M., KANNAN, K., TRASANDE, L. & HERBSTMAN, J. 2020. The association between prenatal exposure to perfluoroalkyl substances and childhood neurodevelopment. *Environ Pollut,* 263**,** 114444.

STEVENSON, D., WOKOSIN, D., GIRKIN, J. & GRANT, M. H. 2002. Measurement of the intracellular distribution of reduced glutathione in cultured rat hepatocytes using monochlorobimane and confocal laser scanning microscopy. *Toxicol In Vitro,* 16**,** 609-19.

STEWART, P. A. & WILEY, M. J. 1981. Structural and histochemical features of the avian blood-brain barrier. *J Comp Neurol,* 202**,** 157-67.

SULTAN, F. & GLICKSTEIN, M. 2007. The cerebellum: Comparative and animal studies. *Cerebellum,* 6**,** 168-76.

SUNDERLAND, E. M., HU, X. C., DASSUNCAO, C., TOKRANOV, A. K., WAGNER, C. C. & ALLEN, J. G. 2019. A review of the pathways of human exposure to poly- and perfluoroalkyl substances (PFASs) and present understanding of health effects. *Journal of Exposure Science & Environmental Epidemiology,* 29**,** 131-147.

SVARCOVA, A., LANKOVA, D., GRAMBLICKA, T., STUPAK, M., HAJSLOVA, J. & PULKRABOVA, J. 2019. Integration of five groups of POPs into one multi-analyte method for human blood serum analysis: An innovative approach within biomonitoring studies. *Science of The Total Environment,* 667**,** 701-709.

SVINGEN, T. & VINGGAARD, A. M. 2016. The risk of chemical cocktail effects and how to deal with the issue. *Journal of Epidemiology and Community Health,* 70**,** 322.

TAIWO, A. M. 2019. A review of environmental and health effects of organochlorine pesticide residues in Africa. *Chemosphere,* 220**,** 1126-1140.

TAVOLONI, T., STECCONI, T., GALARINI, R., BACCHIOCCHI, S., DÖRR, A. J. M., ELIA, A. C., GIANNOTTI, M., SIRACUSA, M., STRAMENGA, A. & PIERSANTI, A. 2021. BFRs (PBDEs and HBCDs) in freshwater species from Lake Trasimeno (Italy): The singular case of HBCDs in red swamp crayfish. *Science of The Total Environment,* 758**,** 143585.

TEHRAN, D. A. & PIRAZZINI, M. Preparation of Cerebellum Granule Neurons from Mouse or Rat Pups and Evaluation of Clostridial Neurotoxin Activity and Their Inhibitors by Western Blot and Immunohistochemistry. 2018.

TOFIGHI, R., WAN IBRAHIM, W. N., REBELLATO, P., ANDERSSON, P. L., UHLÉN, P. & CECCATELLI, S. 2011. Non-dioxin-like polychlorinated biphenyls interfere with neuronal differentiation of embryonic neural stem cells. *Toxicol Sci,* 124**,** 192-201.

UBLACKER, G. A., JOHNSON, J. A., SIEGEL, F. L. & MULCAHY, R. T. 1991. Influence of glutathione S-transferases on cellular glutathione determination by flow cytometry using monochlorobimane. *Cancer Res,* 51**,** 1783-8.

VALLANO, M. L., LAMBOLEZ, B., AUDINAT, E. & ROSSIER, J. 1996. Neuronal activity differentially regulates NMDA receptor subunit expression in cerebellar granule cells. *J Neurosci,* 16**,** 631-9.

VARGAS, A., ZEISSER-LABOUÈBE, M., LANGE, N., GURNY, R. & DELIE, F. 2007. The chick embryo and its chorioallantoic membrane (CAM) for the in vivo evaluation of drug delivery systems. *Advanced Drug Delivery Reviews,* 59**,** 1162-1176.

VARSHAVSKY, J. R., SEN, S., ROBINSON, J. F., SMITH, S. C., FRANKENFIELD, J., WANG, Y., YEH, G., PARK, J.-S., FISHER, S. J. & WOODRUFF, T. J. 2020. Racial/ethnic and geographic differences in polybrominated diphenyl ether (PBDE) levels across maternal, placental, and fetal tissues during mid-gestation. *Scientific Reports,* 10**,** 12247.

VERNER, M.-A., CHEVRIER, J., NGUETA, G., RAUCH, S., BORNMAN, R. & ESKENAZI, B. 2018. Early-life exposure to p,p'-DDT and p,p'-DDE in South African children participating in the VHEMBE study: An assessment using repeated serum measurements and pharmacokinetic modeling. *Environment international,* 119**,** 478-484.

VINGGAARD, A. M., BONEFELD-JØRGENSEN, E. C., JENSEN, T. K., FERNANDEZ, M. F., ROSENMAI, A. K., TAXVIG, C., RODRIGUEZ-CARRILLO, A., WIELSØE, M., LONG, M., OLEA, N., ANTIGNAC, J.-P., HAMERS, T. & LAMOREE, M. 2021. Receptor-based in vitro activities to assess human exposure to chemical mixtures and related health impacts. *Environment International,* 146**,** 106191.

VIZCAINO, E., GRIMALT, J. O., FERNÁNDEZ-SOMOANO, A. & TARDON, A. 2014. Transport of persistent organic pollutants across the human placenta. *Environment International,* 65**,** 107-115.

VOLPE, J. J. 2009. Cerebellum of the Premature Infant: Rapidly Developing, Vulnerable, Clinically Important. *Journal of child neurology,* 24**,** 1085-1104.

VOOGD, J. & GLICKSTEIN, M. 1998. The anatomy of the cerebellum. *Trends in Neurosciences,* 21**,** 370-375.

VUONG, A. M., XIE, C., JANDAROV, R., DIETRICH, K. N., ZHANG, H., SJÖDIN, A., CALAFAT, A. M., LANPHEAR, B. P., MCCANDLESS, L., BRAUN, J. M., YOLTON, K. & CHEN, A. 2020a. Prenatal exposure to a mixture of persistent organic pollutants (POPs) and child reading skills at school age. *International Journal of Hygiene and Environmental Health,* 228**,** 113527.

VUONG, A. M., YOLTON, K., CECIL, K. M., BRAUN, J. M., LANPHEAR, B. P. & CHEN, A. 2020b. Flame Retardants and Neurodevelopment: an Updated Review of Epidemiological Literature. *Current Epidemiology Reports,* 7**,** 220-236.

VUONG, A. M., YOLTON, K., DIETRICH, K. N., BRAUN, J. M., LANPHEAR, B. P. & CHEN, A. 2018. Exposure to polybrominated diphenyl ethers (PBDEs) and child behavior: Current findings and future directions. *Hormones and Behavior,* 101**,** 94-104.

VUONG, A. M., YOLTON, K., WEBSTER, G. M., SJÖDIN, A., CALAFAT, A. M., BRAUN, J. M., DIETRICH, K. N., LANPHEAR, B. P. & CHEN, A. 2016. Prenatal polybrominated diphenyl ether and perfluoroalkyl substance exposures and executive function in school-age children. *Environmental research,* 147**,** 556-564.

WAN IBRAHIM, W. N., TOFIGHI, R., ONISHCHENKO, N., REBELLATO, P., BOSE, R., UHLÉN, P. & CECCATELLI, S. 2013. Perfluorooctane sulfonate induces neuronal and oligodendrocytic differentiation in neural stem cells and alters the expression of PPARγ in vitro and in vivo. *Toxicol Appl Pharmacol,* 269**,** 51-60.

WANG, S., HU, C., LU, A., WANG, Y., CAO, L., WU, W., LI, H., WU, M. & YAN, C. 2021. Association between prenatal exposure to persistent organic pollutants and neurodevelopment in early life: A mother-child cohort (Shanghai, China). *Ecotoxicology and Environmental Safety,* 208**,** 111479.

WHO 2010. Persistent Organic Pollutants: Impact on Child Health, https://apps.who.int/iris/bitstream/handle/10665/44525/9789241501101_eng.pdf

YADAV, A., AMBER, M., ZOSEN, D., LABBA, N. A., HUIBERTS, E. H. W., SAMULIN ERDEM, J., HAUGEN, F., BERNTSEN, H. F., ZIENOLDDINY, S., PAULSEN, R. E., ROPSTAD, E., CONNOLLY, L. & VERHAEGEN, S. 2021. A human relevant mixture of persistent organic pollutants (POPs) and perfluorooctane sulfonic acid (PFOS) enhance nerve growth factor (NGF)-induced neurite outgrowth in PC12 cells. *Toxicol Lett,* 338**,** 85-96.

ZHANG, L., XU, M., REN, Q., LIU, G., MENG, S., XIAHOU, K., ZHANG, Y., JIANG, N. & ZHOU, W. 2020. Human Induced Pluripotent Stem Cell-Derived Neural Cells from Alzheimer's Disease Patients Exhibited Different Susceptibility to Oxidative Stress. *Stem Cells and Development,* 29**,** 1444-1456.

ZHANG, L., YIN, S., ZHAO, Y., SHI, Z., LI, J. & WU, Y. 2017. Polybrominated diphenyl ethers and indicator polychlorinated biphenyls in human milk from China under the Stockholm Convention. *Chemosphere,* 189**,** 32-38.

ZHENG, G., SCHREDER, E., DEMPSEY, J. C., UDING, N., CHU, V., ANDRES, G., SATHYANARAYANA, S. & SALAMOVA, A. 2021. Per- and Polyfluoroalkyl Substances (PFAS) in Breast Milk: Concerning Trends for Current-Use PFAS. *Environmental Science & Technology*.

ZIMMER, K. E., MONTAÑO, M., OLSAKER, I., DAHL, E., BERG, V., KARLSSON, C., MURK, A. J., SKAARE, J. U., ROPSTAD, E. & VERHAEGEN, S. 2011. In vitro steroidogenic effects of mixtures of persistent organic pollutants (POPs) extracted from burbot (Lota lota) caught in two Norwegian lakes. *Sci Total Environ,* 409**,** 2040-8.

9 Papers I-IV

PAPER I

Reproductive Toxicology 100 (2021) 109–119

Contents lists available at ScienceDirect

Reproductive Toxicology

journal homepage: www.elsevier.com/locate/reprotox

A human relevant mixture of persistent organic pollutants (POPs) and perfluorooctane sulfonic acid (PFOS) differentially affect glutamate induced excitotoxic responses in chicken cerebellum granule neurons (CGNs) in vitro

Ajay Yadav [a,b,*], Steven Verhaegen [a], Evelien Verbruggen [b], Marie Kerhoas [b], Eva Henriëtte Willemijn Huiberts [b], Mussie Ghezu Hadera [b], Hanne Friis Berntsen [a,c], Karin Elisabeth Zimmer [d], Erik Ropstad [a], Ragnhild Elisabeth Paulsen [b]

[a] Department of Production Animal Clinical Sciences, Norwegian University of Life Sciences, P.O. Box 369 Sentrum, NO-0102, Oslo, Norway
[b] Section for Pharmacology and Pharmaceutical Biosciences, Department of Pharmacy, University of Oslo, P.O. Box 1068, Blindern, NO-0316, Oslo, Norway
[c] National Institute of Occupational Health, P.O. Box 5330 Majorstuen, NO-0304, Oslo, Norway
[d] Department of Preclinical Sciences and Pathology, Norwegian University of Life Sciences, P.O. Box 369 Sentrum, NO-0102, Oslo, Norway

ARTICLE INFO

Keywords:
Developmental neurotoxicity
Glutathione
Intracellular calcium
NMDA-R
NMDA-R antagonists

ABSTRACT

Primary cultures of cerebellar granule neurons (CGNs) derived from chicken embryos were used to explore the effects on developmental neurotoxicity by a complex defined mixture of persistent organic pollutants (POPs). Its chemical composition and concentrations were based on blood levels in the Norwegian/Scandinavian population. Perfluorooctane sulfonic acid (PFOS) alone, its most abundant compound was also evaluated. Different stages of CGNs maturation, between day *in vitro* (DIV) 1, 3, and 5 were exposed to the POP mixture, or PFOS alone. Their combination with glutamate, an excitatory endogenous neurotransmitter important in neurodevelopment, also known to cause excitotoxicity was evaluated. Outcomes with the mixture at 500x blood levels were compared to PFOS at its corresponding concentration of 20 μM. The POP mixture reduced tetrazolium salt (MTT) conversion at earlier stages of maturation, compared to PFOS alone. Glutamate-induced excitotoxicity was enhanced above the level of that induced by glutamate alone, especially in mature CGNs at DIV5. Glutathione (GSH) concentrations seemed to set the level of sensitivity for the toxic insults from exposures to the pollutants. The role of N-methyl-D-aspartate receptor (NMDA-R) mediated calcium influx in pollutant exposures was investigated using the non-competitive and competitive receptor antagonists MK-801 and CGP 39551. Observations indicate a calcium-independent, but still NMDA-R dependent mechanism in the absence of glutamate, and a calcium- and NMDA-R dependent one in the presence of glutamate. The outcomes for the POP mixture cannot be explained by PFOS alone, indicating that other chemicals in the mixture contribute its overall effect.

1. Introduction

Exposures in humans to complex mixtures of contaminants are suspected to cause adverse health outcomes. Increased prevalence of neurodevelopmental disorders, such as autism, attention-deficit hyperactivity disorder (ADHD), dyslexia, and other cognitive impairments have been linked with exposure to environmental pollutants [1]. Pregnancy and early life stages are particularly vulnerable for exposure to toxicants, including persistent organic pollutants (POPs) [2]. POPs are mostly halogenated compounds that are highly resistant to environmental degradation, and that bioaccumulate and biomagnify in living organisms [3]. Several POPs, including polychlorinated biphenyls (PCBs), organochlorine pesticides (OCPs), polybrominated diphenyl ethers (PBDEs), perfluorooctane sulfonic acid (PFOS), and

* Corresponding author at: Department of Production Animal Clinical Sciences, Norwegian University of Life Sciences, P.O. Box 369 Sentrum, NO-0102, Oslo, Norway.
E-mail addresses: ajay.yadav@nmbu.no (A. Yadav), steven.verhaegen@nmbu.no (S. Verhaegen), evelien.verbruggen@scarlet.be (E. Verbruggen), kerhoas.marie@gmail.com (M. Kerhoas), eva.huiberts@hotmail.com (E.H. Willemijn Huiberts), mughezu@gmail.com (M.G. Hadera), Hanne.Berntsen@stami.no (H.F. Berntsen), karin.zimmer@nmbu.no (K.E. Zimmer), erik.ropstad@nmbu.no (E. Ropstad), r.e.paulsen@farmasi.uio.no (R.E. Paulsen).

https://doi.org/10.1016/j.reprotox.2021.01.008
Received 12 May 2020; Received in revised form 14 December 2020; Accepted 18 January 2021
Available online 23 January 2021
0890-6238/© 2021 The Author(s). Published by Elsevier Inc. This is an open access article under the CC BY license (http://creativecommons.org/licenses/by/4.0/).

perfluorooctanoic acid (PFOA) are supposed to be developmental neurotoxicants [1,4–6].

Human populations are exposed to a complex mixture of contaminants, which could have additive, synergistic or antagonistic effects. Experimental studies carried out *in vitro* and *in vivo* with mixtures showed that low-level exposure to chemicals that are not toxic on an individual basis can together lead to a biological or toxic effect if present in a mixture [7]. This kind of low-dose cocktail or mixture effects are of real concern to humans. Chemicals affecting similar adverse outcomes often act additively when present together in mixtures [8]. Chemical mixtures have often been defined by the modes of action of individual components and three basic types of action have been identified, namely: (I) *similar action* (dose or concentration addition): applied to mixtures in which the chemicals present have a similar mechanism/mode of action and may differ in their potencies (*i.e.* the impact of similar concentrations/doses will differ). In this case the effects of the mixture can be estimated directly from sum of the doses/concentrations, scaled for relative toxicity/potency of the individual substances. (II) *Dissimilar action* (independent action): applied to chemicals with dissimilar modes of action. In this case the action of mixture components can be calculated from the response of individual components (response addition) or the sum of biological responses (effects addition). (III) *Interactions* (synergism and antagonism): applied if the combined effect of two or more chemicals is either stronger (synergistic, potentiating, supra-additive) or weaker (antagonistic, inhibitive, sub-additive, infra-additive) than would be expected on the basis of dose/concentration addition or response addition. In this case the extent of interactions may vary according to the relative dose levels (*e.g.* too low to have such an effect); route of exposure (*e.g.* absorption too low or different metabolism); duration of exposure (including bio-persistence of components); and biological target [9–11].

Studies have shown that there is exposure to POPs in humans as wells in animals. In a Norwegian birth cohort study, concentrations of 27 POPs were reported in breast milk, reflecting the child's early-life exposures, and certain POPs were associated with a neurodevelopmental disorder [12]. Flores-Ramírez et al. [13] showed the levels of multiple POPs in serum samples from children living in high-risk areas in Mexico, indicating that the evaluation of the health risks posed to children living in contaminated areas is a high priority health issue. In another study, González-Mille et al. [14] reported the genotoxic effects in resident wild species exposed to complex mixture of POPs in the delta of the Coatzacoalcos river, Mexico. In the present study, we used a defined POP mixture designed by our group at the Norwegian University of Life Sciences (NMBU), Oslo. The concentration of the individual compounds was based on their respective levels in human blood in the Norwegian/Scandinavian population [15]. PFOS is the compound with the highest concentration present in the total POP mixture and a potent developmental neurotoxicant. In a multi-pollutant analysis of 27 POPs in a Norwegian birth cohort study, early-life exposure to β-hexachlorocyclohexane (HCH) and PFOS was associated with increased risk of ADHD [12]. Recently, European population-based studies including Human Milk Study (HUMIS; Norway) suggested that there may be an increased prevalence of ADHD in girls, in children from nulliparous women, and in children from low-educated mother in association with PFOS and PFOA exposure [16]. Also, our PFOS concentration is comparable to reported concentrations of 20 μM (lowest observed effect concentration) and 38 μM (lethal concentration killing 50 % of the cells) using tetrazolium salt (MTT) assay in rat CGNs [17], and all other component in the mixture had a concentration lower than its effective dose range. We have previously examined the toxicity of each individual PFAAs compounds in the POP mixture in cultured rat CGNs [18]. We observed that the two sulfonated-induced, but not perfluoroalkyl carboxylic acid-induced toxicity was associated with N-methyl-D-aspartate receptor (NMDA-R) and PFOS was the most effective on NMDA-R [18]. This receptor plays an important role in cerebellar development [19]. Here it should be pointed out that in the present study we used PFOS as a single compound with a concentration, which overlaps the concentration of the POP mixture

In addition to its role in motor control and coordination, the cerebellum is involved in learning and memory, language, executive functioning, as well as diseases such as ADHD, autism spectrum disorders, and schizophrenia [20]. The embryonic chicken cerebellum can be used as a model, since it shows developmental stages similar to those in humans [19]. Cerebellar granule neurons (CGNs) form the largest homogeneous neuronal population in the mammalian brain, and are the main excitatory neurons of the cerebellar cortical circuitry [21]. The comparative anatomy studies have shown that the cerebellum is a well-conserved structure between species [22]. The migration of granule neurons through layers of the cerebellar cortex from the external granule layer to the internal granule layer is a key feature for the development of cerebellum. This occurs prenatally before hatching in chicken and to a large extent postnatally in some mammals, including humans [19]. The migration of neurons in a developing brain is guided through N-methyl-D- aspartate receptors (NMDA-R) mediated Ca^{2+} influx, among other signals [23]. Alterations in migration could be indicative of impaired neurodevelopment [19]. CGNs isolated at embryonic day (ED) 17–18 from chicken is comparable to postnatal day 7–8 in the rat [24]. In addition, cultured chicken CGNs develops NMDA-mediated toxicity more rapidly than cultured rat CGNs and respond similarly to glutamate excitotoxicity with ROS production and activation of caspase-3 [24]. CGNs derived from chicken cerebellum serve to study brain development after exposure to different pharmaceuticals, drugs [25–28] and environmental toxins [29]. This is an advantage when considering chicken embryo CGNs as a model for NMDA receptor development and thus makes the cerebellum a potential target organ for developmental toxicity (DNT) induced by POPs.

Glutamate is a major excitatory neurotransmitter in the vertebrate central nervous system (CNS) and under normal circumstances contributes to neural transmission, development, differentiation and plasticity. However, under pathological stimuli excessive glutamate release leads to overactivation of glutamate receptors, resulting in an augmented intracellular Ca^{2+}-influx [30]. This can lead to excitotoxicity, resulting in neuronal death [31,32]. Excitotoxicity is involved in many neurodegenerative diseases such as Huntington's disease, Alzheimer's disease, lateral amyotrophic sclerosis, Parkinson's disease, stroke, or traumatic brain injury [30]. Among different types of glutamate receptors, the N-methyl-D-aspartate receptor (NMDA-R) plays an important role in mediating neuronal death observed in most primary cultured neurons [33]. In CGNs intracellular glutathione (GSH) plays a major role in protecting cells against injury caused by reactive oxygen species (ROS) following excitotoxic insults [34]. A reduction in GSH level can lead to glutamate-induced cell death [35]. Calcium influx plays a critical role in glutamate-induced neurotoxicity [32]. NMDA-R channels are highly Ca^{2+}-permeable and function as heterotetrameric assemblies that typically consist of GluN1 and GluN2 subunits, or GluN2 and GluN3 subunits. The subunit composition of NMDA-Rs changes during development in response to neuronal activity or sensory experiences [36]. Also, *in vitro* the expression of the NMDA-R subunits changes with time and maturation of CGNs [37]. Because of this previously reported time-dependent changes in NMDA-R subunits expression, we conducted the present study at different stages of maturation at day *in vitro* (DIV) 1, 3 and 5. We assume that neuronal cells exposed at DIV5 to express more mature and more sensitive neurons than cells exposed at DIV1 or 3.

A role of NMDA-R in the excitotoxity after exposure to same POP mixture, and PFOS have been shown in rat CGNs as well in chicken CGNs [18,38].The possible involvement of NMDA-Rs in excitotoxicity may be explored by using NMDA-R inhibitors. MK-801 is a non-competitive NMDA-R open channel blocker and binding sites are situated within the ion channel [39,40]. CGP-39551 is a competitive antagonist that binds to the glutamate binding site of the receptor [41].

The hypothesis of the present work was that a complex human

Table 1
The total *in vitro* mixture containing 29 different POPs based on human blood levels, detailed in [15].

Compound	Average human blood levels [a] ng/g lipid	Average human blood levels [b] ng/mL	Total mixture stock nominal concentration [c] mg/mL	Total mixture stock Measured concentration [d] μM
PCBs				
PCB 28	2.13	0.013	0.013	31.1
PCB 52	1.6	0.01	0.01	20.5
PCB 101	1.3	0.008	0.008	24.5
PCB 118	10.67	0.064	0.064	137.9
PCB 138	37	0.222	0.222	429.5
PCB 153	60.33	0.362	0.362	698.3
PCB 180	32.33	0.194	0.194	339
∑ PCBs	145.36	0.873	0.873	1680.8
OCPs				
p,p'-DDE	83.67	0.502	0.502	1065.9
HCB	19.5	0.117	0.117	228.2
α-Chlordane	1.8	0.011	0.011	23.7
Oxychlordane	3.7	0.022	0.022	33
trans-Nonachlor	6.8	0.041	0.041	99.1
α-HCH	1	0.006	0.006	16.8
β-HCH	8.77	0.053	0.053	75.6
γ-HCH	1	0.006	0.006	16.8
Dieldrin	4	0.024	0.024	56.2
∑ OCPs	130.24	0.782	0.782	1615.3
∑ PCBs + OCPs	275.6	1.655	1.655	3296.1
BFRs				
PBDE 47	1.43	0.009	0.009	17.8
PBDE 99	0.59	0.004	0.004	7.5
PBDE 100	0.36	0.002	0.002	3.8
PBDE 153	1.64	0.01	0.001*	2.1
PBDE 154	0.29	0.002	0.002	3
PBDE 209	1.81	0.011	0.011	9.4
HBCD	4.1	0.025	0.025	54.5
∑ BFRs	10.22	0.063	0.053	98.1
PFAAs				
PFHxS	N/A	3.45	3.45	7809.2
PFOS	N/A	29.425	29.425	41522.1
PFOA	N/A	4.523	4.523	4209.4
PFNA	N/A	0.8	0.8	1092.5
PFDA	N/A	0.495	0.495	375.4
PFUnDA	N/A	0.56	0.56	336.8
∑ PFAAs	N/A	39.253	39.253	55345.4

N/A - Not applicable.
Abbreviations: PCBs (polychlorinated biphenyls); OCPs (organochlorine pesticides); BFRs (brominated flame retardants); PFAAs (perfluoroalkyl acids).
[a] Average human blood levels of POPs based on a literature review of Scandinavian values, providing the basis for the *in vitro* mixture.
[b] Average human blood levels of POPs converted to ng/mL. A fat percentage of 0.6 % was used. 1 mL blood was considered to have a weight of 1 g.
[c] Nominal concentration of the various compounds in the total mixture stock – 1000000x the average concentration in blood.
[d] Measured concentrations of the various compounds in the total mixture stock converted to μM.
[*] The nominal concentration of PBDE 153 included in the total mixture stock was ten times lower than originally intended.

relevant POP mixture with defined chemical composition and concentrations could affect NMDA-R signaling and downstream calcium influx, glutathione level, and excitotoxicity, and that the mixture would share some mechanisms with PFOS, a main component of the mixture.

2. Materials and methods

2.1. Chemicals and PFOS, and POP mixture

Basal Eagle's medium (BME) and L-glutamine were purchased from Lonza BioWhittaker (Verviers, Belgium). Penicillin-streptomycin and chicken serum were acquired from Gibco, Life Technologies (Paisley, UK). Dimethyl sulfoxide (DMSO), monochlorobimane (mBCl), cytosine β-D-arabinofuranoside (Ara-C), MK-801, Poly-L-lysine and thiazolyl blue tetrazolium bromide (MTT) powder were all obtained from Sigma-Aldrich (St. Louis, US). Fura-2 AM and Hoechst 33342 were purchased from Invitrogen™ Molecular Probes (Eugene, US). CGP 39551 was from Novartis (Basel, Switzerland). Perfluorooctanesulfonic acid potassium salt (PFOS ≥ 98 %) was purchased from Sigma-Aldrich (St. Louis, MO USA). All other reagents were standard laboratory grade.

The defined POP mixture was designed and prepared by our group at the Norwegian University of Life Sciences (NMBU), Oslo (Norway), detailed in [15]. It contains 29 different compounds: six perfluorinated compounds, seven brominated compounds, and 16 chlorinated compounds (Table 1). The concentrations of the chemicals in the mixture were based on Scandinavian human blood levels. The stocks used in the present study had a concentration of 10^6 times human blood levels and stocks were created using DMSO as a solvent. Working stocks were prepared by creating suitable dilutions in DMSO in glass vials at concentrations 1000 times higher than the final exposure concentrations in the medium of 500x, where x indicates 'times human blood concentrations'. Vials were stored in −80 °C. For MTT conversion and glutathione measurements cells in the culture were exposed to test compounds for 24 h and for intracellular calcium measurements for 90 min.

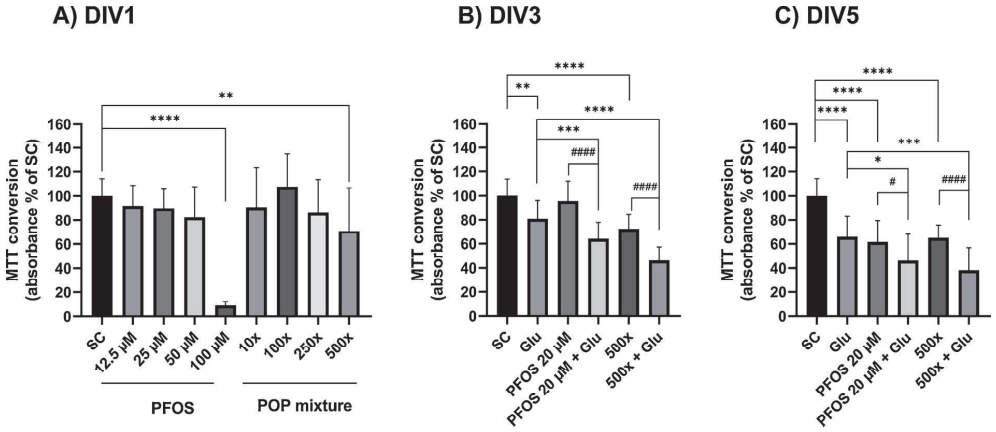

Fig. 1. Assessment of cytotoxicity in CGNs at DIV1 (A) or DIV3 (B) or DIV5 (C) using the tetrazolium MTT conversion assay. CGNs were exposed for 24 h to solvent control (SC, 0.1 % DMSO), glutamate (Glu), 100 µM (together with 10 µM glycine as co-agonist), PFOS (in µM) or POP mixture (x fold human blood levels), alone or in the presence of glutamate. All values were presented relative to the SC (defined as 100 %). Data are mean ± SD, n = 3 to 4 independent experiments (from separate cell isolates), each with replicates >4 per group/exposure, *p < 0.05, **p < 0.01, ***p < 0.001, ****p < 0.0001 one-way ANOVA followed by Dunnett's multiple comparisons test, #p < 0.05, ####p < 0.0001 unpaired *t*-test.

2.2. Chicken egg incubation and isolation of cerebellar granule neurons (CGNs)

Eggs (*Gallus gallus*, weight 50–60 g) were obtained from Nortura Samvirkekylling (Våler, Norway) and incubated at 37.5 °C in 45 % relative humidity in an OvaEasy 380 Advance EXII Incubator (Brinsea, Weston-super-Mare, UK). In accordance with the 3R principles, the mother is excluded from the experiments and the number of fertilized eggs is easy to control. The viability of the embryos was checked with trans-illumination using a LED lamp (Brinsea) by observing spontaneous movement. Cultures of cerebellar granule neurons (CGNs) were prepared on Embryonic Day (ED) 17. The embryos *in ovo* were anaesthetized for 7 min by hypothermia in crushed ice, prior to decapitation. Animals were handled in accordance with the Norwegian Animal Welfare Act and the EU directive 2010/63/EU. The granule neurons were isolated as previously described [42]. Cells for each isolation were obtained from the pooled cerebella of 15–18 chicken embryos and diluted to a centration of 1.8×10^6 cells/mL. From each isolation, 4–6 replicates (sister wells) were prepared per exposure. Each isolation was considered as one independent experiment. In total of 3–4 independent experiments from separate cell isolates were performed. After isolation, cells were seeded onto poly-L-lysine-coated (0.01 mg/mL) dishes (diameter 35 mm) or 96 well plates in BME supplemented with chicken serum (7.5 %), KCl (25 mM), L-glutamine (2 mM), insulin (100 nM) and penicillin-streptomycin (1%) at 37 °C and 5% CO_2 for 24 h. Then the medium was replaced with serum-free BME as described previously [29] supplemented with Ara-C (10 µM) to prevent growth of non-neuronal cells. Cultures contained about 70–80 % neurons. The neurons were exposed with the test compounds on day *in vitro* (DIV) 1, 3 and 5, and then left undisturbed in an incubator until further analysis. For all the assays cells were seeded on the same day DIV0 (day of platting). MTT DIV1 experiment was performed only to find the cytotoxic concentration-range for the POP mixture and PFOS. Based on this a concentration of 500x human blood levels for POP mixture and the corresponding concentration of 20 µM PFOS was used for further mechanistic studies on DIV3 and DIV5.

2.3. Quantification of cell viability by tetrazolium MTT conversion assay

The MTT assay procedure has been described previously [18]. It is based on the conversion of 3-(4,5-dimethylthiazol-2-yl)-2,5-diphenyl tetrazolium bromide (MTT), a pale yellow substrate to a dark blue formazan product by the mitochondrial enzyme succinate dehydrogenase in living cells [43]. MTT was prepared freshly as a stock solution of 5 mg/mL in PBS. DIV1, 3 or 5 cultures were exposed for a further 24 h with the test compounds after which 10 µl MTT stock solution was added to each well of the 96 well plate and subsequently incubated at 37 °C for 3–4 h. Afterwards, the MTT-solution was replaced with 100 µl DMSO/well for dissolution of the formazan salt and after 30 min absorbance was measured at 570 nm in a CLARIOstar® microplate reader (BMG Labtech, Ortenberg, BW, Germany). The average of background value from wells containing cells without MTT, was subtracted from the final optical density. Cell viability was measured as a percentage absorbance of the sample compared with the absorbance of the solvent control.

2.4. Glutathione measurements using monochlorobimane (mBCl) fluorescent probe

Total reduced glutathione (GSH) levels in CGNs were measured with monochlorobimane (mBCl) as described previously [44]. mBCl is a non-fluorescent probe and forms a stable fluorescent conjugate with GSH in a reaction catalyzed by the GSH S-transferases [45]. In brief, cells were seeded in black 96 wells plates and were exposed at DIV3 or DIV5 with the test compounds for 24 h. Then medium was removed and replaced with new medium containing 40 µM of mBCl and incubated further in the dark at 37 °C for 30 min. Subsequently the medium was removed. Plates were washed with freshly prepared experimental buffer containing 140 mM NaCl, 3.5 mM KCl, 15 mM Tris HCl (pH 7.4), 5 mM glucose, 1.2 mM Na_2HPO_4 (pH 7.4), and 2 mM $CaCl_2$. Hundred µl of the buffer was added to each well, and mBCl fluorescence was measured at excitation wavelength of 380 nm (15 nm bandwidth) and emission wavelength of 478 nm (21 nm bandwidth) using a CLARIOstar® plate reader. Further, in the same exposure, we also quantified cell number using nuclei staining with Hoechst 33342. Buffers were replaced with Hoechst 33342 (0.4 µg/mL) and incubated in dark for 1 min. Subsequently, the plate was read at excitation wavelengths of 350 nm (22 nm bandwidth) and emission wavelengths of 461 nm (36 nm bandwidths). This measurement was used to correct for cell number in the calculations for GSH levels after subtraction of blank values.

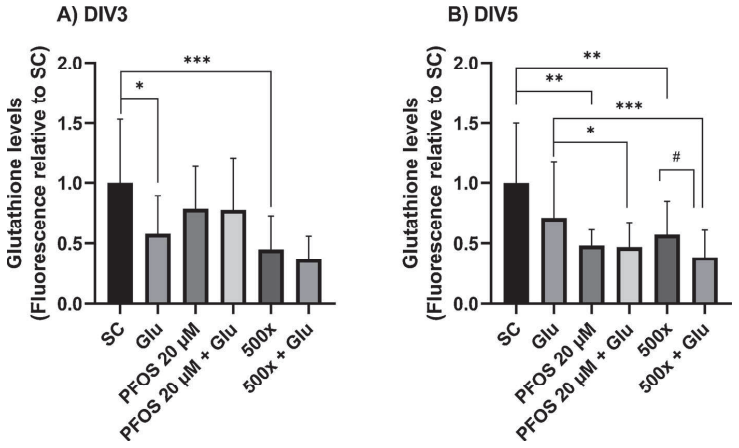

Fig. 2. Assessment of glutathione levels in CGNs at DIV3 (A) or DIV5 (B) using mBCl assay. CGNs were exposed for 24 h to solvent control (SC, 0.1 % DMSO), glutamate (Glu) 100 µM (together with 10 µM glycine as co-agonist), PFOS 20 µM, or POP mixture (500x fold human blood levels), alone or in the presence of glutamate. All values were presented relative to the SC (defined as 1). Data are mean ± SD, n = 3 to 4 experiments (from separate cell isolates), each with replicates >4 per group/exposure, *p < 0.05, **p < 0.01, ***p < 0.001, one-way ANOVA following Dunnett's multiple comparisons test, #p < 0.05 unpaired *t*-test.

2.5. Measurement of intracellular calcium concentrations using Fura-2 AM

The procedure has been described previously [44], with minor modifications. In brief, CGNs were seeded in CELLBIND® 96-Well Microplates, Corning® (Corning Incorporated, Kennebunk, ME, US). On DIV3 or DIV5 cells were loaded with the membrane permeable Ca^{2+}-binding fluorescent probe Fura-2 AM (5.2 µM) in medium and incubated at 37 °C for 40 min. Then the medium was replaced with experimental buffer supplemented with 1 mM $MgSO_4$ (wash buffer) for de-esterification. After 15 min of incubation baseline $[Ca^{2+}]_i$ value was measured at excitation wavelengths 340 nm and 380 nm (12 nm bandwidths) and emission at 510 nm (30 nm bandwidths) using orbital averaging. Subsequently, wash buffer was replaced with test compounds in experimental buffer and $[Ca^{2+}]_i$ value was measured 90 min post treatment. For calculation, the average $[Ca^{2+}]_i$ value obtained at 90 min after treatment was expressed relative to the average $[Ca^{2+}]_i$ value obtained prior to treatment (baseline value) at time point 0 (set to 1). Average of background autofluorescence from wells containing cells without Fura-2 AM were subtracted from excitations at 340 nm and 380 nm before the 340/380 ratio was calculated.

2.6. Statistical analysis

Results are presented as mean ± standard deviation (SD) from n = 3 to 4 independent experiments (from separate cell isolates), each with replicates >4 per group/exposure. So, the total sample size for the calculation of SD was 12–16 replicates. Data was analyzed using Microsoft Excel in addition to Graph pad 8.2 (San Diego, CA). Outlier values were tested for by the built-in feature in GraphPad (Robust regression and Outlier removal, Q = 1%). A one-way analysis of variance (ANOVA) followed by Dunnett's multiple comparison test was used to determine significant differences between treatments and the corresponding control. An unpaired *t*-test was used for comparison when appropriate between two groups. A p-value of < 0.05 was considered significant.

3. Results

3.1. Effects of POP mixture or PFOS on viability in CGNs

To explore the influence of CGNs maturation on exposure outcomes, CGNs at DIV1, DIV3, and DIV5 were used. Cell viability was evaluated by mitochondrial activity as measured by MTT (Fig. 1A-C). On DIV1, in the absence of glutamate a significant reduction in MTT was seen only at 500x by 29 % (P < 0.01) as compared to solvent control. At DIV1, PFOS only reduced MTT activity by 91 % (P < 0.0001) at 100 µM. Concentrations of PFOS in the 20 µM range did not show significant loss of MTT activity before DIV5. Therefore, a concentration of 500x was used for the POP mixture and the corresponding concentration of 20 µM PFOS was used in further studies. In the presence of glutamate, the effect of PFOS already became significant with a reduction of 33 % (P < 0.0001) at DIV3 or by 25 % (P < 0.05) at DIV5, when compared to PFOS alone; and by 21 % (P < 0.001) at DIV3 or by 30 % (P < 0.05) at DIV5 as compared to glutamate (Fig. 1B, C). For the POP mixture MTT activity was significantly reduced by 28 % (P < 0.0001) at DIV3, and by 35 % (P < 0.0001) at DIV5, when compared to solvent control (Fig. 1B, C). Again, in the presence of glutamate this reduction was more pronounced (Fig. 1B, C). In the presence of glutamate, the POP mixture led to a further significant reduction by 36 % (P < 0.0001) at DIV3 or by 41 % (P < 0.0001) at DIV5, when compared to POP mixture alone; and by 43 % (P < 0.0001) at DIV3 or by 42 % (P < 0.001) at DIV5, when compared to glutamate.

3.2. Effects of POP mixture or PFOS on the depletion of intracellular glutathione levels in CGNs

Intracellular levels of glutathione determine the sensitivity of CGNs against chemical induced cytotoxicity. Thus, we tested if the exposures resulted in depletion of the glutathione levels (Fig. 2A, B). Glutamate led to a decrease in glutathione level on both DIV3 and DIV5 by 42 % (P < 0.05 significantly) and by 29 % (P < 0.09 non-significantly), respectively as compared to solvent control. PFOS led to decrease in glutathione levels which were more pronounced on DIV5 and caused a significant reduction by 52 % (P < 0.01), when compared to solvent control. Similarly, the POP mixture resulted in decreased levels of glutathione on both days by 55 % (P < 0.001) at DIV3 and by 43 % (P < 0.01) at DIV5 as compared to solvent control. The combination with glutamate did not alter the effect compared to PFOS alone. However, when combined with the POP mixture a further reduction in intracellular glutathione levels by 18 % (non-significantly) at DIV3 or by 32 % (P < 0.05) at DIV5 as compared to POP mixture was seen; and by 36 % (non-significantly) at DIV3 or by 45 % (P < 0.001) at DV5, when compared to glutamate alone.

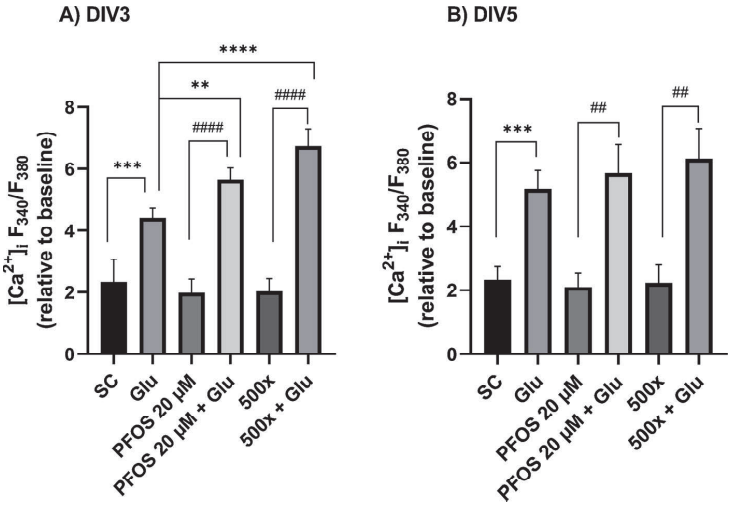

Fig. 3. Intracellular Ca^{2+} measurements in CGNs at DIV3 (A) or DIV5 (B) using Fura-2 AM assay. CGNs were exposed for 90 min to solvent control (SC, 0.1 % DMSO), glutamate (Glu) 100 µM (together with 10 µM glycine as co-agonist), PFOS 20 µM, or POP mixture (500x fold human blood levels), alone or in the presence of glutamate. Before exposure, baseline $[Ca^{2+}]_i$ was measured at time 0. The baseline was set to 1. Cells were exposed to test compounds for 90 min. Measured $[Ca^{2+}]_i$ were expressed relative to the baseline. Data are mean ± SD, n = 3 to 4 experiments (from separate cell isolates), each with replicates >4 per group/exposure, $^{**}p < 0.01$, $^{***}p < 0.001$, $^{****}p < 0.0001$ one-way ANOVA followed by Dunnett's multiple comparisons test, $\#\#p < 0.01$, $\#\#\#\#p < 0.0001$ unpaired *t*-test.

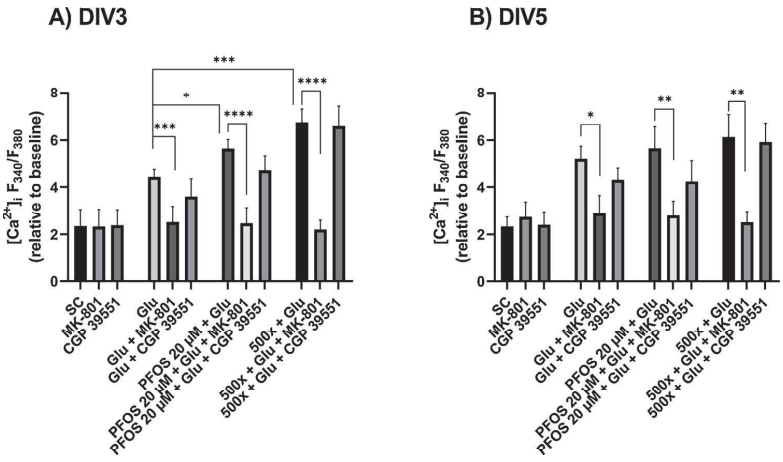

Fig. 4. Intracellular Ca^{2+} measurements in CGNs at DIV3 (A) or DIV5 (B) using Fura-2 AM assay. CGNs were exposed for 90 min to solvent control (SC, 0.1 % DMSO), glutamate (Glu) 100 µM (together with 10 µM glycine as co-agonist), PFOS 20 µM, or POP mixture (500x fold human blood levels) alone or in the presence of glutamate. Cells were treated in the presence and absence of the open NMDA-R channel blocker MK-801 (5 µM) or the competitive NMDA-R antagonist CGP 39551 (100 µM). Before exposure, baseline $[Ca^{2+}]_i$ were measured at time 0. The baseline was set to 1. Cells were exposed to test compounds for 90 min. Measured $[Ca^{2+}]_i$ were expressed relative to the baseline. Datapoints for SC, Glu, PFOS 20 µM + Glu, and 500x + Glu, are identical to Fig. 3. Data are mean ± SD, n = 3 to 4 experiments (from separate cell isolates), each with replicates >4 per group/exposure, $^{*}p < 0.05$, $^{**}p < 0.01$, $^{***}p < 0.001$, $^{****}p < 0.0001$ one-way ANOVA followed by Dunnett's multiple comparisons test.

3.3. Effects of POP mixture or PFOS on intracellular Ca^{2+} concentration in CGNs

Since glutamate excitotoxicity raises intracellular calcium levels, we measured $[Ca^{2+}]_i$ using the Fura-2 AM fluorescent probe following exposures at DIV3 and 5 (Fig. 3A, B). As expected, glutamate alone induced a significant increase in $[Ca^{2+}]_i$ by 89 % ($P < 0.001$) at DIV3 or by 122 % ($P < 0.001$) at DIV5, when compared to solvent control. In contrast, neither PFOS, nor the POP mixture alone were able to increase $[Ca^{2+}]_i$. However, in combination with glutamate they caused a further, significant increase in $[Ca^{2+}]_i$. PFOS in combination with glutamate caused a significant increase in $[Ca^{2+}]_i$ by 185 % ($P < 0.0001$) at DIV3 or by 168 % ($P < 0.01$) at DIV5, when compared to PFOS alone; and POP mixture by 232 % ($P < 0.0001$) at DIV3 or by 174 % ($P < 0.01$) at DIV5, when compared to POP mixture alone.

3.4. Effects of POP mixture or PFOS on intracellular Ca^{2+} concentration in CGNs in combination with NMDA-R antagonists

To examine whether the increases in $[Ca^{2+}]_i$ seen in Fig. 3 could be the results of influx *via* the NMDA-R, we tested the effect of two NMDA-R antagonists, the non-competitive, open channel blocker MK-801 or the competitive antagonist CGP 39551 (Fig. 4A, B).

Neither antagonists alone affected $[Ca^{2+}]_i$ as compared to solvent control on any of the days. In the presence of MK-801, glutamate induced $[Ca^{2+}]_i$ was significantly reversed to control levels on both days ($P < 0.001$ at DIV3 and $P < 0.05$ at DIV5). The reduction by CGP 39551 was less efficient (non-significant). Interestingly, on both DIV3 and 5, MK-801 was capable of reversing the $[Ca^{2+}]_i$ to control levels for both PFOS or the POP mixture combined effect with glutamate. At either of the days, CGP 39551 also reduced $[Ca^{2+}]_i$, induced by the combined effect of PFOS and glutamate, but not statistically significant. CGP 39551 showed no inhibition effect on $[Ca^{2+}]_i$ induced by the combined effect of POP mixture and glutamate.

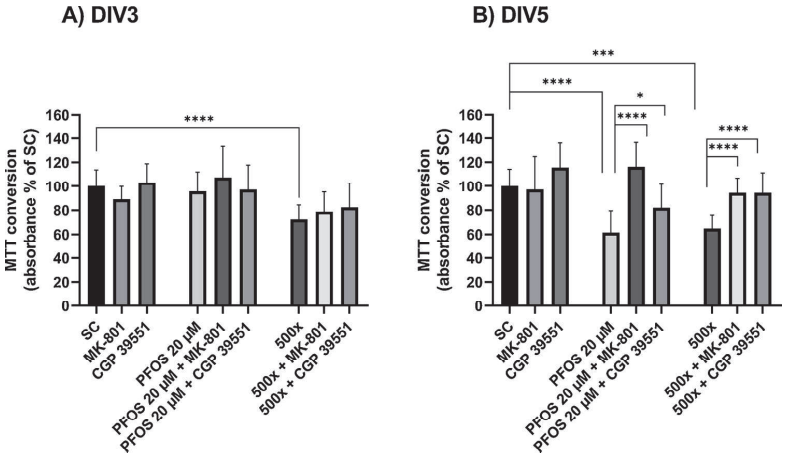

Fig. 5. Assessment of neuroprotective effects of NMDA-R antagonists in PFOS or POP mixture-induced cytotoxicity in the absence of glutamate in CGNs at DIV3 (A) or DIV5 (B) using tetrazolium MTT conversion assay. CGNs were exposed for 24 h to solvent control (SC, 0.1 % DMSO), PFOS 20 μM or POP mixture (500x fold human blood levels). Cells were treated in the presence and absence of the open NMDA-R channel blocker MK-801 (5 μM) or the competitive NMDA-R antagonist CGP 39551 (100 μM). Datapoints for SC, PFOS 20 μM, and 500x, are identical to Fig. 1B and C. All values were presented relative to the SC (defined as 100 %). Data are mean ± SD, n = 3 to 4 experiments (from separate cell isolates), each with replicates >4 per group/exposure, *p < 0.05, ***p < 0.001, ****p < 0.0001 one-way ANOVA followed by Dunnett's multiple comparisons test.

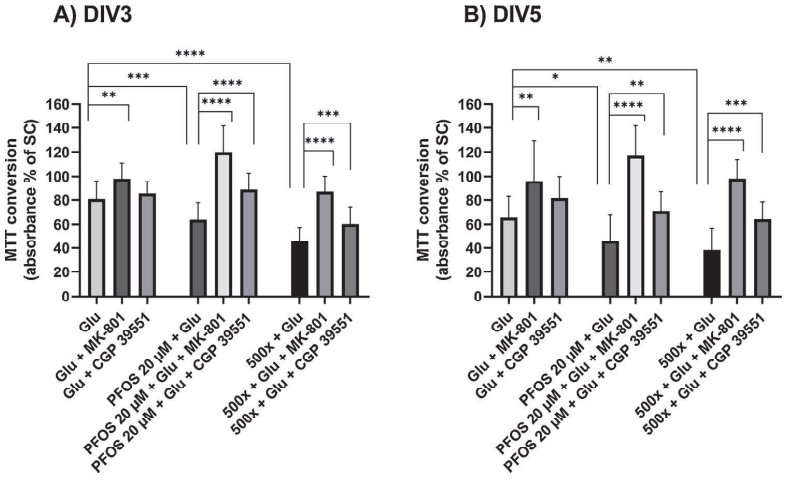

Fig. 6. Assessment of neuroprotective effects of NMDA-R antagonists in PFOS or POP mixture-induced cytotoxicity in the presence of glutamate in CGNs at DIV3 (A) or DIV5 (B) using tetrazolium MTT conversion assay. CGNs were exposed for 24 h to solvent control (SC, 0.1 % DMSO), glutamate (Glu) 100 μM (together with 10 μM glycine as co-agonist), PFOS 20 μM or POP mixture (500x fold human blood levels), alone or in the presence of glutamate. Cells were treated in the presence and absence of the open NMDA-R channel blocker MK-801 (5 μM) or the competitive NMDA-R antagonist CGP 39551 (100 μM). CGNs were exposed to glutamate. All values were presented relative to the SC (defined as 100 %). Datapoints for Glu, PFOS 20 μM + Glu, and 500x + Glu are identical as in Fig. 1B and C. Data are mean ± SD, n = 3 to 4 experiments (from separate cell isolates), each with replicates >4 per group/exposure, *p < 0.05, **p < 0.01, ***p < 0.00, ****p < 0.0001 one-way ANOVA following Dunnett's multiple comparisons test.

3.5. Neuroprotective effects of NMDA-R antagonists on reduced MTT activity in POP mixture or PFOS-induced toxicity

We explored if the NMDA-R antagonists were also capable of rescuing cells from reduced MTT activity, alone or combined with glutamate. We observed the NMDA-R antagonists were still capable of rescuing the CGNs in situations where PFOS and the POP mixture reduced MTT activity (Fig. 1C), albeit in absence of Ca^{2+} influxes (Fig. 3). At DIV 5, MK-801 ($P < 0.0001$) proved more effective than CGP 39551 ($P < 0.05$) in rescuing PFOS-induced toxicity. But both

Table 2
The comparison between PFOS and the POP mixture exposure.

	Without Glutamate			*With Glutamate*		
A) DIV3	*PFOS 20 μM*	*POP mixture 500x*	*Difference between means ± SEM*	*PFOS 20 μM*	*POP mixture 500x*	*Difference between means ± SEM*
MTT conversion	95.61 %	72.50 %	23.11 ± 5.095 ****	63.90 %	46.07 %	17.84 ± 3.183 ****
Glutathione levels	0.7873	0.4504	−0.3369 ± 0.1151 **	0.7775	0.3676	−0.4099 ± 0.09090 ****
$[Ca^{2+}]_i$	1.984	2.030	−0.04679 ± 0.3086	5.648	6.735	−1.087 ± 0.3393 *
B) DIV5						
MTT conversion	61.48 %	64.87 %	−3.395 ± 6.093	46.11%	38.35 %	7.760 ± 5.817
Glutathione levels	0.4828	0.5692	0.08635 ± 0.08092	0.4690	0.3858	−0.08320 ± 0.05387
$[Ca^{2+}]_i$	2.105	2.236	−0.1301 ± 0.4005	5.665	6.131	−0.4660 ± 0.7437

An unpaired *t*-test was performed for the comparison between PFOS and POP mixture, in the absence of glutamate or in the presence of glutamate. *P < 0.05, **P < 0.01, and ****P < 0.0001 considered significant. MTT conversion values were presented relative to the solvent control (defined as 100 %); glutathione levels relative to the solvent control (defined as 1); and $[Ca^{2+}]_i$ relative to the baseline (before exposure, set to 1). A represents DIV3 and B DIV5.

antagonists ($P < 0.0001$) were equally effective at rescuing the POP mixture induced toxicity (Fig. 5B).

In the presence of glutamate, Ca^{2+} influxes were reduced by NMDA-R blockers (Fig. 4). In this situation we found MK-801 was very effective in rescuing cells from reduction of MTT induced by either PFOS or POP mixture (Fig. 6A, B). CGP 39551 also restored MTT activity at either day, albeit in a less efficient manner (Fig. 6A, B).

3.6. Comparison between POP mixture and PFOS at DIV 3 and 5, in absence or presence of glutamate

Table 2 summarizes the direct comparison between the effect for the POP mixture 500x with the corresponding concentration of 20 μM PFOS, at two different stages of maturation (DIV 3 and 5). We observed significant differences in MTT conversion ($P < 0.0001$ for both without and with glutamate) and glutathione levels ($P < 0.01$ without glutamate and $P < 0.0001$ with glutamate) between the exposure of POP mixture and PFOS at DIV3 either alone or in combination of glutamate. However, these differences disappeared at DIV5. Ca^{2+} influxes were at the same order of magnitude for each exposure at each day.

4. Discussion

Our work was aimed at investigating cellular mechanisms of POPs exposures, and the results showed that a POP mixture based on human blood levels from the Norwegian/Scandinavian population affects NMDA-R signaling in CGNs from chicken embryos at critical stages of cerebellar development. NMDA-R signaling is an important event in early development of cerebellum [19] and changes in the expression of this receptors have been linked to neurological disorders [46]. It is difficult to translate pure *in vitro* work into human hazard and risk assessment. Although we noticed effects at 500x blood levels, which might be considered a high concentration, it should be noted that the exposure to POPs is individualistic in nature and certain groups of people may have these levels of exposures for certain POPs similar to these concentrations (summarized in Supplementary Table 2). Our PCBs, chlordane, and PBDEs at 500x are comparable to reported levels in Inuit population [47]. DDE concentration in the 500x mixture is comparable to children in African regions with indoor residual spraying (IRS) of insecticides including DDT, which has reported levels of p, p′-DDE up to 19,772 ng/g lipid (118 ng/mL blood) and 33,605 ng/g lipid (201 ng/g blood), at 12 and 24 months of age, respectively [48]. Extremely high concentration of PFOS has been reported in Chinese factory workers [49], at levels about ten times higher than in our POP mixture at 500×. Most studies examining effects of POPs use single compounds, and often at high concentrations. However, in real life we are exposed simultaneously to a large number of chemicals, thus mixture studies at environmentally relevant concentrations are of great importance. When chemicals co-occur, they may act additively, displaying non-interaction, which is currently believed to be the most common scenario, especially at low concentrations [50,51]. Although less commonly observed, they may also display interactive synergistic (more than additive) or antagonistic (less than additive) effects. Furthermore, it should not be presumed that concentration lower than 500x can be considered safe, because of the fundamental role of the molecular target, namely NMDA-R signaling, in cerebellar development at critical stages of development. It should also be stressed that our *in vitro* exposures are of an acute short-term character, whereas real-life exposures start from conception onwards and are of a chronic nature. Measured concentrations in adult human brain tissues, thereby reflecting long-term exposure levels of PCBs or PBDEs have been reported as summarized in Supplementary Table 3. These levels were associated to neurological disorders [52,53].Together this raises concern about safe lower limits of exposure. Safe limits might potentially be lower for women during pregnancy and lactation in the work environment than for other groups. In addition, the information gained on molecular target and pathways is useful in the Adverse Outcome Pathway (AOP) framework, where it can add knowledge into existing AOPs for DNT [54] and/or form the basis of new AOPs.

PFOS belongs to the chemical class of per- and polyfluoroalkyl substances (PFAS), a family of emerging persistent pollutants of increasing concern with regards to adverse health outcomes, including cognitive outcomes [55]. The POP mixture outcomes were compared with PFOS exposure. The concentration used for PFOS exposure was set to 20 μM, equivalent to its concentration in the POP mixture 500x exposure.

We used MTT assay to quantify direct effect of the exposures on cell viability. Our observations indicated that CGNs sensitivity increases with maturation in culture. Exposure of the CGNs to the excitotoxin glutamate reduced the MTT activity significantly at DIV3, with increased sensitivity at DIV5. The increase in sensitivity at different stages of maturation could also be due to the decrease of cells. In the present study cell viability was evaluated by mitochondrial activity as measured by MTT assay. This mitochondrial integrity/activity may be interpreted as a measure of cell number, proliferation, viability, survival, or toxicity [56]. Expression of different NMDA receptors subunits at DIV3 compared to DIV5 might explain the different sensitivity of glutamate toxicity. In rat CGNs, Ceccon et al. [34] observed a similar lack of response to glutamate before DIV8, followed by increased sensitivity between DIV8 and DIV20. The POP mixture was toxic at either day, whilst PFOS only showed effect at DIV5. Recently Berntsen et al. reported that the same total POP mixture caused toxicity in rat CGNs with a significant impact on viability from 500x, and indicted an involvement of NMDA-R [38]. Similarly, Lee, Lee and Yang [57,58] showed that PFOS concentrations up to 30 μM did not cause any cytotoxicity in rat CGNs. Along the same line, Berntsen et al. [17] showed a lowest observed effect for PFOS at 20 μM in rat CGNs. It should be stressed that our PFOS concentration is comparable to reported concentrations of 26 μM in human serum levels in production workers [59]. Although the POP mixture and PFOS were capable of reducing MTT activity at DIV5, the reduction was more pronounced in presence of glutamate, suggesting an additive effect with the physiological stimulant.

It is interesting to note that the complete POP mixture had negative effects on cellular health already in early stages of CGNs maturation (starting at DIV1), whereas PFOS was most potent in later stages (DIV5). Since the concentration used for PFOS was equivalent to the one present in the total POP mixture, it is obvious PFOS alone cannot mimic the effect of the full mixture. At present, we can only hypothesize about possible mechanisms. Other PFAS compounds present in the total mixture might contribute to a more potent cytotoxic effect. Indeed, all the six PFAS compounds have been found to induce cytotoxicity after 24 h incubation in rat CGNs [17]. Moreover, the other classes of compounds, PCBs, OCPs, and BFRs might contribute to the increased potency of the total mixture. Indeed, both *in vivo* (for example in rat, mice) and *in vitro* (for example in primary CGNs and hippocampal neurons from rat and mice; PC12 and neuroblastoma cells) have shown that PCBs and BFRs could lead to disrupted calcium homeostasis, reduced glutathione levels, formation of ROS, leading to neurotoxicity [60]. Alternatively, since maturation of the CGNs is paralleled with a shift in subunit composition of the NMDA-R [36], it might be that certain compounds in the total mixture might already have an affinity for more immature stages of the receptor, compared to PFOS.

In CGNs the level of intracellular glutathione plays a major role in protecting cells against injury caused by ROS following excitotoxic insults [34]. As such, a reduction in GSH level is involved in glutamate-induced cell death [35]. Direct depletion of mitochondrial and cytoplasmic GSH could result in increased level of ROS, decrease of the mitochondrial transmembrane potential and rapid loss of mitochondrial function [61]. Our observations indicate that glutamate exposure reduced the GSH level at either day, which is in agreement with observations by Sørvik and Paulsen [44]. When exposed to POP mixture or PFOS alone, GSH levels were reduced at either day. However,

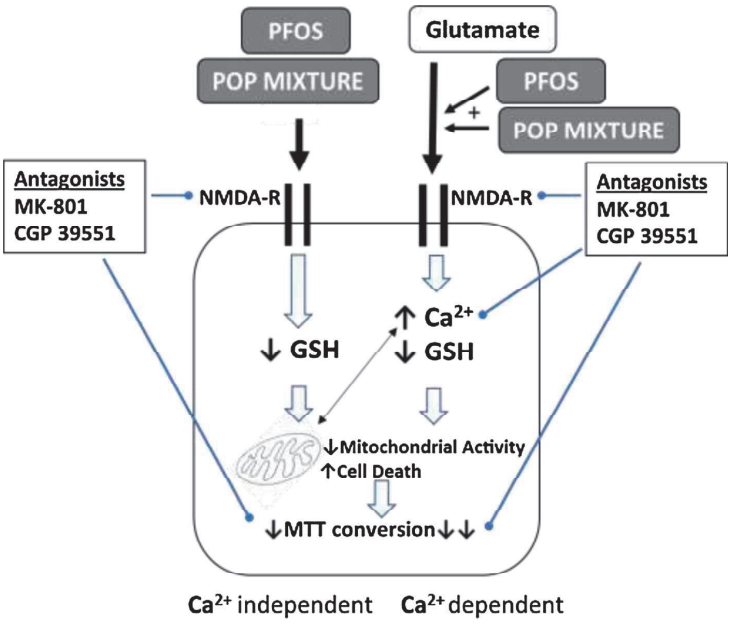

Fig. 7. Overview of the cellular mechanisms involved in CGNs toxicity induced by POP mixture or PFOS alone, in absence or presence of glutamate. Reductions (bold down-arrows) or increases (bold up-arrows) of biological effects are shown. In the absence of glutamate (left side of the figure), exposures with either POP mixture of PFOS alone, reduce intracellular glutathione (GSH) levels and induce CGNs toxicity by a Ca^{2+}-independent mechanism. In the presence of glutamate (right side of the figure), exposures with either POP mixture or PFOS alone, aggravate glutamate-induced excitotoxicity by a Ca^{2+}-dependent mechanism. Competitive (CGP 39551) and non-competitive (MK-801) NMDA-R antagonists can block the underlying mechanisms (indicated by blue lines with blunt end) and rescue CGNs cells from cytotoxicity (For interpretation of the references to colour in this figure legend, the reader is referred to the web version of this article.).

the POP mixture aggravated the effect of glutamate-induced GSH reduction, suggesting an additive effect. No such additive effect was seen for PFOS in the presence of glutamate. For the POP mixture alone, or in combination with glutamate, the reductions in GSH paralleled the reductions seen for MTT activity. This could indicate that the levels of GSH are setting the sensitivity of the CGNs to toxic insult. However, this was not the case for PFOS, suggesting it acts through a different mechanism for induction of toxicity.

NMDA-R channels are highly Ca^{2+}-permeable [36]. Their activation leads to a fast mitochondrial Ca^{2+} uptake, suggesting that Ca^{2+} influx through NMDA receptors has a privileged access to mitochondria, which could result in mitochondrial dysfunction [62,63]. In our hands the chicken CGNs responded to glutamate exposure with an increased Ca^{2+} influx, as previously described by Sørvik and Paulsen [44]. In contrast, neither the POP mixture, nor PFOS induced a Ca^{2+} influx on their own, indicating they do not reproduce the Ca^{2+} signaling induced by glutamate. The absence of a PFOS-induced Ca^{2+} influx could be due to the low concentration. Indeed, Berntsen et al. [18] did not observe Ca^{2+} influx up to the concentration of 100 μM PFOS in rat CGNs. Interestingly, our observations showed that combinations of the POP mixture or the PFOS with glutamate significantly increased the effect of glutamate on Ca^{2+} influx. This indicates that exposure to environmental pollutants can combine with existing excitotoxic processes and aggravate adverse cellular outcomes.

In a second step, we wanted to test whether known inhibitors of NMDA-R mediated Ca^{2+} influx could reverse the effects seen with combined glutamate and POP mixture or PFOS exposure. Glutamate-induced Ca^{2+} influx was reversed to control levels in presence of MK-801. The same trend was seen with CGP 39551, but non-significantly. This is in accordance with previous studies by Jacobs et al. [24,64] using MK-801. MK-801 is also very effective in reversing the Ca^{2+} influx induced by the combination of glutamate and the POP mixture or PFOS. In contrast, CGP 39551 proved far less effective in reversing this influx. It should be noted that MK-801 appeared to have very low voltage-dependency and slow unblocking kinetics to the ion channel [65], which may explain the higher protective effect of MK-801. CGP 39551 on the other hand is a competitive antagonist and acts by binding to the glutamate binding site of the receptor [41].

MK-801 also restored the reduction in MTT activity for the POP exposures in presence of glutamate. Thus, a calcium-dependent NMDA-R mediated toxicity seems at play here. Although CGP 39551 was less effective than MK-801 in blocking the Ca^{2+} influx, it also proved capable of reversing the reduction of MTT. Intriguingly, in absence of glutamate, the antagonists were also able to reverse cytotoxicity induced by either the POP mixture or PFOS. As no Ca^{2+} influx was observed under these conditions, this suggests a role for NMDA-R induced toxicity in a calcium-independent manner. Ca^{2+} flux-independent NMDA-R signaling has been reported previously. This could be due to conformational changes of NMDA-R subunits that subsequently activates intracellular signaling cascades even in the absence of Ca^{2+} influx, and p38 MAP was found to mediate this effect [66].

In general, in our hands the effects of exposures for either POP mixture or PFOS became stronger with increased age of the CGNs cultures *in vitro*. Berntsen, et al. [18] did also observe increased sensitivity of rat CGNs exposed to PFOS from DIV0 to DIV14. Also, neuroprotective effect of NMDA-R antagonists, including MK-801 was more pronounced at DIV14 as compared to DIV8. Recently, in another study Berntsen, et al. observed no toxicity in newly isolated immature rat CGNs when exposed to the same POP mixture from DIV0 to DIV8 as compared to cells exposed at DIV8 [38].This suggest that sensitivity of neurons changes with the maturation in culture. However, in our exposures there was a significant difference on DIV3 between effects of POP mixture and PFOS, whereas on DIV5 the effect of PFOS approached that of POP mixture in magnitude.

We compared the endpoints/mechanism of toxicity of most of the compounds in the mixture from other *in vitro* studies with our POP mixture at 500x (fold human blood levels). As it can be seen from Supplementary Table 1, several of the single compounds have been linked with NMDA-R, ROS and Ca^{2+} homeostasis in neuronal cell models. However, when compared to other studies *in vitro* concentration of each individual compound in the mixture is still lower than concentrations reported. Although POP mixture at 500x looks high relative to

measured blood concentrations, it should be stressed that the concentrations of the individual compounds are lower than those reported in *in vitro* studies.

Our observations indicate PFOS is the major contributor from the PFAAs group, although future experiments are needed to exclude possible additive effects amongst the members of this group. Similarly, we did not investigate the other subgroups separately or combined with PFOS. However, a recent study from our group examined the effects of same total POP mixture as well as Cl, Br, and PFAAs group alone, and their combinations on *in vitro* exposed rat CGNs. They observed that the PFAAs mixture in combination with the Br and/or Cl mixtures exerted a stronger toxic effect than the PFAA mixture alone, indicating a degree of additivity between the sub-classes [38]. Further studies with the sub-mixtures of the different classes, combinations thereof, and the single compounds would be needed to explore the underlying mechanisms.

Our study shows that exposure to POPs could interfere with NMDA glutamate receptors. Exposure to POPs have been associated with an increased prevalence of neurodevelopmental disorders including autism [1]. Changes in the expression of ionotropic glutamate receptors have been observed in autism for example, an upregulation of NMDA-R subunit protein levels has also been reported in the cerebellum of human postmortem samples [46]. In cerebellum the migration of granule neurons through layers of the cerebellar cortex is a key feature for the development of cerebellum and this neuronal migration is modulated by NMDA-R [23]. Perturbations of this process during development for example through exposure of pollutants could lead to developmental neurotoxicity and impaired brain development possibly *via* the involvement of NMDA receptors.

5. Conclusion

Primary chicken embryonal CGNs can be used as an *in vitro* model for evaluation of effects of persistent organic pollutants on developmental neurotoxicity. Our observations, schematized in Fig. 7, indicate that POPs affect different cellular and molecular endpoints in a complex fashion. The outcome depends on maturity of the CGNs. The exposures not only induce toxicity on their own, but also aggravate glutamate-induced excitotoxicity. The effect of the POP mixture cannot be explained by the action of PFOS only. With PFOS our observations in chicken embryo CGNs are similar to those previously reported in rat CGNs. Intracellular glutathione levels seem to set the levels of sensitivity to toxic insult. There seems to be two mechanisms for induction of toxicity, involving either a calcium-dependent or independent NMDA-R pathway. Importantly, antagonists of NMDA-R can inhibit the toxic effect of the exposures.

Declaration of Competing Interest

The authors declare no conflict of interest.

Acknowledgements

This project has received funding from the European Union's Horizon 2020 research and innovation program under the Marie Skłodowska-Curie grant agreement No. 722634 (http://protected.eu.com/). Support from the EU Erasmus + Programme to EV, MK and EHWH is gratefully acknowledged.

Appendix A. Supplementary data

Supplementary material related to this article can be found, in the online version, at doi:https://doi.org/10.1016/j.reprotox.2021.01.008.

References

[1] P. Grandjean, P.J. Landrigan, Neurobehavioural effects of developmental toxicity, Lancet Neurol. 13 (3) (2014) 330–338.
[2] P. Grandjean, P.J. Landrigan, Developmental neurotoxicity of industrial chemicals, Lancet (London, England) 368 (9553) (2006) 2167–2178.
[3] What are POPs? UNEP, 2008 (Accessed 10 April 2020), http://chm.pops.int/TheConvention/ThePOPs/tabid/673/Default.aspx.
[4] R.J. Schmidt, K. Lyall, I. Hertz-Picciotto, Environment and Autism: Current State of the Science, Cut. Edge Psychiatry Pract. 1 (4) (2014) 21–38.
[5] P.R. Kodavanti, Neurotoxicity of persistent organic pollutants: possible mode(s) of action and further considerations, Dose. 3 (3) (2006) 273–305.
[6] B.B. Hoyer, C.H. Ramlau-Hansen, C. Obel, H.S. Pedersen, A. Hernik, V. Ogniev, B. A. Jonsson, C.H. Lindh, L. Rylander, A. Rignell-Hydbom, J.P. Bonde, G. Toft, Pregnancy serum concentrations of perfluorinated alkyl substances and offspring behaviour and motor development at age 5-9 years–a prospective study, Environ. Health 14 (2015) 2.
[7] DENAMIC Report Summary, Project ID: 282957, DENAMIC, 2012. https://cordis.europa.eu/project/id/282957/reporting.
[8] T. Svingen, A.M. Vinggaard, The risk of chemical cocktail effects and how to deal with the issue, J. Epidemiol. Community Health 70 (4) (2016) 322–323.
[9] Chemical Mixtures in Source Water and Drinking-Water, WHO, 2017. https://apps.who.int/iris/bitstream/handle/10665/255543/9789241512374-eng.pdf;jsessionid=301C7A42E1F33E57F83798D68C377636?sequence=1.
[10] Toxicity and Assessment of Chemical Mixtures, Scientific Committee on Health and Environmental Risks (SCHER), SCHER, 2012. https://ec.europa.eu/health/scientific_committees/environmental_risks/docs/scher_o_155.pdf.
[11] S.K. Bopp, R. Barouki, W. Brack, S. Dalla Costa, J.C.M. Dorne, P.E. Drakvik, M. Faust, T.K. Karjalainen, S. Kephalopoulos, J. van Klaveren, M. Kolossa-Gehring, A. Kortenkamp, E. Lebret, T. Lettieri, S. Nørager, J. Rüegg, J.V. Tarazona, X. Trier, B. van de Water, J. van Gils, Å. Bergman, Current EU research activities on combined exposure to multiple chemicals, Environ. Int. 120 (2018) 544–562.
[12] V. Lenters, N. Iszatt, J. Forns, E. Čechová, A. Kočan, J. Legler, P. Leonards, H. Stigum, M. Eggesbø, Early-life exposure to persistent organic pollutants (OCPs, PBDEs, PCBs, PFASs) and attention-deficit/hyperactivity disorder: a multi-pollutant analysis of a Norwegian birth cohort, Environ. Int. 125 (2019) 33–42.
[13] R. Flores-Ramírez, F.J. Pérez-Vázquez, M. Rodríguez-Aguilar, S.E. Medellín-Garibay, E. Van Brussel, A.C. Cubillas-Tejeda, L. Carrizales-Yáñez, F. Díaz-Barriga, Biomonitoring of persistent organic pollutants (POPs) in child populations living near contaminated sites in Mexico, Sci. Total Environ. 579 (2017) 1120–1126.
[14] D.J. González-Mille, C.A. Ilizaliturri-Hernández, G. Espinosa-Reyes, O. Cruz-Santiago, M.D.C. Cuevas-Díaz, C.C. Martín Del Campo, R. Flores-Ramírez, DNA damage in different wildlife species exposed to persistent organic pollutants (POPs) from the delta of the Coatzacoalcos river, Mexico, Ecotoxicol. Environ. Saf. 180 (2019) 403–411.
[15] H.F. Berntsen, V. Berg, C. Thomsen, E. Ropstad, K.E. Zimmer, The design of an environmentally relevant mixture of persistent organic pollutants for use in in vivo and in vitro studies, J. Toxicol. Environ. Health A (2017) 1–15.
[16] J. Forns, M.A. Verner, N. Iszatt, N. Nowack, C.C. Bach, M. Vrijheid, O. Costa, A. Andiarena, E. Sovcikova, B.B. Høyer, J. Wittsiepe, M.J. Lopez-Espinosa, J. Ibarluzea, I. Hertz-Picciotto, G. Toft, H. Stigum, M. Guxens, Z. Liew, M. Eggesbø, Early life exposure to perfluoroalkyl substances (PFAS) and ADHD: a meta-analysis of nine European population-based studies, Environ. Health Perspect. 128 (5) (2020) 57002.
[17] H.F. Berntsen, C.G. Bjorklund, J.N. Audinot, T. Hofer, S. Verhaegen, E. Lentzen, A. C. Gutleb, E. Ropstad, Time-dependent effects of perfluorinated compounds on viability in cerebellar granule neurons: dependence on carbon chain length and functional group attached, Neurotoxicology 63 (2017) 70–83.
[18] H.F. Berntsen, C.G. Bjorklund, R. Strandabo, T.M. Haug, A. Moldes-Anaya, J. Fuentes-Lazaro, S. Verhaegen, R.E. Paulsen, R.A. Tasker, E. Ropstad, PFOS-induced excitotoxicity is dependent on Ca(2+) influx via NMDA receptors in rat cerebellar granule neurons, Toxicol. Appl. Pharmacol. 357 (2018) 19–32.
[19] S. Bjornstad, L.P. Austdal, B. Roald, J.C. Glover, R.E. Paulsen, Cracking the egg: potential of the developing chicken as a model system for nonclinical safety studies of pharmaceuticals, J. Pharmacol. Exp. Ther. 355 (3) (2015) 386–396.
[20] C.J. O'Halloran, G.J. Kinsella, E. Storey, The cerebellum and neuropsychological functioning: a critical review, J. Clin. Exp. Neuropsychol. 34 (1) (2012) 35–56.
[21] M. Manto, C.I. De Zeeuw, Diversity and complexity of roles of granule cells in the cerebellar cortex. Editorial, Cerebellum (London, England) 11 (1) (2012) 1–4.
[22] F. Sultan, M. Glickstein, The cerebellum: comparative and animal studies, Cerebellum (London, England) 6 (3) (2007) 168–176.
[23] H. Komuro, P. Rakic, Modulation of neuronal migration by NMDA receptors, Science 260 (5104) (1993) 95–97.
[24] C.M. Jacobs, P. Aden, G.H. Mathisen, E. Khuong, M. Gaarder, E.M. Løberg, J. Lømo, J. Mæhlen, R.E. Paulsen, Chicken cerebellar granule neurons rapidly develop excitotoxicity in culture, J. Neurosci. Methods 156 (1) (2006) 129–135.
[25] P. Aden, I. Goverud, K. Liestol, E.M. Loberg, R.E. Paulsen, J. Maehlen, J. Lomo, Low-potency glucocorticoid hydrocortisone has similar neurotoxic effects as high-potency glucocorticoid dexamethasone on neurons in the immature chicken cerebellum, Brain Res. 1236 (2008) 39–48.
[26] P. Aden, R.E. Paulsen, J. Maehlen, E.M. Loberg, I.L. Goverud, K. Liestol, J. Lomo, Glucocorticoids dexamethasone and hydrocortisone inhibit proliferation and accelerate maturation of chicken cerebellar granule neurons, Brain Res. 1418 (2011) 32–41.
[27] L.P. Austdal, S. Bjornstad, G.H. Mathisen, P.K. Aden, I. Mikkola, R.E. Paulsen, K. E. Rakkestad, Glucocorticoid effects on cerebellar development in a chicken

embryo model: exploring changes in PAX6 and Metalloproteinase-9 after exposure to dexamethasone, J. Neuroendocrinol. 28 (12) (2016).
[28] M.F. Fjelldal, M.G. Hadera, M. Kongstorp, L.P.E. Austdal, A. Sulovic, J. M. Andersen, R.E. Paulsen, Opioid receptor-mediated changes in the NMDA receptor in developing rat and chicken, Int. J. Dev. Neurosci. 78 (2019) 19–27.
[29] G.H. Mathisen, M. Yazdani, K.E. Rakkestad, P.K. Aden, J. Bodin, M. Samuelsen, U. C. Nygaard, I.L. Goverud, M. Gaarder, E.M. Loberg, A.K. Bolling, R. Becher, R. E. Paulsen, Prenatal exposure to bisphenol A interferes with the development of cerebellar granule neurons in mice and chicken, Int. J. Dev. Neurosci. 31 (8) (2013) 762–769.
[30] A.A. Kritis, E.G. Stamoula, K.A. Paniskaki, T.D. Vavilis, Researching glutamate - induced cytotoxicity in different cell lines: a comparative/collective analysis/ study, Front. Cell. Neurosci. 9 (2015) 91.
[31] D.W. Choi, Glutamate neurotoxicity in cortical cell culture is calcium dependent, Neurosci. Lett. 58 (3) (1985) 293–297.
[32] D.W. Choi, Glutamate neurotoxicity and diseases of the nervous system, Neuron 1 (8) (1988) 623–634.
[33] A.M. Marini, S.M. Paul, N-methyl-D-aspartate receptor-mediated neuroprotection in cerebellar granule cells requires new RNA and protein synthesis, Proc. Natl. Acad. Sci. U.S.A. 89 (14) (1992) 6555–6559.
[34] M. Ceccon, P. Giusti, L. Facci, G. Borin, M. Imbesi, M. Floreani, S.D. Skaper, Intracellular glutathione levels determine cerebellar granule neuron sensitivity to excitotoxic injury by kainic acid, Brain Res. 862 (1-2) (2000) 83–89.
[35] A.B. Fallgren, G.H. Mathisen, J. Maehlen, R. Blomhoff, R.E. Paulsen, Preconditioning with estradiol abolishes its neuroprotection in cerebellar neurons, Biochem. Biophys. Res. Commun. 352 (4) (2007) 966–972.
[36] P. Paoletti, C. Bellone, Q. Zhou, NMDA receptor subunit diversity: impact on receptor properties, synaptic plasticity and disease, Nature reviews, Neuroscience 14 (6) (2013) 383–400.
[37] M.L. Vallano, B. Lambolez, E. Audinat, J. Rossier, Neuronal activity differentially regulates NMDA receptor subunit expression in cerebellar granule cells, J. Neurosci. 16 (2) (1996) 631–639.
[38] H.F. Berntsen, N. Duale, C.G. Bjørklund, O.D. Rangel-Huerta, K. Dyrberg, T. Hofer, K.E. Rakkestad, G. Østby, R. Halsne, G. Boge, R.E. Paulsen, O. Myhre, E. Ropstad, Effects of a human-based mixture of persistent organic pollutants on the in vivo exposed cerebellum and cerebellar neuronal cultures exposed in vitro, Environ. Int. 146 (2020), 106240.
[39] K. Wedzony, K. Golembiowska, M. Zazula, Differential effects of CGP 37849 and MK-801, competitive and noncompetitive NMDA antagonists, with respect to the modulation of sensorimotor gating and dopamine outflow in the prefrontal cortex of rats, Naunyn Schmiedebergs Arch. Pharmacol. 350 (5) (1994) 555–562.
[40] E.H. Wong, J.A. Kemp, T. Priestley, A.R. Knight, G.N. Woodruff, L.L. Iversen, The anticonvulsant MK-801 is a potent N-methyl-D-aspartate antagonist, Proc. Natl. Acad. Sci. U.S.A. 83 (18) (1986) 7104–7108.
[41] G.E. Fagg, H.R. Olpe, M.F. Pozza, J. Baud, M. Steinmann, M. Schmutz, C. Portet, P. Baumann, K. Thedinga, H. Bittiger, et al., CGP 37849 and CGP 39551: novel and potent competitive N-methyl-D-aspartate receptor antagonists with oral activity, Br. J. Pharmacol. 99 (4) (1990) 791–797.
[42] C.M. Jacobs, P. Aden, G.H. Mathisen, E. Khuong, M. Gaarder, E.M. Loberg, J. Lomo, J. Maehlen, R.E. Paulsen, Chicken cerebellar granule neurons rapidly develop excitotoxicity in culture, J. Neurosci. Methods 156 (1-2) (2006) 129–135.
[43] T. Mosmann, Rapid colorimetric assay for cellular growth and survival: application to proliferation and cytotoxicity assays, J. Immunol. Methods 65 (1-2) (1983) 55–63.
[44] I.B. Sørvik, R.E. Paulsen, High and low concentration of 17alpha-estradiol protect cerebellar granule neurons in different time windows, Biochem. Biophys. Res. Commun. 490 (3) (2017) 676–681.
[45] J.C. Fernandez-Checa, N. Kaplowitz, The use of monochlorobimane to determine hepatic GSH levels and synthesis, Anal. Biochem. 190 (2) (1990) 212–219.
[46] D.C. Rojas, The role of glutamate and its receptors in autism and the use of glutamate receptor antagonists in treatment, J. Neural Transm. (Vienna) 121 (8) (2014) 891–905.
[47] B.D. Laird, A.B. Goncharov, H.M. Chan, Body burden of metals and persistent organic pollutants among Inuit in the Canadian Arctic, Environ. Int. 59 (2013) 33–40.
[48] M.-A. Verner, J. Chevrier, G. Ngueta, S. Rauch, R. Bornman, B. Eskenazi, Early-life exposure to p,p'-DDT and p,p'-DDE in South African children participating in the VHEMBE study: An assessment using repeated serum measurements and pharmacokinetic modeling, Environ. Int. 119 (2018) 478–484.
[49] J. Fu, Y. Gao, L. Cui, T. Wang, Y. Liang, G. Qu, B. Yuan, Y. Wang, A. Zhang, G. Jiang, Occurrence, temporal trends, and half-lives of perfluoroalkyl acids (PFAAs) in occupational workers in China, Sci. Rep. 6 (2016) 38039.
[50] A. Kortenkamp, T. Backhaus, M. Faust, State of the Art Report on Mixture Toxicity, Final Report. Executive Summary., The School of Pharmacy University of London (ULSOP), 2009.
[51] O. Martin, M. Scholze, S. Ermler, J. McPhie, S.K. Bopp, A. Kienzler, N. Parissis, A. Kortenkamp, Ten years of research on synergisms and antagonisms in chemical mixtures: a systematic review and quantitative reappraisal of mixture studies, Environ. Int. 146 (2020), 106206.
[52] J.M. Hatcher-Martin, M. Gearing, K. Steenland, A.I. Levey, G.W. Miller, K. D. Pennell, Association between polychlorinated biphenyls and Parkinson's disease neuropathology, Neurotoxicology 33 (5) (2012) 1298–1304.
[53] M.M. Mitchell, R. Woods, L.H. Chi, R.J. Schmidt, I.N. Pessah, P.J. Kostyniak, J. M. LaSalle, Levels of select PCB and PBDE congeners in human postmortem brain reveal possible environmental involvement in 15q11-q13 duplication autism spectrum disorder, Environ. Mol. Mutagen. 53 (8) (2012) 589–598.
[54] M. Sachana, A. Rolaki, A. Bal-Price, Development of the Adverse Outcome Pathway (AOP): chronic binding of antagonist to N-methyl-d-aspartate receptors (NMDARs) during brain development induces impairment of learning and memory abilities of children, Toxicol. Appl. Pharmacol. 354 (2018) 153–175.
[55] M.J. Spratlen, F.P. Perera, S.A. Lederman, V.A. Rauh, M. Robinson, K. Kannan, L. Trasande, J. Herbstman, The association between prenatal exposure to perfluoroalkyl substances and childhood neurodevelopment, Environ. Pollut. 263 (Pt B)) (2020) 114444.
[56] E. Maioli, C. Torricelli, V. Fortino, F. Carlucci, V. Tommassini, A. Pacini, Critical appraisal of the MTT assay in the presence of rottlerin and uncouplers, Biol. Proced. Online 11 (2009) 227–240.
[57] H.G. Lee, Y.J. Lee, J.H. Yang, Perfluorooctane sulfonate induces apoptosis of cerebellar granule cells via a ROS-dependent protein kinase C signaling pathway, Neurotoxicology 33 (3) (2012) 314–320.
[58] Y.J. Lee, H.-G. Lee, J.-H. Yang, Perfluorooctane sulfonate-induced apoptosis of cerebellar granule cells is mediated by ERK 1/2 pathway, Chemosphere 90 (5) (2013) 1597–1602.
[59] T.A. Slotkin, E.A. MacKillop, R.L. Melnick, K.A. Thayer, F.J. Seidler, Developmental neurotoxicity of perfluorinated chemicals modeled in vitro, Environ. Health Perspect. 116 (6) (2008) 716–722.
[60] F. Fonnum, E. Mariussen, Mechanisms involved in the neurotoxic effects of environmental toxicants such as polychlorinated biphenyls and brominated flame retardants, J. Neurochem. 111 (6) (2009) 1327–1347.
[61] U. Wüllner, J. Seyfried, P. Groscurth, S. Beinroth, S. Winter, M. Gleichmann, M. Heneka, P.A. Löschmann, J.B. Schulz, M. Weller, T. Klockgether, Glutathione depletion and neuronal cell death: the role of reactive oxygen intermediates and mitochondrial function, Brain Res. 826 (1) (1999) 53–62.
[62] G. Olmos, N. DeGregorio-Rocasolano, M. Paz Regalado, T. Gasull, M. Assumpcio Boronat, R. Trullas, A. Villarroel, J. Lerma, J.A. Garcia-Sevilla, Protection by imidazol(ine) drugs and agmatine of glutamate-induced neurotoxicity in cultured cerebellar granule cells through blockade of NMDA receptor, Br. J. Pharmacol. 127 (6) (1999) 1317–1326.
[63] T.I. Peng, J.T. Greenamyre, Privileged access to mitochondria of calcium influx through N-methyl-D-aspartate receptors, Mol. Pharmacol. 53 (6) (1998) 974–980.
[64] C.M. Jacobs, M.D. Trinh, T. Rootwelt, J. Lomo, R.E. Paulsen, Dexamethasone induces cell death which may be blocked by NMDA receptor antagonists but is insensitive to Mg2+ in cerebellar granule neurons, Brain Res. 1070 (1) (2006) 116–123.
[65] T. Frankiewicz, B. Potier, Z.I. Bashir, G.L. Collingridge, C.G. Parsons, Effects of memantine and MK-801 on NMDA-induced currents in cultured neurones and on synaptic transmission and LTP in area CA1 of rat hippocampal slices, Br. J. Pharmacol. 117 (4) (1996) 689–697.
[66] P. Montes de Oca Balderas, Flux-independent NMDAR signaling: molecular mediators, cellular functions, and complexities, Int. J. Mol. Sci. 19 (12) (2018).

SUPPLEMENTARY MATERIALS – PAPER I

Supplementary Table 1. The endpoints/mechanism of POPs toxicity: comparison between *in vitro* studies and compounds in POP mixture at 500x (fold human blood levels).

Compound	*Cellular model In vitro*	*Effected endpoints/ Mechanism of toxicity*	*Concentration range in vitro*	*References*	*Compounds in POP mixture at 500x*
PCB					
PCB 52	Rat CGNs	Rapid loss of membrane integrity (correlated with cell death) and decreased mitochondrial membrane potential	10 µM	[1]	10.25 nM
PCB 153	Rat CGNs; neuronal and astrogial cells	Involvement of NMDA-R and ROS; effected cell viability and proliferation	3 - 50 µM; Trypan blue LC50 8 µM; 3 µM exposure led to 8-10% cell death in rat CGNs 3 - 200 µM; MTT IC50 23.6 ± 1.87 µM and trypan blue 32.4 ± 2.57 µM	[2]; [3]	*0.*35 µM
OCP					
DDT	*Rat CGNs*	Caused PKC translocation and perturbations in Ca^{2+} homeostasis (altered Ca^{2+}sequestration)	0 - 100 µM; Mitochondria $^{45}Ca^{2+}$ uptake IC50 (represent the effective concentration that inhibited 50% of the control activity) values 17.1 ± 1.5 µM for o,p`-DDT and 15.9 ± 0.8 µM for p,p`-DDT	[4]	*p,p'*-DDE : 0.5 µM
HCB	Rat CGNs	Modulated the transcriptional activity of genes involved in the classical apoptotic pathway, oxidative stress and cell-cycle control; transcriptional activity of caspase-3	10, 100 µM and 1 mM	[5]	114.1 nM
Chlordane	PC12	Generation of ROS, DNA damage, and increased lipid peroxidation	50 - 200 nM; Concentration-dependent effects of chlordane (50-200 nM) on the release of lactate dehydrogenase (LDH)	[6]	α Chlordane: 11.9 nM
γ-HCH (Lindane)	Rat CGNs; mouse CGNs	Changes in intracellular Ca^{2+} homeostasis through voltage-dependent L-type Ca^{2+} channels and dantrolene-sensitive intracellular Ca^{2+} channels; interaction with inducible $GABA_B$ receptors; interacts with $GABA_A$ and glycine receptors; modulated transcriptional activity of caspase-3 gene	150 and 200 µM; 30 - 300 µM; IC50 value for $GABA_A$ 6.1 µM and glycine receptor 5.0; 10, 100 µM and 1 mM	[7];[8];[9];[5]	8.4 nM

Dieldrin	Mouse CGN; PC12	Interacts with $GABA_A$ and glycine-receptors; induced apoptosis by caspase-3-dependent proteolytic cleavage and activation of PKC-delta; promoted proteolytic cleavage of poly (ADP-ribose) polymerase (PARP) and involvement anti-apoptotic protein Bcl-*2*	0.2 and 3 µM; IC50 value for $GABA_A$ 0.2 µM and for glycine receptor 3.0 µM; 100 - 300 µM; 30 -100 µM	[9]; [10]; [11]	28.1 nM
BFR					
PBDE 47	Rat CGNs; rat hippocampal neurons	Activated MAPK pathway; increased the rate of apoptosis, Ca^{2+}, oxidative stress; protein kinase C (PKC) translocation	0 -100 µM: cytotoxic (% LDH leakage) ≥50 µM; 10 - 50 µM: E50 (represent the concentration that increases 50% of control activity) values of PBDEs on PKC Translocation in rat CGNs: PBDE 47: 34 ± 2 µM; PBDE 99: 36 ± 3 µM; PBDE 100 and PBDE 153: >50 µM	[12]; [13]; [14]	8.9 nM
PBDE 99					3.75 nM
PBDE 100					1.9 nM
PBDE 153					1.05 nM
PBDE 209					4.7 nM
PFAA					
PFHxS	*Rat CGNs*	The toxicity of PFAAs increased with increasing carbon chain length, and for molecules with a similar chain length, a sulfonate functional group led to greater toxicity than a carboxyl group; involvement of NMDA receptors mediated excitotoxity after exposure to two sulfonated but not associated with four carboxylated PFAAs.	200 - 600 µM; LC50 = 500 µM	[15]; [16]	4 µM
PFOS			10 - 100 µM; LC50 = 38 µM		20 µM
PFOA			100 - 600 µM; LC50 = 427 µM		2 µM
PFNA			10 -140 µM; LC50 = 73 µM		0.5 µM
PFDA			10 - 100 µM; LC50 = 33 µM		0.19 µM
PFUnDA			5 - 100 µM; LC50 = 23 µM		0.17 µM

Supplementary Table 2. Comparison between the concentration of certain compounds in the POP mixture at 500x and reported POPs levels in human serum blood in different groups of population.

Compound	***Concentration in human serum blood***	***Concentration in POP mixture at 500x***
Total PCBs[*] [17]	Up to 128 ug/l [a]	304 ng/ml [b]
Chlordane[*] [17]	Up to 45.8 ug/l [c]	34 ng/ml [d]
PBDEs[*] [17]	Up to 10.6 ug/l [e]	7.5 ng/ml [e]
DDE[$] [18]	Up to 19,772 ng/g lipid = 118 ng/ml blood (12 months children) Up to 33,605 ng/g lipid = 201 ng/ml blood (24 months children)	169 ng/ml [f]
PFOS[#] [19]	Up to 118 000 ng/ml	11174 ng/ml

[*] Inuit population in the Canadian Arctic
[a] Congeners: Sum of PCB-28, PCB-52, PCB-99, PCB-101, PCB-105, PCB-118, PCB-128, PCB-138, PCB-153, PCB-156, PCB-170, PCB-180, PCB-183 and PCB-187.
[b] PCB-28, 52,101,118,138 153,180
[c] Sum of cis-nonachlor, trans-nonachlor, and oxychlordane
[d] Sum of α-chlordane, trans-nonachlor, and oxychlordane
[e] Sum of PBDE-47, PBDE-99, PBDE-100
[$] In children in African regions in indoor residual spraying (IRS) of insecticide
[#] Chinese occupational exposure
ng/g lipids = ng/ml, considering a fat percentage of 0.6%, and 1 ml of blood to have a weight of 1 g

Supplementary Table 3: Association between the measured POPs concentrations in human brain samples and neurological disorders.

Study References	*Compound*	*Concentration as reported in the study In Human brain samples*	*Concentration in ng/g of the tissue #*	*Concentration of individual compounds in POP mixture 500x in ng/ml*
PCBs		ng/g of lipid, max. detected		
[20][a]	PCB 28	137.56	68.78	4
	PCB 138	78.30	39.15	77.5
	PCB153	85.87	42.935	126
	PCB 180	76.14	38.07	67
BFRs		ng/g of lipid, max. detected		
[20][a]	PBDE 47	215.54	107.77	4.5
	PBDE 99	87.98	43.99	2
	PBDE 100	29.38	14.69	1
	PBDE 153	81.83	40.91	0.5
	PBDE 154	3.90	1.95	1
PCBs		ng/g wet tissue		
[21][b]	PCB153	2.56 ± 1.81	**2.56 ± 1.81**	126
	PCB 180	2.17 ± 1.87	**2.17 ± 1.87**	67

[#]Considering brain lipids constitute 50% of the brain dry weight

[a]Maximum concentration reported: PCB 28, PCB 180; BDE 99, PBDE 153 in neurotypical controls group (with no known neurodevelopmental abnormalities), and PCB 138, PCB 153; BDE 47, PBDE 100, PBDE 154 in genetic neurodevelopmental disorders group (neurodevelopmental disorders with known genetic basis). POPs congener levels on a panel of human postmortem brain samples from idiopathic ASD, known genetic neurodevelopmental disorders, and controls.

[b]Post-mortem brain samples from control patients and those diagnosed with Parkinson's disease were obtained from the Emory University Bank and from the Nun Study. PCB congeners 153 and 180 were significantly elevated in the brains of Parkinson's disease patients.

References:

[1] Y. Tan, R. Song, D. Lawrence, D.O. Carpenter, Ortho-Substituted but Not Coplanar PCBs Rapidly Kill Cerebellar Granule Cells, Toxicological Sciences 79(1) (2004) 147-156.
[2] E. Mariussen, O. Myhre, T. Reistad, F. Fonnum, The polychlorinated biphenyl mixture aroclor 1254 induces death of rat cerebellar granule cells: the involvement of the N-methyl-D-aspartate receptor and reactive oxygen species, Toxicology and applied pharmacology 179(3) (2002) 137-44.
[3] L.G. Costa, V. Fattori, G. Giordano, A. Vitalone, An in vitro approach to assess the toxicity of certain food contaminants: Methylmercury and polychlorinated biphenyls, Toxicology 237(1) (2007) 65-76.
[4] P.R.S. Kodavanti, T.R. Ward, J.D. McKinney, C.L. Waller, H.A. Tilson, Increased [3H]Phorbol Ester Binding in Rat Cerebellar Granule Cells and Inhibition of45Ca2+Sequestration in Rat Cerebellum by Polychlorinated Diphenyl Ether Congeners and Analogs: Structure–Activity Relationships, Toxicology and applied pharmacology 138(2) (1996) 251-261.
[5] J. Folch, D. Alvira, M. López-Querol, M. Tajes, F.X. Sureda, A. Forsby, V. Rimbau, A. Camins, M. Pallàs, Evaluation of transcriptional activity of caspase-3 gene as a marker of acute neurotoxicity in rat cerebellar granular cells, Toxicology in Vitro 24(2) (2010) 465-471.
[6] D. Bagchi, M. Bagchi, E.A. Hassoun, S.J. Stohs, In vitro and in vivo generation of reactive oxygen species, DNA damage and lactate dehydrogenase leakage by selected pesticides, Toxicology 104(1-3) (1995) 129-40.
[7] R. Rosa, C. Sanfeliu, C. Suñol, A. Pomés, E. Rodríguez-Farré, A. Schousboe, A. Frandsen, The Mechanism for Hexachlorocyclohexane-Induced Cytotoxicity and Changes in Intracellular Ca2+Homeostasis in Cultured Cerebellar Granule Neurons Is Different for the γ- and δ-Isomers, Toxicology and applied pharmacology 142(1) (1997) 31-39.
[8] C. Vale, M.T. Vilaró, E. Rodríguez-Farré, C. Suñol, Effects of the conformationally restricted GABA analogues, Cis-and Trans-4-aminocrotonic acid, on GABA neurotransmission in primary neuronal cultures, Journal of Neuroscience Research 57(1) (1999) 95-105.
[9] C. Vale, E. Fonfra, J. Bujons, A. Messeguer, E. Rodrguez-Farr, C. Suol, The organochlorine pesticides γ-hexachlorocyclohexane (lindane), α-endosulfan and dieldrin differentially interact with GABAA and glycine-gated chloride channels in primary cultures of cerebellar granule cells, Neuroscience 117(2) (2003) 397-403.
[10] M. Kitazawa, V. Anantharam, A.G. Kanthasamy, Dieldrin induces apoptosis by promoting caspase-3-dependent proteolytic cleavage of protein kinase Cδ in dopaminergic cells: relevance to oxidative stress and dopaminergic degeneration, Neuroscience 119(4) (2003) 945-964.
[11] M. Kitazawa, V. Anantharam, A. Kanthasamy, A.G. Kanthasamy, Dieldrin Promotes Proteolytic Cleavage of Poly(ADP-Ribose) Polymerase and Apoptosis in Dopaminergic Cells: Protective Effect of Mitochondrial Anti-Apoptotic Protein Bcl-2, Neurotoxicology 25(4) (2004) 589-598.
[12] C.-Y. Fan, J. Besas, P.R.S. Kodavanti, Changes in mitogen-activated protein kinase in cerebellar granule neurons by polybrominated diphenyl ethers and polychlorinated biphenyls, Toxicology and applied pharmacology 245(1) (2010) 1-8.
[13] J. Chen, C. Liufu, W. Sun, X. Sun, D. Chen, Assessment of the neurotoxic mechanisms of decabrominated diphenyl ether (PBDE-209) in primary cultured neonatal rat hippocampal neurons includes alterations in second messenger signaling and oxidative stress, Toxicology Letters 192(3) (2010) 431-439.
[14] P.R. Kodavanti, T.R. Ward, G. Ludewig, L.W. Robertson, L.S. Birnbaum, Polybrominated diphenyl ether (PBDE) effects in rat neuronal cultures: 14C-PBDE accumulation, biological effects, and structure-activity relationships, Toxicological sciences : an official journal of the Society of Toxicology 88(1) (2005) 181-92.
[15] H.F. Berntsen, C.G. Bjorklund, J.N. Audinot, T. Hofer, S. Verhaegen, E. Lentzen, A.C. Gutleb, E. Ropstad, Time-dependent effects of perfluorinated compounds on viability in cerebellar granule neurons: Dependence on carbon chain length and functional group attached, Neurotoxicology 63 (2017) 70-83.

[16] H.F. Berntsen, C.G. Bjorklund, R. Strandabo, T.M. Haug, A. Moldes-Anaya, J. Fuentes-Lazaro, S. Verhaegen, R.E. Paulsen, R.A. Tasker, E. Ropstad, PFOS-induced excitotoxicity is dependent on Ca(2+) influx via NMDA receptors in rat cerebellar granule neurons, Toxicology and applied pharmacology 357 (2018) 19-32.
[17] B.D. Laird, A.B. Goncharov, H.M. Chan, Body burden of metals and persistent organic pollutants among Inuit in the Canadian Arctic, Environment international 59 (2013) 33-40.
[18] M.-A. Verner, J. Chevrier, G. Ngueta, S. Rauch, R. Bornman, B. Eskenazi, Early-life exposure to p,p'-DDT and p,p'-DDE in South African children participating in the VHEMBE study: An assessment using repeated serum measurements and pharmacokinetic modeling, Environment international 119 (2018) 478-484.
[19] J. Fu, Y. Gao, L. Cui, T. Wang, Y. Liang, G. Qu, B. Yuan, Y. Wang, A. Zhang, G. Jiang, Occurrence, temporal trends, and half-lives of perfluoroalkyl acids (PFAAs) in occupational workers in China, Scientific reports 6 (2016) 38039.
[20] M.M. Mitchell, R. Woods, L.H. Chi, R.J. Schmidt, I.N. Pessah, P.J. Kostyniak, J.M. LaSalle, Levels of select PCB and PBDE congeners in human postmortem brain reveal possible environmental involvement in 15q11-q13 duplication autism spectrum disorder, Environ Mol Mutagen 53(8) (2012) 589-98.
[21] J.M. Hatcher-Martin, M. Gearing, K. Steenland, A.I. Levey, G.W. Miller, K.D. Pennell, Association between polychlorinated biphenyls and Parkinson's disease neuropathology, Neurotoxicology 33(5) (2012) 1298-1304.

PAPER II

Toxicology Letters 338 (2021) 85–96

Contents lists available at ScienceDirect

Toxicology Letters

journal homepage: www.elsevier.com/locate/toxlet

A human relevant mixture of persistent organic pollutants (POPs) and perfluorooctane sulfonic acid (PFOS) enhance nerve growth factor (NGF)-induced neurite outgrowth in PC12 cells

Ajay Yadav[a,b,*], Mazia Amber[c], Denis Zosen[b], Nils Anders Labba[b], Eva Henriette Willemijn Huiberts[b], Johanna Samulin Erdem[d], Fred Haugen[d], Hanne Friis Berntsen[a,d], Shanbeh Zienolddiny[d], Ragnhild Elisabeth Paulsen[b], Erik Ropstad[a], Lisa Connolly[c], Steven Verhaegen[a]

[a] Department of Production Animal Clinical Sciences, Norwegian University of Life Sciences, P.O. Box 369 Sentrum, NO-0102, Oslo, Norway
[b] Section for Pharmacology and Pharmaceutical Biosciences, Department of Pharmacy, University of Oslo, P.O. Box 1068, Blindern, NO-0316, Oslo, Norway
[c] Institute for Global Food Security, Queen's University Belfast, 19 Chlorine Gardens, Belfast, BT9 5DL, Northern Ireland, United Kingdom
[d] National Institute of Occupational Health, P.O. Box 5330 Majorstuen, NO-0304, Oslo, Norway

HIGHLIGHTS

- Nerve growth factor (NGF) induced neuritogenesis in PC12 rat pheochromocytoma cells.
- Persistent organic pollutants (POPs) enhanced NGF-induced neuritogenesis.
- Perfluorooctane sulfonic acid (PFOS) contributed to 50 % of the POP mixture effect.
- Nuclear and mitochondrial health was unaffected by the POP mixture or PFOS.

GRAPHICAL ABSTRACT

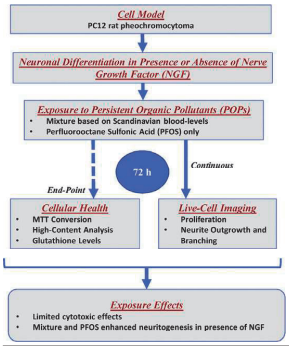

ARTICLE INFO

Article history:
Received 23 October 2020
Received in revised form 1 December 2020
Accepted 6 December 2020
Available online 9 December 2020

Keywords:
Glutathione
Live imaging
Mitochondrial mass
Mitochondrial membrane potential
Rat pheochromocytoma

ABSTRACT

Disruption of neurite outgrowth is a marker for neurotoxicity. Persistent organic pollutants (POPs) are potential developmental neurotoxicants. We investigated their effect on neurite outgrowth in PC12 rat pheochromocytoma cells, in absence or presence of nerve growth factor (NGF), an inducer of neuronal differentiation. Cells were exposed for 72 h to a defined mixture of POPs with chemical composition and concentrations based on blood levels in the Scandinavian population. We also evaluated perfluorooctane sulfonic acid (PFOS) alone, the most abundant compound in the POP mixture. Only higher concentrations of POP mixture reduced tetrazolium salt (MTT) conversion. High-content analysis showed a decrease in cell number, but no changes for nuclear and mitochondrial cellular health parameters. Robust glutathione levels were observed in NGF-differentiated cells. Live imaging, using the IncuCyte ZOOM platform indicated ongoing cell proliferation over time, but slower in presence of NGF. The pollutants did not inhibit neuritogenesis, but rather increased NGF-induced neurite length. PFOS induced neurite

* Corresponding author at: Department of Production Animal Clinical Sciences, Norwegian University of Life Sciences, P.O. Box 369 Sentrum, NO-0102, Oslo, Norway.
E-mail address: ajay.yadav@nmbu.no (A. Yadav).

http://dx.doi.org/10.1016/j.toxlet.2020.12.007
0378-4274/© 2020 The Author(s). Published by Elsevier B.V. This is an open access article under the CC BY license (http://creativecommons.org/licenses/by/4.0/).

outgrowth to about 50 % of the level seen with the POP mixture. Neither the POP mixture nor PFOS affected neurite length in the absence of NGF. Our observations indicate that realistic complex mixtures of environmental pollutants can affect neuronal connectivity via NGF-induced neurite outgrowth.
© 2020 The Author(s). Published by Elsevier B.V. This is an open access article under the CC BY license (http://creativecommons.org/licenses/by/4.0/).

1. Introduction

Normal development of the central nervous system requires the coordinated ontogeny of proliferation, migration, differentiation, synaptogenesis, gliogenesis, myelination and apoptosis (Barone et al., 2000). Perturbations of these processes through exposure to environmental toxicants during development, could affect structures and functions of the brain, leading to lifelong impairment (Grandjean and Landrigan, 2006). Pregnancy and early life stages are particularly vulnerable to exposure to toxicants including persistent organic pollutants (POPs). The growth of dendrites and synapses is fundamental for the development of neuronal circuits that underlie human cognition and behaviour. Disruption of synaptic circuits are associated with intellectual disability, epilepsy, autism spectrum disorder (ASD), schizophrenia and bipolar disorder (Forrest et al., 2018). The chemicals that disrupt the growth of these axonal and dendritic processes (collectively called "neurites") have been linked with developmental neurotoxicity (DNT) *in vivo* (Radio et al., 2008, 2010). Many of the neurodevelopmental processes that occur *in vivo* for example cell differentiation, neurite outgrowth, and synaptogenesis, can be followed using *in vitro* neuronal systems. Among these, the measurement of neurite outgrowth has received the most attention (Radio and Mundy, 2008). Chemicals that can affect the neurite outgrowth include POPs. Various cell lines have been used to study the effects of chemicals on neurons (Radio and Mundy, 2008), including the pheochromocytoma PC12 cell line which has been widely used as a model for the study of neuronal differentiation and neurite outgrowth (Fujita et al., 1989). PC12 is a cell line established from a transplantable rat adrenal pheochromocytoma (Greene and Tischler, 1976). Serum-withdrawal together with stimulation with nerve growth factor (NGF) results in the cells undergoing one doubling and induction of neurite outgrowth (Greene, 1978).

Glutathione (GSH) acts as an important antioxidant. Because of the extensive oxidative metabolism in the brain from mitochondrial respiration, the cells of this organ continuously generate reactive oxygen species. As a result, the antioxidant function of GSH appears to be especially important for the brain. Further, a compromised GSH metabolism contributes to the progression of neurological disorders (Schmidt and Dringen, 2012).

POPs are mostly halogenated compounds that are highly resistant to environmental degradation, and that bioaccumulate and biomagnify in living organisms (UNEP, 2008). Several POPs, including polychlorinated biphenyls (PCBs), organochlorine pesticides (OCPs), polybrominated diphenyl ethers (PBDEs), perfluorooctane sulfonic acid (PFOS), and perfluorooctanoic acid (PFOA) are supposed to be developmental neurotoxicants (Grandjean and Landrigan, 2014; Hoyer et al., 2015; Kodavanti, 2006; Schmidt et al., 2014). Whereas many of the studies on POPs focus on single compound or a small group of contaminants, we are in real life exposed simultaneously to a complex mixture of contaminants, which could have additive, synergistic or antagonistic effects (Bopp et al., 2018; SCHER, 2012; WHO, 2017).

Previously, we designed an environmentally relevant mixture of POPs for use in animal and *in vitro* experimental studies, containing 29 different chlorinated, brominated, and perfluorinated compounds (Berntsen et al., 2017). The mixture used in the present study contained POPs concentrations based on measured human blood concentrations in Scandinavia and aimed to provide a defined and realistic mixture of environmental contaminants for toxicity studies that could reflect the relative levels of POPs to which individuals are exposed (Berntsen et al., 2017).

PFOS belongs to the chemical class of perfluorinated alkyl substances (PFAS), a family of emerging persistent pollutants of increasing concern with regards to adverse health outcomes, including cognitive effects (Spratlen et al., 2020). In our unpublished studies (manuscript under review) we found that the POP mixture at 500x fold human blood levels and PFOS at 20 μM, in a corresponding concentration, induced excitotoxicity via the involvement of N-methyl-D-aspartate receptor (NMDA-R) in cultures of chicken cerebellar granule neurons (CGNs). A similar result has been observed by our group using the same POP mixture at concentrations from 500x, and PFOS in rat as well as in chicken CGNs (Berntsen et al., 2018, 2020). PFOS-induced neurotoxicity has also previously been studied in PC12 cells (Li et al., 2017; Slotkin et al., 2008). As PFOS is the compound occurring at the highest concentration in the POP mixture, we also evaluated PFOS as an individual compound.

High Content Analysis (HCA) is a novel, high-throughput, quantitative fluorescence technique providing an important approach for the detection of compound toxicity at the level of individual cells (O'Brien et al., 2006; Wilson et al., 2016). Cellular health markers like cell number (CN), nuclear area (NA), nuclear intensity (NI), mitochondrial membrane potential (MMP), mitochondrial mass (MM) cover cellular metabolic functions (O'Brien and Haskins, 2007; Wilson et al., 2016). The detection/investigation of these multiple nuclear and mitochondrial parameters allowed us to evaluate cellular health at the end of the differentiation process. Measurements of intracellular GSH levels was used as a marker for possible effects of the POP exposures on the cellular defence mechanism.

Since neuritogenesis is a marker for neuronal differentiation, and neurite outgrowth is very sensitive to neurotoxicants we investigated the effects of POPs on neurite dynamics in the PC12 cell model. We used the IncuCyte ZOOM platform which takes non-perturbing phase-contrast images of neuronal cultures under physiological conditions over an extended period of time (Garay et al., 2016), and has been used to study neurite dynamics in different neuronal cells (Mengel et al., 2019; Yagi et al., 2015). This platform also allowed us to follow cell proliferation over time, which complemented the end point parameters described above.

2. Material and methods

2.1. Chemicals, PFOS, and the POP mixture

Dulbecco's modified Eagle's medium (DMEM) and L-glutamine were obtained from Lonza BioWhittaker (Verviers, Belgium). Penicillin-streptomycin, sodium pyruvate and horse serum were purchased from Gibco, Life Technologies (Paisley, UK). Foetal bovine serum (South America) was from BioWest (Nuaille, France). Dimethyl sulfoxide (DMSO), monochlorobimane (mBCl), thiazolyl blue tetrazolium bromide (MTT), formalin and mouse neural growth factor (NGF) were all supplied by Sigma-Aldrich (Poole, Dorset, UK). Hoechst 33342 nuclear stain and mitochondrial membrane potential dye (MitoTracker™ Red CMXRos) were provided by Thermo Scientific (UK). Valinomycin, perfluorooctanesulfonic acid potassium salt (PFOS ≥ 98

%) as well as all other reagents were from Sigma-Aldrich (St Louis, MO, USA).

In the cell toxicity test PFOS concentrations were chosen in the range of 10–100 μM, based on previous studies in PC12 cells (Berntsen et al., 2018). In the neurite outgrowth study the range was between 10–50 μM, because in the preliminary studies the concentration above 50 μM showed no effect on neurite outgrowth and was associated with fewer cells.

The defined POP mixture was designed and prepared at the Norwegian University of Life Sciences (NMBU), Oslo, Norway (Berntsen et al., 2017). The mixture contained 29 different compounds (Supplementary Table 1), including six perfluorinated (PFAA) (i.e., PFHxS, PFOS, PFOA, PFNA, PFDA, and PFUnDA), seven brominated (Br) (i.e., PBDE 47, PBDE 99, PBDE-100, PBDE 153, PBDE 154, PBDE 209, and HBCD), and sixteen chlorinated compounds (Cl) compounds (i.e., PCB 28, PCB 52, PCB 101, PCB 118, PCB 138, PCB 153, PCB 180, p,p'-DDE, HCB, α-chlordane, oxychlordane, trans-Nonachlor, α-HCH, β-HCH, γ-HCH and Dieldrin). The relative concentrations of the chemicals in the mixture were based on Scandinavian human blood levels and the choice of compounds were based on compounds found at high levels in blood, breastmilk and/or food. The stocks used in the present study had a concentration of 10^6 times measured human blood levels and stocks were created using DMSO as a solvent. We used the POP mixture concentration from 10 to 500x (fold human blood levels), as previously exposure with this mixture showed biological activity in the range of 1/10−500x (fold human blood levels) in a wide variety of cell systems (Doan et al., 2019; McComb et al., 2019; Shannon et al., 2019).

2.2. Cell culture and treatment

The rat pheochromocytoma cell line PC12 was cultivated in growth medium consisting of DMEM with penicillin-streptomycin, sodium pyruvate, and supplemented with 5% horse serum and 10 % foetal bovine serum as described previously (Rakkestad et al., 2014). Cells were seeded out in 96 wells plates (100 μL/well) and 35 mm diameter dishes (1 mL/dish) in a serum free medium and then incubated for 4–6 h for attachment and serum starvation. Without removing the medium, an equal volume of fresh medium containing horse serum (final 2%), NGF (final 50 ng/mL) and test compounds/controls, was thereafter added to each well. Plates were incubated further for 72 h prior to the assay. The exposure scenario is overviewed in Fig. 1.

2.3. MTT conversion assay

Cell viability was measured by MTT colorimetric assay, as described previously (McComb et al., 2019). This assay is based on the conversion of MTT (3-(4,5-dimethylthiazol-2-yl)-2,5-diphenyl tetrazolium bromide, a pale yellow substrate to a dark blue formazan product by the mitochondrial enzyme succinate dehydrogenase in living cells (Mosmann, 1983). Cells were seeded in clear flat-bottomed 96-well plates (Nunc, Roskilde, Denmark) at a density of 1×10^4 cells/cm^2 and exposed to test compounds either in the presence or absence of NGF. Following 72 h exposure with test compounds, the supernatant was discarded, and cells were incubated further with 2 mg/mL MTT (in PBS) solution diluted 1:6 in assay media. Again, the supernatant was removed, and 200 μL/well of DMSO was added to dissolve the formazan crystals. Subsequently, the plate was incubated at 37 °C with agitation for 10 min. Optical density was measured at 570 nm with a reference filter at 630 nm using a Sunrise spectrophotometer (TECAN, Switzerland). Cell viability was measured as the percentage absorbance of the sample compared with the absorbance of the solvent control.

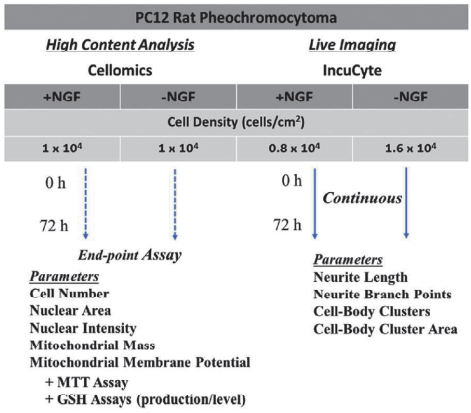

Fig. 1. Exposure overview of experiments.

Valinomycin (Vln) was used as a positive control in the MTT conversion assay and HCA assay. Exposure to Vln induces a dissipation of the mitochondrial transmembrane potential, leading to mitochondrial dysfunction (Abraham et al., 2008).

2.4. Cellular and mitochondrial health assessed by High Content Analysis (HCA)

The experimental procedure was followed as detailed previously (Shannon et al., 2017; Wilson et al., 2016). The Cellomics® HCS reagent series multiparameter cytotoxicity assay was performed following the manufacturer's instructions. Cells were seeded into collagen bio-coat BD Falcon 96 well flat bottomed microtitre plates (BD Biosciences, Bedford, MA, US) at a density of 1×10^4 cells/cm^2 and exposed to test compounds either in the presence or absence of NGF. Briefly, mitochondrial membrane potential dye was prepared by adding 117 μL of anhydrous DMSO to make a 1 mM stock. Following 72 h incubation, 50 μL of live cell stain (final 0.1 μM) was added to each well for 30 min at 37 °C and protected from light. The live stain was removed, and cells were then fixed with a 10 % formalin solution for 20 min at room temperature (RT) and washed with PBS. Hoechst 33342 dye (final 1.6 μM) was added to each well and incubated for 10 min at RT, after which cells were washed with PBS. The wells were then filled with 200 μL PBS, sealed with plate sealer and evaluated on a CellInsight™ NXT High Content Screening Platform (Thermo Fisher Scientific, UK). This instrument analyses epifluorescence of individual cell events using an automated micro-plate reader analyzer interfaced with a Dell precision 136 T5600 workstation.

Hoechst dye was used to measure CN, and nuclear morphology including NI and NA. Mitochondrial membrane potential dye (MitoTracker™ Red CMXRos) was used to measure mitochondrial health, specifically MMP and MM. Data were captured for each plate using a 10x objective magnification in the selected excitation and emission wavelengths of Hoechst dye (Ex/Em 350/461 nm) and mitochondrial membrane potential dye (Ex/Em 554/576 nm). For each well, nine fields of view images were acquired to examine each parameter.

2.5. Glutathione measurements

Total reduced GSH levels in CGNs were measured with mBCl as described previously (Sørvik et al., 2018). In brief, cells were seeded in black 96 wells plates at a density of 1×10^4 cells/cm^2 and

exposed with test compounds for 72 h. Then medium was removed and replaced with new medium containing 40 μM of mBCl and incubated further in the dark at 37 °C for 30 min. Subsequently the medium was removed, and plates were washed with freshly prepared experimental buffer containing 140 mM NaCl, 3.5 mM KCl, 15 mM Tris HCl (pH 7.4), 5 mM glucose, 1.2 mM Na_2HPO_4 (pH 7.4), and 2 mM $CaCl_2$. 100 μl of the buffer was added to each well, and mBCl fluorescence was measured at the excitation wavelength of 380 nm (15 nm bandwidth) and emission wavelength of 478 nm (21 nm bandwidth) using a CLARIOstar® plate reader. Further, in the same exposure, we also quantified cell number using nuclei staining with Hoechst 33342. Buffers were replaced with Hoechst 33342 (0.4 μg/mL) and incubated in dark for 1 min. Subsequently, the plate was read at excitation wavelengths of 350 nm (22 nm bandwidth) and emission wavelengths of 461 nm (36 nm bandwidths). This measurement was used to correct for cell number in the calculations for GSH levels after subtraction of blank values.

2.6. Transfection and luciferase assay for GCLC promoter activity assessment

The procedure has been detailed previously (Sørvik et al., 2018). Cells were seeded in Ø35 mm dishes at a density of 1.25×10^4 cells/cm^2 and allowed to attach for 24 h. On culture day 1, cells were transfected with GCLC (catalytic subunit) promoter coupled to luciferase (GCLC-luc; 0.8 μg; a kind gift from R. Blomhoff, Department of Nutrition, University of Oslo) and internal control vector pRL-TK (0.2 μg; purchased from Promega, WI, US) to a total of 1 μg DNA/mL culture medium. Transfection medium was replaced with fresh medium after 4 h. On culture day 2, cells were exposed with test compounds dissolved in serum free or serum free plus NGF medium. After 48 h luciferase was measured with a luminometer (Lumat LB9507; Berthold Technologies GmbH, Bad Wildbad, Germany) as described previously (Strom et al., 2010). *Renilla* luciferase was measured using the kit Dual-Luciferase® Reporter Assay System in accordance with the manufacturer's instructions (Promega, WI).

2.7. Live cell imaging using the IncuCyte neurite analysis

The IncuCyte ZOOM live-cell imaging system (Essen BioScience, UK) was used to analyse neurite dynamics. Different parameters were quantified over time using an automated IncuCyte® Neurotrack software module, as detailed previously (Garay et al., 2016). PC12 cells were seeded in 96-well TPP (Techno Plastic Products AG, Switzerland) plates and exposed to test compounds either in the presence or absence of NGF, as described above. Cells were seeded at a density of 0.8×10^4 cells/cm^2 in the presence of NGF and 1.6×10^4 cells/cm^2 in the absence of NGF. Plates were scanned every 60 min over a 72 h period using a 10x objective. Four images per well were captured and images were analysed for neurite length, branch points, cell-body clusters number and area. The masks/filters adjustment for Neurotrack phase contrast image analysis were as follows: Segmentation mode: Texture; Hole fill: 0; Adjust size: −5 μm; Min cell width: 8 μm; Neurite filtering: Best;

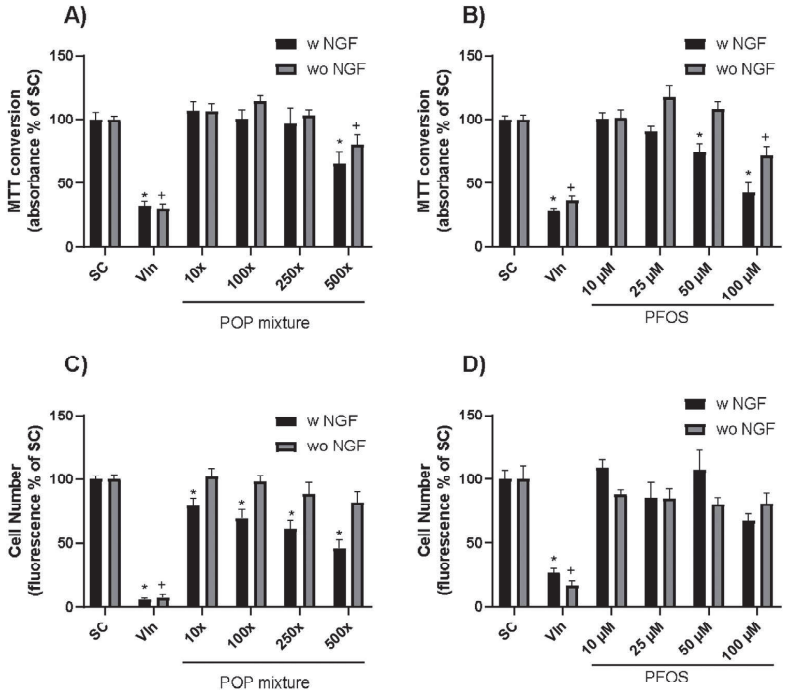

Fig. 2. Assessment of cytotoxic effects in PC12 using the tetrazolium MTT conversion assay or high content analysis (HCA). Cells were exposed in the presence or absence of NGF (50 ng/mL) with solvent control (SC, DMSO 0.1 %), POP mixture (x human blood levels) or PFOS (μM). Valinomycin (Vln, 15 μM) was included as a positive control. Following 72 h exposure to the compounds, cell viability was measured by conventional MTT conversion assay for A) POP mixture, and B) PFOS. Cell number measured by multi-parameter HCA is shown for C) POP mixture, and D) PFOS. Data are mean, n = 3-4 independent experiments, with replicate > 3. All values were presented relative to the corresponding solvent control (SC, 0.1 % DMSO) defined as 100 %, $^*p < 0.05$, compared to SC with NGF and $^+p < 0.05$ compared to SC without NGF, w = with NGF and wo = without NGF.

Neurite sensitivity: 0.35 μm; and Neurite width: 1 μm, detailed in (NeuroTrack™, 2020). The following parameters were quantified:

1 Cell-Body Clusters (CBC) = total number of cell body clusters/ area of image field;
2 Cell-Body Cluster Area (CBCA) = sum of areas of all cell-body clusters pooled/area of image;
3 Neurite Length (NL) = sum of lengths of all neurites pooled/ area of image field;
4 Neurite Branch Points (NBP) = total number of branch points/ area of image field.

2.8. Statistical analysis

Results are presented as mean ± standard error of the mean (SEM), n = 3–4 independent experiments, with replicates > 4 per group. IncuCyte data were analysed using the mixed model personality in JMP Pro 14® (SAS, Cary, USA). Dependent variables were CBC, CBCA, NL and NBP. For the statistical analysis log transformed dependent variables gave a satisfactory fit to the normal distribution. Independent fixed effect variables were: exposure group, time in culture and their interaction. Experiment and the nested effect of time within experiment were entered as random effects allowing for repeated measurements along the time scale. Dunnett's test was used to compare differences between groups exposed to chemicals and control (solvent control, 0.1 % DMSO). The effect of NGF on log transformed dependent variables (CBC, CBCA, NL and NBP) was explored in a separate mixed model using a subset of data including only controls. Independent variables included as fixed effects were time in culture, NGF and their interaction. All other data were analysed using Graph pad 8.2 (San Diego, CA, US). Outlier values were tested for by the built-in feature in GraphPad (Robust regression and Outlier removal, Q = 1%). A one-way analysis of variance (ANOVA) followed by Dunnett's multiple comparisons test was used to determine significant differences between treatments and solvent control. An unpaired *t*-test was used for comparison when appropriate between two groups. A *p*-value of < 0.05 was considered significant.

3. Results

3.1. Effects of POP mixture or PFOS on cytotoxicity as measured by MTT conversion assay

In a first approach, cytotoxic effects of pollutants on PC12 cells viability were evaluated using the MTT conversion assay. Both in the presence and absence of NGF, exposure to the POP mixture reduced MTT activity only at the highest concentration tested (Fig. 2A). PFOS alone reduced MTT activity significantly at 50 and 100 μM,which were 2.5 and 5 times higher than the corresponding concentration in the POP mixture at 500x (Fig. 2B). In the absence of NGF, reduced MTT activity was only observed at 100 μM (Fig. 2B).

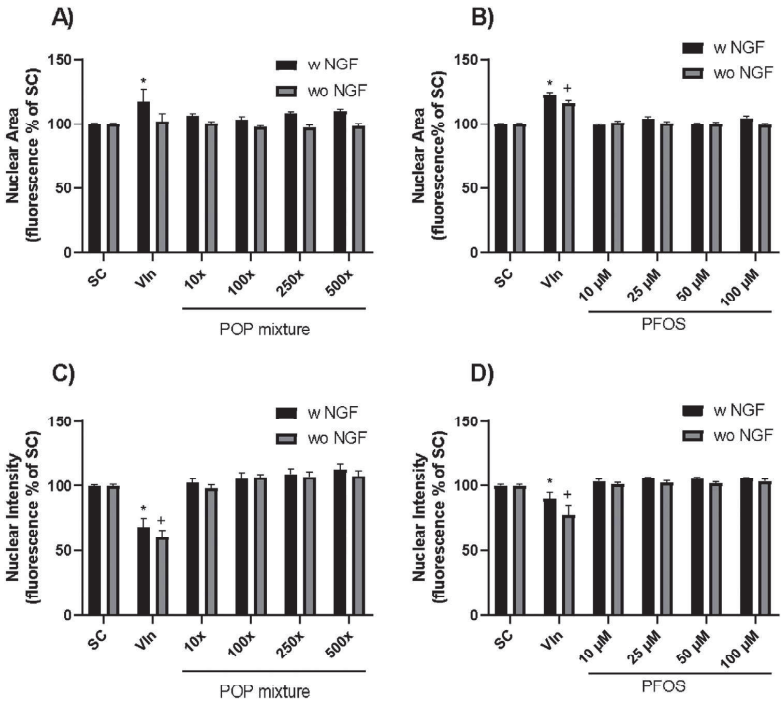

Fig. 3. Assessment of changes in nuclear health in PC12 using high content analysis (HCA). Cells were exposed in the presence or absence of NGF (50 ng/mL) with solvent control (SC, DMSO 0.1 %), POP mixture (x human blood levels) or PFOS (μM). Valinomycin (Vln, 15 μM) was included as a positive control. Multiparameter HCA endpoints were measured following 72 h exposure to the test compounds. Results for nuclear area is shown for A) POP mixture, and B) PFOS. Nuclear intensity is shown for C) POP mixture, and D) PFOS. Data are mean, n = 3-4 independent experiments, with replicate > 3. All values were presented relative to the corresponding solvent control (SC, 0.1 % DMSO) defined as 100 %. $^{*}p < 0.05$, compared to SC with NGF and $^{+}p < 0.05$ compared to SC without NGF, w = with NGF and wo = without NGF.

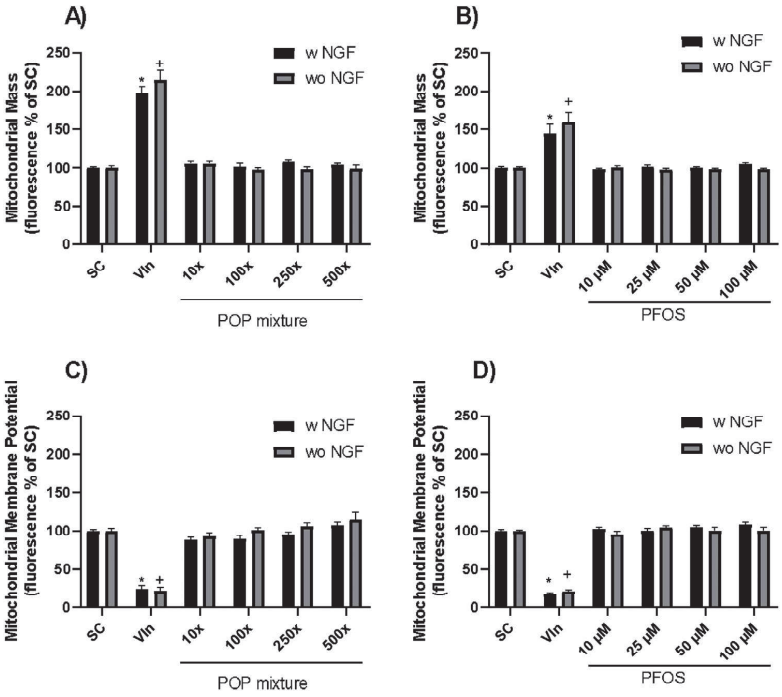

Fig. 4. Assessment of changes in mitochondrial health in PC12 using high content assay (HCA). Cells were exposed in the presence or absence of NGF (50 ng/mL) with solvent control (SC, DMSO 0.1 %), POP mixture (x human blood levels) or PFOS (µM). Valinomycin (Vln, 15 µM) was included as a positive control. Multiparameter HCA endpoints were measured following 72 h exposure to the test compounds. Results for mitochondrial mass is shown for A) POP mixture, and B) PFOS. Mitochondrial membrane potential is shown for C) POP mixture, and D) PFOS. Data are mean, n = 3-4 independent experiments, with replicate >3. All values were presented relative to the corresponding solvent control (SC, 0.1 % DMSO) defined as 100 %. $^{*}p < 0.05$, compared to SC with NGF and $^{+}p < 0.05$ compared to SC without NGF, w = with NGF and wo = without NGF.

3.2. Effect of POP mixture or PFOS on cell number measured by HCA

To investigate whether decreases in MTT activity was due to a reduction in cell number we evaluated cell number independently by HCA. For the POP mixture in the presence of NGF, reductions in cell number as measured by HCA were already significant at 10x (fold human blood levels, Fig. 2C). However, in the absence of NGF the cell number remained unaffected at any of the concentrations tested (Fig. 2C). For PFOS alone no significant concentration-response was observed for cell number in the presence or absence of NGF (Fig. 2D).

3.3. Effects of POP mixture or PFOS on cytotoxicity as measured by nuclear and mitochondrial health using HCA

Alternatively, MTT activity can be affected by diminished mitochondrial health resulting in cell loss via cell death. Thus, we investigated additional HCA toxicity parameters for nuclear and mitochondrial health. Both in the presence or absence of NGF, exposure to either the POP mixture or PFOS did not affect the nuclear (Fig. 3A–D) or mitochondrial parameters (Fig. 4A–D).

HCA images using Hoechst dye (nuclear staining) and mitochondrial potential dye (mitochondrial staining) are illustrated in Supplementary Fig. 1.

3.4. Effects of POP mixture or PFOS on glutathione levels and GCLC promoter activity

Since intracellular GSH levels are important for cell survival, we measured the effects of pollutants on total levels of GSH by mBCl probe, as well as the production of GSH by GCLC promoter activity. In the presence of NGF the POP mixture significantly increased glutathione levels at 10x blood levels, whereas at higher concentrations the glutathione levels were comparable with control levels. In the absence of NGF, glutathione levels were reduced in a concentration-dependent manner to half the level seen in the solvent control (SC, 0.1 % DMSO; Fig. 5A). Both in the presence or absence of NGF the GCLC promoter activity following 48 h exposure to POP mixture 500x remained unaffected. This suggests that the synthesis of GSH did not change following the exposure to POP mixture (Fig. 5B).

3.5. Effects of POP mixture or PFOS on cell body clusters and area in PC12 cells with and without NGF

We quantified the number of cell body clusters (CBC) and area (CBCA) using IncuCyte live cell imaging which can be interpreted as a measure of proliferation and cell body size, respectively. CBC number and CBCA increased with time in culture for all conditions

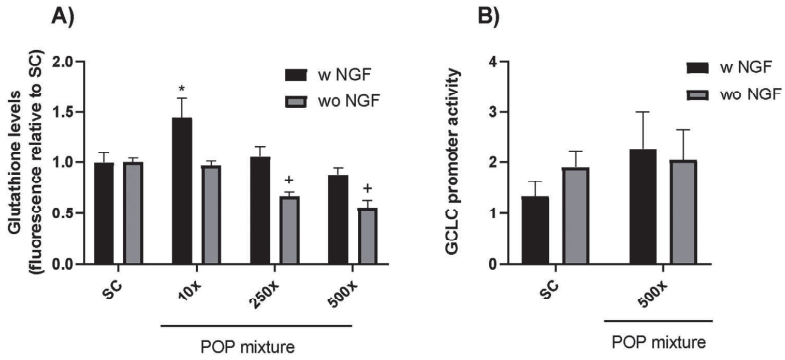

Fig. 5. Assessment of glutathione (GSH) levels and GSH production levels. Cells were exposed in the presence or absence of NGF (50 ng/mL) with solvent control (SC, DMSO 0.1 %) or POP mixture (x human blood levels) or PFOS (μM). A) GSH level using mBCl was measured following 72 h exposure, and B) GCLC promoter activity following 48 exposure. Data are mean, n = 3-4 independent experiments, with replicate > 3. All values were presented relative to the corresponding solvent control (SC, 0.1 % DMSO) defined as 1 for GSH, $^{*}p < 0.05$, compared to SC with NGF and $^{+}p < 0.05$ compared to SC without NGF, w = with NGF and wo = without NGF.

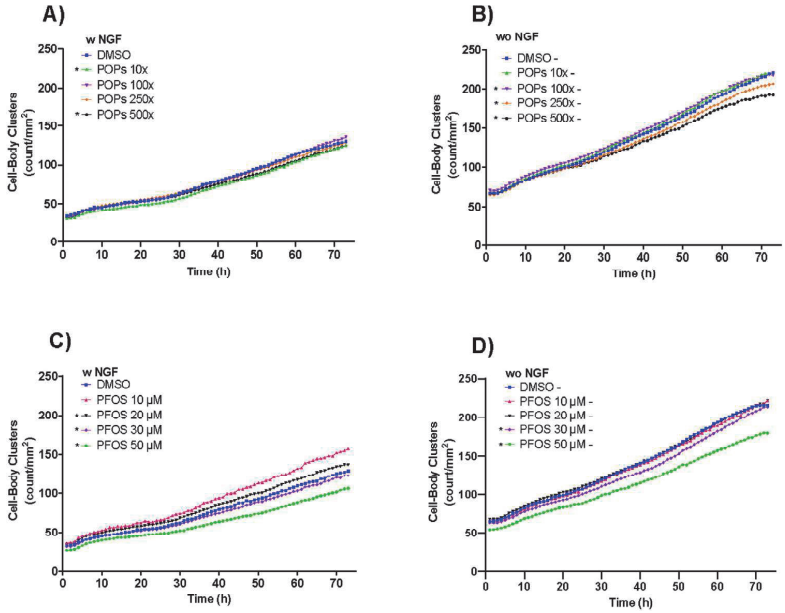

Fig. 6. Assessment of changes in cell body clusters (CBC) in PC12 cells after exposure to POP mixture or PFOS using live-cell imaging. Effect of the compounds in presence of NGF (50 ng/mL) (A and C) or its absence (B and D) were evaluated. Cell were exposed to the POP mixture (A and B), or to PFOS (C and D). Solvent control was DMSO 0.1 %. Concentration of the POP mixture is indicated as POPs x human blood levels. PFOS concentrations are in μM. Average CBC (total number of cell body clusters/area of image field) were automatically measured by Neuro Track software, every 60 min, followed for 72 h. For clarity, the graph is presented only with mean value at different time points. Data are mean, n = 3-4 independent experiments, with replicate > 3 per group. Statistical difference between the overall average of the exposed groups and the solvent control (0.1 % DMSO) is indicated on the left-hand side of the figure legends ($^{*}p < 0.05$), w = with NGF and wo = without NGF.

tested (Figs. 6 and 7). CBC number for DMSO control tripled for PC12 cells stimulated with NGF alone (Fig. 6A, C) and nearly quadrupled without NGF (Fig. 6B, D). NGF exposure was associated with a significant decrease in the overall least squares (LS) mean log CBC and log CBCA (Figs. 6 and 7; Supplementary Table 3). Exposure to high concentrations of POP mixture and PFOS was associated with a significant decrease in log CBC and log CBCA whereas low and intermediate concentrations had variable effects (Supplementary Table 2; Figs. 6 and 7).

Phase contrast IncuCyte images and images after applying Neuro Track masks for CBCs and neurites are illustrated in Supplementary Figs. 2 and 3.

3.6. Effects of POP mixture or PFOS on neurite length and branch points in PC12 cells with and without NGF

We quantified neurite length and neurite branch points as measures of neurite outgrowth using IncuCyte live cell imaging. NL

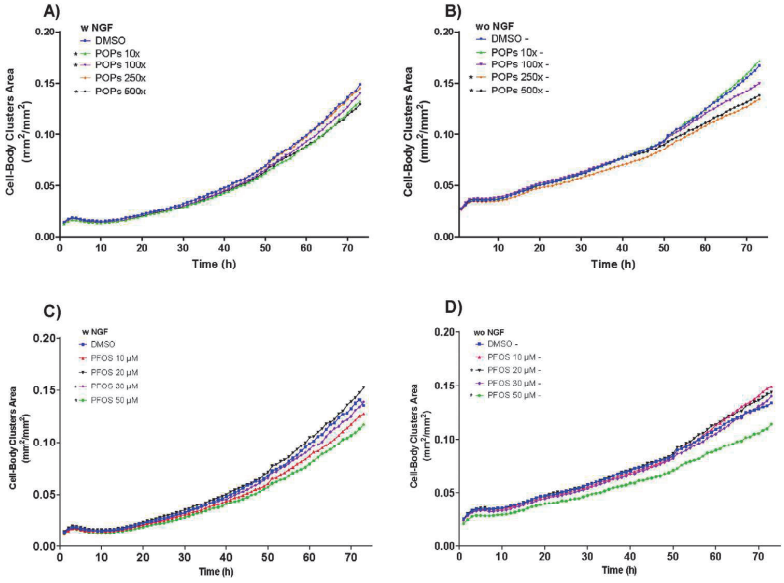

Fig. 7. Assessment of changes in Cell-Body Cluster Area (CBCA) in PC12 cells after exposure to POP mixture or PFOS using live-cell imaging. Effect of the compounds in presence of NGF (50 ng/mL) (A and C) or its absence (B and D) were evaluated. Cell were exposed to the POP mixture (A and B), or to PFOS (C and D). Solvent control was DMSO 0.1 %. Concentration of the POP mixture is indicated as POPs x human blood levels. PFOS concentrations are in μM. Average CBCA (sum of areas of all cell-body clusters pooled/area of image) were automatically measured by Neuro Track software, every 60 min, followed for 72 h. For clarity, the graph is presented only with mean value at different time points. Data are mean, n = 3-4 independent experiments, with replicate > 3 per group. Statistical difference between the overall average of the exposed groups and the solvent control (0.1 % DMSO) is indicated on the left-hand side of the figure legends (*$p < 0.05$), w = with NGF and wo = without NGF.

and NBP increased with time in culture for all conditions in the presence of NGF (Figs. 8A, C, and 9 A, C, respectively). Only a marginal increase was observed with time in culture when NGF was not present (Figs. 8B, D and 9 B, D, respectively).

In PC12 cells stimulated with NGF, the POP mixture significantly increased the neurite length in a concentration-dependent manner compared to the effect of NGF alone (Fig. 8A; Supplementary Table 2). PFOS had a similar, but less pronounced effect. PFOS at concentrations of 20 μM and above significantly increased the neurite length compared to NGF alone over the 72 h period (Fig. 8C; Supplementary Table 2). In the absence of NGF, the effects of POPs and PFOS on NL were marginal (Fig. 8B, D; Supplementary Table 2).

Similar patterns were observed for the number of branch points (Fig. 9A–D; Supplementary Table 2).

4. Discussion

We investigated if a POP mixture based on human blood levels from the Scandinavian population can affect cellular health and neurite dynamics, using PC12 cells as a model. Outcomes were compared to PFOS alone, the most abundant compound in the POP mixture.

Cytotoxicity of the POP mixture exposure after 72 h evaluated by MTT conversion was only seen at higher concentrations. Reduced conversion of MTT to formazan by PC12 cells could indicate a reduction of mitochondrial activity, rather than reduced proliferation or loss of cells. However, a decrease in cell number was measured by HCA. Yet, the HCA nuclear and mitochondrial parameters remained unchanged and were indicative of healthy cells. This suggests that the reduction seen in MTT was mainly due to a reduced proliferation. The IncuCyte experiments allowed us to follow cell proliferation in a dynamic way over the full 72 h exposure. Indeed, the number of cell body clusters (CBC) can be interpreted as a measurement of cell proliferation, although it gives no information about the number of cells in each individual cluster. This can be gathered from the cell cluster area (CBCA), a measurement of the total area of cell clusters per image field. In all exposures, both CBC number and CBCA increased linearly over time, indicative of continued cell proliferation. However, the rise was slower in the presence of NGF, indicating a negative effect of NGF on cell proliferation. This is in accordance with the observations that NGF-induced differentiation in PC12 cells is linked with reduced cell proliferation (Greene and Tischler, 1976). During the 72 h period the most potent POP mixture concentration (500x) slowed down the rate of CBC number increase compared to solvent control. However, in the absence of NGF, the same concentration had more outspoken effect on the rate of reduction in CBC number increase. This could be related to the relative lower level of GSH as discussed below.

For PFOS in the presence of NGF, no reduction in MTT was seen at lower concentrations (10 and 25 μM), although higher concentrations (50 and 100 μM) showed a reduction compared to control. No significant changes in cell number at any concentration could be observed. As with the POP mixture, no effects were seen on nuclear and mitochondrial parameters. PFOS at lower concentration (10 and 20 μM) seemed to have a stimulating effect on the rate of CBC number increase compared to control, whereas higher concentrations (30 and 50 μM) led to lower rate. Thus, we can conclude PFOS concentrations (20 and 25 μM) relevant to those present in the total POP mixture did not adversely affect neither cell proliferation nor cellular toxicity. In the absence of NGF, only at 100 μM a reduction in MTT activity was observed, but this PFOS concentration is about 5 times higher than relevant to the POP mixture. Again, no significant effects on cell

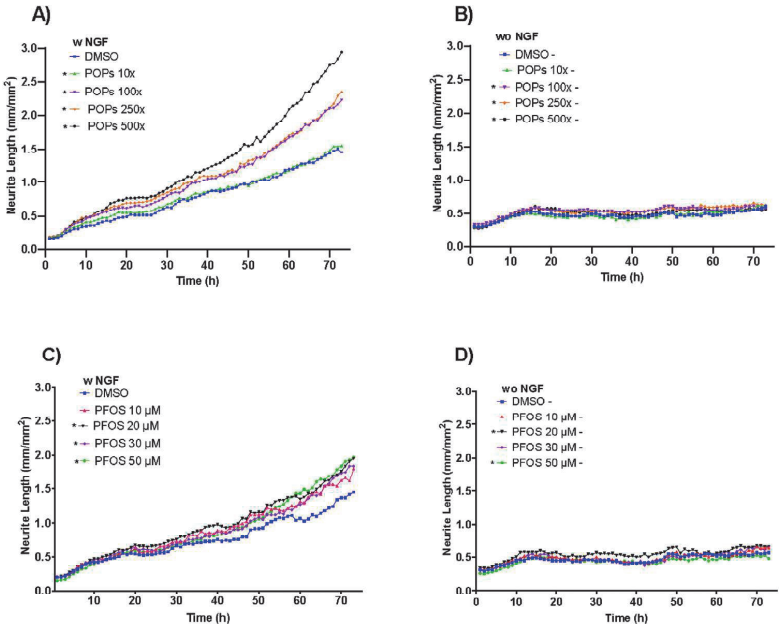

Fig. 8. Assessment of changes in neurite length over time in PC12 cells after exposure to POP mixture or PFOS using live-cell imaging. Effect of the compounds in presence of NGF (50 ng/mL) (A and C) or its absence (B and D) were evaluated. Cell were exposed to the POP mixture (A and B), or to PFOS (C and D). Solvent control was DMSO 0.1 %. Concentration of the POP mixture is indicated as POPs x human blood levels. PFOS concentrations are in µM. Average neurite lengths (sum of lengths of all neurites pooled/area of image field in mm/mm^2) were automatically measured by Neuro Track software, every 60 min, followed for 72 h. For clarity, the graph is presented only with mean value at different time points. Data are mean, n = 3-4 independent experiments, with replicate > 3 per group. Statistical difference between the overall average of the exposed groups and the solvent control (0.1 % DMSO) is indicated on the left-hand side of figure legends (*$p < 0.05$), w = with NGF and wo = without NGF.

number and cellular health parameters in HCA were observed. However, concentrations of 30 and 50 µM lead to decrease in CBC number.

Intracellular GSH levels are important for cell survival and protect the cells against injury caused by ROS. We have previously observed that the POP mixture and PFOS negatively affected GSH levels in chicken cerebellar granule cells (manuscript under review). Thus, we tested if PC12 cells were equally affected. In the presence of NGF, low concentrations of POP mixture raised GSH level, which was absent for the higher concentrations. In the absence of NGF, POP mixture exposure led to a decrease in GSH, suggesting that NGF-differentiated cells have a more robust GSH defence mechanism. Indeed, treatment with NGF has been shown to increase the level of GSH in PC12 cells (Kamata et al., 1996). We found no evidence that either in the presence or absence of NGF, the POP mixture at 500x affected GCLC promotor activity, suggesting it did not affect production rates of GSH.

NGF can stimulate neurite outgrowth in PC12 cells, and neurite outgrowth can be used as a marker for neuronal differentiation (Radio and Mundy, 2008). Indeed, in our system NGF alone was a sufficient driver for altering the cellular and neurite dynamics compared to DMSO control. Chemicals, including POPs, could potentially affect neuronal outgrowth (Addae et al., 2013; Angus and Contreras, 1995; Radio et al., 2008). However, it seems exposure to the POP mixture cannot mimic the NGF-receptor signal on its own. We found that exposure to the POP mixture did enhance NGF-induced neurite length and branched networks of neurites in a concentration- and time-dependent manner. This suggests that the POP mixture might have potentially influenced the NGF neurotrophic system. Similar to our results, Angus and Contreras (1995) found that Aroclor 1254 (a technical mixture of PCBs) enhanced NGF-stimulated neurite outgrowth in PC12 cells and caused an increase in the affinity of binding of NGF to the high-affinity NGF receptors. However, Aroclor 1254 is an industrial mixture with a lot-to-lot variation of *ortho*- and non-*ortho*-PCB composition (Kodavanti et al., 2001). In contrast, our mixture is chemically defined and contains mainly non-dioxin like PCBs. Thus, our observations indicate that non-dioxin-like PCBs might contribute to neuritogenesis. The effects of PFOS on both neurite length and branch point parameters in absolute numbers were about 50 % of the full mixture. The effect of PFOS seemed to plateau from 20 µM onwards. This also represents the concentration of PFOS present in the POP mixture at 500 ×. Thus, PFOS alone can explain part of the effect seen with the POP mixture, but additional compounds contribute to the overall effect. At present, mechanisms are not known.

Studies *in vitro* have shown the differential effects of individual POPs on neurite outgrowth using different neuronal cells. PCB 153 or PCB 180 at 100 nM facilitated the neurite outgrowth associated with a decrease in cell proliferation, indicating an increase in neuronal differentiation in primary rat embryonic neural stem cells (Tofighi et al., 2011). In the POP mixture at 500x, PCB 153 is present at 349 nM and PCB 180 at 170 nM. Generally, OCPs have been shown to reduce neurite outgrowth. p,p`-DDT and o,p`-DDT decreased the neurite outgrowth dose dependently (1–50 µM) and induced apoptosis in NGF-stimulated PC12 cells. p,p`-DDE also revealed a similar effect but to a lesser extent (Shinomiya and Shinomiya, 2003). In the POP mixture at 500x, p,p`-DDE is present at 0.5 µM. Christen et al. (2017) reported that the different organochlorine pesticides including dieldrin at 10 or 100 µM suppressed the neurite outgrowth in PC12 cells co-treated with NGF, but this compound is only present at 28 nM in the POP

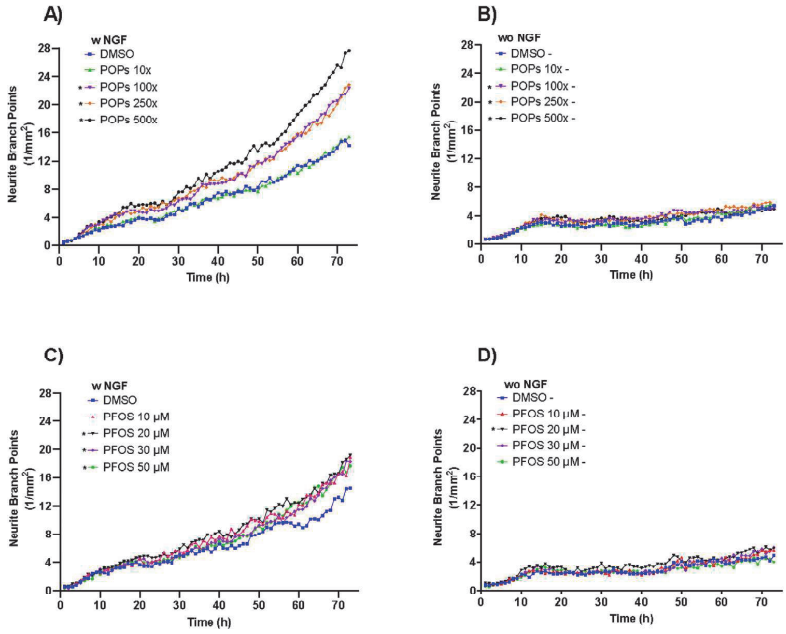

Fig. 9. Assessment of changes in neurite branch points in PC12 cells after exposure to POP mixture or PFOS using live-cell imaging. Effect of the compounds in presence of NGF (50 ng/mL) (A and C) or its absence (B and D) were evaluated. Cell were exposed to the POP mixture (A and B), or to PFOS (C and D). Solvent control was DMSO 0.1 %. Concentration of the POP mixture is indicated as POPs x human blood levels. PFOS concentrations are in µM. Average neurite branch points (total number of branch points/area of image field) were automatically measured by NeuroTrack software, every 60 min, followed for 72 h. For clarity, the graph is presented only with mean value at different time points. Data are mean n = 3-4 independent experiments, with replicate > 3 per group. Statistical difference between the overall average of the exposed groups and the solvent control (0.1 % DMSO) is indicated on the left-hand side of figure legends (*$p < 0.05$), w = with NGF and wo = without NGF.

mixture at 500 × . Treatment with HCB at 0.5 nM repressed neurite outgrowth but did not affect cell viability in mouse embryonic stem (ES) cells (Addae et al., 2013). This compound is present in the POP mixture (500x) at 114 nM. Commercial PBDEs decabromodiphenyl ether (deca-BDE) at 15 µM, inhibited the neurite growth in cultured rat hippocampal neuron (Liao et al., 2008a). In our mixture, individual BFRs are present at nanomolar range. Nanomolar concentrations of PFOS, have been shown to facilitate neurite outgrowth associated with decreased cell proliferation in rat primary embryonic neuronal cells (Wan Ibrahim et al., 2013). However, micromolar concentrations of PFAAs, comparable to ours, inhibited the neurite outgrowth in cultured rat hippocampal neurons cells (Liao et al., 2009, 2008b). These discrepancies in outcomes might be explained by many factors, such as concentration ranges, differences in different types of neurons, or the experimental conditions used. The effects of POPs on neurite outgrowth in PC12 could also be species specific or cell type specific effect. In contrast to other neurons from the central nervous system, PC12 is lacking functional expression of NMDA receptors. This receptor mediates glutamate induced excitotoxicity and can result in excessive calcium influx leading to cell death in many neurological disorders (Edwards et al., 2007). Another possible reason could be an ontogenetic effect, linked to the developmental stage of the cells used. In the present, we examined the effects of POPs in PC12 cells that were not exposed previously to NGF (i.e. not differentiated, unprimed). Although not examined in the present study, the other possible way would be to determine the effects of POPs in PC12 that have been exposed previously to NGF (primed). Parran et al. (2003) observed that in unprimed PC12 cells, mercuric chloride exposure increased NGF-stimulated neurite outgrowth. However, in primed PC12 cells, this compound inhibited NGF-stimulated neurite outgrowth. It should be noted that our POP mixture contains 29 different compounds which could have additive, synergistic or antagonistic effects.

It should be stressed that neurite length number returned by the IncuCyte image analysis software relates to the summation of the individual lengths of outgrowths per image fields, rather than a mean length of individual neurites. Similarly, the number of branch points returns a count per image field. Also, it does not differentiate between true branch points (one extension splitting in 2 or more) or crossings formed by overlapping outgrowths. Nevertheless, we found both parameters are highly correlated, and their increases suggest that cells are investing in the formation of more neurite material, and that the complexity of the outgrowths increases.

Our POP mixture did not induce immediate cell death. Rather, the inhibition of neurite outgrowth has been considered an important mode of action for specific developmental neurotoxicants (Radio et al., 2008). However, in our study POP mixture and PFOS lead to enhanced neurite outgrowth indicating lack of cytotoxicity. Some effects on the rate of cell proliferation were observed, but nuclear and mitochondrial health parameters remained unaffected.

The neurite outgrowth occurs in a strictly controlled way. During development of the nervous system, many more neurons are generated than ultimately integrate into neuronal circuits and survive (Mattson, 2008). Although pollutants showed no cytotoxic effects in these circumstances, overactive neuritogenesis at the wrong timing might also be detrimental. For example, studies have found that spine density is increased in ASD, which could suggest a developmental alteration in spine morphogenesis (Forrest et al., 2018).

Future studies could take into account effects of sub-mixtures and individual mixture constituents, and also further validate our observation of neurite outgrowth with alternative methods, such as measuring the length of individual neurites (Christen et al., 2017) or quantification by labeling with intracellular neurite specific markers, such as anti-βIII tubulin (Radio et al., 2010).

5. Conclusion

Exposure of differentiating neurons to complex mixtures of POPs might not result in neurotoxicity by cell loss, yet we cannot exclude possible adverse effects on developmental outcomes with regards to improper neuronal connectivity. PFOS contributes to a considerable part of the neuritogenesis seen with the total POP mixture, but other compounds present amplify the effect.

Declaration of Competing Interest

The authors declare that they have no known competing financial interests or personal relationships that could have appeared to influence the work reported in this paper.

Acknowledgements

This project has received funding from the European Union's Horizon 2020 research and innovation program under the Marie Skłodowska-Curie grant agreement No. 722634 (http://protected.eu.com/). Support from the EU Erasmus+Programme to EHWH is gratefully acknowledged.

Appendix A. Supplementary data

Supplementary material related to this article can be found, in the online version, at doi:https://doi.org/10.1016/j.toxlet.2020.12.007.

References

Abraham, V.C., Towne, D.L., Waring, J.F., Warrior, U., Burns, D.J., 2008. Application of a high-content multiparameter cytotoxicity assay to prioritize compounds based on toxicity potential in humans. J. Biomol. Screen. 13, 527–537.
Addae, C., Cheng, H., Martinez-Ceballos, E., 2013. Effect of the environmental pollutant hexachlorobenzene (HCB) on the neuronal differentiation of mouse embryonic stem cells. Int. J. Environ. Res. Public Health 10, 5244–5256.
Angus, W.G., Contreras, M.L., 1995. Aroclor 1254 alters the binding of 125I-labeled nerve growth factor in PC12 cells. Neurosci. Lett. 191, 23–26.
Barone Jr., S., Das, K.P., Lassiter, T.L., White, L.D., 2000. Vulnerable processes of nervous system development: a review of markers and methods. Neurotoxicology 21, 15–36.
Berntsen, H.F., Berg, V., Thomsen, C., Ropstad, E., Zimmer, K.E., 2017. The design of an environmentally relevant mixture of persistent organic pollutants for use in in vivo and in vitro studies. J. Toxicol. Environ. Health A 1–15.
Berntsen, H.F., Bjorklund, C.G., Strandabo, R., Haug, T.M., Moldes-Anaya, A., Fuentes-Lazaro, J., Verhaegen, S., Paulsen, R.E., Tasker, R.A., Ropstad, E., 2018. PFOS-induced excitotoxicity is dependent on Ca(2+) influx via NMDA receptors in rat cerebellar granule neurons. Toxicol. Appl. Pharmacol. 357, 19–32.
Berntsen, H.F., Duale, N., Bjørklund, C.G., Rangel-Huerta, O.D., Dyrberg, K., Hofer, T., Rakkestad, K.E., Østby, G., Halsne, R., Boge, G., Paulsen, R.E., Myhre, O., Ropstad, E., 2020. Effects of a human-based mixture of persistent organic pollutants on the in vivo exposed cerebellum and cerebellar neuronal cultures exposed in vitro. Environ. Int. 146, 106240.
Bopp, S.K., Barouki, R., Brack, W., Dalla Costa, S., Dorne, J.C.M., Drakvik, P.E., Faust, M., Karjalainen, T.K., Kephalopoulos, S., van Klaveren, J., Kolossa-Gehring, M., Kortenkamp, A., Lebret, E., Lettieri, T., Nørager, S., Rüegg, J., Tarazona, J.V., Trier, X., van de Water, B., van Gils, J., Bergman, Å., 2018. Current EU research activities on combined exposure to multiple chemicals. Environ. Int. 120, 544–562.
Christen, V., Rusconi, M., Crettaz, P., Fent, K., 2017. Developmental neurotoxicity of different pesticides in PC-12 cells in vitro. Toxicol. Appl. Pharmacol. 325, 25–36.
Doan, T.Q., Berntsen, H.F., Verhaegen, S., Ropstad, E., Connolly, L., Igout, A., Muller, M., Scippo, M.L., 2019. A mixture of persistent organic pollutants relevant for human exposure inhibits the transactivation activity of the aryl hydrocarbon receptor in vitro. Environ. Pollut. 254, 113098.
Edwards, M.A., Loxley, R.A., Williams, A.J., Connor, M., Phillips, J.K., 2007. Lack of functional expression of NMDA receptors in PC12 cells. Neurotoxicology 28, 876–885.
Forrest, M.P., Parnell, E., Penzes, P., 2018. Dendritic structural plasticity and neuropsychiatric disease. Nat. Rev. Neurosci. 19, 215–234.
Fujita, K., Lazarovici, P., Guroff, G., 1989. Regulation of the differentiation of PC12 pheochromocytoma cells. Environ. Health Perspect. 80, 127–142.
Garay, et al., 2016. CellPlayer™ 96-Well Kinetic NeuroTrack™ Assay Essen BioScience. Ann Arbor, Michigan. .
Grandjean, P., Landrigan, P.J., 2006. Developmental neurotoxicity of industrial chemicals. Lancet 368, 2167–2178.
Grandjean, P., Landrigan, P.J., 2014. Neurobehavioural effects of developmental toxicity. Lancet Neurol. 13, 330–338.
Greene, L.A., 1978. Nerve growth factor prevents the death and stimulates the neuronal differentiation of clonal PC12 pheochromocytoma cells in serum-free medium. J. Cell Biol. 78, 747–755.
Greene, L.A., Tischler, A.S., 1976. Establishment of a noradrenergic clonal line of rat adrenal pheochromocytoma cells which respond to nerve growth factor. Proc. Natl. Acad. Sci. U. S. A. 73, 2424–2428.
Hoyer, B.B., Ramlau-Hansen, C.H., Obel, C., Pedersen, H.S., Hernik, A., Ogniev, V., Jonsson, B.A., Lindh, C.H., Rylander, L., Rignell-Hydbom, A., Bonde, J.P., Toft, G., 2015. Pregnancy serum concentrations of perfluorinated alkyl substances and offspring behaviour and motor development at age 5-9 years–a prospective study. Environ. Health 14, 2.
Kamata, H., Tanaka, C., Yagisawa, H., Hirata, H., 1996. Nerve growth factor and forskolin prevent H2O2-induced apoptosis in PC12 cells by glutathione independent mechanism. Neurosci. Lett. 212, 179–182.
Kodavanti, P.R., 2006. Neurotoxicity of persistent organic pollutants: possible mode (s) of action and further considerations. Dose. 3, 273–305.
Kodavanti, P.R., Kannan, N., Yamashita, N., Derr-Yellin, E.C., Ward, T.R., Burgin, D.E., Tilson, H.A., Birnbaum, L.S., 2001. Differential effects of two lots of aroclor 1254: congener-specific analysis and neurochemical end points. Environ. Health Perspect. 109, 1153–1161.
Li, C., Liu, X., Liu, Q., Li, S., Li, Y., Hu, H., Shao, J., 2017. Protection of taurine against PFOS-induced neurotoxicity in PC12 cells. Adv. Exp. Med. Biol. 975 (Pt 2), 907–916.
Liao, C., Duan, S., Jiang, G., 2008a. Effect of polybrominated diphenyl ether on development of cultured hippocampal neuron. Sci. China Ser. B Chem. 51, 62–68.
Liao, C.Y., Li, X.Y., Wu, B., Duan, S., Jiang, G.B., 2008b. Acute enhancement of synaptic transmission and chronic inhibition of synaptogenesis induced by perfluorooctane sulfonate through mediation of voltage-dependent calcium channel. Environ. Sci. Technol. 42, 5335–5341.
Liao, C., Wang, T., Cui, L., Zhou, Q., Duan, S., Jiang, G., 2009. Changes in synaptic transmission, calcium current, and neurite growth by perfluorinated compounds are dependent on the chain length and functional group. Environ. Sci. Technol. 43, 2099–2104.
Mattson, M.P., 2008. Glutamate and neurotrophic factors in neuronal plasticity and disease. Ann. N. Y. Acad. Sci. 1144, 97–112.
McComb, J., Mills, I.G., Muller, M., Berntsen, H.F., Zimmer, K.E., Ropstad, E., Verhaegen, S., Connolly, L., 2019. Human blood-based exposure levels of persistent organic pollutant (POP) mixtures antagonise androgen receptor transactivation and translocation. Environ. Int. 132, 105083.
Mengel, D., Hong, W., Corbett, G.T., Liu, W., DeSousa, A., Solforosi, L., Fang, C., Frosch, M.P., Collinge, J., Harris, D.A., Walsh, D.M., 2019. PrP-grafted antibodies bind certain amyloid β-protein aggregates, but do not prevent toxicity. Brain Res. 1710, 125–135.
Mosmann, T., 1983. Rapid colorimetric assay for cellular growth and survival: application to proliferation and cytotoxicity assays. J. Immunol. Methods 65, 55–63.
I.Z., NeuroTrack™ . IncuCyte™ ZOOM NeuroTrack™ Processing Overview. last accessed December 17th, 2020. IncuCyte™ ZOOM NeuroTrack™ Processing Overview https://www.essenbioscience.com/media/uploads/files/8000-0194-C00_ZOOM_NeuroTrack_PHASE_Procesing_Tech_Note.pdf.
O'Brien, P., Haskins, J.R., 2007. In vitro cytotoxicity assessment. In: Taylor, D.L., Haskins, J.R., Giuliano, K.A. (Eds.), High Content Screening (Methods in Molecular Biology). Humana Press, NJ, USA, pp. 415–425.
O'Brien, P.J., Irwin, W., Diaz, D., Howard-Cofield, E., Krejsa, C.M., Slaughter, M.R., Gao, B., Kaludercic, N., Angeline, A., Bernardi, P., Brain, P., Hougham, C., 2006. High concordance of drug-induced human hepatotoxicity with in vitro cytotoxicity measured in a novel cell-based model using high content screening. Arch. Toxicol. 80, 580–604.
Parran, D.K., Barone Jr., S., Mundy, W.R., 2003. Methylmercury decreases NGF-induced TrkA autophosphorylation and neurite outgrowth in PC12 cells. Brain Res. Dev. Brain Res. 141, 71–81.
Radio, N.M., Mundy, W.R., 2008. Developmental neurotoxicity testing in vitro: models for assessing chemical effects on neurite outgrowth. Neurotoxicology 29, 361–376.
Radio, N.M., Breier, J.M., Shafer, T.J., Mundy, W.R., 2008. Assessment of chemical effects on neurite outgrowth in PC12 cells using high content screening. Toxicol. Sci. 105, 106–118.
Radio, N.M., Freudenrich, T.M., Robinette, B.L., Crofton, K.M., Mundy, W.R., 2010. Comparison of PC12 and cerebellar granule cell cultures for evaluating neurite outgrowth using high content analysis. Neurotoxicol. Teratol. 32, 25–35.
Rakkestad, K.E., Mathisen, G., Austdal, L.P., Paulsen, R.E., 2014. Neurodevelopmental effects of bisphenol A and phthalates studied in in ovo exposed chicken to model prenatal exposure. Toxicol. Lett. 229, S47.
SCHER, 2012. Toxicity and Assessment of Chemical Mixtures Scientific Committee on Health and Environmental Risks (SCHER). . https://ec.europa.eu/health/scientific_committees/environmental_risks/docs/scher_o_155.pdf.

Schmidt, M.M., Dringen, R., 2012. Glutathione (GSH) synthesis and metabolism. Neural Metabolism In Vivo. Advances in Neurobiology, vol. 4. Springer, Boston, MA, pp. 1029–1050.
Schmidt, R.J., Lyall, K., Hertz-Picciotto, I., 2014. Environment and autism: current state of the science. Cut. Edge Psychiatry Pract. 1, 21–38.
Shannon, M., Green, B., Willars, G., Wilson, J., Matthews, N., Lamb, J., Gillespie, A., Connolly, L., 2017. The endocrine disrupting potential of monosodium glutamate (MSG) on secretion of the glucagon-like peptide-1 (GLP-1) gut hormone and GLP-1 receptor interaction. Toxicol. Lett. 265, 97–105.
Shannon, M., Xie, Y., Verhaegen, S., Wilson, J., Berntsen, H.F., Zimmer, K.E., Ropstad, E., Green, B.D., Connolly, L., 2019. A human relevant defined mixture of persistent organic pollutants (POPs) affects in vitro secretion of glucagon-like peptide 1 (GLP-1), but does not affect translocation of its receptor. Toxicol. Sci. 172, 359–367.
Shinomiya, N., Shinomiya, M., 2003. Dichlorodiphenyltrichloroethane suppresses neurite outgrowth and induces apoptosis in PC12 pheochromocytoma cells. Toxicol. Lett. 137, 175–183.
Slotkin, T.A., MacKillop, E.A., Melnick, R.L., Thayer, K.A., Seidler, F.J., 2008. Developmental neurotoxicity of perfluorinated chemicals modeled in vitro. Environ. Health Perspect. 116, 716–722.
Sørvik, I.B., Solum, E.J., Labba, N.A., Hansen, T.V., Paulsen, R.E., 2018. Differential effects of some novel synthetic oestrogen analogs on oxidative PC12 cell death caused by serum deprivation. Free Radic. Res. 52, 273–287.
Spratlen, M.J., Perera, F.P., Lederman, S.A., Rauh, V.A., Robinson, M., Kannan, K., Trasande, L., Herbstman, J., 2020. The association between prenatal exposure to perfluoroalkyl substances and childhood neurodevelopment. Environ. Pollut. 263, 114444.
Strom, B.O., Aden, P., Mathisen, G.H., Lomo, J., Davanger, S., Paulsen, R.E., 2010. Transfection of chicken cerebellar granule neurons used to study glucocorticoid receptor regulation by nuclear receptor 4A (NR4A). J. Neurosci. Methods 193, 39–46.
Tofighi, R., Wan Ibrahim, W.N., Rebellato, P., Andersson, P.L., Uhlén, P., Ceccatelli, S., 2011. Non-dioxin-like polychlorinated biphenyls interfere with neuronal differentiation of embryonic neural stem cells. Toxicol. Sci. 124, 192–201.
UNEP, 2008. What are POPs? . http://chm.pops.int/TheConvention/ThePOPs/tabid/673/Default.aspx.
Wan Ibrahim, W.N., Tofighi, R., Onishchenko, N., Rebellato, P., Bose, R., Uhlén, P., Ceccatelli, S., 2013. Perfluorooctane sulfonate induces neuronal and oligodendrocytic differentiation in neural stem cells and alters the expression of PPARγ in vitro and in vivo. Toxicol. Appl. Pharmacol. 269, 51–60.
WHO, 2017. Chemical Mixtures in Source Water and Drinking-water. . https://apps.who.int/iris/bitstream/handle/10665/255543/9789241512374-eng.pdf;jsessionid=301C7A42E1F33E57F83798D68C377636?sequence=1.
Wilson, J., Berntsen, H.F., Zimmer, K.E., Frizzell, C., Verhaegen, S., Ropstad, E., Connolly, L., 2016. Effects of defined mixtures of persistent organic pollutants (POPs) on multiple cellular responses in the human hepatocarcinoma cell line, HepG2, using high content analysis screening. Toxicol. Appl. Pharmacol. 294, 21–31.
Yagi, H., Ohkawara, B., Nakashima, H., Ito, K., Tsushima, M., Ishii, H., Noto, K., Ohta, K., Masuda, A., Imagama, S., Ishiguro, N., Ohno, K., 2015. Zonisamide enhances neurite elongation of primary motor neurons and facilitates peripheral nerve regeneration in vitro and in a mouse model. PLoS One 10, e0142786.

SUPPLEMENTARY MATERIALS – PAPER II

Supplementary Table 1. The total *in vitro* mixture containing 29 different POPs based on human blood levels, detailed in (Berntsen et al., 2017).

Compound	*Average human blood levels [a] ng/g lipid*	*Average human blood levels [b] ng/ml*	*Total mixture stock nominal concentration [c] mg/ml*	*Total mixture stock Measured concentration [d] µM*	*Compounds in POP mixture at 500x µM*
PCBs					
PCB 28	2.13	0.013	0.013	31.1	0.016
PCB 52	1.6	0.01	0.01	20.5	0.010
PCB 101	1.3	0.008	0.008	24.5	0.012
PCB 118	10.67	0.064	0.064	137.9	0.069
PCB 138	37	0.222	0.222	429.5	0.215
PCB 153	60.33	0.362	0.362	698.3	0.349
PCB 180	32.33	0.194	0.194	339	0.170
∑ PCBs	145.36	0.873	0.873	1680.8	0.840
OCPs					
p,p'-DDE	83.67	0.502	0.502	1065.9	0.533
HCB	19.5	0.117	0.117	228.2	0.114
α-Chlordane	1.8	0.011	0.011	23.7	0.012
Oxychlordane	3.7	0.022	0.022	33	0.017
trans-Nonachlor	6.8	0.041	0.041	99.1	0.050
α-HCH	1	0.006	0.006	16.8	0.008
β-HCH	8.77	0.053	0.053	75.6	0.038
γ-HCH	1	0.006	0.006	16.8	0.008
Dieldrin	4	0.024	0.024	56.2	0.028
∑ OCPs	130.24	0.782	0.782	1615.3	0.808
∑ PCBs + OCPs	275.6	1.655	1.655	3296.1	1.648
BFRs					
PBDE 47	1.43	0.009	0.009	17.8	0.009
PBDE 99	0.59	0.004	0.004	7.5	0.004
PBDE 100	0.36	0.002	0.002	3.8	0.002
PBDE 153	1.64	0.01	0.001*	2.1	0.001
PBDE 154	0.29	0.002	0.002	3	0.002
PBDE 209	1.81	0.011	0.011	9.4	0.005
HBCD	4.1	0.025	0.025	54.5	0.027
∑ BFRs	10.22	0.063	0.053	98.1	0.049
PFAAs					
PFHxS	N/A	3.45	3.45	7809.2	3.905
PFOS	N/A	29.425	29.425	41522.1	20.761
PFOA	N/A	4.523	4.523	4209.4	2.105
PFNA	N/A	0.8	0.8	1092.5	0.546
PFDA	N/A	0.495	0.495	375.4	0.188
PFUnDA	N/A	0.56	0.56	336.8	0.168
∑ PFAAs	N/A	39.253	39.253	55345.4	27.673

[a] Average human blood levels of POPs based on a literature review of Scandinavian values, providing the basis for the in vitro mixture.
[b] Average human blood levels of POPs converted to ng/ml. A fat percentage of 0.6 % was used. 1 ml blood was considered to have a weight of 1 g.
[c] Nominal concentration of the various compounds in the total mixture stock – 1000000x the average concentration in blood.
***The nominal concentration of PBDE 153 included in the total mixture stock was ten times lower than originally intended.**
[d] Measured concentrations of the various compounds in the total mixture stock converted to µM.
500x fold human blood levels
N/A - Not applicable
Abbreviations: PCBs (polychlorinated biphenyls); OCPs (organochlorine pesticides); BFRs (brominated flame retardants); PFAAs (perfluoroalkyl acids)

Supplementary Table 2. Differences in overall means of the dependent variables* Cell Body Cluster (CBC), area (CBCA), Neurite Length (NL), and Neurite Branching Points (NBP) between cells exposed to POPs and the solvent control (SC, 0.1% DMSO). Cells were exposed to the POPs mixture (POPs 10x - 500x fold human blood levels) or PFOS (10 - 50 μM) in the presence and absence of neurite growth factor (NGF). P-values <0.05 were considered significant and indicated in bold.

	With NGF			*Without NGF*		
Exposure group and dependent variable	***Difference in overall mean against SC***	***Lower 95% confidence limit***	***Upper 95% confidence limit***	***Difference in overall mean against SC***	***Lower 95% confidence limit***	***Upper 95% confidence limit***
CBC						
POPs 10x	**-0.080**	-0.093	-0.067	0.011	-0.003	0.024
POPs 100x	0.004	-0.010	0.017	**0.033**	0.020	0.047
POPs 250x	0.010	-0.003	0.024	**-0.040**	-0.054	-0.026
POPs 500x	**-0.026**	-0.039	-0.013	**-0.061**	-0.075	-0.048
PFOS 10 μM	-0.001	-0.025	0.024	**-0.016**	-0.032	-0.001
PFOS 20 μM	**0.079**	0.058	0.100	0.015	-0.001	0.031
PFOS 30 μM	**-0.056**	-0.077	-0.035	**-0.059**	-0.075	-0.044
PFOS 50 μM	**-0.205**	-0.227	-0.184	**-0.203**	-0.219	-0.188
CBCA						
POPs 10x	**-0.101**	-0.145	-0.058	0.003	-0.029	0.036
POPs 100x	**-0.047**	-0.090	-0.004	-0.002	-0.034	0.031
POPs 250x	0.013	-0.030	0.057	**-0.106**	-0.138	-0.073
POPs 500x	**-0.062**	-0.105	-0.018	**-0.052**	-0.084	-0.020
PFOS 10 μM	-0.003	-0.061	0.056	-0.007	-0.042	0.029
PFOS 20 μM	0.051	-0.001	0.102	**0.037**	0.001	0.072
PFOS 30 μM	**-0.074**	-0.125	-0.022	-0.027	-0.063	0.008
PFOS 50 μM	**-0.214**	-0.265	-0.162	**-0.185**	-0.221	-0.150
NL						
POPs 10x	**0.085**	0.048	0.122	-0.007	-0.044	0.031
POPs 100x	**0.281**	0.245	0.318	**0.150**	0.113	0.188
POPs 250x	**0.327**	0.290	0.364	**0.146**	0.108	0.183
POPs 500x	**0.448**	0.411	0.485	**0.083**	0.046	0.121
PFOS 10 μM	0.008	-0.037	0.053	0.017	-0.022	0.055
PFOS 20 μM	**0.222**	0.183	0.261	**0.116**	0.077	0.154
PFOS 30 μM	**0.118**	0.078	0.157	0.020	-0.018	0.059
PFOS 50 μM	**0.122**	0.082	0.161	**-0.099**	-0.138	-0.061
NBP						
POPs 10x	0.045	-0.025	0.115	0.069	-0.005	0.142
POPs 100x	**0.316**	0.246	0.385	**0.183**	0.109	0.256
POPs 250x	**0.322**	0.252	0.391	**0.104**	0.031	0.178
POPs 500x	**0.455**	0.385	0.525	**0.154**	0.080	0.227
PFOS 10 μM	0.041	-0.046	0.128	0.016	-0.055	0.087
PFOS 20 μM	**0.262**	0.186	0.338	**0.178**	0.107	0.248
PFOS 30 μM	**0.105**	0.029	0.182	0.054	-0.017	0.124
PFOS 50 μM	**0.123**	0.047	0.200	-0.042	-0.113	0.028

* Differences are based on the Dunnett's multiple comparisons test using the Mixed Model personality in JMP Pro 14® (SAS, Cary, USA). The dependent variables CBC, CBCA, NL and NBP were log transformed to give a satisfactory fit to the normal distribution. Independent fixed effect variables were: exposure group, time in culture and their interaction. Experiment and the nested effect of time within experiment were entered as random effects allowing for repeated measurements along the time scale. If the value for lower and upper limit crosses zero, the difference is not significant.

Supplementary Table 3. Estimated effects of neurite growth factor (NGF) on measured IncuCyte endpoints. Cells were exposed to solvent control (SC, 0.1% DMSO) in the presence and absence of (NGF). The parameters: Neurite Length (NL), Neurite Branching Points (NBP), Cell Body Cluster (CBC) and area (CBCA) were dependent variables analysed in mixed models after log transformation*. The Table shows the effects of the log-transformed least squares (LS) means with confidence limits. LS means with different letters indicate a significant effect of NGF exposure ($p < 0.05$).

Effect of NGF on measured IncuCyte endpoints			
NGF YES/NO	***LS means (Estimate)***	***Lower 95% confidence limit***	***Upper 95% confidence limit***
Log NL			
No	-0.834	-1.373	-0.295
YES	-0.422	-0.961	0.118
Log NBP			
No	0.935	0.338	1.533
YES	1.608	1.011	2.206
Log CBC			
No	4.860	4.424	5.296
YES	4.228	3.792	4.665
Log CBCA			
No	-2.653	-3.202	-2.103
YES	-3.232	-3.782	-2.682

* Differences are based on Student's t-test after using the Mixed Model personality in JMP Pro 14® (SAS, Cary, USA). The dependent variables CBC, CBCA, NL and NBP were log transformed to give a satisfactory fit to the normal distribution. Independent fixed effect variables were: exposure group (+NGF or –NGF), time in culture and their interaction. Experiment and the nested effect of time within experiment were entered as random effects allowing for repeated measurements along the time scale.

HCA Images

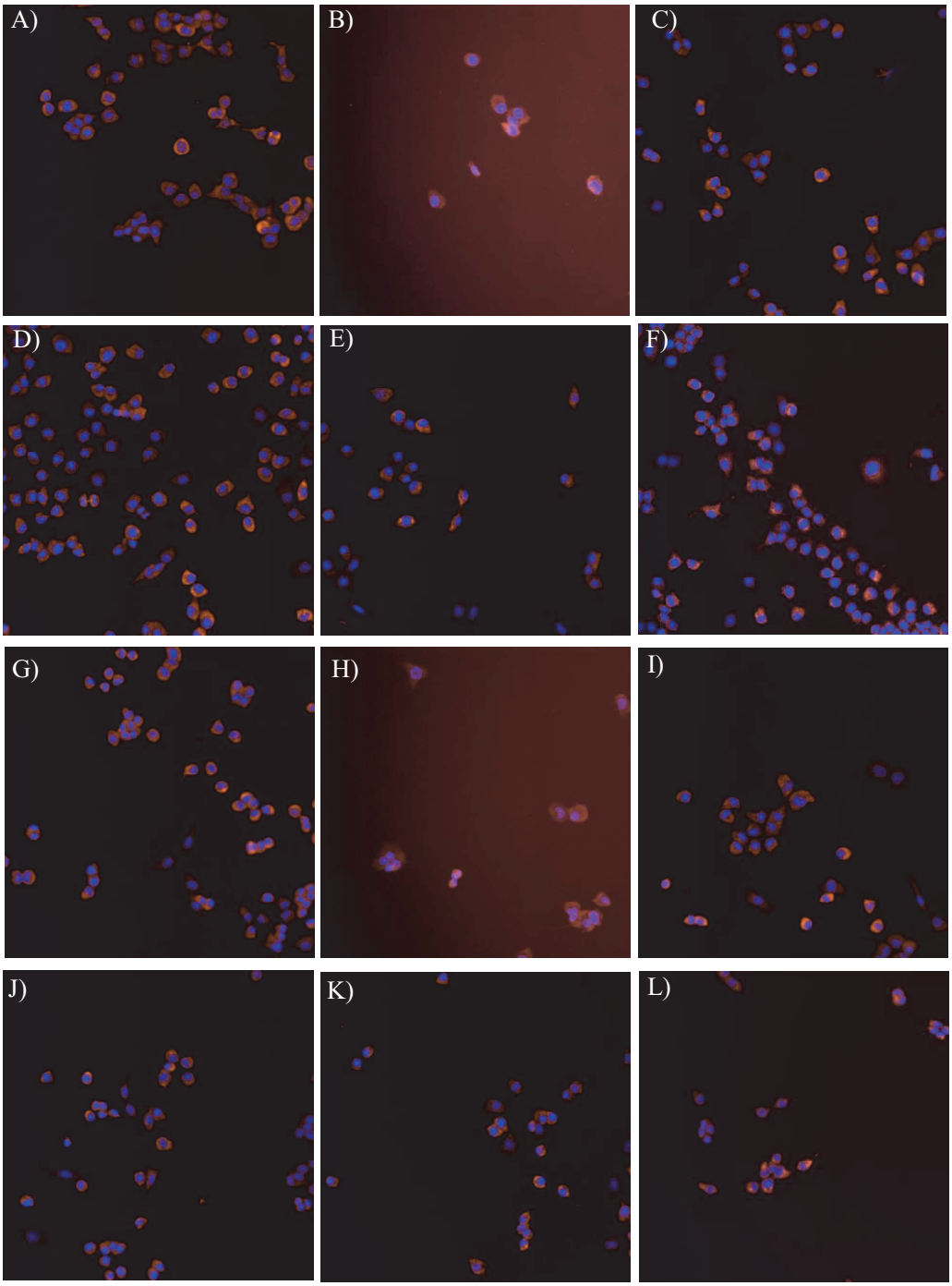

Supplementary Fig. 1. HCA images A and G solvent control (SC, DMSO 0.1%); B and H valinomycin (Vln, 15 μM positive control); C and I POP mixture 10x (fold human blood levels); D and J POP mixture 250x; E and K POP mixture 500x; and F and L PFOS 50 μM, following 72 h exposure. A, B, C, D, E and F were in the presence of NGF (50 ng/ml); and G, H, I, J, K and L were in the absence of NGF. Each image was acquired at 20x objective magnification using Hoechst dye (blue: nuclear staining) and mitochondrial potential dye (orange: mitochondrial staining). All images at scale bar = 200 μm.

IncuCyte Images

0 h 72 h

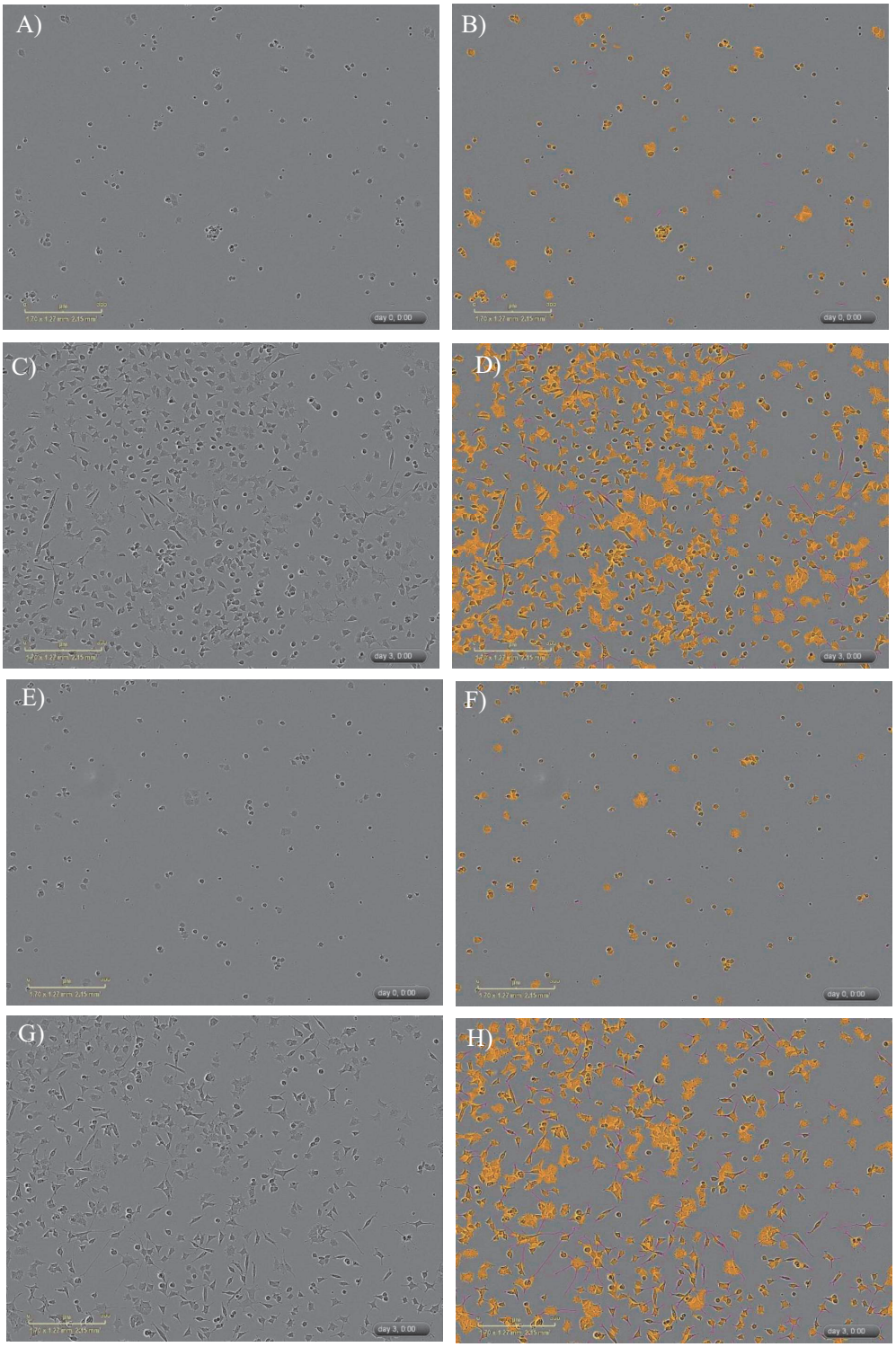

Supplementary Fig. 2. Phase contrast IncuCyte images for solvent control (SC, DMSO 0.1%) A and C ; and for POP mixture 500x (fold human blood levels) E and G, in the presence of NGF (50 ng/ml). B, D, F and H are the corresponding Images of A, C, E and G respectively, after applying Neuro Track masks, cell body clusters (orange) and neurites (violet). Each image was acquired at 10x magnification (Scale bar = 300 μm).

IncuCyte Images

0 h 72 h

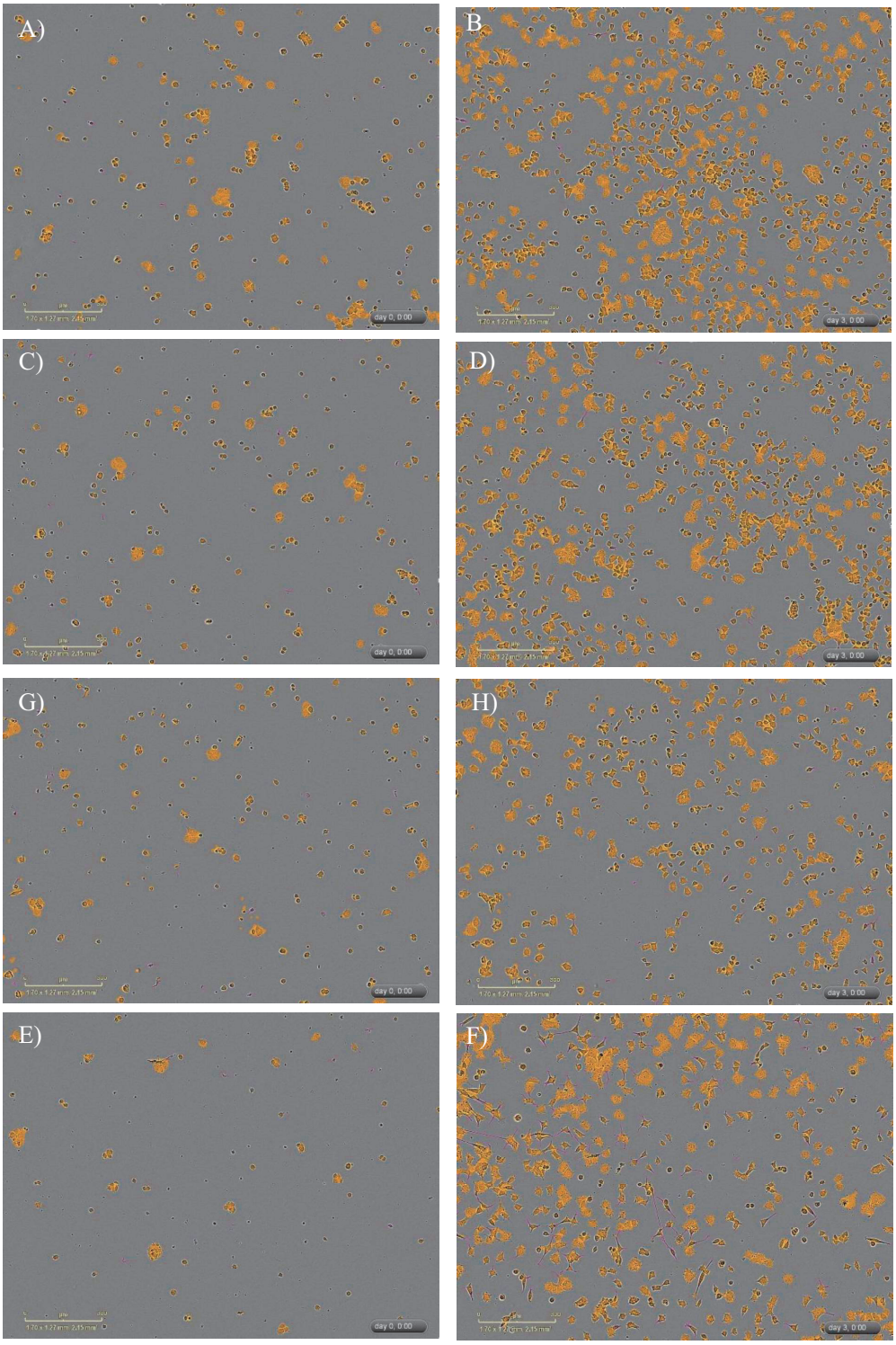

Supplementary Fig. 3. IncuCyte images after applying Neuro Track masks, cell body clusters (orange) and neurites (violet). A and B are solvent control (SC, DMSO 0.1%); C and D are POP mixture 500x (fold human blood levels), in the absence of NGF. G and H are PFOS 50 µM in the absence of NGF; and E and F are PFOS 50 µM in the presence of NGF (50 ng/ml). Each image was acquired at 10x magnification (Scale bar = 300 µm).

PAPER III

Peripherally Administered Persistent Organic Pollutants Distribute to the Brain of Developing Chicken Embryo in Concentrations Relevant for Human Exposure

Ajay Yadav[1,2], Steven Verhaegen[1], Mussie Ghezu Hadera[2], Hanne Friis Berntsen[1,3], Vidar Berg[4], Jan Ludvig Lyche[4], Azemira Sabaredzovic[5], Line Småstuen Haug[5], Oddvar Myhre[5], Karin Elisabeth Zimmer[6], Ragnhild Elisabeth Paulsen[2*], Erik Ropstad[1], Fernando Boix[7]

[1]Department of Production Animal Clinical Sciences, Norwegian University of Life Sciences, P.O. Box 369 Sentrum, NO-0102, Oslo, Norway

[2]Section for Pharmacology and Pharmaceutical Biosciences, Department of Pharmacy, University of Oslo, P.O. Box 1068, Blindern, NO-0316 Oslo, Norway

[3]National Institute of Occupational Health, P.O. Box 5330 Majorstuen, NO-0304, Oslo, Norway

[4]Department of Food Safety and Infection Biology, Faculty of Veterinary Medicine, Norwegian University of Life Sciences, P.O Box 369 Sentrum, 0102, Oslo, Norway

[5]Department of Environmental Health, Norwegian Institute of Public Health, PO Box 222 Skøyen, N-0213 Oslo, Norway.

[6]Department of Preclinical Sciences and Pathology, Norwegian University of Life Sciences, P.O. Box 369 Sentrum, NO-0102, Oslo, Norway

[7]Section for Drug Abuse Research, Dept. of Forensic Sciences, Division of Laboratory Medicine, Oslo University Hospital, PO Box 4404, Nydalen, 0403 Oslo, Norway

E-Mail Adresse: ajay.yadav@nmbu.no (A. Yadav), steven.verhaegen@nmbu.no (S. Verhaegen), mughezu@gmail.com (M. G. Hadera), Hanne.Berntsen@stami.no (H. F. Berntsen), vidar.berg@nmbu.no (V. Berg), jan.l.lyche@nmbu.no (J. L. Lyche), Azemira.Sabaredzovic@fhi.no (A. Sabaredzovic), LineSmastuen.Haug@fhi.no (L. S. Haug), oddvar.Myhre@fhi.no (O. Myhre), karin.zimmer@nmbu.no (K. E. Zimmer), r.e.paulsen@farmasi.uio.no (R. E. Paulsen), erik.ropstad@nmbu.no (E. Ropstad), rmfees@ous-hf.no (F. Boix)

*Corresponding author: R. E. Paulsen, e-mail address: r.e.paulsen@farmasi.uio.no

Abstract:

Persistent organic pollutants (POPs) can reach the fetal brain and contribute to developmental neurotoxicity. To explore the distribution of POPs to the fetal brain, we exposed chicken embryos to a POP mixture, containing 29 different compounds with concentrations based on blood levels measured in the Scandinavian human population. The mixture was injected into the allantois at embryonic day 13 (E13), aiming at a theoretical concentration of 10 times human blood levels. POPs concentrations in the brain were measured at 0.5, 1, 2, 4, 6, 24, 48, and 72 h after administration. Twenty-seven of the individual compounds were detected during at least one of the time-points analyzed. Generally, the concentrations of most of the measured compounds were within the order of magnitude of those reported in human brain samples. Differences in the speed of distribution to the brain were observed for the per- and polyfluoroalkyl substances (PFASs) which have protein binding potential, versus the lipophilic polychlorinated biphenyls (PCBs), organochlorine pesticides (OCPs) and brominated flame retardants (BFRs). Based on human pharmacokinetic modeling, protein binding PFASs were best described by a one compartment model. PFASs displayed relatively slow elimination *(Kel)* and persisted at high levels in the brain. Lipophilic OCPs and PCBs could be fitted to a 2-compartment model. These showed high levels in the brain relative to the dose administrated as calculated by area under the curve (AUC)/Dose. Altogether our study showed that chicken is a relevant model to explore the distribution of POPs in the developing brain at human relevant exposure.

Keywords*:*

allantois; brain concentration; chicken embryo; human pharmacokinetic model; POP mixture

Highlights:

- Different POPs reach the chicken embryo brain at varying speed and concentrations
- Brain concentrations were in the human relevant exposure range after an injection
- POPs can be analyzed by different human pharmacokinetic models
- Chicken embryo is a relevant model for distribution of POPs in the developing brain

1. Introduction

Persistent organic pollutants (POPs) are halogenated industrial chemicals highly resistant to environmental degradation. Worldwide concern exists because of their tendency to bioaccumulate and bio-magnify in living organisms. Exposure to POPs has been associated with a variety of adverse health effects. These include cancer, allergies and hypersensitivity, reproductive disorders, alterations of the hormonal system as well as effects on the nervous and immune systems (Secretariat of the Stockholm Convention, 2019b). POPs include chlorinated, brominated, and per- and polyfluoroalkyl substances (PFASs) (Secretariat of the Stockholm Convention, 2019a). Chlorinated and brominated POPs are predominantly distributed in lipid rich tissues such as adipose tissue and blood lipids, whereas PFASs are associated with proteins, and are found in the highest concentrations in liver, kidney, and blood. (Karrman et al., 2006, Lau, 2015). All three classes of compounds have been detected in the human brain (Dewailly et al., 1999, Maestri et al., 2006, Mitchell et al., 2012, Pérez et al., 2013). The accumulation of POPs in the body starts *in utero*, through maternal exposure to POPs, and later continues via contaminated food, air or water (WHO, 2008). Development of the blood brain barrier (BBB) and maturation of barrier transporter systems are vital for protection of the fetal brain from exposure to toxic substances, excluding them from the fetal CNS (Goasdoué et al., 2017). Several industrial compounds including POPs can transfer to the fetus via the placenta and to the infant through breast milk. The BBB protects only partially against the entry of these compounds into the brain (Grandjean and Landrigan, 2014), and POPs are detected in the brain of human fetuses (Mamsen et al., 2019). This leads to exposure to these chemicals in early life and potentially adverse effects on brain development, which may lead to neurodevelopmental disorders such as cognitive and neurobehavioral impairment (Grandjean and Landrigan, 2014).

We have previously designed an environmentally relevant mixture of POPs for use in animal and *in vitro* experimental studies, containing 29 different chlorinated, brominated, and PFASs (Berntsen et al., 2017a). The mixture contains POPs at concentrations based on those measured in human blood in Scandinavia, and is aimed to provide a defined and realistic mixture of environmental contaminants for toxicity studies that could reflect the relative levels of POPs to which the general human population are exposed (Berntsen et al., 2017a).

The abundance of potential hazardous chemicals in the brains is of special relevance for brain development. Because this organ could be a potential target for developmental neurotoxicity (DNT) by altering its normal tissue architecture and/or molecular mechanisms. Studies *in vitro* and *in vivo* in animal models have reported neurodevelopmental effects caused by polychlorinated biphenyls (PCBs) and brominated flame retardants (BFRs) (Fonnum and Mariussen, 2009), or PFASs (Berntsen et al., 2017b, Berntsen et al., 2018, Berntsen et al., 2020, Yadav et al., 2021b). In our recent study we found transfer of POPs to mice offspring brains after maternal exposure with a mixture of similar composition as the one used in chicken embryos, resulting in gene expression changes related to brain function (Myhre et al. 2020, in press Chemosphere). In addition, the same POP mixture showed adverse effects on neuronal cell function and development (Berntsen et al., 2020, Davidsen et al., 2021, Yadav et al., 2021a). Human epidemiological studies have also showed associations between POP exposure and neurodevelopmental effects. For example, in a multi-pollutant analysis of 27 POPs in a Norwegian birth cohort study, early-life exposure to β-hexachlorocyclohexane (β-HCH) and perfluorooctanesulfonic acid (PFOS) was associated with increased risk of attention-deficit hyperactivity disorder (ADHD) (Lenters et al., 2019). Further, Sagiv et al. (2012) reported an association between organochlorines and neuropsychological measures of attention among 8

year old children prenatally exposed to organochlorines. In another study, they found singificant associations of prenatal exposure to polybrominated diphenyl ethers (PBDEs) with poorer attention and executive function later in childhood (Sagiv et al., 2015).

Limited information is available about which individual POPs reach the fetal brain and at what final concentrations. An embryo model without maternal distribution and mother-embryo transfer could be useful for gathering such information. In the present study, we injected a defined mixture of POPs (Berntsen et al., 2017a) into chicken eggs and measured their distribution to the developing fetal brain. Chicken embryos have previously been used as an animal model to study brain development after exposure to POPs (Berntsen et al., 2020, Yadav et al., 2021b), different pharmaceuticals (Aden et al., 2008, Austdal et al., 2016) and environmental toxicants (Mathisen et al., 2013). Several aspects of the stages of neuronal development in chickens are well characterized (Bjornstad et al., 2015). The development of the chorioallantoic membrane (CAM) is fully differentiated by embryonic day 13 (E13) (Nowak-Sliwinska et al., 2014), whereas the BBB in chicken matures between E10 and E16 (Stewart and Wiley, 1981). Injection experiments using horseradish peroxidase into the allantoic vein of chick embryos indicated a decreasing permeability of the brain blood vessels from E13 of development onwards (Wakai and Hirokawa, 1978), suggesting maturation of the BBB.

In the current study, we explore the distribution of the chemicals present in this mixture of POPs to the brain of developing chicken embryo after injection into the allantois at E13. We predict that injected pollutants will distribute in the allantoic fluid, be absorbed through CAM, and distribute to the brain via the blood stream, followed by an elimination from the brain (P1). This prediction is based on LC-MS analysis of the drug methadone which rapidly reached the

132 developing chicken embryo brain in concentrations comparable to those obtained in rat (Hadera
133 et al., 2017).

134 It is expected that small lipid soluble compounds such as chlorinated and brominated
135 POPs will readily diffuse across the BBB. Other compounds, such as protein binding PFASs
136 would need carrier or receptor-mediated transport (Goasdoué et al., 2017). In general, PFASs
137 do not readily cross the mature BBB since the levels of perfluorooctanoic acid (PFOA) and
138 PFOS in the cerebral spinal fluid in adult humans were about 1% of those in serum (Harada et
139 al., 2007). However, there may be potential for some PFASs to cross the immature blood-brain
140 barrier (Borg et al., 2010, Chang et al., 2009, Ishida et al., 2017). Based on this we predict that
141 concentrations of the compounds reaching the brain will depend on the chemical property of
142 the individual compounds (P2).

143 Furthermore, we assume that although the POPs are administered as a single injection
144 of a highly concentrated mixture, its dilution into the egg volume and subsequent distribution
145 will result in concentrations of individual compounds in the brain that are in the human relevant
146 exposure range (P3).

147 We also postulate that distribution to the developing chicken fetal brain would follow
148 standard pharmacokinetics (P4), which could be modelled using pharmacokinetic software
149 previously applied to calculate the different pharmacokinetic parameters determining the levels
150 of drugs in blood and brain in mice (Andersen et al., 2009, Boix et al., 2013).

151

2. Material and methods

2.1. POP mixture

The POP mixture was designed and prepared at the Norwegian University of Life Sciences (NMBU), Oslo, Norway (Berntsen et al., 2017a). The mixture contained 29 different compounds (Supplementary Table 1), including six PFASs (perfluorohexanesulfonic acid (PFHxS), PFOS, PFOA, perfluorononanoic acid (PFNA), perfluorodecanoic acid (PFDA), and perfluoroundecanoic acid (PFUnDA)); seven brominated (Br) compounds (PBDE 47, PBDE 99, PBDE-100, PBDE 153, PBDE 154, PBDE 209, and hexabromocyclododecane (HBCD)); and sixteen chlorinated (Cl) compounds (PCB 28, PCB 52, PCB 101, PCB 118, PCB 138, PCB 153, PCB 180, *p,p'*-dichlorodiphenyldichloroethylene (DDE), hexachlorobenzene (HCB), α-chlordane, oxychlordane, *trans*-nonachlor, α-hexachlorocyclohexane (HCH), β-HCH, γ-HCH (lindane) and dieldrin). The compounds were selected from their respective compound groups based on prevalence in blood, breastmilk and/or food, and their relative concentrations based on Scandinavian human blood levels. The stocks used in the present study had a concentration of 10^6 times blood levels in DMSO and stored in glass vials at -80°C (Berntsen et al., 2017a).

2.2. Injection of chicken eggs and exposure of developing embryos to POPs

Eggs (*Gallus gallus*, weight 50-55 g, fertilized) were obtained from Nortura Samvirkekylling (Våler, Norway) and incubated at 37.5°C in 45% relative humidity in an OvaEasy 380 Advance EXII Incubator (Brinsea,Weston-super-Mare, UK). Sex determination of embryos was not performed. Prior to injection, eggs were weighed, and the POP mixture was diluted in 0.9% saline. On E13, eggs were trans-illuminated with a LED lamp (Brinsea) to visualize spontaneous movements confirming living embryos. For injection, the POP mixture

stock was diluted 1/100 in saline. This solution was injected into each egg (1 µl saline solution/gram egg weight). Injection was performed through the CAM into the allantois with a 29-gauge needle. Injection was guided by trans-illumination with the LED lamp to avoid injecting into blood vessels. This resulted in a final exposure concentration of 10x (times) human blood levels compounds, assuming uniform distribution of the compounds throughout all compartments of the egg. At 0.5, 1, 2, 4, 6, 24, 48, and 72 h after administration, the embryos were anesthetized by hypothermia by submerging the eggs in crushed ice for 7 min, hatched, and immediately decapitated. The skull was opened along the cranial sutures and the cranium was removed to expose the brain. The whole brain was isolated with a spatula and the meninges were removed with forceps. The brains were snap-frozen in liquid nitrogen and stored at -80 °C until further processing. Two or three eggs were injected per sampling time-point. Animals were handled in accordance with the Norwegian Animal Welfare Act and the EU directive 2010/63/EU, and the study was approved by the Norwegian Food Safety Authority (application ID: FOTS 13896). The exposure scenario is shown in Figure 1.

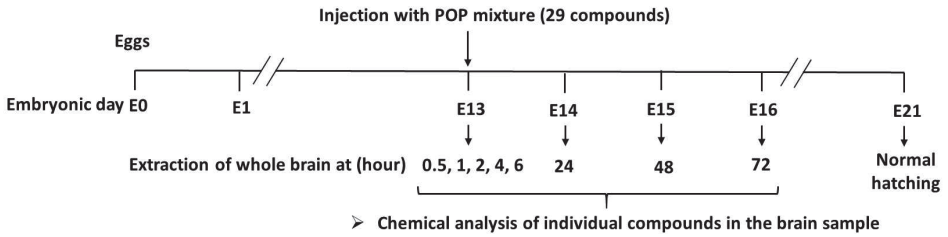

Figure 1. Illustration of the experimental timeline. The POP mixture (29 compounds) was administrated by injection through CAM into the allantois at embryonic day (E) 13. At 0.5, 1,

2, 4, 6, 24, 48 and 72 h after administration, the whole brain was isolated and chemical analysis of individual compounds in the brain was performed.

2.3. Measurement of POPs concentration in chicken embryo brains

Analysis of brain samples for PFASs was performed at the Department of Environmental Health at the Norwegian Institute of Public Health (Oslo, Norway) as described previously (Haug et al., 2009). In short, PFASs were extracted with methanol. Concentrations of PFASs were determined using column-switching liquid chromatography (LC) coupled to a triple-quadrupole mass spectrometer (MS). For the chemical analysis of these compounds, a single measurement was performed from three individual brains each, Table 1A.

The rest of the compounds (PCBs, PBDEs and OCPs) were analyzed in brains from a different set of exposures at the Norwegian University of Life Sciences (NMBU), Department of Food Safety and Infection Biology, Laboratory of Environmental Toxicology. Extractions were performed with cyclohexane/acetone and water. It was followed by gel permeation column or sulphuric acid for clean-up. Separation and detection of the OCPs and PCBs were performed on a GC coupled to Electron Capture Detector (ECD) and low-resolution mass spectrometry (LRMS). Detection of PBDEs and HBCD was performed on a HRGC–LRMS (Polder et al., 2014). For each collected time-point two brains were pooled for a single chemical quantitation of individual OCPs, PCBs and BFRs, Table 1B. Details from the extraction, clean-up and instrument run for the samples and quality control parameters can be found in Supplementary material.

Table 1. Chemical concentrations of POP mixture in chicken embryo brain. Chicken embryos on E13 were exposed with a POP mixture containing 29 compounds resulting in a final concentration equivalent to 10x human blood levels in the egg. After 0.5, 1, 2, 4, 6, 24, 28 and 72 h exposure individual compounds were analyzed in embryonic brains. A) Measured concentrations represent the mean value ± SEM of PFASs of three brains at each time point (n=3); B) Measured concentrations represent single measurements of OCPs, PCBs and BFRs in the brain at each time-point.

Individual Compounds in POP mixture	***Detection limit***	***Time h***							
A) ng/g wet weight		0.5	1	2	4	6	24	48	72
*PFASs**									
PFHxS	0.50	nd	nd	nd	3.52 ± 0.26	8.60 ± 1.90	21.19 ± 3.05	20.64 ± 1.67	14.74 ± 0.83
PFOS	0.50	5.10 ± 0.29	1.54 ± 0.36	25.74 ± 3.51	77.57 ± 10.55	201.81 ± 25.36	190.89 ± 28.40	132.45 ± 8.04	83.18 ± 6.29
PFOA	0.50	#0.15 ± 0.00	nd	nd	0.07 ± 0.02	0.72 ± 0.25	3.70 ± 1.09	5.79 ± 0.87	5.23 ± 0.51
PFNA	0.50	nd	nd	nd	0.93 ± 0.14	1.54 ± 0.21	2.70 ± 0.39	3.00 ± 0.48	1.66 ± 0.24
PFDA	0.50	nd	nd	nd	0.96 ± 0.18	2.02 ± 0.37	2.20 ± 0.22	2.62 ± 0.07	1.53 ± 0.10
PFUnDA	0.50	0.10 ± 0.02	0.05 ± 0.00	0.67 ± 0.09	1.58 ± 0.13	3.48 ± 0.46	3.60 ± 0.41	4.26 ± 0.32	3.26 ± 0.31
B) ng/g of lipid									
OCPs									
HCB	0.01	50.00	26.84	6.92	19.63	11.07	2.92	2.57	1.67
α-HCH	0.03	4.21	nd	nd	nd	nd	nd	nd	nd
β-HCH	0.05	38.42	12.11	5.39	5.56	3.93	nd	nd	nd
γ-HCH	0.04	10.53	nd	nd	2.22	nd	nd	nd	nd
Oxychlordane	0.02	14.21	7.90	nd	5.56	2.50	nd	nd	nd
alpha-chlordane	0.02	7.90	4.74	3.46	4.82	2.50	nd	nd	nd
trans-Nonachlor	0.01	18.95	13.16	15.39	22.96	13.93	1.83	nd	nd
p,p'-DDE	0.11	154.21	139.47	164.23	354.07	205.00	26.27	18.29	11.67
Dieldrin	0.40	40.00	nd	nd	22.22	19.29	nd	nd	nd
PCBs									
PCB-101	0.04	nd	5.26	5.39	10.37	5.36	nd	nd	nd
PCB-118	0.01	12.28	10.70	18.59	46.79	28.33	3.41	2.10	1.94
PCB-138	0.01	17.90	17.37	59.23	223.33	170.71	20.07	10.00	7.71
PCB-153	0.01	19.83	20.35	82.95	364.32	297.38	36.73	19.91	15.76
PCB-180	0.01	1.75	1.75	15.13	129.01	149.05	50.48	19.52	11.32
BFRs									
PBDE-47	0.01	2.11	1.58	1.54	5.56	3.21	nd	nd	nd
PBDE-99	0.02	nd	2.11	0.77	2.96	1.79	nd	nd	nd
PBDE-100	0.01	1.05	1.58	0.77	2.22	1.79	3.70	0.86	nd
PBDE-153	0.02	1.05	na	1.15	1.11	nd	nd	nd	nd
PBDE-154	0.02	1.58	1.05	nd	0.74	1.43	nd	nd	nd
PBDE-209	0.11	nd	nd	nd	nd	nd	nd	nd	4.79
HBCD	0.11	nd	6.33	nd	10.14	nd	nd	nd	nd

Abbreviations: nd (not detected); PCB (polychlorinated biphenyls); OCP (organochlorine pesticides); BFR (brominated flame retardants); PFASs (per- and polyfluoroalkyl substances). *Limit of quantitation (LOQ): about 0.5 pg/mg, results were indicated below the LOQ when the chromatogram showed a distinct peak. #0.15 ± 0.00 detected in only one sample.

2.4. Pharmacokinetics modelling

We applied the pharmacokinetic software package Kinetica 5.1 (Thermo Fisher Scientific Inc., Waltham, MA, USA) to model the distribution to the embryonic chicken egg with the brain considered as an extravascular compartment. This package has been applied in previous studies to calculate the different pharmacokinetic parameters determining the levels of drugs in blood and brain after administration in mice (Andersen et al., 2009, Boix et al., 2013). A one-compartment or two-compartment extravascular pharmacokinetic model with or without lag was selected based on the lowest Akaike's Information Criteria and subsequent visual inspection of the fitted curves. This allowed us to calculate the pharmacokinetic distribution parameters (Table 2) based on the concentrations curves and the absolute dose injected. The ratio between the area under the curve (AUC) and dose (*AUC/Dose*) was also calculated. The log of the n-octanol/water partition coefficient (*logKow*), defined as the ratio of the concentration of a chemical in n-octanol and water at equilibrium at a specified temperature, was obtained from available public sources (referenced in Table 2).

3. *Results*

3.1. Concentrations of POP mixture compounds in chicken embryo brain

First, PFASs were quantified for each time-point. PFOS reached maximum concentrations at 6 h after injection, whereas the other PFASs reached maximum concentration at 24 and 48 h after injection. The highest concentration was for PFOS (201.81 ± 25.36 ng/g) at 6 h, followed by PFHxS (21.19 ± 3.05 ng/g) at 24 h post injection (Table 1A).

These observations based on 3 biological replicates and summarized in Supplementary Table 3 also indicate consistency and reproducibility of the injections. For example, at 6 h the SEM is 12.57% of the mean for PFOS, and 13.21% for PFUnDA. Data for the remaining compounds were therefore based on a single measurement in two pooled brains at each time-point (Table 1B).

Of the 29 compounds, 27 were found in the brain samples, and only PCB 28 and PCB 52 could not be detected. Most compounds were already detectable in the brain 0.5 h after injection into the allantois (Table 1B). Variability in the time reaching the maximum brain concentrations between compounds was observed. The OCPs were at their maximum 0.5-1 h after exposure, except *trans*-nonachlor and *p,p`*-DDE which, like the PCBs, peaked at 4-6 h. Other lipophilic compounds (BFRs) peaked between 0.5 and 6 h. Interestingly, the peak concentrations were lower than what would have been expected with a uniform distribution throughout the egg, consistent with barriers preventing free diffusion and emphasizing the importance of such analyses. After reaching the maximum peak, the brain concentrations of OCPs declined rapidly and only DDE was above the detection limit at 72 h post exposure. followed by BFRs, which PFASs persisting at relative high levels in the brain for relative long times. The levels of PCBs are still detectable but relatively low whereas the levels of PFASs

were all relatively high at the end of the study (72 h) compared to maximum peak. The levels of PBDEs were under the detection limit at 72 h post exposure.

3.2.*Pharmacokinetic (PK) modelling*

The experimental data in Table 1 seemed to follow different distribution pattern depending on the chemical class of compound. We used an available human pharmacokinetic package to derive pharmacokinetic parameters based on the concentration measured on the brain. Based on these, PFASs showed a good fit to a one-compartment model with lag, OCPs fitted predominantly to a 2 compartments model, and PCBs to a two-compartments model with lag (Table 2 and Figures 2 to 4).

PFASs showed the lowest rates of transfer (*Ka*) from the injection site to the brain than the PCBs. The two OCPs, DDE and HCB modelled showed different transfer rates to the brain. On the other hand, a relationship between the elimination rate constant (*Kel)* and the different classes of POPs was revealed. Thus, whereas the OCPs showed the highest elimination rates, being therefore the compounds disappearing fastest from the embryo brain, PFASs were the ones with the lowest *Kel*, showing relatively high concentrations still 72 hours after administration, with data for PCBs in-between those two. The ratios of AUC/Dose were also closely related to compound class, with PCBs showing much higher AUC/Dose ratios than PFASs, while data for OCPs were in between those two. Reported logKow values (Table 2) were the highest for PCBs whereas OCPs and PFASs have lower values.

Despite the relations between type of compounds and pharmacokinetic parameters, there were also obvious differences within compound classes. PFUnDa sticked out by its much

lower *Kel* than the other PFASs, which also reflected in its residence time and its AUC/Dose, whereas the two OCPs analyzed showed a very high discrepancy in their *Ka*.

Table 2. Dose administered, pharmacokinetics parameters in the brain of chicken embryos, and logKow of selected POPs injected into the allantois of the chicken egg.

Compound	*Model*	*Dose*	*Ka*	*lag*	*Kel*	*AUC*	*MRT*	*Cmax Calc*	*Tmax calc*	*AUC Dose*	*logKow*
		ng	h-1	h	h-1	(h)*(ng/µL)	h	ng/g	h		
PFASs											
PFOS	1 C - lag	12291.40	0.60	3.41	0.017	15750.70	56.33	237.79	9.58	1.28	6.43 (Wang et al., 2011)
PFHxS	1 C - lag	1886.48	0.06	2.00	0.016	2234.02	61.47	22.30	30.98	1.18	5.17 (Wang et al., 2011)
PFOA	1 C - lag	958.62	0.02	3.69	0.017	810.21	54.75	5.56	57.04	0.84	5.30 (Wang et al., 2011)
PFUnDA	1 C - lag	104.49	0.29	1.54	0.003	1585.80	377.61	4.00	18.01	15.18	7.15 (Wang et al., 2011)
OCPs											
p,p'-DDE	2 C - lag	186.44	0.63	1.68	0.266	3786.76	35.29	377.45	3.33	20.31	6.51 (Desban et al., 1989)
HCB	2 C - no lag	35.74	3.74		0.404	349.35	26.20	57.96	0.30	9.77	5.47 (Tolls et al., 2003)
PCBs											
PCB153	2 C - lag	138.60	1.12	1.84	0.085	5969.54	58.61	364.93	3.86	43.07	6.87 (Li et al., 2003)
PCB138	2 C - lag	85,25	1.58	1.86	0.093	3189.71	47.67	229.14	3.47	37.42	7.22 (Li et al., 2003)
PCB180	2 C - lag	73.71	0.54	1.86	0.054	3847.56	32.62	149.05	6.00	52.20	7.16 (Li et al., 2003)
PCB118	2 C - lag	24.76	0.60	1.72	0.244	535.14	45.31	48.89	3.43	21.61	6.69 (Li et al., 2003)

Model: Pharmacokinetic model best fitting concentrations of POP in the chicken brain. *Dose*: Absolute dose injected in allantoic fluid. *Ka*: Absorption rate constant from injection site. *Lag*: Time taken to appear in the brain following administration. *Kel*: Elimination rate constant from brain. *AUC*: Area under the curve. *MRT*: Mean residence time (Time spend by molecules in the brain). *Cmax calc*: Theoretical calculated maximal concentration. *Tmax calc*: Theoretical calculated time at which Cmax is achieved. *AUC/Dose*: Relation between AUC and dose administered. *logKow*: Logarithm of the n-octanol/water partition coefficient (Kow) as obtained from the literature (references in brackets).

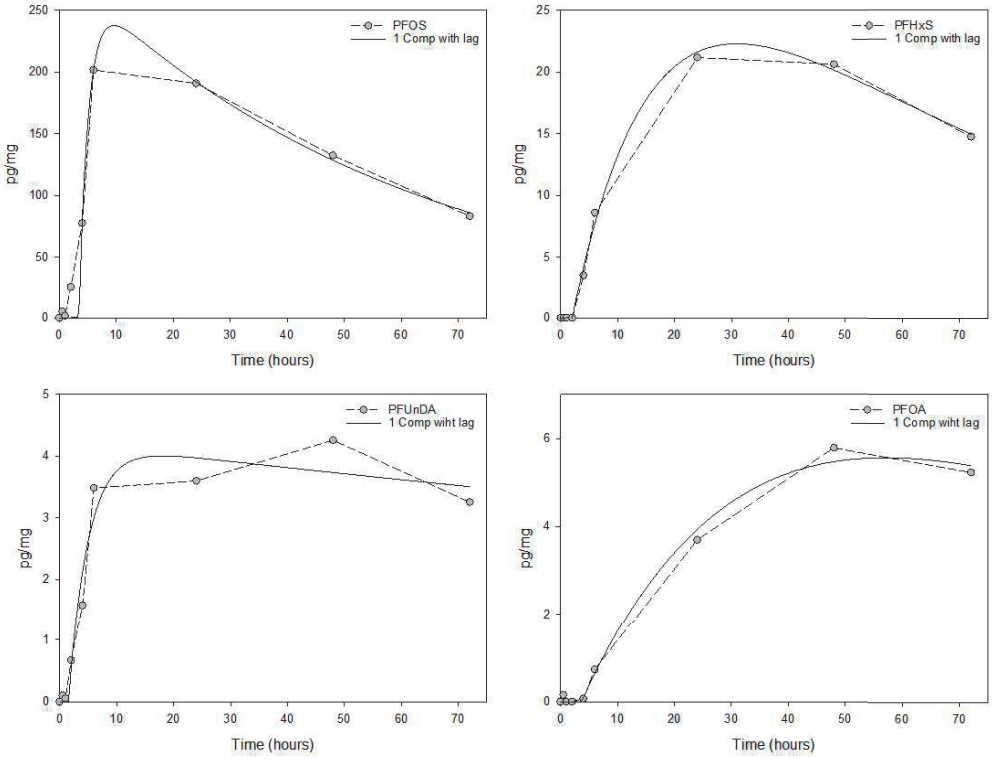

302

303 **Figure 2**. Mean concentrations (grey circles, dashed line) of PFASs (PFOS, PFHxS,
304 PFUnDA, PFOA,) in the brain of chicken embryos taken at different time-points after their
305 injection in the allantoic fluid of chicken eggs and theoretical values (continuous black
306 spline), calculated in half hour intervals, from the pharmacokinetic model fitted (specified in
307 the legends of the graphs).

308

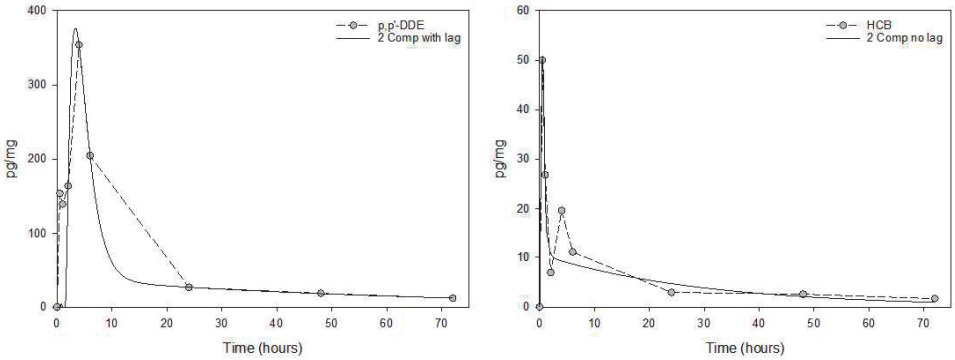

309

310 **Figure 3.** Concentrations (grey circles, dashed line) of OCPs (*p,p'*-DDE, HCB) in the brain of
311 chicken embryos taken at different time-points after their injection in the allantoic fluid of
312 chicken eggs and theoretical values (continuous black spline), calculated in half hour interval,
313 from the pharmacokinetic model fitted (specified in the legends of the graphs).

314

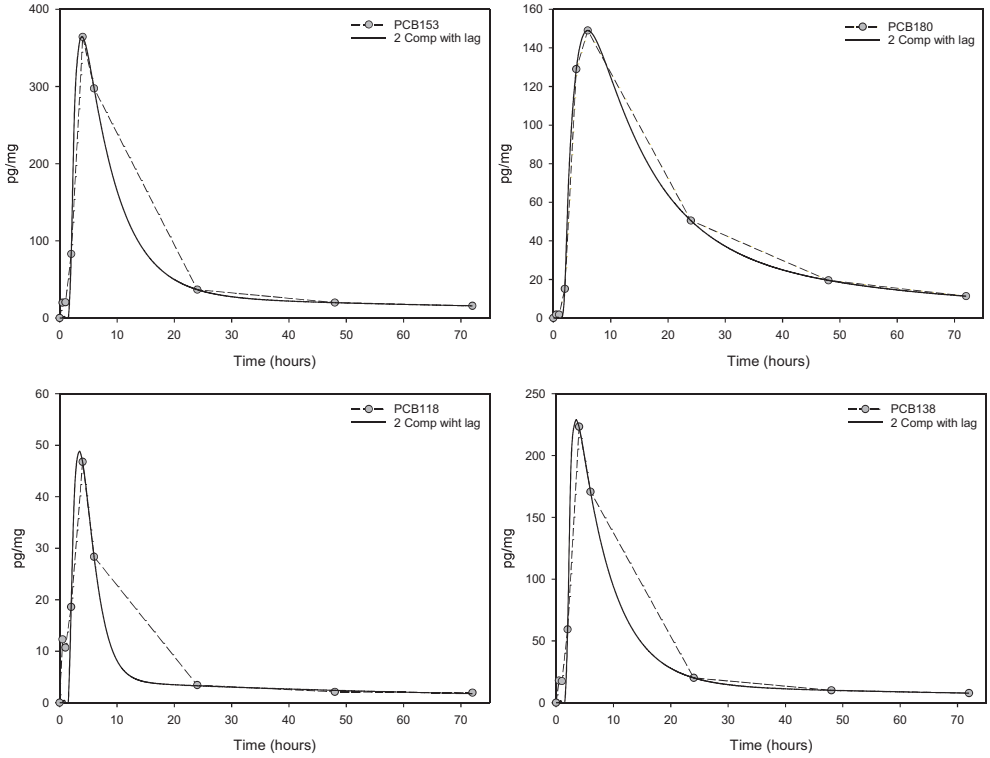

315

316 **Figure 4**. Concentrations (grey circles, dashed line) of PCBs (PCB 153, PCB 180, PCB 118,
317 PCB 138) in the brain of chicken embryos taken at different time-points after their injection in
318 the allantoic fluid of chicken eggs and theoretical values (continuous black spline), calculated
319 in half hour intervals, from the pharmacokinetic model fitted (specified in the legends of the
320 graphs).

321

4. Discussion

POPs and different drugs/chemicals have shown to cause neurodevelopmental effects in the chicken embryo model (Austdal et al., 2016, Berntsen et al., 2020, Mathisen et al., 2013, Yadav et al., 2021b). In this study we exposed chicken embryos at E13 with a POP mixture containing 29 compounds resulting in a final concentration equivalent to 10x human blood levels in the egg by injection into the allantois. After administration, 27 of 29 of the individual compounds were detected in the developing brain during at least one of the time-points analyzed. Concentration reached a peak value, followed by a decline over time. This confirms our prediction (P1) that the compounds in our mixture reach the embryonic brain via the blood stream and are subject to elimination.

We observed differences in the speed of distribution to the brain, with the protein binding compounds (PFASs) being slower than the lipophilic (PCBs, OCPs, BFRs), which confirms P2. Moreover, it suggests the presence of a functional barrier at this time-point, most likely the BBB.

The concentrations of most of the measured compounds in chicken embryo brains were within the same order of magnitude as those reported in human brain samples (Supplementary Table 2), supporting P3. However, the levels of PFOS in the chicken brain were relatively high compared to levels measured in human brain samples. As exposure to POPs is individualistic in nature, certain groups of people may have higher body burden of certain POPs. A Chinese study reported levels of PFOS up to 118000 ng/ml and PFOA up to 32000 ng/ml in serum from occupationally exposed workers (Fu et al., 2016). Although there are few studies reporting levels of PFASs in the human brain, according to Maestri et al. (2006) the concentrations in the brain of PFOS and PFOA can be expected to be the 25% and 17% of their concentrations

345 in serum, respectively. Thus, this would correspond to brain concentrations up to 29500 ng/ml
346 for PFOS and 5440 ng/ml for PFOA in Fu et al. (2016).

347 The POPs studied can be differentiated based on which pharmacokinetic model fits
348 them best. Thus, whereas pharmacokinetic modelling for PFASs was best fitted by a standard
349 one compartment extravascular model, OCPs (HCB, DDE) and PCBs could be best fitted by
350 standard two compartmental extravascular model. In pharmacokinetics, multi-compartmental
351 models are used to mathematically describe non-linear kinetics of a drug during the elimination
352 phase, which can be detected using a semilogarithmic plot. Accordingly, the fitting of a one or
353 two compartments model merely expresses if the pharmacokinetics is linear (one compartment)
354 or not (two or more compartments). These compartments have been associated to anatomical
355 locations in the organism where the drug distributes. However, non-linearity can be due to
356 other physiological processes, for example the kinetics of the metabolic enzymatic reactions
357 (Macheras and Iliadis, 2016). Thus, the compartmental modelling distinguishing PFASs from
358 OCPs and PCBs would imply that probably different physiological mechanisms or routes are
359 responsible for the distribution of these compounds to the brain. Which process, or processes,
360 determines the non-linearity in the distribution of these compounds to the chicken embryo brain
361 demands a more advanced knowledge of this experimental model. OCPs are characterized by
362 fitting a model without lag, indicating a faster absorption. Indeed, they presented larger
363 absorption rates (Ka). Considering the elimination constant (Kel), OCPs showed a more rapid
364 accumulation followed by a faster elimination from brain than PCBs compared to the PFASs,
365 which still persisted at relatively high levels in the brain at the end of the study (3 day post
366 injection). PFUnDA had the lowest Kel, indicating a mean residence time of more than 300
367 hours. Thus, PFUnDA would stay at relatively significant levels in the brain for at least until

368 hatching. PFUnDA is one of the most abundant PFASs in the brains of polar bears from
369 Greenland (Eggers Pedersen et al., 2015). Also, in brain samples from harbour seals and red-
370 throated divers the longer chained PFASs such as PFUnDA have been found to accumulate to
371 a higher extent in brain relative to blood, than shorter chained compounds (Ahrens et al., 2009,
372 Rubarth et al., 2011). In addition, we have previously examined the toxicity of each individual
373 PFASs present in the POP mixture in cultured rat cerebellar granule neurons (Berntsen et al.,
374 2017b). We observed that toxicity of PFASs increased with increasing carbon chain length,
375 with PFUnDA being the most potent inducer of cytotoxicity. The longer residence time of this
376 compound and its possible higher neurotoxicity could potentially make this a compound of
377 high concern with respect to developmental neurotoxicity. This concern is amplified by the fact
378 that production and use of PFUnDA in a multitude of consumer products, is not regulated by
379 any national or international legislation.

380 The calculated AUC/Dose, which can give valuable information about total exposure
381 in the brain in relation to the dose administered, is lowest for PFASs and increases with HCB,
382 DDE and PCBs. This would imply that, If the same dose of each compound were to be
383 administered, the brain exposure would be highest for PCBs, followed by DDE, HCB and
384 PFASs, except for PFUnDA. This information can be especially useful to estimate the possible
385 impact of the levels found in humans in the development of the embryonic brain.

386 The differences in the pharmacokinetics between the studied compounds can be related
387 to their lipophilicity. One common measure of lipophilicity is the n-Octanol/Water Partition
388 Coefficient (Kow), which is the ratio of the concentration of a chemical in n-octanol and water
389 at equilibrium. Kow is normally expressed as a logarithm (logKow). LogKow is generally
390 directly related to solubility in fat (as measured in n-octanol in this case), is proportional to the

391 molecular weight of a substance, and can predict the distribution of pollutants in tissues
392 (Hellou et al., 2002). Despite overlaps, the different POPs groups are also clustered by their
393 logKow. On the other hand, a negative, correlation (Pearson's r=-0.5594) with the lag,
394 accompanied by positive correlations with the mean residential time MRT and the AUC/Dose
395 (Pearson's r=0.3115 and r=0.7518 respectively), were observed. This would indicate that the
396 most lipophilic substances are able to get faster into and remain longer in the brain, possibly
397 due to the relative high content of fatty compounds in this organ. However, logKow might not
398 be a good predictor for PFASs as we have to consider their values as uncertain since they are
399 both hydrophobic and oleophobic. Therefore logKow cannot easily be experimentally
400 determined and can only be estimated from their structure (Liu et al., 2019). Together, this
401 indicates that a human pharmacokinetic model can be applied to the observed concentrations
402 in the chicken brain and can be related to their chemical and physical properties, in line with
403 prediction P4.
404 The importance of pharmacokinetic knowledge is furthermore illustrated for humans
405 hazard assessments, where measurements of PCBs or PBDE concentrations in human brain
406 tissues (Dewailly et al., 1999) are associated to neurological disorders (Corrigan et al., 1996,
407 Corrigan et al., 1998, Hatcher-Martin et al., 2012, Mitchell et al., 2012). Such levels were
408 approximately in the same brain level range of maternally exposed mice offspring (exhibiting
409 disturbed hippocampal gene expression) in our recent experiment (Myhre et al. 2020, in press
410 Chemosphere) and in the present study.
411
412
413

5. Conclusion

Individual compounds from a human relevant mixture of POPs injected into the allantois distributed to the brain of developing chicken embryos. For most of the compounds, the concentrations measured in chicken embryonic brains were within the same order of magnitude of those reported in human brain samples. However, differences in the speed of distribution to the brain were observed for the lipophilic PCBs, OCPs versus the PFASs which have protein binding potential. Thus, PCBs showed high exposure in the brain in relation to the dose administrated, probably contributing more to CNS toxicity than estimated only from their dose and, most likely, blood concentrations alone. This could be related to the chemical properties of different classes of compound in the mixture. However, how far these differences are reflecting their inherent physicochemical properties should be further investigated. Furthermore, our study shows that chicken is a relevant model to explore the distribution of POPs in developing brain at human relevant exposures.

Acknowledgements

This project has received funding from the European Union's Horizon 2020 research and innovation program under the Marie Skłodowska-Curie grant agreement No. 722634 (http://protected.eu.com/).

References

ADEN, P., GOVERUD, I., LIESTOL, K., LOBERG, E. M., PAULSEN, R. E., MAEHLEN, J. & LOMO, J. 2008. Low-potency glucocorticoid hydrocortisone has similar neurotoxic effects as high-potency glucocorticoid dexamethasone on neurons in the immature chicken cerebellum. *Brain Res,* 1236**,** 39-48.

AHRENS, L., SIEBERT, U. & EBINGHAUS, R. 2009. Total body burden and tissue distribution of polyfluorinated compounds in harbor seals (Phoca vitulina) from the German Bight. *Marine Pollution Bulletin,* 58**,** 520-525.

ANDERSEN, J. M., RIPEL, A., BOIX, F., NORMANN, P. T. & MØRLAND, J. 2009. Increased locomotor activity induced by heroin in mice: pharmacokinetic demonstration of heroin acting as a prodrug for the mediator 6-monoacetylmorphine in vivo. *J Pharmacol Exp Ther,* 331**,** 153-61.

AUSTDAL, L. P., BJORNSTAD, S., MATHISEN, G. H., ADEN, P. K., MIKKOLA, I., PAULSEN, R. E. & RAKKESTAD, K. E. 2016. Glucocorticoid Effects on Cerebellar Development in a Chicken Embryo Model: Exploring Changes in PAX6 and Metalloproteinase-9 After Exposure to Dexamethasone. *J Neuroendocrinol,* 28.

BERNTSEN, H. F., BERG, V., THOMSEN, C., ROPSTAD, E. & ZIMMER, K. E. 2017a. The design of an environmentally relevant mixture of persistent organic pollutants for use in in vivo and in vitro studies. *J Toxicol Environ Health A***,** 1-15.

BERNTSEN, H. F., BJORKLUND, C. G., AUDINOT, J. N., HOFER, T., VERHAEGEN, S., LENTZEN, E., GUTLEB, A. C. & ROPSTAD, E. 2017b. Time-dependent effects of perfluorinated compounds on viability in cerebellar granule neurons: Dependence on carbon chain length and functional group attached. *Neurotoxicology,* 63**,** 70-83.

BERNTSEN, H. F., BJORKLUND, C. G., STRANDABO, R., HAUG, T. M., MOLDES-ANAYA, A., FUENTES-LAZARO, J., VERHAEGEN, S., PAULSEN, R. E., TASKER, R. A. & ROPSTAD, E. 2018. PFOS-induced excitotoxicity is dependent on Ca(2+) influx via NMDA receptors in rat cerebellar granule neurons. *Toxicol Appl Pharmacol,* 357**,** 19-32.

BERNTSEN, H. F., DUALE, N., BJØRKLUND, C. G., RANGEL-HUERTA, O. D., DYRBERG, K., HOFER, T., RAKKESTAD, K. E., ØSTBY, G., HALSNE, R., BOGE, G., PAULSEN, R. E., MYHRE, O. & ROPSTAD, E. 2020. Effects of a human-based mixture of persistent organic pollutants on the in vivo exposed cerebellum and cerebellar neuronal cultures exposed in vitro. *Environ Int,* 146**,** 106240.

BJORNSTAD, S., AUSTDAL, L. P., ROALD, B., GLOVER, J. C. & PAULSEN, R. E. 2015. Cracking the Egg: Potential of the Developing Chicken as a Model System for Nonclinical Safety Studies of Pharmaceuticals. *J Pharmacol Exp Ther,* 355**,** 386-96.

BOIX, F., ANDERSEN, J. M. & MØRLAND, J. 2013. Pharmacokinetic modeling of subcutaneous heroin and its metabolites in blood and brain of mice. *Addict Biol,* 18**,** 1-7.

BORG, D., BOGDANSKA, J., SUNDSTRÖM, M., NOBEL, S., HÅKANSSON, H., BERGMAN, Å., DEPIERRE, J. W., HALLDIN, K. & BERGSTRÖM, U. 2010. Tissue distribution of 35S-labelled perfluorooctane sulfonate (PFOS) in C57Bl/6 mice following late gestational exposure. *Reproductive Toxicology,* 30**,** 558-565.

CHANG, S.-C., EHRESMAN, D. J., BJORK, J. A., WALLACE, K. B., PARKER, G. A., STUMP, D. G. & BUTENHOFF, J. L. 2009. Gestational and lactational exposure to potassium perfluorooctanesulfonate (K+PFOS) in rats: Toxicokinetics, thyroid hormone status, and related gene expression. *Reproductive Toxicology,* 27**,** 387-399.

CORRIGAN, F. M., FRENCH, M. & MURRAY, L. 1996. Organochlorine compounds in human brain. *Hum Exp Toxicol,* 15**,** 262-4.

CORRIGAN, F. M., MURRAY, L., WYATT, C. L. & SHORE, R. F. 1998. Diorthosubstituted Polychlorinated Biphenyls in Caudate Nucleus in Parkinson's Disease. *Experimental Neurology,* 150**,** 339-342.

DAVIDSEN, N., LAUVÅS, A. J., MYHRE, O., ROPSTAD, E., CARPI, D., GYVES, E. M.-D., BERNTSEN, H. F., DIRVEN, H., PAULSEN, R. E., BAL-PRICE, A. & PISTOLLATO, F. 2021. Exposure to human relevant mixtures of halogenated persistent organic pollutants (POPs) alters neurodevelopmental processes in human neural stem cells undergoing differentiation. *Reproductive Toxicology,* 100**,** 17-34.

DESBAN, M., GAUCHY, C., KEMEL, M. L., BESSON, M. J. & GLOWINSKI, J. 1989. Three-dimensional organization of the striosomal compartment and patchy distribution of striatonigral projections in the matrix of the cat caudate nucleus. *Neuroscience,* 29**,** 551-566.

DEWAILLY, E., MULVAD, G., PEDERSEN, H. S., AYOTTE, P., DEMERS, A., WEBER, J. P. & HANSEN, J. C. 1999. Concentration of organochlorines in human brain, liver, and adipose tissue autopsy samples from Greenland. *Environ Health Perspect,* 107**,** 823-8.

EGGERS PEDERSEN, K., BASU, N., LETCHER, R., GREAVES, A. K., SONNE, C., DIETZ, R. & STYRISHAVE, B. 2015. Brain region-specific perfluoroalkylated sulfonate (PFSA) and carboxylic acid (PFCA) accumulation and neurochemical biomarker Responses in east Greenland polar Bears (Ursus maritimus). *Environmental Research,* 138**,** 22-31.

FONNUM, F. & MARIUSSEN, E. 2009. Mechanisms involved in the neurotoxic effects of environmental toxicants such as polychlorinated biphenyls and brominated flame retardants. *J Neurochem,* 111**,** 1327-47.

FU, J., GAO, Y., CUI, L., WANG, T., LIANG, Y., QU, G., YUAN, B., WANG, Y., ZHANG, A. & JIANG, G. 2016. Occurrence, temporal trends, and half-lives of perfluoroalkyl acids (PFAAs) in occupational workers in China. *Sci Rep,* 6**,** 38039.

GOASDOUÉ, K., MILLER, S. M., COLDITZ, P. B. & BJÖRKMAN, S. T. 2017. Review: The blood-brain barrier; protecting the developing fetal brain. *Placenta,* 54**,** 111-116.

GRANDJEAN, P. & LANDRIGAN, P. J. 2014. Neurobehavioural effects of developmental toxicity. *Lancet Neurol,* 13**,** 330-8.

HADERA, M. G., ANDERSEN, J. M. & PAULSEN, R. E. 2017. Effects of methadone in the developing chicken embryo as a model of neurodevelopmental toxicity. *Reproductive Toxicology,* 72**,** 216-217.

HARADA, K. H., HASHIDA, S., KANEKO, T., TAKENAKA, K., MINATA, M., INOUE, K., SAITO, N. & KOIZUMI, A. 2007. Biliary excretion and cerebrospinal fluid partition of perfluorooctanoate and perfluorooctane sulfonate in humans. *Environmental Toxicology and Pharmacology,* 24**,** 134-139.

HATCHER-MARTIN, J. M., GEARING, M., STEENLAND, K., LEVEY, A. I., MILLER, G. W. & PENNELL, K. D. 2012. Association between polychlorinated biphenyls and Parkinson's disease neuropathology. *Neurotoxicology,* 33**,** 1298-1304.

HAUG, L. S., THOMSEN, C. & BECHER, G. 2009. A sensitive method for determination of a broad range of perfluorinated compounds in serum suitable for large-scale human biomonitoring. *J Chromatogr A,* 1216**,** 385-93.

HELLOU, J., LEONARD, J. & ANSTEY, C. 2002. Dietary Exposure of Finfish to Aromatic Contaminants and Tissue Distribution. *Archives of Environmental Contamination and Toxicology,* 42**,** 470-476.

ISHIDA, K., TSUYAMA, Y., SANOH, S., OHTA, S. & KOTAKE, Y. 2017. Perfluorooctane sulfonate induces neuronal vulnerability by decreasing GluR2 expression. *Archives of Toxicology,* 91**,** 885-895.

KARRMAN, A., VAN BAVEL, B., JARNBERG, U., HARDELL, L. & LINDSTROM, G. 2006. Perfluorinated chemicals in relation to other persistent organic pollutants in human blood. *Chemosphere,* 64**,** 1582-91.

LAU, C. 2015. Perfluorinated Compounds: An Overview. *In:* DEWITT, J. C. (ed.) *Toxicological Effects of Perfluoroalkyl and Polyfluoroalkyl Substances.* Cham: Springer International Publishing.

LENTERS, V., ISZATT, N., FORNS, J., ČECHOVÁ, E., KOČAN, A., LEGLER, J., LEONARDS, P., STIGUM, H. & EGGESBØ, M. 2019. Early-life exposure to persistent organic pollutants (OCPs, PBDEs, PCBs, PFASs) and attention-deficit/hyperactivity disorder: A multi-pollutant analysis of a Norwegian birth cohort. *Environment International,* 125**,** 33-42.

LI, N., WANIA, F., LEI, Y. D. & DALY, G. L. 2003. A Comprehensive and Critical Compilation, Evaluation, and Selection of Physical–Chemical Property Data for Selected Polychlorinated Biphenyls. *Journal of Physical and Chemical Reference Data,* 32**,** 1545-1590.

LIU, W., WU, J., HE, W. & XU, F. 2019. A review on perfluoroalkyl acids studies: Environmental behaviors, toxic effects, and ecological and health risks. *Ecosystem Health and Sustainability,* 5**,** 1-19.

MACHERAS, P. & ILIADIS, A. 2016. Deterministic Compartmental Models. *In:* MACHERAS, P. & ILIADIS, A. (eds.) *Modeling in Biopharmaceutics, Pharmacokinetics and Pharmacodynamics: Homogeneous and Heterogeneous Approaches.* Cham: Springer International Publishing.

MAESTRI, L., NEGRI, S., FERRARI, M., GHITTORI, S., FABRIS, F., DANESINO, P. & IMBRIANI, M. 2006. Determination of perfluorooctanoic acid and perfluorooctanesulfonate in human tissues by liquid chromatography/single quadrupole mass spectrometry. *Rapid Commun Mass Spectrom,* 20**,** 2728-34.

MAMSEN, L. S., BJORVANG, R. D., MUCS, D., VINNARS, M. T., PAPADOGIANNAKIS, N., LINDH, C. H., ANDERSEN, C. Y. & DAMDIMOPOULOU, P. 2019. Concentrations of perfluoroalkyl substances (PFASs) in human embryonic and fetal organs from first, second, and third trimester pregnancies. *Environ Int,* 124**,** 482-492.

MATHISEN, G. H., YAZDANI, M., RAKKESTAD, K. E., ADEN, P. K., BODIN, J., SAMUELSEN, M., NYGAARD, U. C., GOVERUD, I. L., GAARDER, M., LOBERG, E. M., BOLLING, A. K., BECHER, R. & PAULSEN, R. E. 2013. Prenatal exposure to bisphenol A interferes with the development of cerebellar granule neurons in mice and chicken. *Int J Dev Neurosci,* 31**,** 762-9.

MITCHELL, M. M., WOODS, R., CHI, L. H., SCHMIDT, R. J., PESSAH, I. N., KOSTYNIAK, P. J. & LASALLE, J. M. 2012. Levels of select PCB and PBDE congeners in human postmortem brain reveal possible environmental involvement in 15q11-q13 duplication autism spectrum disorder. *Environ Mol Mutagen,* 53**,** 589-98.

NOWAK-SLIWINSKA, P., SEGURA, T. & IRUELA-ARISPE, M. L. 2014. The chicken chorioallantoic membrane model in biology, medicine and bioengineering. *Angiogenesis,* 17**,** 779-804.

PÉREZ, F., NADAL, M., NAVARRO-ORTEGA, A., FÀBREGA, F., DOMINGO, J. L., BARCELÓ, D. & FARRÉ, M. 2013. Accumulation of perfluoroalkyl substances in human tissues. *Environment International,* 59**,** 354-362.

POLDER, A., MÜLLER, M. B., LYCHE, J. L., MDEGELA, R. H., NONGA, H. E., MABIKI, F. P., MBISE, T. J., SKAARE, J. U., SANDVIK, M., SKJERVE, E. & LIE, E. 2014. Levels and patterns of persistent organic pollutants (POPs) in tilapia (Oreochromis sp.) from four different lakes in Tanzania: Geographical differences and implications for human health. *Science of The Total Environment,* 488-489**,** 252-260.

RUBARTH, J., DREYER, A., GUSE, N., EINAX, J. W. & EBINGHAUS, R. 2011. Perfluorinated compounds in red-throated divers from the German Baltic Sea: new findings from their distribution in 10 different tissues. *Environmental Chemistry,* 8**,** 419-428.

SAGIV, S. K., KOGUT, K., GASPAR, F. W., GUNIER, R. B., HARLEY, K. G., PARRA, K., VILLASEÑOR, D., BRADMAN, A., HOLLAND, N. & ESKENAZI, B. 2015. Prenatal and childhood polybrominated diphenyl ether (PBDE) exposure and attention and executive function at 9-12 years of age. *Neurotoxicol Teratol,* 52**,** 151-61.

SAGIV, S. K., THURSTON, S. W., BELLINGER, D. C., ALTSHUL, L. M. & KORRICK, S. A. 2012. Neuropsychological measures of attention and impulse control among 8-year-old children exposed prenatally to organochlorines. *Environ Health Perspect,* 120**,** 904-9.

SECRETARIAT OF THE STOCKHOLM CONVENTION. 2019a. *All POPs listed in the Stockholm Convention.* *http://chm.pops.int/TheConvention/ThePOPs/AllPOPs/tabid/2509/Default.aspx* [Online]. [Accessed 8 January 2021].

SECRETARIAT OF THE STOCKHOLM CONVENTION. 2019b. *What are POPs?* *http://chm.pops.int/TheConvention/ThePOPs/tabid/673/Default.aspx* [Online]. [Accessed 8 January 2021].

STEWART, P. A. & WILEY, M. J. 1981. Structural and histochemical features of the avian blood-brain barrier. *J Comp Neurol,* 202**,** 157-67.

TOLLS, J., BODO, K., DE FELIP, E., DUJARDIN, R., KIM, Y. H., MOELLER-JENSEN, L., MULLEE, D., NAKAJIMA, A., PASCHKE, A., PAWLICZEK, J.-B., SCHNEIDER, J., TADEO, J.-L., TOGNUCCI, A. C., WEBB, J. & ZWIJZEN, A. C. 2003. Slow-stirring method for determining the n-octanol/water partition coefficient (pow) for highly hydrophobic chemicals: Performance evaluation in a ring test. *Environmental Toxicology and Chemistry,* 22**,** 1051-1057.

WAKAI, S. & HIROKAWA, N. 1978. Development of the blood-brain barrier to horseradish peroxidase in the chick embryo. *Cell Tissue Res,* 195**,** 195-203.

WANG, Z., MACLEOD, M., COUSINS, I. T., SCHERINGER, M. & HUNGERBÜHLER, K. 2011. Using COSMOtherm to predict physicochemical properties of poly- and perfluorinated alkyl substances (PFASs). *Environmental Chemistry,* 8**,** 389-398.

WHO 2008. WHO on POPs. https://www.who.int/ceh/capacity/POPs.pdf.

YADAV, A., AMBER, M., ZOSEN, D., LABBA, N. A., HUIBERTS, E. H. W., SAMULIN ERDEM, J., HAUGEN, F., BERNTSEN, H. F., ZIENOLDDINY, S., PAULSEN, R. E., ROPSTAD, E., CONNOLLY, L. & VERHAEGEN, S. 2021a. A human relevant mixture of persistent organic pollutants (POPs) and perfluorooctane sulfonic acid (PFOS) enhance nerve growth factor (NGF)-induced neurite outgrowth in PC12 cells. *Toxicol Lett,* 338**,** 85-96.

YADAV, A., VERHAEGEN, S., VERBRUGGEN, E., KERHOAS, M., WILLEMIJN HUIBERTS, E. H., HADERA, M. G., BERNTSEN, H. F., ZIMMER, K. E., ROPSTAD, E. & PAULSEN, R. E. 2021b. A human relevant mixture of persistent organic pollutants (POPs) and perfluorooctane sulfonic acid (PFOS) differentially affect glutamate induced excitotoxic responses in chicken cerebellum granule neurons (CGNs) in vitro. *Reprod Toxicol,* 100**,** 109-119.

SUPPLEMENTARY MATERIALS – PAPER III

Supplementary Table 1. Description of the total *in vitro* mixture containing 29 different POPs based on human blood levels, detailed in (Berntsen et al., 2017).

Compound	*Average human blood levels [a] ng/g lipid*	*Average human blood levels [b] ng/ml*	*Total mixture stock nominal concentration [c] mg/ml*	*Total mixture stock Measured concentration [d] µM*
PCBs				
PCB 28	2.13	0.013	0.013	31.1
PCB 52	1.6	0.01	0.01	20.5
PCB 101	1.3	0.008	0.008	24.5
PCB 118	10.67	0.064	0.064	137.9
PCB 138	37	0.222	0.222	429.5
PCB 153	60.33	0.362	0.362	698.3
PCB 180	32.33	0.194	0.194	339
∑ PCBs	145.36	0.873	0.873	1680.8
OCP				
p,p'-DDE	83.67	0.502	0.502	1065.9
HCB	19.5	0.117	0.117	228.2
α-Chlordane	1.8	0.011	0.011	23.7
Oxychlordane	3.7	0.022	0.022	33
trans-Nonachlor	6.8	0.041	0.041	99.1
α-HCH	1	0.006	0.006	16.8
β-HCH	8.77	0.053	0.053	75.6
γ-HCH	1	0.006	0.006	16.8
Dieldrin	4	0.024	0.024	56.2
∑ OCPs	130.24	0.782	0.782	1615.3
∑ PCBs + OCPs	275.6	1.655	1.655	3296.1
BFRs				
PBDE 47	1.43	0.009	0.009	17.8
PBDE 99	0.59	0.004	0.004	7.5
PBDE 100	0.36	0.002	0.002	3.8
PBDE 153	1.64	0.01	0.001*	2.1
PBDE 154	0.29	0.002	0.002	3
PBDE 209	1.81	0.011	0.011	9.4
HBCD	4.1	0.025	0.025	54.5
∑ BFRs	10.22	0.063	0.053	98.1
PFASs				
PFHxS	N/A	3.45	3.45	7809.2
PFOS	N/A	29.425	29.425	41522.1
PFOA	N/A	4.523	4.523	4209.4
PFNA	N/A	0.8	0.8	1092.5
PFDA	N/A	0.495	0.495	375.4
PFUnDA	N/A	0.56	0.56	336.8
∑ PFASs	N/A	39.253	39.253	55345.4

[a] Average human blood levels of POPs based on a literature review of Scandinavian values, providing the basis for the in vitro mixture.

[b] Average human blood levels of POPs converted to ng/ml. A fat percentage of 0.6 % was used. 1 ml blood was considered to have a weight of 1 g.

[c] Nominal concentration of the various compounds in the total mixture stock – 1000000x the average concentration in blood.

****The nominal concentration of PBDE 153 included in the total mixture stock was ten times lower than originally intended.***

[d] Measured concentrations of the various compounds in the total mixture stock converted to µM.

N/A - Not applicable

Abbreviations: PCBs (polychlorinated biphenyls); OCPs (organochlorine pesticides); BFRs (brominated flame retardants); PFASs (per- and polyfluoroalkyl substances)

Chemical analyses

Extraction of the OCPs, PCBs and BDEs has been described by Polder *et al.* (2014). Briefly the samples were weighed, and added internal standards (PCB 29, 112 and 207 (Ultra Scientific, RI, USA); BDE 77, 119 and 181 and 13C12-BDE 209 (Cambridge Isotope Laboratories, Inc., MA, USA)) and solvents (cyclohexane/acetone/water), followed by homogenization using a T25 Ika Ultra-Turrax®. The removal of lipids for the determination of dieldrin was performed using a gel permeation column, filled with Bio-Beads S-X3, 200–400 mesh (Bio-Rad Laboratories, Inc., CA, USA) installed on a Gilson Model 233 combined injector and fractionating system (Gilson, Inc., WI, USA). The removal of lipids for the determination of the rest of the OCPs, PCBs, BDEs and HBCD was performed using ≥ 97.5% H2SO4 (Fluka Analytical®).

Separation and detection of the OCPs and PCBs were performed on a GC coupled to Electron Capture Detector (ECD) and low resolution mass spectrometry (LRMS) (Agilent6890 Series; agilent Technologies), as described by (Polder et al., 2014). PCB 28, 52 and 101, and dieldrin were quantified using a 63Ni micro μ-ECD (Agilent 6890 μ-ECD). The rest of the PCBs and pesticides were quantified, using a MS detector (Agilent 5975C; Agilent Technologies), which was operated by negative chemical ionization (NCI) in selected ion monitoring (SIM) mode. The target ions used were at m/z 71 (HCHs), 284 (HCB), 359 (oxychlordane), 410 (α-chlordane), 444 (trans-nonachlor), 318 (p,p'- DDE), 326 (PCB 118), 360 (PCB 138 and 153), 396 (PCB 180). Detection of BDEs and HBCD was performed on a HRGC–LRMS (Agilent 6890 Series; Agilent Technologies), equipped with an autosampler (Agilent 7683 Series; Agilent Technologies) and coupled to a MS detector (Agilent 5973 Network; Agilent Technologies) (Polder et al., 2014). The BDEs and HBCD were monitored using negative chemical ionization (NCI) in selected ion monitoring (SIM) mode at m/z 79/81. BDE 209 was monitored at m/z 484/486 and 13C12-BDE-209 at m/z 495/497.

The laboratory is accredited by the Norwegian Accreditation for testing the analyzed chemicals in biological material according to the requirements of the NS-EN ISO/IEC 17025 (TEST 137). The details of the analytical quality system have been described in (Polder et al., 2014). Briefly, every analytical series included three procedural blanks (solvents), one blind (non-spiked clean feed), two spiked samples of clean feed for recoveries and the laboratory's own reference materials (LRMs) of blubber of harp seal (*Pagophilus groenlandicus*). The lowest levels of detection (LODs) for individual compounds were defined as three times the noise level. Relative recoveries % were for HCB 96 %, HCHs 109-110%, p,p'- DDE 108%, dieldrin 125%, PCBs 95-102%, chlordanes 76-99%, BDEs 92-102% (BDE209 147%) and HBCD 240%. Positive consistent blanks in media were found for PCBs 118, 153, 138 and 180, (0.02, 0.18, 0.17 and 0.02 ng/g respectively), HCB (0.32) and for BDEs 47, 99 and 100 (0.04, 0,02 and 0,09 ng/g respectively). The results were corrected for these blanks. The quality control parameters were within the accepted ranges for the methods applied. The Analytical quality is regularly approved by routinely analyzing relevant Certified Reference Materials (CRM) such as mackerel oil (CRM 350) and by participation in relevant intercalibration tests such as the 2011 MOE Interlaboratory study for the Northern Contaminants Program (NCP) III — phase 6 on lake trout (Salvelinus namaycush) and brown trout (*Salmo trutta*) organized by the Ontario Ministry of the Environment, Laboratory Services Branch.

Supplementary Table 2. Concentrations reported for individual POPs in human brain samples from other studies and comparison with concentrations detected in the embryonic chicken brain in the present study.

Study References	*Compound*	*Concentration as reported in the studies (human samples)*	*[a]Maximum concentration in the chicken brain for POP mixture 10x in ng/g (present study)*	*[b]Maximum concentration from the pharmacokinetic fitted model in chicken brain for POP mixture 10x in ng/g (present study)*
PCBs		ng/g of lipid, max. detected*		
(Mitchell et al., 2012)	PCB 138	78.30	223	229
	PCB 153	85.87	364	365
	PCB 180	76.14	149	149
		µg/kg lipid		
(Dewailly et al., 1999)	PCB 118	38	47	49
	PCB 138	134	223	229
	PCB 153	198	364	365
	PCB 180	145	149	149
OCPs		µg/kg lipid		
(Dewailly et al., 1999)	*p,p'*-DDE	319	354	377
	HCB	260	50	58
PFASs		ng/g of tissue		
(Maestri et al., 2006)	PFOS	1.3	202	238
	PFOA	0.5	6	6
		Mean ng/g wet weight		
(Pérez et al., 2013)	PFOS	4.9	202	238
	PFHxS	3.2	21	22

*PCB 180 in neurotypical controls group (with no known neurodevelopmental abnormalities)
*PCB 138, PCB 153 in genetic neurodevelopmental disorders group (neurodevelopmental disorders with known genetic basis)
Abbreviations: PCB (polychlorinated biphenyls); OCP (organochlorine pesticides); PFASs (per- and polyfluoroalkyl substances)
a = represents the same values that are presented in Table 1 by LC-MS analysis
b = represents the same values (Cmax) that are presented in Table 2 by applying pharmacokinetic fitted model

Supplementary Table 3.Chemical concentrations of POP mixture in chicken embryo brain. Chicken embryos on E13 were exposed with a POP mixture containing 29 compounds resulting in a final concentration equivalent to 10x human blood levels in the egg. After 0.5, 1, 2, 4, 6, 24, 28 and 72 h exposure individual compounds were analyzed in embryonic brains. Measured concentrations represent the mean value (SEM% of the mean) of PFASs of three brains at each time point (n=3). These are the same values that were presented in Table 1A.

Compound POP mixture	***Detection limit***	***Time h***							
Mean pg/mg wet weight		0.5	1	2	4	6	24	48	72
PFASs									
PFHxS	0.50	nd	nd	nd	3.52 (7.38%)	8.60 (22.09%)	21.19 (14.25%)	20.64 (8.09%)	14.74 (5.73%)
PFOS	0.50	5.10 (5.68%)	1.54 (23.37%)	25.74 (13.63%)	77.57 (13.60%)	201.81 (12.57%)	190.89 (14.87%)	132.45 (6.07%)	83.18 (7.56%)
PFOA	0.50	0.15[#]	nd	nd	0.07 (28.57%)	0.72 (34.72%)	3.70 (29.45%)	5.79 (15.029%)	5.23 (9.57%)
PFNA	0.50	nd	nd	nd	0.93 (15.05%)	1.54 (13.63%)	2.70 (14.44%)	3.00 (16%)	1.66 (14.45%)
PFDA	0.50	nd	nd	nd	0.96 (18.75%)	2.02 (18.31%)	2.20 (10%)	2.62 (2.67%)	1.53 (6.53%)
PFUnDA	0.50	0.10 (20%)	0.05 (<0.01%)	0.67 (13.43%)	1.58 (8.23%)	3.48 (13.21%)	3.60 (11.38%)	4.26 (7.51%)	3.26 (9.50%)

*Limit of quantitation (LOQ): about 0.5 pg/mg, results were indicated below the LOQ when the chromatogram showed a distinct peak; [#]detected in only one sample

References:

BERNTSEN, H. F., BERG, V., THOMSEN, C., ROPSTAD, E. & ZIMMER, K. E. 2017. The design of an environmentally relevant mixture of persistent organic pollutants for use in in vivo and in vitro studies. *J Toxicol Environ Health A*, 1-15.

DEWAILLY, E., MULVAD, G., PEDERSEN, H. S., AYOTTE, P., DEMERS, A., WEBER, J. P. & HANSEN, J. C. 1999. Concentration of organochlorines in human brain, liver, and adipose tissue autopsy samples from Greenland. *Environ Health Perspect,* 107**,** 823-8.

MAESTRI, L., NEGRI, S., FERRARI, M., GHITTORI, S., FABRIS, F., DANESINO, P. & IMBRIANI, M. 2006. Determination of perfluorooctanoic acid and perfluorooctanesulfonate in human tissues by liquid chromatography/single quadrupole mass spectrometry. *Rapid Commun Mass Spectrom,* 20**,** 2728-34.

MITCHELL, M. M., WOODS, R., CHI, L. H., SCHMIDT, R. J., PESSAH, I. N., KOSTYNIAK, P. J. & LASALLE, J. M. 2012. Levels of select PCB and PBDE congeners in human postmortem brain reveal possible environmental involvement in 15q11-q13 duplication autism spectrum disorder. *Environ Mol Mutagen,* 53**,** 589-98.

PÉREZ, F., NADAL, M., NAVARRO-ORTEGA, A., FÀBREGA, F., DOMINGO, J. L., BARCELÓ, D. & FARRÉ, M. 2013. Accumulation of perfluoroalkyl substances in human tissues. *Environment International,* 59**,** 354-362.

POLDER, A., MÜLLER, M. B., LYCHE, J. L., MDEGELA, R. H., NONGA, H. E., MABIKI, F. P., MBISE, T. J., SKAARE, J. U., SANDVIK, M., SKJERVE, E. & LIE, E. 2014. Levels and patterns of persistent organic pollutants (POPs) in tilapia (Oreochromis sp.) from four different lakes in Tanzania: Geographical differences and implications for human health. *Science of The Total Environment,* 488-489**,** 252-260.

PAPER IV

Exposure to a Human Relevant Mixture of Persistent Organic Pollutants (POPs) or to Perfluorooctane Sulfonic Acid (PFOS) Alone Dysregulates the Developing Cerebellum of Chicken Embryo

Ajay Yadav[1,2], Steven Verhaegen[1], Panagiotis Filis[3], Diana Domanska[4], Robert Lyle[5,6], Arvind Y.M. Sundaram[5], Magnus Leithaug[5], Gunn Charlotte Østby[1], Mona Aleksandersen[7], Hanne Friis Berntsen[1,8], Karin Elisabeth Zimmer[7], Paul A. Fowler[3], Ragnhild Elisabeth Paulsen[2], Erik Ropstad[1*]

[1]Department of Production Animal Clinical Sciences, Norwegian University of Life Sciences, P.O. Box 369 Sentrum, NO-0102, Oslo, Norway

[2]Section for Pharmacology and Pharmaceutical Biosciences, Department of Pharmacy, University of Oslo, P.O. Box 1068, Blindern, NO-0316 Oslo, Norway

[3] Institute of Medical Sciences, School of Medicine, Medical Sciences & Nutrition, University of Aberdeen, Foresterhill, Aberdeen AB25 2ZD, UK

[4]Department of Pathology, Institute of Clinical Medicine, University of Oslo, Oslo, Norway

[5]Department of Medical Genetics, Oslo University Hospital and University of Oslo, Oslo, Norway

[6]Centre for Fertility and Health, Norwegian Institute of Public Health, Oslo, Norway

[7]Department of Preclinical Sciences and Pathology, Norwegian University of Life Sciences, P.O. Box 369 Sentrum, NO-0102, Oslo, Norway

[8]National Institute of Occupational Health, P.O. Box 5330 Majorstuen, NO-0304, Oslo, Norway

*Corresponding author: Prof. Erik Ropstad, erik.ropstad@nmbu.no

Abstract

Prenatal exposure to POPs is associated with neurodevelopmental disorders. In the present study, we explored whether a human-relevant POP mixture affects the development of the chicken embryo cerebellum. We used a defined mixture of 29 POPs, at human-relevant concentrations. We also evaluated exposure to a prominent compound in the mixture, perfluorooctane sulfonic acid (PFOS), alone. Embryos were exposed by injection directly into the allantois at embryonic day 13 (E13). Cerebella were isolated at E17 and subjected to morphological, RNA-seq and shot-gun proteomics analyses. There was up to 19% thinning of the molecular layer in both exposure scenarios. Exposure to the POP mixture significantly affected expression of 65 of 13,800 transcripts, and 43 of 2,568 proteins, when compared to solvent control. PFOS alone affected expression of 80 of 13,859 transcripts, and 69 of 2,555 proteins. Twenty-five genes and 15 proteins were common for both exposure groups. These point to alterations in molecular events linked to retinoid X receptor (RXR) signalling, neuronal cell proliferation and migration, cellular stress responses including unfolded protein response, lipid metabolism, and myelination. Exposure to the POP mixture increased methionine oxidation, whereas PFOS decreased oxidation. Several of the altered genes and proteins are involved in a wide variety of neurological disorders. We conclude that POP exposure can interfere with fundamental aspects of neurodevelopment, altering molecular pathways that are associated with adverse neurocognitive and behavioural outcomes.

Keywords:

Chicken embryo; Environmental chemicals; Neurodevelopment; Prenatal exposure; Proteomics; RNA-seq transcriptomics

1. Introduction:

Exposure to man-made chemicals, together with other factors, including nutrition, stress, and gene-environment interactions, are suspected as underlying causes for the rise in neurodevelopmental impairments, such as attention deficit hyperactivity disorder (ADHD), autism spectrum disorders (ASD), and cognitive impairment (Grandjean et al., 2017). Environmental contaminants tend to bio-magnify in food chains and, consequently, diet is a major route of lifelong exposures. Mother-child transfer during pregnancy and lactation results in perinatal exposure of the developing infant. This may impair neurodevelopmental processes, which could affect brain structures and functions, leading to lifelong behavioural and cognitive impairments (Rice and Barone, 2000, Grandjean and Landrigan, 2014, Sunyer and Dadvand, 2019) associated with huge societal costs (Bellanger et al., 2015).

Several studies in cultured neuronal cells have reported that exposure to persistent organic pollutants (POPs) can induce oxidative stress as a mechanism of toxicity (Chen et al., 2010, Costa et al., 2007, Mariussen, 2012, Mariussen et al., 2002). Similarly, exposure to a POP mixture led to up-regulation of genes related to the antioxidant defence in cultured rat CGNs, also indicating mixture toxicity involves oxidative stress (Berntsen et al., 2020). In animal studies exposure to POPs induces oxidative stress in the brain tissues of rats (Hassoun et al., 2000, Hassoun et al., 2002). POPs at low levels commonly present in the environment are found to be associated with increased oxidative stress in healthy humans from a general population (Kumar et al., 2014).

The migration of neurons in a developing brain is modulated by N-methyl-D-aspartate receptor (NMDA-R) mediated Ca^{2+} influx, where the GluN2B subunits are especially important (Komuro and Rakic, 1993, Llansola et al., 2005). This takes place prenatally before hatching in chickens and to a large extent postnatally in some mammals, including humans. Alterations in migration could be indicative of impaired neurodevelopment (Bjornstad et al.,

2015). For example, prenatal exposure to toxicants interfered with the development of CGNs and disturbed the morphology of the cerebellum in mice and chicken (Mathisen et al., 2013).

The cerebellum is a well-conserved structure between species (Sultan and Glickstein, 2007). The developing chicken embryo has been used as a model to study cerebellar development after exposure to POPs (Berntsen et al., 2020, Yadav et al., 2021b), various pharmaceuticals (Aden et al., 2008, Austdal et al., 2016) and environmental toxicants (Mathisen et al., 2013). In addition to its role in motor control and coordination, the cerebellum is involved in learning and memory, language and executive functioning (O'Halloran et al., 2012).

We have previously designed an environmentally relevant mixture of persistent organic pollutants, containing 29 different chlorinated, brominated, and perfluorinated substances (Berntsen et al., 2017). The mixture contains POPs at concentrations based on those measured in human blood in Scandinavia, and provides a defined and realistic mixture of environmental contaminants for toxicity studies (Berntsen et al., 2017). Perfluorooctanesulfonic acid (PFOS) is the compound with the highest concentration in the POP mixture and is a potent developmental neurotoxicant. In our previous studies the exposure with this POP mixture, or PFOS alone, has affected NMDA-R signalling and downstream Ca^{2+}-influx, glutathione levels, and excitotoxicity in cultured chicken CGNs (Yadav et al., 2021b). Prenatal exposure to a POP mixture of similar composition in mice and PFOS exposure *in ovo* in chicken affect NR2B protein expression in cerebellum, indicating a developmental disruption caused by POP exposure (Berntsen et al., 2020). Following maternal mouse exposure to this POP mixture, POPs were detected in the offspring's brains, which also showed brain function-related gene expression changes (Myhre et al., 2021). Exposure to this POP mixture in the allantoic fluid led to human-relevant exposure levels of POPs in the developing chicken brain (Yadav et. al. under review). In addition, the same POP mixture had adverse effects on neuronal cell function

and development in differentiating human neural stem cells and PC12 cells (Davidsen et al., 2021, Yadav et al., 2021a). Associations between POP exposure and neurodevelopmental effects have also been reported in human epidemiological studies. For example, in a multi-pollutant analysis of 27 POPs in a Norwegian birth cohort study, early-life exposure to β-hexachlorocyclohexane (β-HCH) and PFOS was associated with increased risk of ADHD (Lenters et al., 2019). Further, Sagiv et al. (2015) reported associations of prenatal exposure to polybrominated diphenyl ethers (PBDEs) with poorer attention and executive function, measured with parent report and direct neuropsychological testing of the child. Among the perfluoroalkyl acid (PFAA) compounds present in the mixture, PFOS was the most potent in terms of NMDA-receptor mediated toxicity in cultured rat CGNs (Berntsen et al., 2018).

Based on the role of NMDA receptors in cerebellar development described above we predicted that exposure to a mixture of POPs and PFOS (as a single compound with a concentration, which overlaps the concentration of the POP mixture) at human-relevant composition and concentrations would alter the morphology of cerebellum in developing chicken embryo. We expected changes in molecules related to the NMDA receptor pathway and down-stream effects, such as altered Ca^{2+} homeostasis, as well as glutathione and antioxidant defences. Since NMDA excitotoxicity leads to increased ROS formation, we expect higher levels of protein oxidation. Finally, findings from the RNA-seq and proteome study can give insight in novel mechanisms for disturbed neurodevelopment and provide links to adverse neurobehavioral outcomes.

2. *Material and methods*

2.1. POP mixture and PFOS

The POP mixture was designed and prepared at the Norwegian University of Life Sciences (NMBU), Oslo, Norway (Berntsen et al., 2017). The mixture contained 29 different compounds (Supplementary Table 1), including six PFAAs (perfluorohexanesulfonic acid (PFHxS), PFOS, PFOA, perfluorononanoic acid (PFNA), perfluorodecanoic acid (PFDA), and perfluoroundecanoic acid (PFUnDA)); seven brominated (Br) compounds (PBDE 47, PBDE 99, PBDE 100, PBDE 153, PBDE 154, PBDE 209, and hexabromocyclododecane (HBCD)); and sixteen chlorinated (Cl) compounds (PCB 28, PCB 52, PCB 101, PCB 118, PCB 138, PCB 153, PCB 180, *p,p'*-dichlorodiphenyldichloroethylene (DDE), hexachlorobenzene (HCB), α-chlordane, oxychlordane, *trans*-nonachlor, α-hexachlorocyclohexane (HCH), β-HCH, γ-HCH (lindane) and dieldrin). The compounds were selected from their respective compound groups based on prevalence in blood, breastmilk and/or food, and their relative concentrations based on Scandinavian human blood levels. The stocks used in the present study had a concentration of 10^6 times blood levels in DMSO and were stored in glass vials at -80°C (Berntsen et al., 2017)

Perfluorooctanesulfonic acid potassium salt (PFOS ≥ 98%) was obtained from Sigma-Aldrich (St Louis, MO, USA). All other reagents were standard laboratory grade.

It should be noted that in the present study we exposed chicken embryo with POP mixture at 10x (human blood levels) or PFOS alone at 0.4 μM, a similar concentration as present in the POP mixture.

Animals

Eggs (*Gallus gallus*, weight 50-55 g, fertilized) were obtained from Nortura Samvirkekylling (Våler, Norway) and incubated at 37.5°C in 45% relative humidity in an

OvaEasy 380 Advance EXII Incubator (Brinsea,Weston-super-Mare, UK). Sex determination of embryos was not performed. Prior to injection, eggs were weighed, and the POP mixture was diluted in 0.9% saline. On E13, eggs were trans-illuminated with a LED lamp (Brinsea) to visualize spontaneous movements confirming living embryos. For injection, the POP mixture or PFOS stock was diluted 1/100 in saline. This solution was injected into each egg (1 µl saline solution/gram egg weight). Injection was performed through the CAM into the allantois with a 29-gauge needle. Injection was guided by trans-illumination with the LED lamp to avoid injecting into blood vessels. This resulted in a final exposure concentration of POP mixture at 10x (times) human blood levels compounds and PFOS 0.4 µM, assuming uniform distribution of the compounds throughout all compartments of the egg. On E17 the embryos were anesthetised by hypothermia by submerging the eggs in crushed ice for 7 min, hatched, and immediately decapitated. The whole brains or cerebella were isolated with a spatula and the meninges were removed with forceps. The brains or cerebella were snap-frozen in liquid nitrogen and stored at -80 °C until further processing. Animals were handled in accordance with the Norwegian Animal Welfare Act and the EU directive 2010/63/EU, and the study was approved by the Norwegian Food Safety Authority (application ID: FOTS 13896). The exposure scenario is shown in Figure 1.

2.2. Brain weight and Histology

The embryos were sacrificed at E17 and the brains were removed and weighed. Brains for histology were collected as described by (Austdal et al., 2016). The sculls of chicken embryos prepared for histology were opened along the cranial sutures and whole heads were fixed for 24 h in 10% buffered formalin (VWR Chemicals). After fixation, the brains were divided in the coronary plane, and the dorsal part were routinely processed and embedded in paraffin.

Tissue blocks were trimmed until at least three cerebellar lobuli were visible and sections of 3 mm thickness were cut, mounted, and stained with haematoxylin and eosin.

Histological slides were examined blindly by a board-certified veterinary pathologist. Photomicrographs of cerebellar lobuli were taken (Figure 2.) and image analysis were done using ImageJ (NIH, Bethesda, MD, USA). Quantifications of cerebellar cortical layers were performed, and only optimally oriented slides were included. Thickness of external granular layer (EGL), molecular layer (ML) and internal granular layer (IGL) were measured in five locations per slide.

2.3. RNA extraction and RNA sequencing transcriptomic analyses

RNA from cerebella was extracted following Qiagen miRNeasy mini Protocol. Gene expression (RNA-seq) was carried out at the Department of Medical Genetics (Oslo University Hospital) and Norwegian Sequencing Centre (Oslo University Hospital). RNA-seq libraries were preparated using TruSeq stranded RNA-prep (Illumina, USA) following manufacturer's protocol. 96 libraries were pooled together, and 75 bp paired end sequencing were performed on a single HiSeq 3/4000 (Illumina, USA) run. Raw data from the sequencer was demultiplexed using bcl2fastq v2.20.0.422. Low quality reads were trimmed/removed along with any reads mapping to the PhiX spike-in used during sequencing using BBDuk (2021) (part of BBMap v34.56). Cleaned reads were mapped to the Chicken genome (ENSEMBL GRCg6a) using HISAT V2.1.0 (parameter:rna-strandness RF) (Kim et al., 2019). Resulting sam files were handled using samtools v1.2.

2.4. Protein extraction and proteomics analysis

Protein expression measured by label-free LC-MS-detection based proteomics was carried out during at the Aberdeen Proteomics facility. Protein from cerebellar tissues was extracted

using Qiagen AllPrep kits (#80004, Qiagen, Manchester, UK), following manufacturer's instructions. Briefly, whole cerebella were lysed using appropriate amounts of RLT buffer (600 µL per 30 mg of tissue). 600 µL of lysate were processed to protein pellets, dissolved in 100 µL of resuspension buffer (6.8 M Urea, 2 M thiourea, 20 mM dithiothreitol, and 0.1% w/v Rapigest detergent), and stored at −80 °C until further analysis.

Tissue proteins were identified and quantified using a Q Exactive Plus hybrid quadrupole Orbitrap mass spectrometer fitted with an EASY-Spray nano-ESI source (Thermo Scientific) as detailed in (Filis et al., 2018, Siemienowicz et al., 2019). Briefly,10 µg of tissue proteins was diluted to a final volume of 100 µL in 50 mM NH_4HCO_3 (BioUltra grade, Sigma Aldrich). Proteins were digested in solution according to the PRIME-XS protocol and reduced by using 2 mM dithiothreitol (Sigma Aldrich, > 99%) for 25 min at 60 °C and S-xalkylated in 4 mM iodoacetamide (Sigma Aldrich, > 99%) for 30 min at 25 °C in the dark, then digested by sequencing-grade modified trypsin (Promega, Southampton, UK, cat.no. V5111) at a 1:10 ratio of trypsin:protein overnight at 37 °C. The reaction was stopped by freezing at − 80 °C. Then samples were thawed and dried by vacuum centrifugation (SpeedVac Plus SC110A, Savant), and dissolved in 10 µL 2% acetonitrile/0.1% formic acid. The equivalent of 2 µg of peptides (assuming no losses) were analysed by liquid chromatography-tandem mass spectrometry (LC-MS/MS).

Raw mass spectrophotometric output files were processed by MaxQuant (v 1.5.3.30) (Cox and Mann, 2008). MaxQuant runs were performed under the default parameters except that trypsin was set as the digestion enzyme and matching between runs was enabled. All peptide searches were performed against all the Refseq proteins retrieved from NCBI. Protein intensities across samples were normalized using the maxLFQ algorithm (Cox et al., 2014).

2.5. Statistical analysis

Each exposure group consisted of 7-8 individual eggs per group for transcriptomics, 8 individual eggs per group for proteomics, and 9 samples per group for brain weight and histological analysis.

The thickness of the external granular layer, the molecular and internal granular layers showed a satisfactory fit to the normal distribution and were analysed by a mixed model where exposure group and the individual were included as independent variables. Exposure group was entered as a fixed effect and the individual as a random effect. Differences between exposure groups were assessed using the Tukey HSD test. Comparison of brain weights between exposure groups was analysed by ANOVA followed by a Tukey HSD test.

The raw gene counts were used for downstream transcriptomic analyses. Genes were filtered, normalised and differential expression was performed using the default parameters of *edgeR* package in R v3.5.1. The normalised protein intensities and the site occupancies for methionine oxidation were used for the downstream proteomic analyses. Only proteins and site occupancies with 75% of valid values across the samples compared were used for differential expression analysis. The *limma* package in R v3.5.1 was used for statistical comparisons.

3. Results

3.1. Effect of POP mixture or PFOS on brain weight and histopathological changes

We observed no significant alteration of brain weight in chicken embryos exposed to POP mixture or PFOS. Results are summarized in Supplementary Table 2. Microscopic examination did not show strong visual histopathological changes for either the POP mixture, or the PFOS exposure. However, quantitative image analysis revealed that the ML was significantly thinner following exposure to the POP mixture, and PFOS alone compared to the control group. The thickness of the EGL and IGL were unaffected by either exposure (Fig 2, Table 1).

3.2. Expression profile of genes and proteins after exposure to POP mixture

After quality filtering, a total of 13,800 transcripts were compared between the control and POP mixture exposure groups (Supplementary data 1). Using $P<0.05$ and log2 fold change $>\pm 0.7$ (equivalent to ±1.6 fold) cut-offs, the POP mixture affected expression of a total 65 transcripts (Figure 3 and Supplementary data 1). Similarly, a total of 2,568 proteins were compared between the control and POP mixture exposure groups (Supplementary data 2). Using $P<0.05$ and log2 fold change $>\pm 0.7$ (equivalent to ±1.6 fold) cut-offs, POP mixture affected expression of a total 43 proteins (Figure 3 and Supplementary data 2). No common elements were identified in both the gene and protein set (Figure 4). However, several identified genes and proteins often described a common pathway or process. Thus, transcriptional regulators were affected at the level of genes (*HES5*, *ZBTB32*), as well as proteins (PBX1, ZNF423, EIF2B2). Similarly, the insulin-signalling pathway was also affected at gene (*IGF-I*, *CCN3*) and protein level (IGFBP7). In addition, members of the RXR signalling pathway were affected (*RXRG*, *RDH10,* RBP4). Growth factor genes including *VEGFD*, *BMP3* were modulated. Several myelination-related genes were found to be down-regulated (*CDH19, PLP1, PLLP*). Several cell surface transporters genes were affected (*ABCB11*, *SLC1A2*,

SLC6A4, *SLC27A6*). Protein levels for ANXA1, a membrane-localized protein that binds phospholipids and has anti-inflammatory activity and multiple roles in cell proliferation, differentiation, and migration was found downregulated. Indeed, many systems involved in cell survival and death, and cellular stress responses were affected: regulators of cell cycle and apoptosis (CCAR1, DAD1); the unfolded protein response and ubiquitination (*CHAC1*, *CA4*, *SCRG-1*, UBE2D3, NACAD); protection against DNA damage and apoptosis (FAM168A); and mitochondrial health (OPA1).

Genes related to cellular trafficking were affected, including chemokine receptors (*ACKR4, S100A12*) and regulators immune cell infiltration (*AvBD1, LECT2*). The neuronal cell adhesion gene *IMPG1* was up-regulated, whereas *DCX*, a marker of migrating and immature neurons (*DCX*) was found to be down-regulated.

System controlling cellular architecture were affected. For example, a gene coding for a member of the superfamily of intermediate filament proteins was down-regulated (*KRT40*). Proteins controlling neuronal cytoskeletal stability (TPM1, RMDN1) and axon formation (CDH13, NAA25) were affected, as well as a component of the linker of nucleoskeleton and cytoskeleton complex, SYNE1.

In addition, neurotransmitter receptors were found to be modulated (*GABPR*, *CHRNA9*). *CNGA3*, a marker for synaptic plasticity was upregulated. A number of channel related genes were affected. The ion channel *PKD2L2* gene was upregulated whereas the potassium voltage-gated channel subfamily gene *KCNQ2* was down-regulated. The gene for the receptor for arginine vasotocin, *AVPR2* was up-regulated.

The plasma lipoprotein APOH was found downregulated. Golgi-lipoprotein transporter (MIA3), and a cholesterol transfer protein that regulates Golgi structure and function (OSBLPL1) were modulated. A protein HCAD2 related to fatty acid metabolism was down-regulated.

Two haemoglobin-related proteins were found downregulated (HBZ, HBBR). SRSF7 (spliceosome) was upregulated. Protein level of an enzyme that catalyses branched-chain amino acids (BCAT1) was found downregulated.

Some genes and proteins not previously described in brain context were down-regulated (*TMEM125, SCEL, MAEL,* SYCP2).

3.3. Expression profile of genes and proteins after exposure to PFOS

After quality filtering, a total of 13,859 transcripts were compared between the control and PFOS exposure groups (Supplementary data 3). Using $P<0.05$ and log2 fold change $>\pm 0.7$ (equivalent to ±1.6 fold) cut-offs, PFOS affected expression of a total 80 transcripts (Figure 3 and Supplementary data 3). Among others, PFOS exposure affected 25 genes that were common with POP mixture exposure (Figure 4 and Table 2). Similarly, a total of 2,555 proteins were compared between the control and PFOS exposure groups (Supplementary data 4). Using $P<0.05$ and log2 fold change $>\pm 0.7$ (equivalent to ±1.6 fold) cut-offs, PFOS affected expression of a total 69 proteins (Figure 3 and Supplementary data 4). Among others, PFOS exposure affected 15 proteins that were common with POP mixture (Figure 4 and Table 3).

In addition to genes and proteins in common with POP mixture, the following were also strongly affected by PFOS exposure. The transcriptional regulators *SIX6* and *ZBTB20* were downregulated. Two genes for small nucleolar RNAs, *SNORD14* and *SNORD79,* were up-regulated. Membrane transporters (*SLC38A4, SLC35D5*) were found to be affected. Genes related to sodium-voltage regulated channel (*SCN4B*), potassium Voltage-gated channel subfamily member (*KCNQ1*) and the myelin marker (*MBP*) were down-regulated. In addition, the ten strongest up-regulated proteins included a nuclear receptor binding protein (NRBP1), the cytoskeletal component beta-actin (ACTB), a mitochondrial inner membrane transport molecule (TIMM23B), the solute carrier protein SLC27A4 involved in fatty acid transport, a

311 neuroprotective transcription factor (ADNP), and LIN7A, a molecule involved in correct
312 localization of NMDA-R subunits. Among the bottom ten down-regulated transcripts we report
313 the non-receptor phosphatase PTPN12, mitochondrial 3-hydroxyisobutyrate dehydrogenase
314 enzyme HIBADH), co-chaperone with mitochondrial function (DNAJA1), an acyl-CoA
315 dehydrogenase involved in fatty acid metabolism ACADSB, and the vacuolar protein sorting
316 member (VPS11).
317
318 ***3.4. Protein oxidation after exposure to POP mixture or PFOS***
319 The POP mixture exposure group showed a trend for increased oxidation ratios.
320 Amongst 213 peptides that were oxidized on a methionine residue, 33 showed significantly
321 increased oxidation ratios ($p < 0.05$ and log2 fold change $\geq \pm 0.7$) when compared with control
322 (Figure 3 and Supplementary data 5). Those altered oxidised peptide ratios are derived from
323 different sites, the blood (e.g. ALB, HBA), the cytosol (e.g. ARHGDIA), and are also in the
324 nucleus (e.g. Histone H2B) and cytoskeleton (e.g. VIM, TUBA4A).
325 In the PFOS exposure group there was a trend of decreased methionine oxidation ratio.
326 Amongst 166 peptides oxidised on a methionine residue, 21 showed significantly decreased
327 oxidized ratios ($p < 0.05$ and log2 fold change $\geq \pm 0.7$), (Figure 3 and Supplementary data 6).
328 Those altered oxidised ratios were not derived from blood proteins and there are almost no
329 proteins from the nucleus. Many of them are cytoskeletal e.g. tubulin (TUBB2B, TUBB3,
330 TUBB2B) or actin (ACTC1, ACTC2).
331

4. Discussion

It is thought that POPs reaching the fetal brain can interfere with neurodevelopmental processes and cause developmental neurotoxicity (DNT). Our results indicate that either exposure to the POP mixture or PFOS alone elicited alterations in a common set of genes and proteins involved in pathways and processes resulting in dysregulation of normal CNS development as illustrated in Fig. 5.

Our histological analysis revealed thinning of the ML in cerebellum after POP exposure. This ML thinning could well be due to the observed dysregulation of genes and proteins involved in proliferative and/or migratory pathways. For example, *IGF-1* and *VEFG-D*, are modulators of migration of interneurons in different layers of cerebellum. *DCX* has also been reported to be strongly expressed by neurons in the cerebellum during periods of migration, and mutations in the human gene cause a disruption of cortical neuronal migration (Freemyer et al., 2019, Gleeson et al., 1999).

NMDA-R is important for neural stem cell proliferation and differentiation (Chakraborty et al., 2017), establishment or elimination of synapses and migration of neurons (Komuro and Rakic, 1993). Exposure to POPs induces excitotoxicity in cultured chicken CGNs via either a Ca^{2+}-dependent or independent NMDA-R pathway (Yadav et al., 2021b). In the present data set no significant changes in glutamate ionotropic NMDA-Rs or subunit types were observed. However, *VEGF-D*, is a ligand for the VEGF receptor VEGFR-2 (Flk1) (Achen et al., 1998) and in complexing with NMDAR subunits can enhance Ca^{2+} influx in immature granular cells before synapse formation (Meissirel et al., 2011). *IGF-1* has also been reported to alleviate NMDA-induced neurotoxicity through the IGF-AKT-mTor pathway in microglia (Riikonen, 2016). We also found changes in RMDN1, a paralog of RMDN3 which is involved in calcium homeostasis (Fecher et al., 2019). This indicates that POP exposure affected

regulators of the NMDA-R systems and calcium signalling, and thus could modulate excitotoxicity.

Our POP mixture reduced GSH levels in chicken CGNs in culture (Yadav et al., 2021b), however the genes and proteins in our data set do not point strongly to changes in GSH metabolism or antioxidant defence systems, in discordance with our expectations. However, our proteomics analysis revealed increased methionine oxidation of peptides following exposure to the POP mixture. This oxidation is an abundant non-enzymatic post-translational modification which is indicative of oxidative stress and can act as a removal mechanism for cellular ROS, preventing the irreversible oxidation of other biomolecules (Walker et al., 2019). Cytosolic as well as nuclear proteins were affected. In addition, oxidised proteins from blood (e.g. ALB, HBA) were detected. This is suggestive of an organism-wide increase in oxidative stress. Strikingly, the PFOS only exposure led to decreased methionine oxidation. Since the concentration used for PFOS was equivalent to the one present in the total POP mixture, PFOS alone cannot mimic the effect of the full mixture, in accordance with previous *in vitro* studies using chicken CGNs and rat PC12 cells (Yadav et al., 2021a, Yadav et al., 2021b). We suggest that compounds other than PFOS present in the POP mixture may be responsible for stimulating methionine protein oxidation. For instance, PBDE congeners (PBDE-47, PBDE-99, PBDE-100, PBDE-153, and PBDE-209) which are also present in our POP mixture, can induce oxidative stress (Huang et al., 2010).

Oxidation of proteins will lead to unfolded and/or misfolded proteins and this can cause ER stress, a condition where the accumulation of unfolded and misfolded proteins takes place in the ER lumen. This results in activation of the unfolded protein response (UPR) and ubiquitination process. Indeed, our data set included several important components of pathways related to ER stress, unfolded protein response or ubiquitination, such as *CHAC*1, *CA4,* UBE2D3, *ZBT32* and NACAD. The *CHAC*1 enzyme acts as an inhibitor of Notch signalling

that promotes embryonic neurogenesis (Chi et al., 2012). *CHAC1* degrades glutathione and is associated with ER stress and apoptosis pathways (Perra et al., 2018). As well as being a component of the unfolded protein response (UPR) pathway, *CHAC1* is also a probable substrate-recognition component of an E3 ubiquitin-protein ligase complex which mediates the ubiquitination and subsequent proteasomal degradation of target proteins (Furukawa et al., 2003). Furthermore, *ZBTB32* is involved in the control of autophagy related proteins (Zhang et al., 2015) and autophagy is an important intracellular catabolic mechanism involved in the removal of misfolded proteins. In different wildlife species exposure to POPs led to genotoxic effects (DNA damage) (González-Mille et al., 2019). In our dataset we found UBE2D3 and FAM168A associated with DNA damage, thus it is conceivable that exposure to the POP chemicals might lead to direct or indirect DNA damage, for example through generation of reactive oxygen or nitrogen species.

Both increased oxidative stress and altered calcium homeostasis due to ER stress can cause mitochondrial dysfunction (Chaudhari et al., 2014), leading to lowered mitochondrial transmembrane potentials and rapid loss of mitochondrial function (Wüllner et al., 1999). In *vitro* studies using the same POP mixture or different PFAS exposures, including PFOS revealed changes in mitochondrial mass and mitochondrial membrane potentials in several non-neuronal cell systems (Shannon et al., 2019, Wilson et al., 2016a), so a similar effect in neuronal cells cannot be excluded. Indeed, in the present analysis following exposure to either POP mixture or PFOS alone, we found alterations in OPA1 and *HEBP2* which are related to mitochondrial health.

In addition to the above targets linked to known modes of actions of POPs, we also identified novel networks affected by POP exposure. These include transcription factors and their regulators (PBX1, *RXRG*, *HES5*, *CHAC1*) with known roles in the cerebellum. As a pioneer transcription factor, PBX1 is particularly well-suited to initiate cell fate changes

406 (Grebbin and Schulte, 2017), conferring regional identity in the embryo. It also increases
407 expression of the neuroprotective gene Nfe2L1. A PBX1 transcriptional network controls
408 dopaminergic neuron development and is impaired in Parkinson's disease (Villaescusa et al.,
409 2016). Thus, POP exposure can affect central regulators of neuroprotective mechanisms
410 thereby interfering with processes protecting against DNT.

411 RXRs are ligand-activated transcription factors that play a central role in early
412 embryonic morphogenetic patterning, inflammation and the immune system, and the
413 physiology of the CNS (Mey, 2017). Thus, we placed it as top-regulatory mechanism in our
414 schematic overview in Fig. 5. The presence of RXRG and two additional entities RBP4A and
415 *RDH10* in our data set suggests that POP exposure might affect retinoid acid receptor
416 FRAR/RXR signalling. *RXR-G* acts as a positive regulator of endogenous oligodendrocyte
417 precursor cell differentiation and CNS remyelination (Huang et al., 2011). Despite its up-
418 regulation, several genes or proteins that regulates myelin forming cells (oligodendrocyte) or
419 myelination were down-regulated. This might be explained by the observed up-regulation of
420 the transcription factor *HES5*, a negative regulator of myelin gene expression. Indeed, Liu et
421 al. (2006) reported up-regulated myelin gene expression in *HES5* knock-out mice compared to
422 wild-type siblings. *CDH19* is a marker for myelin-producing cells. Interestingly, *CDH19* is
423 expressed both in Schwann cells (in the peripheral nervous system) and oligodendrocytes (in
424 the brain) in the chicken embryo throughout development, suggesting that *CDH19* is
425 selectively expressed by myelin-forming cells and might play a role in myelin formation (Lin
426 et al., 2010). Myelin proteolipid *PLP1* is the major structural protein maintaining the
427 compaction of CNS myelin sheaths. In *PLP1* deletion patients, myelin sheaths showed splitting
428 and decompaction of myelin (Laukka et al., 2016). In the PLP-null (mice) CNS, axons large
429 enough to be myelinated often lacked myelin entirely or were surrounded by abnormally thin
430 sheaths (Rosenbluth et al., 2006). Plasmolipin (*PLLP*) is a plasma membrane proteolipid and a

major myelin membrane component in the vertebrate nervous system and is detected in developing rat cerebellum (Sapirstein et al., 1992). This however requires further histological and immunohistochemical confirmation.

Excess prenatal glucocorticoid stimulation disturbs normal development of the cerebellum in the chicken embryo model (Austdal et al., 2016). The present exposures did not lead to changes in glucocorticoid receptor (GR) levels. However, ANXA1 a gene transcriptionally regulated by GR was down-regulated. ANXA1 is a potent endogenous, broad-spectrum anti-inflammatory effector (Zub et al., 2019), suggesting POP exposure might facilitate inflammatory responses. When tested in a GR translocation assay *in vitro* the POP mixture did not affect GR transactivation *in vitro,* although the individual POPs, *p,p`*-DDE, PFOS, PFDA and PBDE 47 modulate GR activity (Wilson et al., 2016b). However, *in vivo*, a similar POP mixture affected the stress response as measured by corticosterone level, in female mice and their offspring (Hudecova et al., 2018). Ligated RARα/RXR can interact with ligated GR, resulting in an enhanced transcriptional activity of the GR (Tóth et al., 2011). Our observation that POP exposure up-regulate *RXR-G* provides a new mechanism for the dysregulation of the glucocorticoid axis. Indeed, a dexamethasone-responsive gene, *SCRG1* (Ochi et al., 2006) was also down-regulated. This gene is involved in maintenance of pluripotency (Ochi et al., 2006) and autophagy and has also been linked with neurodegenerative diseases (Dron et al., 2006, López-Pérez et al., 2020).

Maturation of the BBB in chick embryos occurs from E13 onwards (Wakai and Hirokawa, 1978). Following injection of the POP mixture, 27 of 29 of the individual compounds could be detected in the developing brain between E13 and E16 (Yadav et al, under review). ANXA1 is expressed on BBB endothelial cells during human fetal development, supporting a role for the protein in prenatal brain development (McArthur et al., 2016). *ANXA1*$^{-/-}$mice exhibited an increase in permeability of the blood brain barrier (Purvis et al.,

2019). In our experiments, ANXA1 expression decreases, suggesting that POP exposure might negatively be affecting the integrity of the BBB. However, *VEGF-D*, a mitogenic for endothelial cells (Achen et al., 1998) was up-regulated, whereas *BMP3* a regulator of pericytes (Lei et al., 2017) was down-regulated. *CA4*, a gene located on the luminal surface of cerebral capillaries, and a regulator of carbon dioxide and bicarbonate homeostasis (Halmi et al., 2006) was down-regulated. This suggests POP exposure can affect development of brain vascularisation, as well as function and integrity of the BBB at several levels.

Finally, POP exposure affected genes or proteins related to cytokines and their receptors, and regulators of inflammation and immune cell infiltration such as *SELE*, *CCN3*, ANXA1, *AvBD1*, *LECT-2*, *IGF-1*, *EPX*. Currently, we cannot distinguish whether this indicates alteration of normal neuroimmunological development or if POP exposure elicits an inflammatory response.

5. Conclusion

Our study showed that exposure to a POP mixture or PFOS led to morphological changes in cerebellar development, with plausible linkage to some affected pathways. Both exposures affected similar biological and molecular pathways that are involved in several key neurodevelopmental processes. However, some exposure effects were different with regards to protein oxidation: the POP mixture leading to increased protein oxidation whereas PFOS decreased protein oxidation. The genes or proteins affected by POP exposures are involved in several neurological disorders (summarized in Table 5). These include molecules involved in GABAergic and serotonergic neurotransmitter systems which have a primary function in some cognitive processes (Myhrer, 2003). The present study provides a possible mechanistic explanation for the epidemiological associations between POP exposure and adverse neurodevelopmental and cognitive outcomes.

Acknowledgements

This project has received funding from the European Union's Horizon 2020 research and innovation program under the Marie Skłodowska-Curie grant agreement No. 722634 (http://protected.eu.com/). The authors gratefully acknowledge the Proteomics Core Facility of the University of Aberdeen for their support & assistance in this work.

References

ACHEN, M. G., JELTSCH, M., KUKK, E., MÄKINEN, T., VITALI, A., WILKS, A. F., ALITALO, K. & STACKER, S. A. 1998. Vascular endothelial growth factor D (VEGF-D) is a ligand for the tyrosine kinases VEGF receptor 2 (Flk1) and VEGF receptor 3 (Flt4). *Proc Natl Acad Sci U S A,* 95**,** 548-53.

ADEN, P., GOVERUD, I., LIESTOL, K., LOBERG, E. M., PAULSEN, R. E., MAEHLEN, J. & LOMO, J. 2008. Low-potency glucocorticoid hydrocortisone has similar neurotoxic effects as high-potency glucocorticoid dexamethasone on neurons in the immature chicken cerebellum. *Brain Res,* 1236**,** 39-48.

AUSTDAL, L. P., BJORNSTAD, S., MATHISEN, G. H., ADEN, P. K., MIKKOLA, I., PAULSEN, R. E. & RAKKESTAD, K. E. 2016. Glucocorticoid Effects on Cerebellar Development in a Chicken Embryo Model: Exploring Changes in PAX6 and Metalloproteinase-9 After Exposure to Dexamethasone. *J Neuroendocrinol,* 28.

BBDUK 2021. https://sourceforge.net/projects/bbmap/.

BELLANGER, M., DEMENEIX, B., GRANDJEAN, P., ZOELLER, R. T. & TRASANDE, L. 2015. Neurobehavioral deficits, diseases, and associated costs of exposure to endocrine-disrupting chemicals in the European Union. *J Clin Endocrinol Metab,* 100**,** 1256-66.

BERNTSEN, H. F., BERG, V., THOMSEN, C., ROPSTAD, E. & ZIMMER, K. E. 2017. The design of an environmentally relevant mixture of persistent organic pollutants for use in in vivo and in vitro studies. *J Toxicol Environ Health A***,** 1-15.

BERNTSEN, H. F., BJORKLUND, C. G., STRANDABO, R., HAUG, T. M., MOLDES-ANAYA, A., FUENTES-LAZARO, J., VERHAEGEN, S., PAULSEN, R. E., TASKER, R. A. & ROPSTAD, E. 2018. PFOS-induced excitotoxicity is dependent on Ca(2+) influx via NMDA receptors in rat cerebellar granule neurons. *Toxicol Appl Pharmacol,* 357**,** 19-32.

BERNTSEN, H. F., DUALE, N., BJØRKLUND, C. G., RANGEL-HUERTA, O. D., DYRBERG, K., HOFER, T., RAKKESTAD, K. E., ØSTBY, G., HALSNE, R., BOGE, G., PAULSEN, R. E., MYHRE, O. & ROPSTAD, E. 2020. Effects of a human-based mixture of persistent organic pollutants on the in vivo exposed cerebellum and cerebellar neuronal cultures exposed in vitro. *Environ Int,* 146**,** 106240.

BJORNSTAD, S., AUSTDAL, L. P., ROALD, B., GLOVER, J. C. & PAULSEN, R. E. 2015. Cracking the Egg: Potential of the Developing Chicken as a Model System for Nonclinical Safety Studies of Pharmaceuticals. *J Pharmacol Exp Ther,* 355**,** 386-96.

BLANDINA, P., PROVENSI, G., PASSSANI, M. B., CAPASSO, C. & SUPURAN, C. T. 2020. Carbonic anhydrase modulation of emotional memory. Implications for the treatment of cognitive disorders. *J Enzyme Inhib Med Chem,* 35**,** 1206-1214.

BOND, A. M., BHALALA, O. G. & KESSLER, J. A. 2012. The dynamic role of bone morphogenetic proteins in neural stem cell fate and maturation. *Developmental neurobiology,* 72**,** 1068-1084.

CHAKRABORTY, A., MURPHY, S. & COLEMAN, N. 2017. The Role of NMDA Receptors in Neural Stem Cell Proliferation and Differentiation. *Stem Cells and Development,* 26**,** 798-807.

CHAUDHARI, N., TALWAR, P., PARIMISETTY, A., LEFEBVRE D'HELLENCOURT, C. & RAVANAN, P. 2014. A Molecular Web: Endoplasmic Reticulum Stress, Inflammation, and Oxidative Stress. *Frontiers in Cellular Neuroscience,* 8.

CHEN, J., LIUFU, C., SUN, W., SUN, X. & CHEN, D. 2010. Assessment of the neurotoxic mechanisms of decabrominated diphenyl ether (PBDE-209) in primary cultured neonatal rat hippocampal neurons includes alterations in second messenger signaling and oxidative stress. *Toxicology Letters,* 192**,** 431-439.

COSTA, L. G., FATTORI, V., GIORDANO, G. & VITALONE, A. 2007. An in vitro approach to assess the toxicity of certain food contaminants: methylmercury and polychlorinated biphenyls. *Toxicology,* 237**,** 65-76.

COX, J., HEIN, M. Y., LUBER, C. A., PARON, I., NAGARAJ, N. & MANN, M. 2014. Accurate proteome-wide label-free quantification by delayed normalization and maximal peptide ratio extraction, termed MaxLFQ. *Mol Cell Proteomics,* 13**,** 2513-26.

COX, J. & MANN, M. 2008. MaxQuant enables high peptide identification rates, individualized p.p.b.-range mass accuracies and proteome-wide protein quantification. *Nat Biotechnol,* 26**,** 1367-72.

DANDOY-DRON, F., GRIFFOND, B., MISHAL, Z., TOVEY, M. G. & DRON, M. 2003. Scrg1, a novel protein of the CNS is targeted to the large dense-core vesicles in neuronal cells. *Eur J Neurosci,* 18**,** 2449-59.

DAVIDSEN, N., LAUVÅS, A. J., MYHRE, O., ROPSTAD, E., CARPI, D., GYVES, E. M.-D., BERNTSEN, H. F., DIRVEN, H., PAULSEN, R. E., BAL-PRICE, A. & PISTOLLATO, F. 2021. Exposure to human relevant mixtures of halogenated persistent organic pollutants (POPs) alters neurodevelopmental processes in human neural stem cells undergoing differentiation. *Reproductive Toxicology,* 100**,** 17-34.

DRON, M., BAILLY, Y., BERINGUE, V., HAEBERLÉ, A.-M. & GRIFFOND, B. 2006. SCRG1, a Potential Marker of Autophagy in TSE. *Autophagy,* 2**,** 58-60.

DRON, M., BAILLY, Y., BERINGUE, V., HAEBERLÉ, A.-M., GRIFFOND, B., RISOLD, P.-Y., TOVEY, M. G., LAUDE, H. & DANDOY-DRON, F. 2005. Scrg1 is induced in TSE and brain injuries, and associated with autophagy. *European Journal of Neuroscience,* 22**,** 133-146.

FECHER, C., TROVÒ, L., MÜLLER, S. A., SNAIDERO, N., WETTMARSHAUSEN, J., HEINK, S., ORTIZ, O., WAGNER, I., KÜHN, R., HARTMANN, J., KARL, R. M., KONNERTH, A., KORN, T., WURST, W., MERKLER, D., LICHTENTHALER, S. F., PEROCCHI, F. & MISGELD, T. 2019. Cell-type-specific profiling of brain mitochondria reveals functional and molecular diversity. *Nature Neuroscience,* 22**,** 1731-1742.

FILIS, P., HOMBACH-KLONISCH, S., AYOTTE, P., NAGRATH, N., SOFFIENTINI, U., KLONISCH, T., O'SHAUGHNESSY, P. & FOWLER, P. A. 2018. Maternal smoking and high BMI disrupt thyroid gland development. *BMC Med,* 16**,** 194.

FREEMYER, A., NEAL, C., NELSON-BRANTLEY, J., STAECKER, H. & DURHAM, D. 2019. Early Onset Region and Cell Specific Alterations of Doublecortin Expression in the CNS of Animals with Sound Damage Induced Hearing Loss. *IBRO reports,* 7**,** 129-140.

GLEESON, J. G., LIN, P. T., FLANAGAN, L. A. & WALSH, C. A. 1999. Doublecortin Is a Microtubule-Associated Protein and Is Expressed Widely by Migrating Neurons. *Neuron,* 23**,** 257-271.

GONZÁLEZ-MILLE, D. J., ILIZALITURRI-HERNÁNDEZ, C. A., ESPINOSA-REYES, G., CRUZ-SANTIAGO, O., CUEVAS-DÍAZ, M. D. C., MARTÍN DEL CAMPO, C. C. & FLORES-RAMÍREZ, R. 2019. DNA damage in different wildlife species exposed to persistent organic pollutants (POPs) from the delta of the Coatzacoalcos river, Mexico. *Ecotoxicol Environ Saf,* 180**,** 403-411.

GRANDJEAN, P., KISHI, R. & KOGEVINAS, M. 2017. Prevention of Developmental Neurotoxicity. *Epidemiology,* 28**,** 157-158.

GRANDJEAN, P. & LANDRIGAN, P. J. 2014. Neurobehavioural effects of developmental toxicity. *Lancet Neurol,* 13**,** 330-8.

GREBBIN, B. M. & SCHULTE, D. 2017. PBX1 as Pioneer Factor: A Case Still Open. *Frontiers in cell and developmental biology,* 5**,** 9-9.

HALMI, P., PARKKILA, S. & HONKANIEMI, J. 2006. Expression of carbonic anhydrases II, IV, VII, VIII and XII in rat brain after kainic acid induced status epilepticus. *Neurochemistry International,* 48**,** 24-30.

HASSOUN, E. A., LI, F., ABUSHABAN, A. & STOHS, S. J. 2000. The relative abilities of TCDD and its congeners to induce oxidative stress in the hepatic and brain tissues of rats after subchronic exposure. *Toxicology,* 145**,** 103-113.

HASSOUN, E. A., WANG, H., ABUSHABAN, A. & STOHS, S. J. 2002. INDUCTION OF OXIDATIVE STRESS IN THE TISSUES OF RATS AFTER CHRONIC EXPOSURE TO TCDD, 2,3,4,7,8-

585 PENTACHLORODIBENZOFURAN, AND 3,3',4,4',5-PENTACHLOROBIPHENYL. *Journal of*
586 *Toxicology and Environmental Health, Part A,* 65**,** 825-842.
587 HENTRICH, T., WASSOUF, Z., EHRHARDT, C., HAAS, E., MILLS, J. D., ARONICA, E., OUTEIRO, T. F.,
588 HÜBENER-SCHMID, J., RIESS, O., CASADEI, N. & SCHULZE-HENTRICH, J. M. 2020. Increased
589 expression of myelin-associated genes in frontal cortex of SNCA overexpressing rats and
590 Parkinson's disease patients. *Aging (Albany NY),* 12**,** 18889-18906.
591 HUANG, S. C., GIORDANO, G. & COSTA, L. G. 2010. Comparative cytotoxicity and intracellular
592 accumulation of five polybrominated diphenyl ether congeners in mouse cerebellar granule
593 neurons. *Toxicol Sci,* 114**,** 124-32.
594 HUDECOVA, A. M., HANSEN, K. E. A., MANDAL, S., BERNTSEN, H. F., KHEZRI, A., BALE, T. L., FRASER, T.
595 W. K., ZIMMER, K. E. & ROPSTAD, E. 2018. A human exposure based mixture of persistent
596 organic pollutants affects the stress response in female mice and their offspring.
597 *Chemosphere,* 197**,** 585-593.
598 KIM, D., PAGGI, J. M., PARK, C., BENNETT, C. & SALZBERG, S. L. 2019. Graph-based genome alignment
599 and genotyping with HISAT2 and HISAT-genotype. *Nature Biotechnology,* 37**,** 907-915.
600 KIM, S. H., SHIM, K. S. & LUBEC, G. 2002. Human brain nascent polypeptide-associated complex alpha
601 subunit is decreased in patients with Alzheimer' s disease and Down syndrome. *J Investig Med,*
602 50**,** 293-301.
603 KOMURO, H. & RAKIC, P. 1993. Modulation of neuronal migration by NMDA receptors. *Science,* 260**,**
604 95-7.
605 KUMAR, J., MONICA LIND, P., SALIHOVIC, S., VAN BAVEL, B., LIND, L. & INGELSSON, E. 2014. Influence
606 of persistent organic pollutants on oxidative stress in population-based samples.
607 *Chemosphere,* 114**,** 303-309.
608 LANG, U. E., PULS, I., MULLER, D. J., STRUTZ-SEEBOHM, N. & GALLINAT, J. 2007. Molecular mechanisms
609 of schizophrenia. *Cell Physiol Biochem,* 20**,** 687-702.
610 LAUKKA, J. J., KAMHOLZ, J., BESSERT, D. & SKOFF, R. P. 2016. Novel pathologic findings in patients with
611 Pelizaeus-Merzbacher disease. *Neurosci Lett,* 627**,** 222-32.
612 LENTERS, V., ISZATT, N., FORNS, J., ČECHOVÁ, E., KOČAN, A., LEGLER, J., LEONARDS, P., STIGUM, H. &
613 EGGESBØ, M. 2019. Early-life exposure to persistent organic pollutants (OCPs, PBDEs, PCBs,
614 PFASs) and attention-deficit/hyperactivity disorder: A multi-pollutant analysis of a Norwegian
615 birth cohort. *Environment International,* 125**,** 33-42.
616 LIN, J., LUO, J. & REDIES, C. 2010. Cadherin-19 expression is restricted to myelin-forming cells in the
617 chicken embryo. *Neuroscience,* 165**,** 168-178.
618 LIU, A., LI, J., MARIN-HUSSTEGE, M., KAGEYAMA, R., FAN, Y., GELINAS, C. & CASACCIA-BONNEFIL, P.
619 2006. A molecular insight of Hes5-dependent inhibition of myelin gene expression: old
620 partners and new players. *Embo j,* 25**,** 4833-42.
621 LLANSOLA, M., SANCHEZ-PEREZ, A., CAULI, O. & FELIPO, V. 2005. Modulation of NMDA receptors in
622 the cerebellum. 1. Properties of the NMDA receptor that modulate its function. *Cerebellum,*
623 4**,** 154-61.
624 LÓPEZ-PÉREZ, Ó., BADIOLA, J. J., BOLEA, R., FERRER, I., LLORENS, F. & MARTÍN-BURRIEL, I. 2020. An
625 Update on Autophagy in Prion Diseases. *Frontiers in Bioengineering and Biotechnology,* 8.
626 MA, D. Q., WHITEHEAD, P. L., MENOLD, M. M., MARTIN, E. R., ASHLEY-KOCH, A. E., MEI, H., RITCHIE,
627 M. D., DELONG, G. R., ABRAMSON, R. K., WRIGHT, H. H., CUCCARO, M. L., HUSSMAN, J. P.,
628 GILBERT, J. R. & PERICAK-VANCE, M. A. 2005. Identification of Significant Association and
629 Gene-Gene Interaction of GABA Receptor Subunit Genes in Autism. *The American Journal of*
630 *Human Genetics,* 77**,** 377-388.
631 MARIUSSEN, E. 2012. Neurotoxic effects of perfluoroalkylated compounds: mechanisms of action and
632 environmental relevance. *Arch Toxicol,* 86**,** 1349-67.
633 MARIUSSEN, E., MYHRE, O., REISTAD, T. & FONNUM, F. 2002. The polychlorinated biphenyl mixture
634 aroclor 1254 induces death of rat cerebellar granule cells: the involvement of the N-methyl-
635 D-aspartate receptor and reactive oxygen species. *Toxicol Appl Pharmacol,* 179**,** 137-44.

MATHISEN, G. H., YAZDANI, M., RAKKESTAD, K. E., ADEN, P. K., BODIN, J., SAMUELSEN, M., NYGAARD, U. C., GOVERUD, I. L., GAARDER, M., LOBERG, E. M., BOLLING, A. K., BECHER, R. & PAULSEN, R. E. 2013. Prenatal exposure to bisphenol A interferes with the development of cerebellar granule neurons in mice and chicken. *Int J Dev Neurosci,* 31**,** 762-9.

MCARTHUR, S., LOIOLA, R. A., MAGGIOLI, E., ERREDE, M., VIRGINTINO, D. & SOLITO, E. 2016. The restorative role of annexin A1 at the blood–brain barrier. *Fluids and Barriers of the CNS,* 13**,** 17.

MEISSIREL, C., RUIZ DE ALMODOVAR, C., KNEVELS, E., COULON, C., CHOUNLAMOUNTRI, N., SEGURA, I., DE ROSSI, P., VINCKIER, S., ANTHONIS, K., DELÉGLISE, B., DE MOL, M., ALI, C., DASSONVILLE, K., LOYENS, E., HONNORAT, J., MICHOTTE, Y., ROGEMOND, V., SMOLDERS, I., VOETS, T., VIVIEN, D., VANDEN BERGHE, P., VAN DEN BOSCH, L., ROBBERECHT, W., CHÉDOTAL, A., OLIVIERO, S., DEWERCHIN, M., SCHMUCKER, D., THOMASSET, N., SALIN, P. & CARMELIET, P. 2011. VEGF modulates NMDA receptors activity in cerebellar granule cells through Src-family kinases before synapse formation. *Proceedings of the National Academy of Sciences,* 108**,** 13782.

MEY, J. 2017. RAR/RXR-Mediated Signaling. *Gene Regulation, Epigenetics and Hormone Signaling.*

MYHRE, O., ZIMMER, K. E., HUDECOVA, A. M., HANSEN, K. E. A., KHEZRI, A., BERNTSEN, H. F., BERG, V., LYCHE, J. L., MANDAL, S., DUALE, N. & ROPSTAD, E. 2021. Maternal exposure to a human based mixture of persistent organic pollutants (POPs) affect gene expression related to brain function in mice offspring hippocampus. *Chemosphere,* 276**,** 130123.

MYHRER, T. 2003. Neurotransmitter systems involved in learning and memory in the rat: a meta-analysis based on studies of four behavioral tasks. *Brain Res Brain Res Rev,* 41**,** 268-87.

O'HALLORAN, C. J., KINSELLA, G. J. & STOREY, E. 2012. The cerebellum and neuropsychological functioning: a critical review. *J Clin Exp Neuropsychol,* 34**,** 35-56.

OCHI, K., DERFOUL, A. & TUAN, R. S. 2006. A predominantly articular cartilage-associated gene, SCRG1, is induced by glucocorticoid and stimulates chondrogenesis in vitro. *Osteoarthritis and Cartilage,* 14**,** 30-38.

PURVIS, G. S. D., SOLITO, E. & THIEMERMANN, C. 2019. Annexin-A1: Therapeutic Potential in Microvascular Disease. *Frontiers in Immunology,* 10.

REN, H., GUAN, L., ZHAO, L., LIN, Y., WANG, Y., YANG, Z., LI, X., MA, X., CHENG, X., DENG, W., AITCHISON, K. J., CAO, L. & LI, T. 2018. Contribution of genes in the GABAergic pathway to bipolar disorder and its executive function deficit in the Chinese Han population. *American Journal of Medical Genetics Part B: Neuropsychiatric Genetics,* 177**,** 50-67.

RICE, D. & BARONE, S., JR. 2000. Critical periods of vulnerability for the developing nervous system: evidence from humans and animal models. *Environ Health Perspect,* 108 Suppl 3**,** 511-33.

RIIKONEN, R. 2016. Treatment of autistic spectrum disorder with insulin-like growth factors. *European Journal of Paediatric Neurology,* 20**,** 816-823.

ROSENBLUTH, J., NAVE, K. A., MIERZWA, A. & SCHIFF, R. 2006. Subtle myelin defects in PLP-null mice. *Glia,* 54**,** 172-82.

SAGIV, S. K., KOGUT, K., GASPAR, F. W., GUNIER, R. B., HARLEY, K. G., PARRA, K., VILLASEÑOR, D., BRADMAN, A., HOLLAND, N. & ESKENAZI, B. 2015. Prenatal and childhood polybrominated diphenyl ether (PBDE) exposure and attention and executive function at 9-12 years of age. *Neurotoxicol Teratol,* 52**,** 151-61.

SHANNON, M., XIE, Y., VERHAEGEN, S., WILSON, J., BERNTSEN, H. F., ZIMMER, K. E., ROPSTAD, E., GREEN, B. D. & CONNOLLY, L. 2019. A Human Relevant Defined Mixture of Persistent Organic Pollutants (POPs) Affects In Vitro Secretion of Glucagon-Like Peptide 1 (GLP-1), but Does Not Affect Translocation of Its Receptor. *Toxicol Sci,* 172**,** 359-367.

SIEMIENOWICZ, K. J., FILIS, P., SHAW, S., DOUGLAS, A., THOMAS, J., MULROY, S., HOWIE, F., FOWLER, P. A., DUNCAN, W. C. & RAE, M. T. 2019. Fetal androgen exposure is a determinant of adult male metabolic health. *Sci Rep,* 9**,** 20195.

SULTAN, F. & GLICKSTEIN, M. 2007. The cerebellum: Comparative and animal studies. *Cerebellum,* 6**,** 168-76.

SUNYER, J. & DADVAND, P. 2019. Pre-natal brain development as a target for urban air pollution. *Basic & Clinical Pharmacology & Toxicology,* 125**,** 81-88.

TÓTH, K., SARANG, Z., SCHOLTZ, B., BRÁZDA, P., GHYSELINCK, N., CHAMBON, P., FÉSÜS, L. & SZONDY, Z. 2011. Retinoids enhance glucocorticoid-induced apoptosis of T cells by facilitating glucocorticoid receptor-mediated transcription. *Cell Death & Differentiation,* 18**,** 783-792.

VAN DER MEER, D., HOEKSTRA, P. J., BRALTEN, J., VAN DONKELAAR, M., HESLENFELD, D. J., OOSTERLAAN, J., FARAONE, S. V., FRANKE, B., BUITELAAR, J. K. & HARTMAN, C. A. 2016. Interplay between stress response genes associated with attention-deficit hyperactivity disorder and brain volume. *Genes Brain Behav,* 15**,** 627-36.

VILLAESCUSA, J. C., LI, B., TOLEDO, E. M., RIVETTI DI VAL CERVO, P., YANG, S., STOTT, S. R., KAISER, K., ISLAM, S., GYLLBORG, D., LAGUNA-GOYA, R., LANDREH, M., LÖNNERBERG, P., FALK, A., BERGMAN, T., BARKER, R. A., LINNARSSON, S., SELLERI, L. & ARENAS, E. 2016. A PBX1 transcriptional network controls dopaminergic neuron development and is impaired in Parkinson's disease. *The EMBO journal,* 35**,** 1963-1978.

WAKAI, S. & HIROKAWA, N. 1978. Development of the blood-brain barrier to horseradish peroxidase in the chick embryo. *Cell Tissue Res,* 195**,** 195-203.

WALKER, E. J., BETTINGER, J. Q., WELLE, K. A., HRYHORENKO, J. R. & GHAEMMAGHAMI, S. 2019. Global analysis of methionine oxidation provides a census of folding stabilities for the human proteome. *Proceedings of the National Academy of Sciences,* 116**,** 6081.

WILSON, J., BERNTSEN, H. F., ZIMMER, K. E., FRIZZELL, C., VERHAEGEN, S., ROPSTAD, E. & CONNOLLY, L. 2016a. Effects of defined mixtures of persistent organic pollutants (POPs) on multiple cellular responses in the human hepatocarcinoma cell line, HepG2, using high content analysis screening. *Toxicol Appl Pharmacol,* 294**,** 21-31.

WILSON, J., BERNTSEN, H. F., ZIMMER, K. E., VERHAEGEN, S., FRIZZELL, C., ROPSTAD, E. & CONNOLLY, L. 2016b. Do persistent organic pollutants interact with the stress response? Individual compounds, and their mixtures, interaction with the glucocorticoid receptor. *Toxicol Lett,* 241**,** 121-32.

WÜLLNER, U., SEYFRIED, J., GROSCURTH, P., BEINROTH, S., WINTER, S., GLEICHMANN, M., HENEKA, M., LÖSCHMANN, P. A., SCHULZ, J. B., WELLER, M. & KLOCKGETHER, T. 1999. Glutathione depletion and neuronal cell death: the role of reactive oxygen intermediates and mitochondrial function. *Brain Research,* 826**,** 53-62.

YADAV, A., AMBER, M., ZOSEN, D., LABBA, N. A., HUIBERTS, E. H. W., SAMULIN ERDEM, J., HAUGEN, F., BERNTSEN, H. F., ZIENOLDDINY, S., PAULSEN, R. E., ROPSTAD, E., CONNOLLY, L. & VERHAEGEN, S. 2021a. A human relevant mixture of persistent organic pollutants (POPs) and perfluorooctane sulfonic acid (PFOS) enhance nerve growth factor (NGF)-induced neurite outgrowth in PC12 cells. *Toxicol Lett,* 338**,** 85-96.

YADAV, A., VERHAEGEN, S., VERBRUGGEN, E., KERHOAS, M., WILLEMIJN HUIBERTS, E. H., HADERA, M. G., BERNTSEN, H. F., ZIMMER, K. E., ROPSTAD, E. & PAULSEN, R. E. 2021b. A human relevant mixture of persistent organic pollutants (POPs) and perfluorooctane sulfonic acid (PFOS) differentially affect glutamate induced excitotoxic responses in chicken cerebellum granule neurons (CGNs) in vitro. *Reprod Toxicol,* 100**,** 109-119.

ZHOU, F. C., XU, Y., BLEDSOE, S., LIN, R. & KELLEY, M. R. 1996. Serotonin transporter antibodies: production, characterization, and localization in the brain. *Molecular Brain Research,* 43**,** 267-278.

ZOLEZZI, J. M., SANTOS, M. J., BASTÍAS-CANDIA, S., PINTO, C., GODOY, J. A. & INESTROSA, N. C. 2017. PPARs in the central nervous system: roles in neurodegeneration and neuroinflammation. *Biol Rev Camb Philos Soc,* 92**,** 2046-2069.

ZUB, E., CANET, G., GARBELLI, R., BLAQUIERE, M., ROSSINI, L., PASTORI, C., SHEIKH, M., REUTELINGSPERGER, C., KLEMENT, W., DE BOCK, F., AUDINAT, E., GIVALOIS, L., SOLITO, E. &

737 MARCHI, N. 2019. The GR-ANXA1 pathway is a pathological player and a candidate target in
738 epilepsy. *The FASEB Journal,* 33**,** 13998-14009.

739

740 ***Figure Legends:***

741 **Figure 1.** POP mixture (29 compounds) or PFOS was administrated by injection through CAM
742 into the allantois at embryonic day (E) 13. At E17 after administration, the whole brain or
743 cerebellum was isolated and study of changes in the transcriptome and proteome in developing
744 cerebellum was performed. The effects of POPs on developmental changes in whole brain
745 weight and cerebellar morphology were also explored.

746

747 **Figure 2.** Photomicrographs of chicken cerebellum at embryonic day (E) 17.

748 a. The whole cerebellum with its lobuli is shown. Hematoxylin and eosin-stained section.
749 Ce; cerebellum. 25x

750 b. Part of a cerebellar lobuli with the different cortical layers is shown. Hematoxylin and
751 eosin-stained section. Egl; external granular layer, ml; molecular layer, igl; internal
752 granular layer. 100x.

753

754 **Figure 3.** Proportion of down-regulated and up-regulated genes or proteins. Significant
755 differently expressed genes or proteins ($p<0.05$ and with a log2 fold change $>\pm0.7$) are
756 represented by jittered dots: blue = down-regulated and red = up-regulated. Violin plot
757 represents significant log2 fold change score. DMSO vs POP mixture 10x RNA-seq, DMSO
758 vs PFOS proteomics, DMSO vs PFOS RNA-seq, DMSO vs PFOS proteomics, DMSO vs POP
759 mixture 10x protein oxidation and DMSO vs PFOS Protein oxidation

760

761 **Figure 4.** Venn diagrams showing the number (percentage) of significantly differentially
762 expressed genes or proteins in chicken cerebella following exposure to POP mixture or PFOS.
763 Within either the POP mixture exposure or the PFOS exposure, no commonality was found
764 between genes and proteins. However, within the RNAseq set, twenty-five common gene

765 transcripts were found between the POP mixture and PFOS exposure. Similarly, within the
766 proteomics set, 15 common proteins were found between the POP mixture and PFOS exposure.
767
768 **Figure 5.** Overview of biological pathways and processes affected by exposure to POP mixture
769 or PFOS alone. Exposure to environmental toxicants has been associated with adverse
770 neurodevelopmental outcomes (light grey curved arrow). Developing chicken cerebella
771 exposed to POP mixture or PFOS alone showed alterations in morphology and protein
772 oxidation. Also, expression of a set of common genes and proteins. These signalling pathways
773 and biochemical functions are schematized above. Several of these pathways and processes are
774 interlinked (arrows). Specific examples of these genes and proteins are listed in **Table 4**, as
775 well as additional supportive observations in other studies (number in stars). A number of these
776 genes and proteins have been shown to be involved in a wide variety of neurological disorders
777 (references in **Table 5**). This provides possible causal mechanistic understanding between
778 exposure to environmental pollutants and adverse developmental neurotoxicity (DNT)
779 outcomes, strengthening the existing associative epidemiological links.
780
781

782 **Figure 1.**

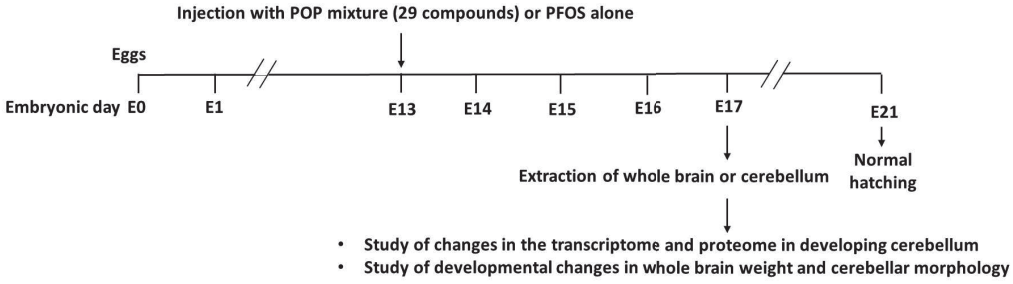

783

784

785 **Figure 2**.

786

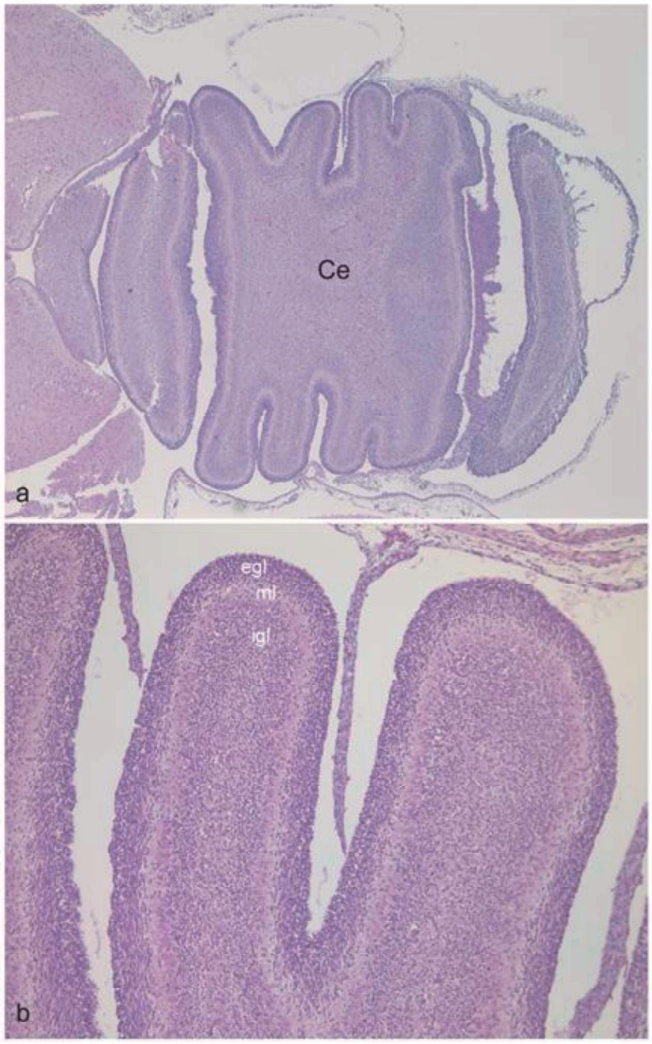

807

808

Figure 3.

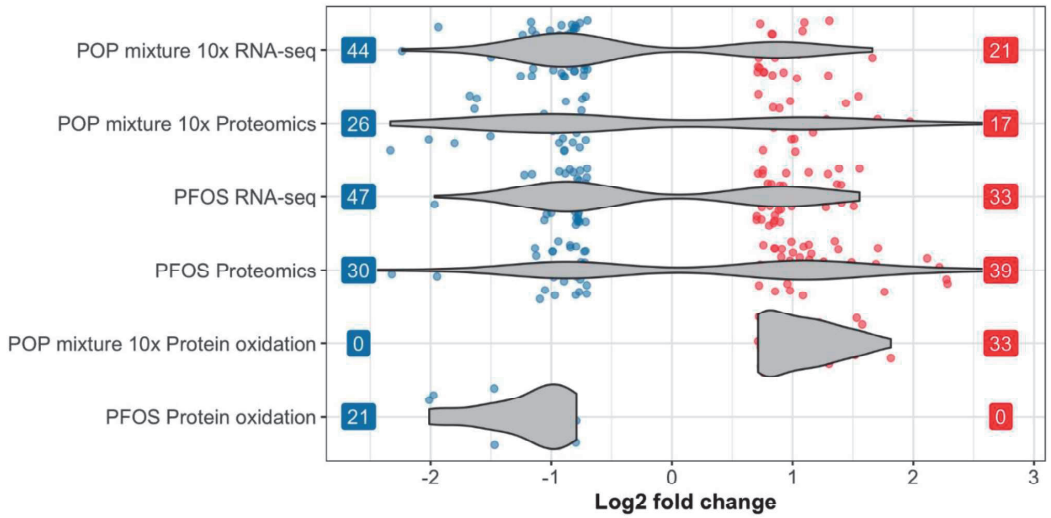
POP mixture 10x RNA-seq
POP mixture 10x Proteomics
PFOS RNA-seq
PFOS Proteomics
POP mixture 10x Protein oxidation
PFOS Protein oxidation
44
21
26
17
47
33
30
39
0
33
21
0
-2
-1
0
1
2
3
Log2 fold change

Figure 4.

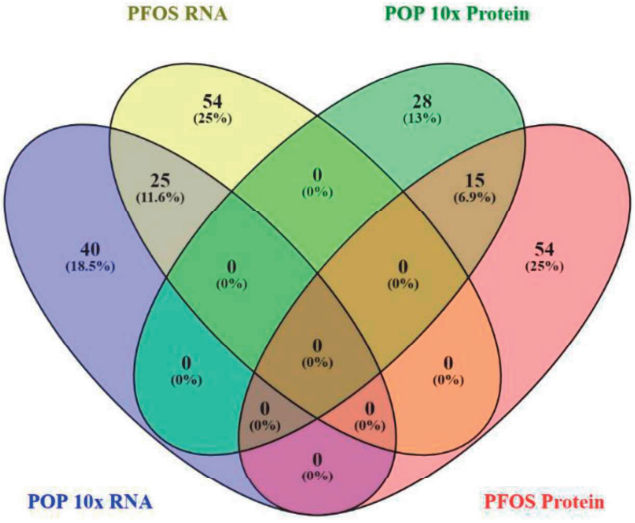
PFOS RNA
POP 10x Protein
54
(25%)
28
(13%)
25
(11.6%)
0
(0%)
15
(6.9%)
40
(18.5%)
0
(0%)
0
(0%)
54
(25%)
0
(0%)
0
(0%)
0
(0%)
0
(0%)
0
(0%)
0
(0%)
POP 10x RNA
PFOS Protein

Figure 5.

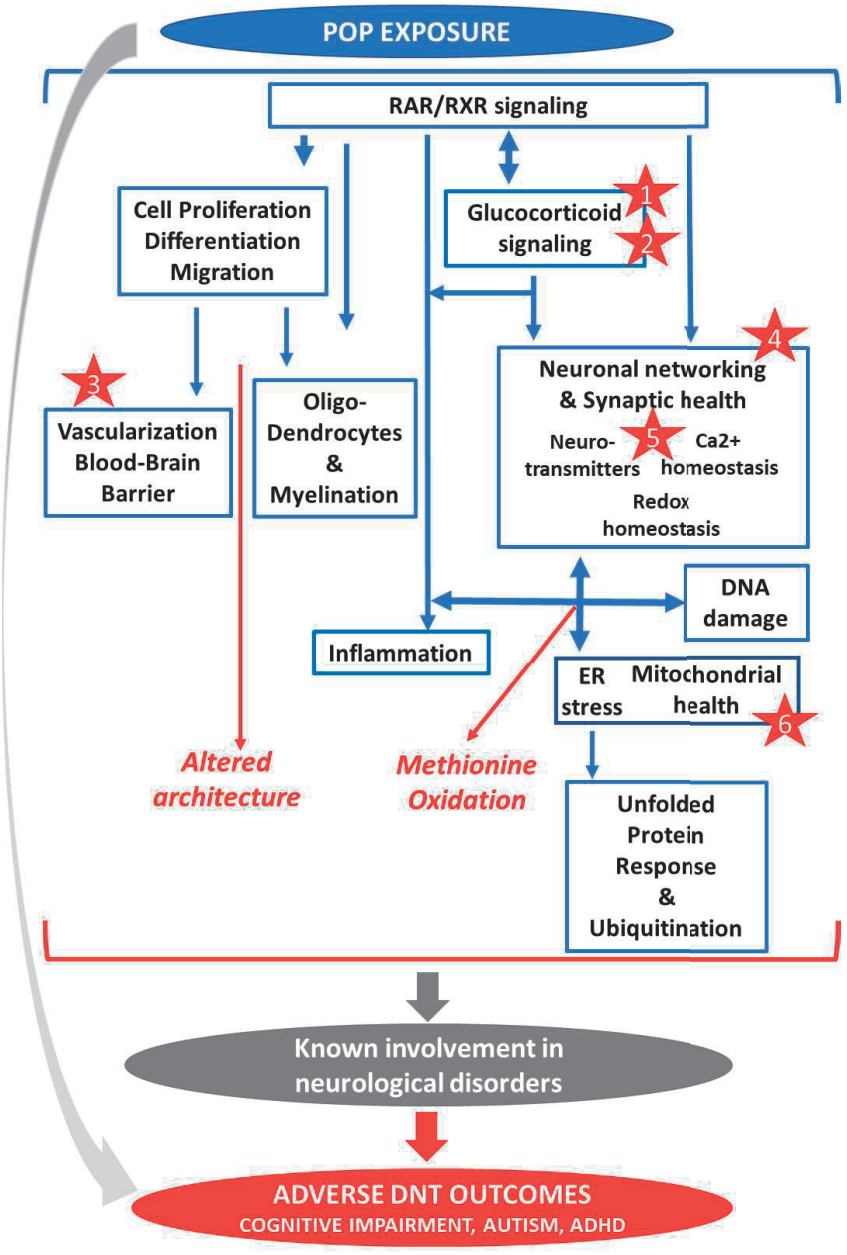
POP EXPOSURE
RAR/RXR signaling
Cell Proliferation
Differentiation
Migration
Glucocorticoid signaling
1
2
3
Vascularization
Blood-Brain
Barrier
Oligo-
Dendrocytes
&
Myelination
4
Neuronal networking
& Synaptic health
Neuro-
transmitters
5
Ca2+
homeostasis
Redox
homeostasis
DNA
damage
Inflammation
ER
stress
Mitochondrial
health
6
Altered
architecture
Methionine
Oxidation
Unfolded
Protein
Response
&
Ubiquitination
Known involvement in
neurological disorders
ADVERSE DNT OUTCOMES
COGNITIVE IMPAIRMENT, AUTISM, ADHD

820 **Table 1.** Effect of exposures on thickness of the respective cellular layers in cerebellum of
821 developing chicken embryos. Cerebellar layers thickness was analysed in a mixed model with
822 exposure group as a fixed effect and the individual as a random factor. Data shown are Least
823 squares (LS) means in mm with standard errors and 95% confidence limits (CL) based on 5
824 repeated measurements of each layer per individual. A. Exposures to POP mixture and PFOS
825 compared to control. Here the concentration of PFOS (0.4 μM) alone overlaps the
826 concentration of PFOS in POP 10x (mixture). Each exposure group consists of 9 chicks per
827 group. EGL= external granular layer; ML= molecular layer; IGL= internal granular layer. *LS
828 mean values differ significantly from control ($p \leq 0.05$).

Exposure group	Cerebellar layer	LS means mm	Std Error	Lower 95% CL	Upper 95% CL
DMSO control	EGL	0.99	0.03	0.92	1.06
POP mixture 10x	EGL	0.96	0.03	0.89	1.03
PFOS	EGL	1.00	0.03	0.93	1.07
DMSO control	ML	0.74	0.02	0.70	0.79
POP mixture 10x	ML	**0.63***	0.02	0.58	0.67
PFOS	ML	**0.60***	0.02	0.56	0.65
DMSO control	IGL	1.56	0.09	1.37	1.75
POP mixture 10x	IGL	1.57	0.09	1.38	1.76
PFOS	IGL	1.49	0.09	1.30	1.68

829

830

831 **Table 2.** Common transcripts between POP mixture and PFOS exposure based on cut-off
832 values for significance of p<0.05 and with a log2 fold change >±0.7

RNA-seq transcripts		POP mixture		PFOS	
ID	**Gene**	**P Value**	**LogFC**	**P Value**	**LogFC**
Upregulated					
ENSGALG00000038364	***CCN3***	0.00162355	1.66118029	0.013932	1.384964
ENSGALG00000040730	***RXRG***	0.007167761	1.30436263	0.008934	1.367174
ENSGALG00000016791	***SLC9A2***	0.036054025	1.29570501	0.041498	1.29327
ENSGALG00000041491	***ACKR4***	0.000229811	1.09709331	1.33E-08	1.506378
ENSGALG00000016558	***VEGFD***	0.007210225	1.051434	0.032908	0.793624
ENSGALG00000015897	***IMPG1***	0.007490512	1.03575956	0.000579	1.405499
ENSGALG00000006120	***PKD2L2***	0.018657854	0.80468934	0.048601	0.702702
ENSGALG00000039826	***CNGA3***	0.030627314	0.73116232	0.03455	0.884197
ENSGALG00000009497	***AVPR2***	0.049429426	0.71884589	0.00056	1.275254
ENSGALG00000001141	***HES5***	0.000513484	0.71338272	0.000133	0.753101
ENSGALG00000002152	***GABRP***	0.00993585	0.7093588	0.005189	0.823913
Downregulated					
ENSGALG00000000112	***PLP1***	0.047524117	-0.7002252	0.002481	-1.12965
ENSGALG00000033376	***APOH***	0.002527203	-0.8291049	0.005611	-1.05762
ENSGALG00000053697	***TMEM125***	0.003243833	-0.8511434	0.00523	-1.06644
ENSGALG00000014268	***CHRNA9***	0.001828774	-0.8583561	0.011306	-0.77632
ENSGALG00000001391	***PLLP***	0.034696778	-0.8719167	0.008951	-1.37532
ENSGALG00000019716	***KRT40***	0.012128976	-0.8861578	0.000431	-1.32345
ENSGALG00000013775	***CDH19***	0.003089066	-0.8964305	0.00321	-1.15967
ENSGALG00000027514	***SCEL***	0.001036455	-0.8979882	0.000798	-0.99983
ENSGALG00000047990	***SCRG1***	0.000715431	-1.0194793	0.038799	-0.78173
ENSGALG00000019211	***MAEL***	0.000352765	-1.0683372	0.009412	-0.95985
ENSGALG00000004246	***SLC6A4***	0.004770037	-1.1501515	0.038442	-0.8472
ENSGALG00000005360	***CA4***	0.002540797	-1.1618113	0.0291	-0.80444
ENSGALG00000038540	***ZBTB32***	0.000494656	-1.1671055	0.011645	-1.07877
ENSGALG00000027874	***CHAC1***	0.00000199	-1.9362278	8.8E-07	-1.96661

833 **Table 3.** Common proteins between POP 10 mixture and PFOS exposure based on cut-off
834 values for significance of $p<0.05$ and with a log2 fold change $\geq \pm 0.7$

Proteomics	POP mixture		PFOS		
ID	**Protein name**	**P Value**	**logFC**	**PValue**	**logFC**
Upregulated					
XP_004939171.2	**NACAD**	0.001492	2.826486	0.018064	2.778713
XP_025004922.1	**LOC776992**	0.00245	1.972114	0.032837	1.690717
NP_001001760.1	**CDH13**	0.043196	1.703826	0.017349	2.27518
NP_001034398.1	**OPA1**	0.000661	1.169173	0.016594	1.25752
NP_001025835.2	**NAA25**	0.028407	0.990431	0.043288	1.058891
XP_015136489.1	**FAM168A**	0.039566	0.837654	0.035407	0.910865
Downregulated					
NP_990077.1	**PBX1**	0.01593	-0.71459	0.013932	-0.72148
NP_001004390.1	**HBBR**	0.005335	-0.78311	0.000813	-0.98994
NP_990569.1	**RBP4A**	0.004826	-0.79091	0.002934	-0.7832
NP_001026324.1	**UBE2D3**	0.011188	-0.82191	0.023831	-0.89254
NP_996789.1	**ANXA1**	0.018446	-0.87991	0.046458	-0.75984
XP_004944240.2	**ZNF423**	0.046982	-0.89053	0.023975	-0.84985
NP_001264341.1	**RMDN1**	0.012601	-0.93477	0.025308	-0.97869
NP_001004374.1	**HBZ**	0.000397	-1.06057	8.46E-05	-1.0944
NP_990732.1	**TPM1**	0.045329	-1.6364	0.015319	-2.32081

835

836

837

838 **Table 4**. Examples of genes and proteins affected by POP mixture or PFOS exposure in context
839 of the biological functions and outcomes. Additional supportive published evidence is also
840 referenced.
841

Biological function/Outcome	Gene/Protein symbol	Other POPs and/or PFOS observations
RARA/RXR signalling	*RXRG*, *RDH10,* RBP4A	
Glucocorticoid signalling	ANXA1, *SCRG1*	(1) POP mixture affects stress response (Hudecova et al., 2018). (2) Glucocorticoids effects on cerebellar development in a chicken embryo development (Austdal et al., 2016)
Cell proliferation, differentiation, migration	PBX1, *CCN3*, *CHAC1*, ANXA1	
Vascularization, blood-brain barrier	*VEGFD*, *CCN3*, *SLC9A2*, *CA4*	(3) POP mixture distributes to the developing chicken brain at human relevant exposure level (Yadav et al.,2021 under review).
Oligodendrocytes	*CDH19*	
Myelination	*HES5*, *PLP1, PLLP*	
Neuronal networking & Synaptic health **Neurotransmitters** **Ca^{2+}-homeostasis** **Redox homeostasis** **Mitochondrial health**	 *SLC6A4*, *GABR*P RMDN1 *CHAC1*, HEBP2 OPA1, HEBP2	(4) POPs and PFOS increase neuritogenesis (Yadav et al., 2021a). (5) POP mixture and PFOS aggravate glutamate-excitotoxicity; Ca^{2+} dependent and independent mechanism exist (Yadav et al., 2021b) (6) POP mixture and single POPs affect mitochondrial mass and mitochondrial membrane potential (Shannon et al., 2019, Wilson et al., 2016a).
ER stress	*CHAC*1,	
Unfolded protein response	*CHAC1*, *CA4*	
Ubiquitination	UBE2D3, *ZBT16*, NACAD1	
Inflammation	*ACKR4*, *SELE*, *CCN3*, ANXA1	
DNA damage	UBE2D3	

842
843

844 **Table 5.** An overview of genes and proteins differentially regulated by POP mixture or PFOS
845 exposure with a known link to neurocognitive and neurobehavioral outcomes, as well as
846 neurodegenerative disorders.

Gene/Protein symbol	Function	Disorders association	Reference
ANX1	Neuroinflammatory, neurovascular and metabolic disease, repairing blood–brain barrier damage	Multiple sclerosis, Alzheimer's disease, neurovascular disease, and stroke	(McArthur et al., 2016, Purvis et al., 2019)
BMP	Neural stem cell fate and maturation, neural development	Cognitive decline associated with normal aging and neurodegenerative diseases	(Bond et al., 2012)
CA4	Carbon dioxide and bicarbonate homeostasis	phobias, obsessive-compulsive disorder, generalized anxiety, and post-traumatic stress disorders	(Blandina et al., 2020)
GABRP	Associated with GABA	Autism, schizophrenia, bipolar I disorder	(Ma et al., 2005, Lang et al., 2007, Ren et al., 2018)
IGF-1	Cellular proliferation and differentiation during embryonic and postnatal development including brain growth	Autism	(Riikonen, 2016)
NACAD	Prevents mistargeting of nascent polypeptide chains to the endoplasmic reticulum membranes	Alzheimer's disease	(Kim et al., 2002)
PLP1	Major structural protein maintaining the compaction of CNS myelin sheaths	Parkinson's disease	(Hentrich et al., 2020)
PPAR-α	Lipid catabolism, brain inflammation	Alzheimer's, Parkinson's, Huntington's disease	(Zolezzi et al., 2017)
RMDN1	Calcium and lipid transfer	Alzheimer's disease	(Fecher et al., 2019)
RXR-G	Remyelination	Multiple sclerosis	(Huang et al., 2011)
SCRG1	Mouse scrapie responsive gene, cell growth suppression and differentiation, glucocorticoid signalling	Transmissible spongiform encephalopathies	(Dandoy-Dron et al., 2003, Dron et al., 2005)
SLC6A4	Reuptake of Serotonin and terminates Serotonin transmission	Mood and personality disorders, obsessive compulsive disorders, anxiety, insomnia, and eating disorders, ADHD	(Zhou et al., 1996, van der Meer et al., 2016)
UBE2D3	E2 ubiquitin-conjugating enzyme family	Gordon Holmes syndrome (characterized by reproductive and neurological problems)	From GeneCards and MalaCards database

847

SUPPLEMENTARY MATERIALS – PAPER IV

Supplementary materials

Due to the large file size, the supplementary materials for this Omics draft (**paper IV**) are provided as a Zip folder attached in the Email.

ISBN: 978-82-575-1837-0
ISSN: 1894-6402

Norwegian University
of Life Sciences

Postboks 5003
NO-1432 Ås, Norway
+47 67 23 00 00
www.nmbu.no

111678 / ANDVORDGRAFISK.NO